UNIVERSITY OF NAPLES
"FEDERICO II"

Doctorate School in Molecular Medicine

Doctorate Program in
Genetics and Molecular Medicine
Coordinator: Prof. Lucio Nitsch
XXVII Cycle

"Identification of *PATZ1*-Targeting miRNAs in thyroid cancer"

Michela Vitiello

Naples 2015

“Identification of *PATZ1*-Targeting miRNAs in thyroid cancer”

TABLE OF CONTENTS

LIST OF PUBLICATION

This dissertation is based upon the following publications and manuscripts in preparation:

1. **Vitiello M**, Valentino T, De Menna M, De Vita G, Palmieri D, Fusco A and Fedele M. Targeting of PATZ1 by miR-29b is a downstream effect of oncogenic Ras signaling in thyroid cells. (The main body of the dissertation - Manuscript in preparation)

2. **Vitiello M**, Valentino T, Chiappetta G, Pasquinelli R, Monaco M, Palma G, Luciano A, Aiello C, Rea D, Losito SN, Arra C, Fusco A and Fedele M. Loss of one or two PATZ1 alleles enhances RET/PTC1 tumorigenesis in mice. (Manuscript in preparation)

3. Chiappetta G, Valentino T, **Vitiello M**, Pasquinelli R, Monaco M, Palma G, Sepe R, Luciano A, Pallante PL, Palmieri D, Aiello C, Rea D, Losito SN, Arra C, Fusco A and Fedele M. PATZ1 acts as a tumor suppressor in thyroid cancer via targeting p53-dependent genes involved in EMT and cell migration. Oncotarget, advance publications, **2014**. Published: December 16, 2014. Online ISSN: 1949-2553. (Attached at the end)

4. Valentino T, Palmieri D, **Vitiello M**, Pierantoni GM, Fusco A, Fedele M. PATZ1 interacts with p53 and regulates expression of p53-target genes enhancing apoptosis or cell survival based on the cellular context. Cell Death Dis. **2013** Dec 12;4:e963. doi: 10.1038. (Attached at the end)

5. **Vitiello M**, Valentino T, De Menna M, Serpico L, Mansueto S, De Vita G, Fusco A and Fedele M. Targeting of PATZ1 by miR-29b is a downstream effect of oncogenic Ras signaling in thyroid cells. Endocrine Abstracts **2013**. Vol 32. ISSN 1479-6848. (Attached at the end)

6. Valentino T, Palmieri D, **Vitiello M**, Simeone A, Palma G, Arra C, Chieffi P, Chiariotti L, Fusco A, Fedele M. Embryonic defects and growth alteration in mice with homozygous disruption of the Patz1 gene. J Cell Physiol. **2013** Mar;228(3):646-53. (Attached at the end)

7. Valentino T, **Vitiello M**, Pasquinelli R, Palmieri D, Monaco M, Palma G, Arra C, Fusco A, Chiappetta G, Fedele M. PATZ1 is a New Candidate Tumour-Suppressor in Thyroid Cancer. European Journal of Cancer **2012.** Vol. 48, suppl. 5 S25–S288. (Attached at the end)

8. Chiappetta G, Valentino T, **Vitiello M,** Pasquinelli R, Monaco M, Palma G, Arra C, Fusco A and Fedele M. PATZ1 is a new candidate tumor-suppressor gene in thyroid cancer. Endocrine Abstracts. **2012**. Vol. 29 ISSN1470-3947 (Print). ISSN 1479-6848. (Attached at the end)

Besides these, during my PhD program I also contributed to the following study that was in progress in our laboratory:

1. Palmieri D, Valentino T, De Martino I, Esposito F, Cappabianca P, Wierinckx A, **Vitiello M**, Lombardi G, Colao A, Trouillas J, Pierantoni GM, Fusco A, Fedele M. PIT1 upregulation by HMGA proteins has a role in pituitary tumorigenesis. Endocr Relat Cancer. **2012** Apr 10;19(2):123-35. (Attached at the end)

LIST OF ABBREVIATION

TF, Transcriptional Factor
POK, Poxviruses and Zinc-finger (POZ) and *Krüppel*
BTB, Broad Complex, Tramtrack, and Bric a' brac
POZ, Poxviruses and Zinc-finger
PATZ1, POZ/BTB A-T Hook Zinc-finger 1
EWS, Ewing Sarcoma
HDAC, Histone DeACetylase
HMGA, High Mobility Group A
CNS, Central Nervous System
OFT, Out-Flow Tract
MEF, Murine Embryonic Fibroblast
ICM, Inner Cell Mass
ESC, Embryonic Stem Cell
iPSCs, induced Pluripotent Stem Cells
MET, Mesenchimal- Epithelial Transition
EMT, Epithelial- Mesenchimal Transition
FTA, Follicular Thyroid Adenoma
PTC, Papillary Thyroid Cancer
FTC, Follicular Thyroid Cancer
ATC, Anaplastic Thyroid Cancer / Undifferentiated Thyroid Cancer
PDTC, Poor Differentiated Thyroid Cancer
WDTC, Well Differentiated Thyroid Cancer
MAPK, Mitogen-Activated Protein Kinase
TK, Tyrosine Kinase
miRNA/ miR, microRNA
RISC, RNA-Induced Silencing Complex
RNAi, RNA Interference
UTR, UnTranslated Region
AML, Acute Myeloid Leukemia
MCL, Mantle Cell Lymphoma
CLL, Chronic Lymphoid Leukemia
ALL, Acute lymphoblastic Leukemia
TSH, Thyroid-stimulating hormone
6H, 6 Hormones
qRT-PCR, quantitative Real Time- Polymerase Chain Reaction
CS, Calf Serum

ABSTRACT

Thyroid cancer is one of the most frequent malignancies of the endocrine system, and its incidence is predicted to become the fourth leading cancer diagnosis by 2030. In spite of the progressive knowledge of the molecular mechanisms involved in thyroid transformation, its prognosis remains unpredictable and the identification of new biological markers are needed in addition to already known molecules, to correctly stratify patients at risk of recurrence and progression, eventually providing new targeted therapies. We recently showed that the transcriptional regulator PATZ1 is constantly down-regulated in human thyroid cancer and acts as a tumor suppressor in thyroid cancer cell lines by targeting p53-dependent genes involved in Epithelial-Mesenchymal Transition and cell migration. The aim of the present work was to elucidate the upstream signaling pathway regulating PATZ1 expression during thyroid transformation. We first identified miR-23b and miR-29b to specifically target PATZ1 expression, which was inversely correlated to their expression in rat thyroid cells stimulated to proliferate with Thyroid-stimulating hormone (TSH). Next, using an inducible cell system, we found that miR-29b was up-regulated by oncogenic Ras during transformation of FRTL-5 rat thyroid cells toward an undifferentiated phenotype resembling that of anaplastic carcinomas and characterized by the acquisition of a migratory and invasive behavior. Conversely, PATZ1 was down-regulated, with an inverse correlation compared to miR-29b expression, and was specifically targeted by miR-29b in untransformed FRTL-5 cells. Restoration of PATZ1 expression in FRTL-5 cells stably expressing oncogenic Ras inhibited cell proliferation and migration, indicating a key role of PATZ1 in Ras-driven thyroid transformation. These results confirm the tumor suppressor role of PATZ1 in thyroid cancer and suggest that its downregulation in thyroid cancer requires the activation of Ras GTPase signaling via miR-29b.

1. BACKGROUND

1.1 The POK protein family

Transcription factors (TFs) play a key role in several biological mechanisms by which specific genes are expressed in a temporal and tissue-specific manner and, as modular proteins, they can be classified mainly based on the structure of their DNA binding or protein-protein interacting domains. The POK (Poxviruses and Zinc-finger (POZ) and *Krüppel*) family of transcription repressors is characterized by a typical structure, consisting in an amino-terminal POZ/Broad Complex, Tramtrack, and Bric a' brac (BTB) domain and several *Krüppel*-type zinc fingers at the carboxyterminal side (Lee and Maeda 2012; Costoya 2007) (Figure 1). The BTB domain, also known as Poxviruses and Zinc-finger (POZ) domain, is an evolutionary conserved protein-protein interaction domain. In most cases this domain is associated with C2H2 zinc finger motifs in TFs involved in transcriptional regulation through chromatin re-modeling (Kelly and Daniel 2006). C2H2 *Krüppel*-type name is due to the fact that it resembles the Drosophila segmentation protein *Krüppel*. It represents one of the most common types of DNA binding domains, with approximately more than 600 genes in the human genome encoding C2H2 motifs (Venter et al. 2001), suggesting that this class of TFs represents a substantial portion of the genes in the human genome. The biological functions of POK proteins are defined on the basis of the homo- and hetero-dimerization as well as protein-protein interactions properties conferred by the BTB/POZ domain, while the *Krüppel*-like C2H2 zinc fingers mediate the specific binding to DNA sequences located within gene-regulatory regions. Thus, the BTB/POZ domain promotes homo- and hetero-dimerization and exerts its transcriptional role through its interaction with transcriptional co-factors, including SIN3A, SMRT, NCOR1 and other co-repressors, which in turn recruit HDACs (Histone DeACetylases). On the other hand, transcription is highly dependent on DNA packaging. DNA can be tightly compacted, thus preventing accessibility of TFs, or can be available to TFs via modification of the nucleosome, fundamental subunit of chromatin. This architecture of chromatin is strongly influenced by post-translational modifications of the histones. POK proteins are able to act as a molecular switch opening or closing the chromatin through the deacetylation of the histones, and therefore regulating the transcription of their target genes (Costoya 2007). Most POK proteins studied so far have displayed a consistent trans-repressive activity in a variety of cell types and on various promoters, although it remains possible that the transcriptional activity of POK proteins may be dependent on the cellular environment and may include the ability to trans-

activate (Kobayashi et al. 2000). There are many proteins belonging to the POK family, involved in several biological and pathological processes, such as development, stem cell biology, and cancer. Among them there is the POZ/BTB and AT-hook-containing Zinc finger protein 1, also known as PATZ1.

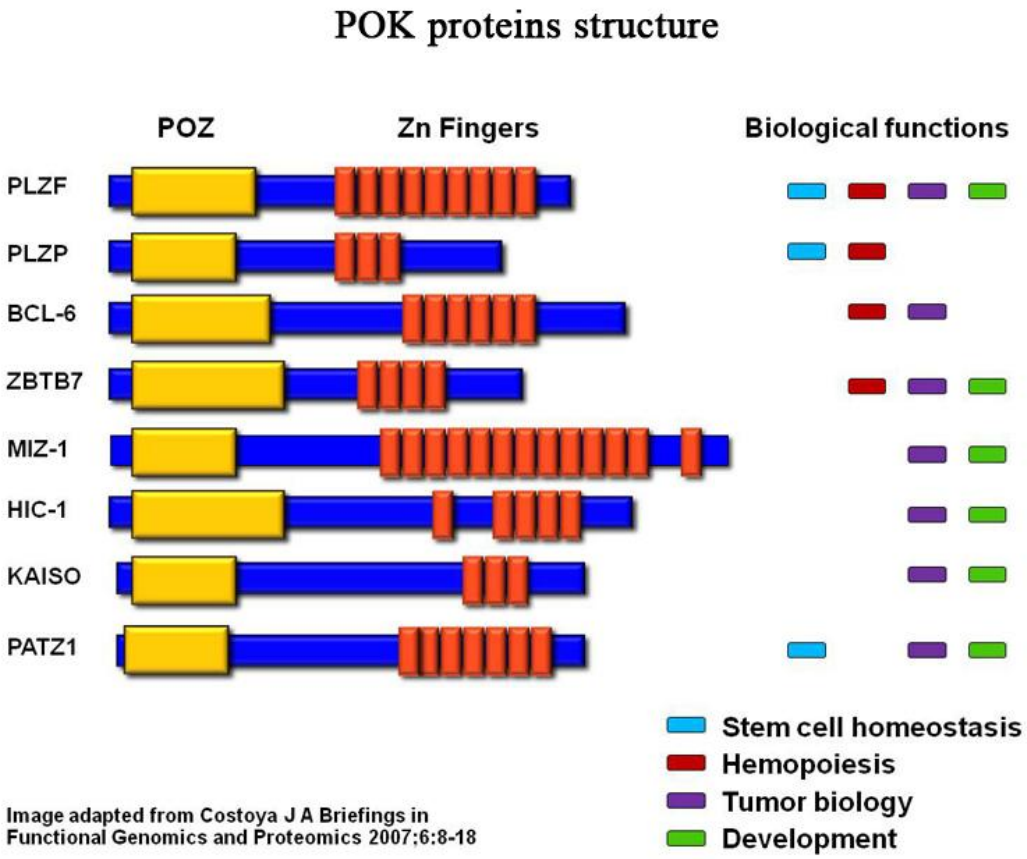

Figure 1. Structure of selected POK transcription factors. These proteins are characterized by the same structure: an amino-terminal POZ/BTB domain and several carboxy-terminal *Krüppel*-type zinc fingers. They have been shown to play important roles in hemopoiesis, cancer, development and stem cell biology.

1.2 *PATZ1* gene and protein structure: the discovery

The POZ/BTB and AT-hook-containing Zinc finger protein1 (PATZ1), also known as Zinc finger Sarcoma Gene (ZSG), MAZ-Related factor (MAZR) or Zinc Finger Protein 278 (ZNF278/Zfp278), is coded by the *PATZ1* gene, located on human chromosome 22 at the position 22q12. It was originally cloned in the 2000, by three independent groups (Fedele et al. 2000; Kobayashi et al. 2000; Mastrangelo et al. 2000). Mastrangelo and co-workers described a submicroscopic inversion of chromosome 22q in a patient presenting a small round cell sarcoma with a t(1;22)(p36.1;q12) translocation. The result of the mutation was a chimeric transcript contained exon 8 of the Ewing sarcoma (*EWS*) gene fused in-frame to exon 1 of the *PATZ1* gene, creating a protein with the transactivation domain of EWS fused to the zinc finger domains of PATZ1. Subsequently, the same group found that this paracentric inversion of chromosome 22q12 interrupted the *UQCRH* gene, with the breakpoint in intron 3, and created fusion genes with both *EWS* on der(22) and *PATZ1* on der(1). At the same time, Kobayashi and co-workers, as well as our group, isolated PATZ1 by yeast 2-hybrid screenings. As a bait, Kobayashi and co-workers used the POZ domain of Bach2, while our group used the RING finger protein-4 (RNF4) (Fedele et al. 2000; Kobayashi et al. 2000).

PATZ1 gene consists of 6 exons and encodes, by alternative splicing that give rise to PATZ1 variants 1-4, four protein isoforms (ranging from 537 to 687 amino acids) that share a common modular structure consisting of a N-terminal BTB/POZ domain, one AT-hook (in the central region) and four to seven C2H2 Zinc fingers at the C-terminus (Fedele et al. 2000) (Figure 2). Although such motifs are common to factors involved in transcriptional regulation, the presence of all these domains in the same protein appears to be an unique feature of PATZ1. The AT-hook motif is a small AT-rich DNA binding domain that was first described in the high mobility group non-histone chromosomal protein (HMGA1) and then identified in a few other proteins such as HMGA2 and ALL-1, and is involved in the binding to the minor groove in correspondence of AT-rich regions (Fedele et al. 1998). The BTB/POZ and zinc finger domains makes PATZ1 a member of the POK family of transcriptional repressors (Costoya 2007). Consistent with its protein structure and with the presence of typical features of nuclear proteins, including two nuclear localization signals, the subcellular localization of PATZ1, at least in physiological conditions, is in the nucleus, with a typical speckled distribution (Figure 3) (Fedele et al. 2000).

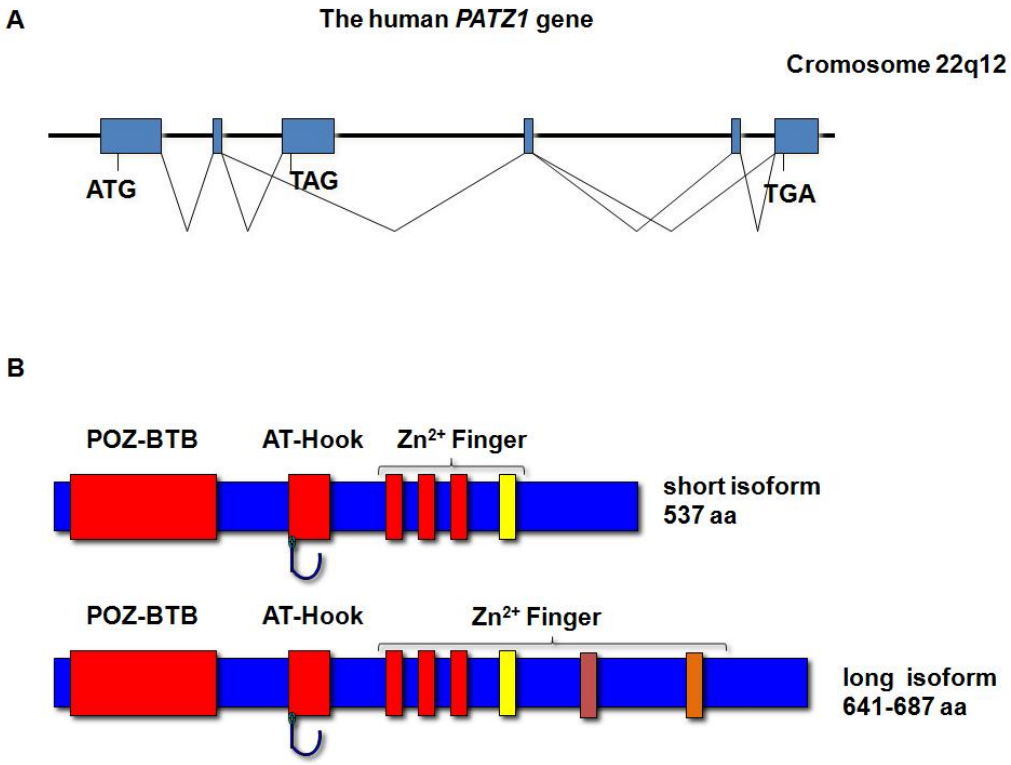

Figure 2. Schematic representation of human *PATZ1* gene and its encoded protein isoforms. (A) The human *PATZ1* gene consists of 6 exons, which give rise, trough alternative splicing, to 4 mRNA variants and 4 protein isoforms (depicted by exons-connecting lines). (B) Two short isoforms of 537 aa and the two long isoforms of 641 and 687 aa are represented by their characteristic domains.

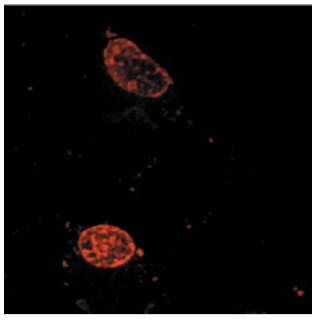

Figure 3. PATZ1 localization. The PATZ1 localization was detected with anti-PATZ rabbit polyclonal antibodies and Texas red-conjugated goat anti-rabbit IgG (Fedele et al. 2000).

1.3 Transcriptional activity of the *PATZ1* gene

Similarly to the other BTB/POZ proteins, the transcriptional activity of PATZ1 requires the POZ domain (Fedele et al. 2000). However, the mechanisms by which transcriptional regulation by PATZ1 occurs remain to be elucidated. The POZ domain of the POK proteins BCL6 and PLZF, as well as other POZ domain containing proteins, associates with the SMRT-mSin3AHDAC-1 complex and forms a multimeric repressor complex involving histone deacetylation activity (Huynh and Bardwell 1998). PATZ1 may also be involved in the formation of such complex, since we have demonstrated that its binding to gene promoters is influenced by HDACs inhibitors (unpublished data). Moreover, it is likely that the zinc finger motifs could target the PATZ1 protein to specific G-rich sequences (Kobayashi et al. 2000; Ow et al. 2014). PATZ1 has been shown to regulate expression of different genes in either a positive or negative manner. This dual behavior is in the nature of POZ-containing TFs, because their transcriptional activity is due to the POZ-mediated oligomers formation, and therefore they may function either as activators or repressors depending on the presence of proteins able to interact with them, which may be different depending on the cellular context. Moreover, PATZ1 contains an AT-hook, a motif characteristic of architectural transcriptional factors, such as the HMGA proteins, whose activity in gene transcription depends on the cellular context (Fedele and Fusco 2010).

For all these reasons, there are several studies in literature, reporting that PATZ1 can be either an activator or a repressor of transcriptional regulation. Fedele and co-workers showed that PATZ1 acts as a transcriptional repressor of basal transcription, as a co-repressor of RNF4 RING finger protein, on the *c-myc*, *CDC6*, *galectin-1* and *SV40* promoters (Fedele et al. 2000). On the other hand, it has been reported that PATZ1 acts as a transcriptional activator of the *c-myc* promoter in B cells and that the c-myc transcriptional activation by BACH2 is enhanced by its interaction with the BTB/POZ domain of PATZ1 (Kobayashi et al. 2000). Moreover, PATZ1 is able to activate mouse Mast cell protease 6 (mMCP-6) (Morii et al. 2002) and FGF4 (Kobayashi et al. 2000), and to repress androgen receptor (Pero et al. 2002), *CD8* (Bilic et al. 2006) and *BCL-6* genes (Pero et al. 2012). Consistent with the CD8 regulation, it has been shown that PATZ1 plays a key role in the transcription factor network that controls the CD4 *versus* CD8 lineage fate of double-positive thymocytes (Sakaguchi et al. 2010).

Recently, our group has demonstrated that the cellular context can influence the regulatory activity of PATZ1. In fact, we showed that PATZ1 is able to interact with the tumor suppressor p53 and enhance the expression of p53-dependent gene promoters, such as *BAX*, *CDKN1A* and *MDM2*, increasing the susceptibility to apoptosis. Consistently, knockdown of PATZ1 in p53-wild type human cell line (HEK293) reduces promoter activity of these genes and inhibits their expression.

However, PATZ1 binds p53-target genes also independently from p53, exerting, in the absence of p53, an opposite function on their expression. Indeed, knockdown of PATZ1 in p53-null osteosarcoma cells (SAOS-2) upregulates BAX expression and decreases cell survival (Valentino et al. 2013a). A recent work by Ma and co-workers, in collaboration with our group, using global gene expression analysis, showed that histone deacetylases, such as HDAC2, 4 and 11, were generally down-regulated upon Patz1 loss, while histone acetylases, such as Hat1 and Kat2a, were up-regulated. This implies that Patz1 may crosstalk with many epigenetic factors and modulate chromatin modification (Ma et al. 2014a).

1.4 PATZ1 expression and role in development

There are several studies in literature about the physiological role of PATZ1, but its function is still not completely known. Among them, Fedele and co-workers described an important role in testis development and spermatogenesis. Indeed, PATZ1 is expressed in spermatogonia, in which it could exert the role of transcriptional repressor to maintain the stem cell pool, and its lack led to increased apoptosis of the spermatocytes and total absence of spermatids and spermatozoa with subsequent male infertility (Fedele et al. 2008). On the other side, PATZ1 is strongly and widely expressed during the early steps of the mouse embryogenesis, in particular between 8.5 and 17.5 days post coitum (dpc), the period during which the most critical events of organogenesis take place. Indeed, the expression of PATZ1 in the central nervous system (CNS) is clearly restricted to the actively proliferating neuroblasts in the periventricular neocortical neuroepithelium, in the telencephalic cortical plate, in the hippocampus, and in the striatal neuroepithelium and subventricular zone; then, even though it keeps to be ubiquitously expressed, it is still abundant in restricted organs during the medium and late developmental stages (Valentino et al. 2013b). Its ubiquitous expression is kept in the adult life, but it is generally lower than in embryonic tissues and is still abundant in selected tissues, including skeletal muscle, spinal cord and thyroid (Fedele, unpublished data). In order to understand the role of PATZ1 in development, adult life and cancer, a Patz1 knock-out mouse model has been generated in our laboratory. The analysis of Patz1 -/- mouse embryos showed defects in the CNS with a clear reduction of periventricular cells, and altered positioning of the cardiac out-flow tract (OFT) suggesting that this gene plays an important role in the development of the CNS and the cardiac OFT. Moreover, most Patz1 -/- embryos dye in utero: homozygous mutant pups totaled only 4% of the newborn offspring from heterozygous intercrosses, instead of the expected 25%, indicating that most PATZ1-null mice died during embryogenesis, probably because of defects accumulated during CNS and cardiac OFT development. The few Patz1 -/- mice that survived showed a general growth retardation and defects

in spermatogenesis, resulting in infertility (i.e. increased apoptosis of the spermatocytes and total absence of spermatids and spermatozoa (Fedele et al. 2008; Valentino et al. 2013b). The growth defects may be due, at least in part, to alterations in cell cycle progression and premature senescence. In fact, Patz1 -/- mouse embryonic fibroblasts (MEFs) showed arrest at or beyond the restriction point in either G1 or G2 phase and enter into premature cellular senescence (Valentino et al. 2013b). The results obtained on the Patz1-null MEFs are consistent with recent data showing that knockdown of PATZ1 in young cells induced cellular senescence, which was confirmed by growth arrest and increased p53 protein levels and SA-β-gal activity, and accumulation of phospho-H2AX foci; conversely, the upregulation of PATZ1 in old cells reversed senescence phenotype (Cho et al. 2012).

1.5 PATZ1 in stem cells

Embryonic stem cells (ESCs) are obtained by culturing the inner cell mass (ICM) of the preimplantation stage blastocyst *in vitro*. They are pluripotent, and can be self-renewed by culturing with leukemia inhibitory factor (LIF) and bone morphogenetic protein 4 (Bmp4) for murine ESCs (mESCs) or basic fibroblast growth factor (bFGF) and transforming growth factor β (TGFβ) for human ESCs (hESCs) (Ow et al. 2014). The intrinsic transcriptional network that maintains pluripotency is conserved, with Oct4, Sox2 and Nanog as the master regulators that control this network (Masui et al, 2007). The importance of these factors in stem cell maintenaince is testified by their pivotal role in induced pluripotent stem cells (iPSCs) (Takahashi K and S Yamanaka 2006). Recent studies have shown that several zinc finger proteins are crucial for maintaining pluripotent ESCs. Among them, Sal14 is important in the regulation of Oct4 and interacts with Nanog to control many downstream genes; Zic3 suppresses differentiation of ESCs into the endodermal lineage through direct interaction with Nanog; Zfp206 acts as a transcriptional activator of Nanog and Oct4. Moreover, Zfp143 and Zfp281 are able to activate Nanog (Ow et al. 2014). Among the zinc finger proteins, PATZ1 was found highly expressed in the pluripotent mouse ICM compared to the nonpluripotent trophectoderm (Yoshikawa al. 2006), and in Oct4^{+} cells relative to Oct4^{-} cells (Tang et al. 2010). In addition, the *Patz1* genomic region is bound by various important transcription factors, such as Oct4, Nanog, Sox2, Klf4 and c-Myc (Nishiyama et al. 2009). Together, these data suggest that PATZ1 potentially regulates pluripotency in ESCs, even though its mechanism of action function is poorly studied. In a recent study, Ow and co-workers have shown that, through *Patz1* knock-down and Chromatin Immuno-Precipitation assays (CHIP), PATZ1 binds to the regulatory elements of the master pluripotency

regulators Oct4 and Nanog and directly activates their gene transcription. The consequent down-regulation of Nanog and Oct4 led to differentiation and loss of pluripotency in *Patz1*-knocked-down cells, reduction of alkaline phosphatase staining, and up-regulation of germ layer markers (Ow et al. 2014). All these data highlighted the importance of PATZ1 in maintaining the expression of pluripotency regulators, thus sustaining ESCs in the undifferentiated state. Subsequently, the same authors, in collaboration with our group, showed a role for PATZ1 also in the reprogramming process (Ma et al. 2014a).

It is well known that the pluripotent state can be generated from mouse somatic cells by ectopic expression of transcription factors Oct4, Sox2, Klf4 and c-Myc (OKSM) (Takahashi K and S Yamanaka 2006). These induced pluripotent stem cells (iPSCs) resemble ESCs, possessing the abilities to self-sustain pluripotency and to differentiate into many cell types (Ma et al. 2014a). However, the acquisition of induced pluripotency remains a relatively slow and inefficient process. Indeed, there are cellular "barriers" for a somatic cell to overcome in order to be reprogrammed into a pluripotent stem cell. Several study have revealed that the cell fate conversion from somatic cells to iPSCs is a dynamic process that involves a cascade of cellular events, such as silencing lineage-specific genes and reactivation of pluripotency genes, mesenchymal to epithelial transition (MET), overcoming cellular senescence and acquisition of cell immortality, reactivation of X chromosome and resetting the chromatin signatures (Apostolou, 2014). Ma and co-workers showed that the overexpression of PATZ1 inhibits the acquisition of pluripotency, while interference or heterozygous loss of PATZ1 enhances iPSC generation. On the other hand, complete knockout of PATZ1 seriously affects the reprogramming process by inducing cellular senescence. This suggests that a critical control of PATZ1 dosage is essential for the generation of iPSCs (Figure 4). In particular, heterozygous knockout of PATZ1 in mouse embryonic fibroblasts (MEFs) down-regulates repressive histone marks and upregulates active histone markers, creating a more open chromatin accessible for transcriptional activation of pluripotency factors, thus facilitating the reprogramming. In the absence of PATZ1 (Patz1-/- MEFs), p53/p16 axis is activated, and the cells undergo cellular senescence. When only one of Patz1 alleles is disrupted (Patz1+/- MEFs), Ink4a/Arf locus is repressed, whereby preventing the cells from senescence induction. Conversely, overexpression of PATZ1 robustly activates p53 and p16, thereby inhibiting cell proliferation in MEFs (Ma et al. 2014a).

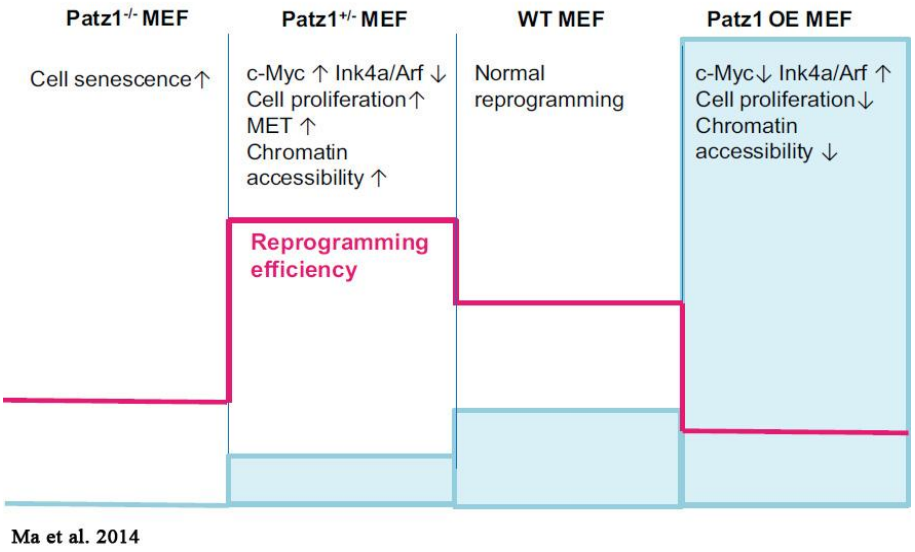

Fig. 4 Proposed role of Patz1 during somatic cell reprogramming. Overexpression of Patz1 (Patz1 OE) creates a condensed chromatin, which represses the reprogramming process; Patz1 overexpression also represses c-Myc and induces cell senescence inhibiting reprogramming. Heterozygous knockout of *Patz1* can promote MET, activate c-Myc, overcome *Ink4a/Arf* barrier to surpass senescence and also create an open, hyperdynamic chromatin structure accessible for pluripotency gene reactivation, thus enhancing cellular reprogramming. Patz1-/- MEFs undergo cell senescence and are hard to be reprogrammed (Ma et al. 2014a).

1.6 PATZ1 in cancer

Recently it has been produced a wide literature about the involvement of PATZ1 in cancer but its cancer-related function is still debated between being a tumor suppressor or an oncogene. In support of the view that PATZ1 is a tumor suppressor, Mastrangelo and co-workers demonstrated that the human *PATZ1* gene maps on the FRA22B fragile site (on chromosome 22) which suffers loss of heterozygosity in several solid tumors. Indeed, it has been found rearranged with *EWS* gene in a small round cell sarcoma, with the loss of heterozygosis of the wild-type *PATZ1* allele (Mastrangelo et al. 2000; Burrow et al. 2009). In recent years, our research group has supported the tumor suppressor role for PATZ1, conducting different studies. First, we showed that in some cell lines PATZ1 is able to reduce the promoter activity of the proto-oncogene c-myc and may cooperate with the oncoprotein BCL6 in the inhibition of its own promoter. In particular, we demonstrated that PATZ1 can bind *BCL6* exon 1 and negatively modulate *BCL6* promoter activity in GC-derived lymphoma B cells, thus acting as a tumor suppressor in lymphomagenesis (Fedele et al. 2000, Pero et al. 2012).

Moreover, we demonstrated that in testicular seminomas, teratomas and embryonal carcinomas there is a significant overexpression of PATZ1; however, it localized in cytoplasm rather than nucleus, suggesting a reduction of its transcriptional function (Fedele et al. 2008). Interestingly, it has been also shown that the delocalization of PATZ1 in testicular seminomas depends on estrogen receptor-β levels and the translocation from cytoplasm to the nucleus is mediated by cAMP (Esposito et al. 2012a), as it was previously demonstrated in other cell systems, such as PC3M prostate carcinoma cells and normal fibroblasts (Yang et al. 2010). Yang and co-workers demonstrated that PATZ1 binds the RIα subunit of the cAMP-dependent protein kinase in the cytoplasm, and it is known that alteration of RIα expression, and then of the cAMP signaling, may confer cell growth advantage. Therefore, the sequestration of PATZ1 in the cytoplasm through its interaction with RIα would enable PATZ1 to translocate into nucleus and transactivate/repress its target genes upon activation of the cAMP pathway (Yang et al. 2010). More recently, once again in support of a tumor suppressor role for PATZ1, we showed that PATZ1 could play a key role in opposing to thyroid carcinogenesis. Indeed, we demonstrated that PATZ1 is down-regulated in thyroid carcinomas compared to normal thyroid tissues, with an inverse correlation to the degree of cell differentiation. In particular, PATZ1 has been found significantly further down-regulated in poorly differentiated and anaplastic thyroid cancers compared to the papillary histotype, also resulting increasingly delocalized from the nucleus to the cytoplasm proceeding from differentiated to undifferentiated thyroid carcinomas. More interestingly, restoration of PATZ1 expression in three thyroid cancer-derived cell lines, all characterized by fully dedifferentiated cells, significantly inhibited their malignant behaviors, including *in vitro* proliferation, anchorage-independent growth, migration and invasion, as well as *in vivo* tumor growth. Consistent with recent studies showing a role for PATZ1 in the p53 pathway, we showed that ectopic expression of PATZ1 in thyroid cancer cells activates p53-dependent pathways opposing epithelial-mesenchymal transition (EMT) and cell migration to prevent invasiveness (Chiappetta et al. 2014). Finally, a strong effort to the tumor-suppressor hypothesis derived by the analysis of PATZ1 knock-out mice carried out in our laboratory. In fact, we have shown that both heterozygous and homozygous Patz1 knock-out mice spontaneously develop tumors, including BCL6-expressing Non-Hodgkin lymphomas, sarcomas, hepatocellular carcinomas and rare lung adenocarcinomas (Pero et al. 2012). In particular, at the age of 4-24 months (average of 19 months), pathological analysis demonstrated that 9 out 63 *Patz1* +/+ mice, 50 out of 75 *Patz1* +/- mice, and 9 out of 11 *Patz1* -/- mice developed multiple neoplastic lesions, including both malignant tumors and benign lymphoproliferative diseases (Pero et al. 2012). All the tumors raised in heterozygous animals do not lose or mutate the second wild-type allele, and express the wild-type PATZ1 protein, thus excluding loss of

heterozygosity as an explanation for the increased occurrence of tumors in *Patz1* +/- mice compared to *Patz1* +/+ mice and suggesting an haploinsufficient tumor suppressor role for PATZ1. Consistent with the role of PATZ1 in BCL6 autoregulation, *Patz1*-knock-out mice developed thymus hyperplasias or lymphomas and showed increased levels of BCL6, thus suggesting that PATZ1 causes up-regulation of BCL6 expression, which in turn could be responsible for the thymus pathological phenotype. This hypothesis was validated crossing *Patz1* +/- mice with *Bcl6* +/- mice to generate double mutants that had shown a normal phenotype rescue, indicating a key role for BCL6 expression in its pathologic development (Pero et al. 2012).

On the other hand, an oncogenic role for PATZ1 has also been suggested. It has been shown that PATZ1 is capable to activate c-myc in a B cellular context (Kobayashi et al. 2000), is overexpressed in colon carcinomas (Tian et al. 2008) and its down-regulation by siRNA either blocks the growth or induces apoptosis of cell lines derived from colorectal cancer or gliomas, respectively (Tian et al. 2008; Tritz et al. 2008). In addition, a recent paper by Keskin and co-workers showed that PATZ1 can interact and inhibit the DNA binding and transcriptional activity of p53 in colon cancer cells, once again suggesting an oncogenic role for PATZ1 in colon cancer (Keskin et al. 2015).

The controversial role of PATZ1 in tumorigenesis could be easily explained considering that its transcriptional modulation is highly dependent on specific molecular partners of a particular cellular context. Moreover, as for other well known architectural factors, it is possible an involvement in the development of neoplastic disease either if hyper- or hypo-expressed, stressing the great importance of the correct gene dosage for these factors.

1.7 Thyroid cancer

Thyroid cancer is the most common endocrine malignancy and its incidence is predicted to become the fourth leading cancer diagnosis by 2030 (Rahib et al. 2014). Many studies have provided evidences for this increase; however, why thyroid cancer incidence keeps rising is still debated and there are conflicting reports of factors leading to the increase in its incidence (Ito et al. 2013; Rahib et al. 2014). The thyroid carcinoma is a good multi-step carcinogenesis model because it differs in malignant potential as a result of different genetic alterations (Figure 5). The majority of thyroid carcinomas (over 95%) derive from follicular thyroid cells, also known as thyroid epithelium or thyroid principal cells, responsible for thyroid hormone production and secretion, while a minority (3-5%), named medullary thyroid carcinomas, originates from para-follicular or C-cells (Kondo et al. 2006; Rossing 2013). Thyroid tumors are divided into benign

and malignant tumors; while benign tumors are represented by goiters and follicular adenomas (FTA), malignant tumors, histologically thyroid carcinomas, can be classified into papillary (PTC), follicular (FTC), and anaplastic thyroid cancer (ATC) (Guan et al. 2009). The most common follicular cell-derived carcinomas are PTCs, which account for 80–90% of all thyroid cancers and have a 5-year survival above 90% (Kondo et al. 2006). PTCs are characterized by the classic papillary architecture and cells with typical nuclear alterations (ground-glass nuclei). Often, they are multifocal and tends to metastasize to regional lymph nodes (De Lellis et al. 2004). The second most common follicular cell-derived carcinomas are FTCs, accounting for 10% of thyroid cancers (Kondo et al. 2006). The frequency of distant metastases at the time of diagnosis of FTCs is up to 20%. Nevertheless, the prognosis of FTCs is still favorable with a 5-year survival close to 90% (Kondo et al. 2006). FTCs are the malignant counterparts of benign FTAs, which represent the most common follicular cell-derived tumors of the thyroid (Faquin 2008). The sole morphological feature differentiating follicular thyroid adenomas from FTCs is the lack of invasion (capsular and/or vessel); indeed, invasion is the diagnostic criterion for FTCs (Faquin 2008). Poorly differentiated (PDTC) and undifferentiated thyroid cancer, also known as ATC, represent a small subset of follicular cell-derived cancers with a poor prognosis. The growth patterns of ATCs and PDTCs are highly invasive and more than 50% of patients have distant metastases at the time of diagnosis (Kondo et al. 2006). The 5-year survival rate of ATCs is no more than 5%, illustrating why this tumor is considered one of the most fatal human cancers (Kebebew et al. 2005). PDTCs and ATCs can develop *de novo* although many of them arise through the process of stepwise dedifferentiation of PTCs and FTCs (Nikiforov and Nikiforova 2011). The theory of sequential progression of well-differentiated thyroid carcinoma (WDTC) trough the spectrum of PDTC to ATC is supported by the presence of pre- or co- existing WDTC with less differentiated types and the common core of genetic loci with identical allelic imbalances in co-existing well-differentiated components (van der Laan et al. 1993). Similar to other cancer types, thyroid tumor initiation and progression may be separate events and occur through gradual accumulation of various genetic (rearrangements that activate proto-oncogenes, point mutations and loss of tumor suppressor function) and epigenetic alterations, including activating and inactivating somatic mutations, alteration in gene expression patterns, micro-RNA dysregulation and aberrant gene methylation (Kim et al. 2014). A molecular analyses conducted by Jung and co-workers revealed three important trends in the mutational composition of PTCs over time: (1) the overall proportion of *Ras* point mutations increased significantly after 2000, and this was entirely due to increases in the follicular variant of PTC, (2) the proportion of *BRAF* mutations was largely stable, although it increased significantly within the classic papillary type of PTC, and (3) the proportion

of *RET/PTC* rearrangements significantly decreased, suggesting that recent increases in thyroid cancer are likely not due to ionizing radiation exposure (Jung et al. 2014).

In PTCs non overlapping mutations of genes involved in the activation pathway of mitogen-activated protein kinase (MAPK), such as RET, TRK, RAS and BRAF, have been found in about 70% of the cases (Kimura e al. 2003, Soares et al. 2003, Frattini et al. 2004). Indeed, a fraction of about 30% of PTCs present a typical gene alteration consisting in the rearrangement of the RET proto-oncogene (Santoro et al 2004). The RET/PTC rearrangement consists in the fusion of the tyrosine kinase domain (TK) of RET with other genes that provide the chimeric gene of promoter and 5' coding region. In about 10% of PTC cases, rearrangements of the gene coding for TRK, another TK protein, which determines its fusion to partner genes similarly to RET/PTC rearrangements, were identified. At least ten different types of RET/PTC rearrangements have been reported (Nikiforov 2002). RET/PTC1 was generated by the fusion of RET TK domain with the 5' terminal region of the gene CCD6 (Grieco et al. 1990), whereas in RET/PTC3 the TK domain of RET is fused to the RFG gene (Santoro et al. 2004).

Approximately 45% of PTCs and 25% of PTCs-derived ATCs harbor a thymine-to-adenine transversion (T1799A) point mutation, in the gene encoding the serine/threonine-kinase B-type Raf kinase (BRAF), with substitution of valine by glutamate (V600E). Mutated BRAF generates a constitutive activation of the MAPK signaling pathway, which plays a critical role in transmitting proliferative signals generated by cell surface receptors and cytoplasmic signaling elements, to the nucleus (Lopes and Fonseca 2011; Guan et al. 2009). In PTCs, BRAF mutation and RET/PTC rearrangements are mutually exclusive and cannot be found simultaneously in the same patients, yet they are not completely equivalent, since it has been shown that PTCs positive for BRAF are more aggressive than those positive for RET/PTC (Kimura et al. 2003; Soares et al. 2003).

Ras genes (K-RAS, H-RAS, and N-RAS) mutations represent early molecular lesions. Point mutation in codons 12, 13 and 61, are observed in 10-20% of PTCs (Namba et al. 1990; Vasko et al. 2004), and are frequently found in FTAs, which are considered FTCs precursors. Mutations of *Ras* genes are also observed in 40-50% of conventional FTCs, while 35% of conventional FTCs presents the PAX8/PPARγ rearrangement (Pallante et al. 2010). The PAX8/PPARγ rearrangement leads to the fusion between a portion of the PAX8 gene, which encodes a paired domain transcription factor, and PPARγ gene (Kroll et al. 2000); this fusion results in strong overexpression of the chimeric PAX8/PPARγ protein (Kroll et al. 2000; Sahin et al. 2005), although the mechanism of its transforming activity remains to be fully understood.

In PDTCs RET/PTC rearrangements (13%) and mutations in the *Ras* (46-55%) and *BRAF* (12-17%) genes were identified, while in the ATC only mutations of *Ras* (6-52%) and *BRAF* (25-29%) genes were reported. In more advanced stages of thyroid carcinogenesis, alterations of PI3K and PTEN were also found (Paes and Ringel 2008). The molecular alteration that characterizes ATCs compared with WDTCs is the mutation of the p53 tumor suppressor gene. Almost all ATCs show inactivation of p53 and is therefore highly probable that it is the deficiency of p53, combined with mutations of oncogenes such as *Ras* and *BRAF*, to determine the high proliferative index and high aggressiveness of this tumor. Indeed, p53 mutations are common to both PDTCs (17-38%) and ATCs (67-88%), but rare or absent (0-9%) in WDTCs (Ito et al. 1992; Donghi et al. 1993; Fagin et al. 1993). Even though critical molecular mechanisms of thyroid carcinogenesis have been clarified, other molecular steps of neoplastic progression still need to be investigated.

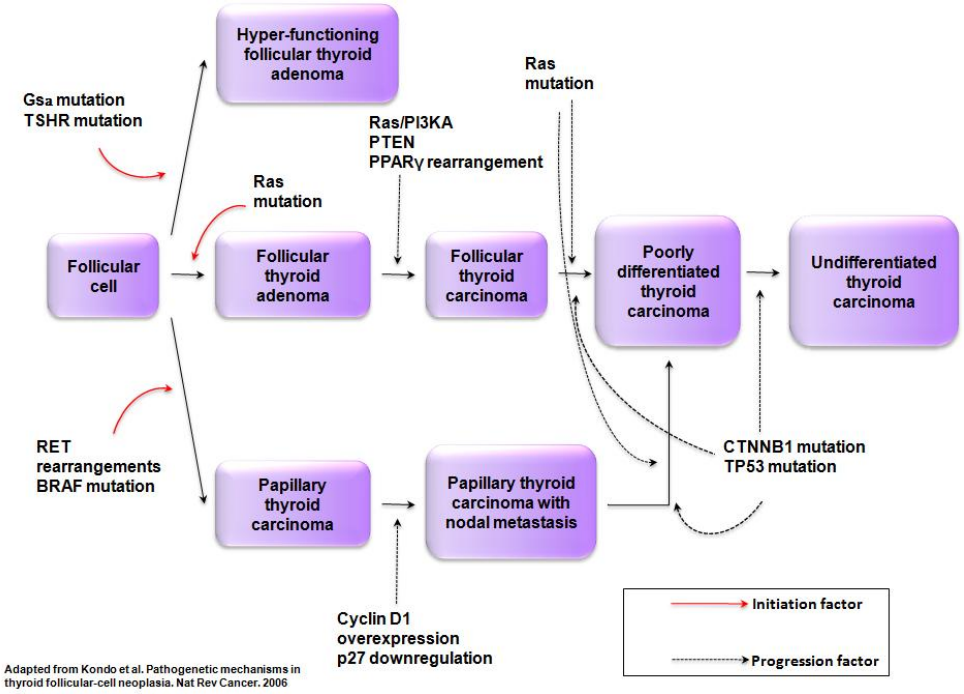

Figure 5. Model of multi-step carcinogenesis of thyroid tumors. Three distinct pathways have been proposed for the initiation of thyroid tumors including hyper-functioning follicular thyroid adenoma, FTC and PTC. Genetic defects that result in activation of RET or BRAF represent frequent early initiating events associated with radiation exposure that leads to PTC development. Ras mutations represent frequent early initiating events, associated with iodine deficiency, that lead to FTC development. By contrast, most PDTCs and ATCs are considered to derive from pre-existing well-differentiated thyroid carcinoma through the accumulation of additional genetic events that include nuclear accumulation of β-catenin (encoded by CTNNB1) and p53 inactivation.

1.8 MicroRNA

MicroRNAs (miRNAs or miRs) are endogenous small non-coding single-stranded RNAs of ~22 nucleotides in length, first described in 1993 when Ambros and colleagues discovered a gene, *Lin4*, that affected the development in *Caenorhabditis Elegans* (Lee et al. 1993). After these seminal findings, the cloning and characterization of small, ~22 nucleotides long, members of the non-protein coding RNA family, has led to the identification of more than 1300 miRNAs, for which the main feature is to negatively regulate the gene expression at post-transcriptional level (Iorio and Croce 2009; Croce 2009; Pallante et al. 2014).

MiRNA genes are evolutionarily conserved and may be located either within the introns or exons of protein-coding genes (70%) or in intergenic areas (30%). Most of the intronic or exonic miRNAs are oriented in sense with their host gene, suggesting that they are transcribed in parallel with their host transcript, while others are transcribed from intergenic regions or gene deserts comprising independent transcription units. Frequently, miRNAs are located in clusters and transcribed as polycistrons, therefore showing similar expression patterns (Garzon et al. 2009; Nikiforova et al. 2009). Generally, they are transcribed by Polymerase II into long primary transcripts, up to several kilobases, called pri-miRNA, that are subsequently processed in the nucleus by the enzyme Drosha to become ~70-nt-long precursor strands, or pre-miRNA (Figure 6). Subsequently, this precursor is exported by exportin 5 to the cytoplasm, where it is bound to the RNAse Dicer and to the RNA-induced silencing complex (RISC). RISC is composed of the transactivation-responsive RNA binding protein (TRBP) and Argonaute 2 (Ago2). First, Ago2 cleaves the pre-miRNA 12 nt from its 3' end (forming Ago2-cleaved precursor miRNA) and then the Dicer cleaves the Ago2-cleaved precursor miRNA into a mature ~22 nt miRNA duplex. While the active or mature strand is retained in RISC, the passenger strand is removed and degraded (Garzon et al. 2009). At this point, the active and mature miRNAs can negatively regulate their targets in one of two ways depending on the degree of complementarity between the miRNA and its target. MiRNAs that bind with perfect or nearly perfect complementarity to protein coding mRNA sequences induce the RNA-mediated interference (RNAi) pathway. Briefly, mRNA transcripts are cleaved by ribonucleases in the miRNA-associated, multiprotein RNAinduced- silencing complex (miRISC), which results in the degradation of target mRNAs. This mechanism of miRNA-mediated gene silencing is commonly found in plants, but miRNA-directed mRNA cleavage has also been shown to occur in mammals. However, most animal miRNAs are thought to use a second mechanism of gene regulation that does not involve the cleavage of their mRNA targets. These miRNAs exert their regulatory effects by binding to imperfect complementary sites within the 3′ untranslated regions

(UTRs) of their mRNA targets, and they repress target-gene expression post-transcriptionally, at the level of translation, through a RISC complex that is similar to, or possibly identical with, the one that is used for the RNAi pathway. Consistent with translational control, miRNAs that use this mechanism reduce the protein levels of their target genes, but the mRNA levels of these genes are barely affected. However, recent findings indicate that miRNAs that share only partial complementarity with their targets can also induce mRNA degradation, but it is unclear if translational inhibition precedes destabilization of the gene targets in these cases (Esquela-Kerscher and Slack 2006). The interplay between miRNAs and mRNAs constitutes a powerful regulatory network that is involved in several fundamental processes, such as cell growth and differentiation, development, metabolic regulation and apoptosis as well as in pathological processes, including cancer in a range of organisms, such as *C. Elegans*, plants, *D. Melanogaster* and mammals (including humans) (Croce 2009; Pallante et al. 2014). This regulatory network is extremely complex; in fact, in humans a single miRNA is able to regulate several mRNAs, and one gene can be under the control of multiple miRNAs (Pallante et al. 2014).

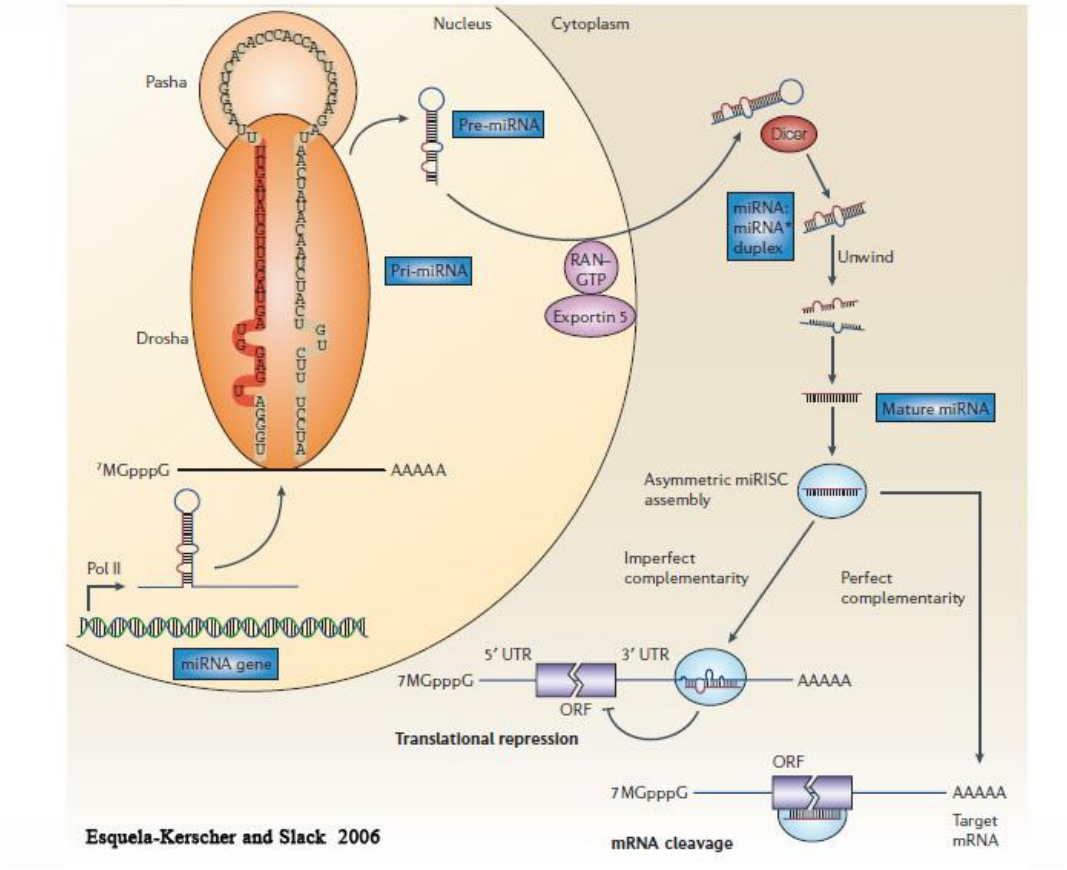

Figure 6. The biogenesis of microRNAs. MicroRNA (miRNA) genes are transcribed by RNA Polymerase II in the nucleus to form large pri-miRNA transcripts, then processed by Drosha and its co-factor, Pasha, to release the ~70-nucleotide pre-miRNA precursor product (the mature miRNA sequence is shown in red) RAN–GTP and Exportin 5 transport the pre-miRNA into the cytoplasm. Subsequently, Dicer processes the pre-miRNA to generate a transient ~22- nucleotide miRNA duplex. This duplex is then loaded into the miRISC complex, where the mature single-stranded miRNA (red) is preferentially retained. The mature miRNA then binds to complementary sites in the mRNA target to negatively regulate gene expression in one of two ways that depend on the degree of complementarity. The full complementarity leads to mRNA cleavage, while the imperfect complementarity leads to translational repression (Esquela-Kerscher and Slack 2006).

1.9 MicroRNA in thyroid cancer.

Increasing evidences have revealed the involvement of miRNAs in human malignancies. The deregulation of miRNAs expression is believed to be an important regulator of tumor development and progression. Due to its repression effect, deregulation of specific miRNAs could lead to the repression of tumor suppressor gene and/or increase of oncogene expression. Consequently, these molecular changes favor cell proliferation, differentiation and apoptosis (Li et al. 2013). Like a protein-coding gene, miRNAs can act either as tumor suppressors or oncogenes; in fact, their loss or gain of function can initiate or contribute to the malignant transformation of a normal cell. Moreover, miRNA expression profiles resulted in being different not only between tumors and normal tissues, but also between different subtypes of tumors and between primary tumors and metastatic tumors (Li et al. 2013; Pallante et al. 2014). Several studies have analyzed miRNA expression in numerous and different types of thyroid tumors, evidencing a miRNA deregulation in cancer tissues compared to their normal counterpart (Pallante et al. 2006; He et al. 2005; Takakura et al. 2008). In thyroid tumors 32% of all known human miRNAs resulted upregulated and 38% downregulated with more then 2-fold change as compared to normal tissues (Nikiforova et al. 2009). Moreover, the miRNA expression profile presents a significant variability between different kinds of thyroid cancers, even if they originate from the same type of thyroid cells (Nikiforova et al. 2008). In fact, papillary tumors, conventional follicular tumors (adenomas and carcinomas), and oncocytic follicular tumors (adenomas and carcinomas) revealed separate clusters. Less differentiated tumors (PDTCs and ATCs) did not show individual clusters and were scattered within the PTC and FTC clusters or separately, supporting the concept of stepwise progression and dedifferentiation of thyroid tumors (Nikiforova et al. 2009).

In the last years, several studies by the group of Prof. Fusco, a major contributor in this field, demonstrated that several miRNAs have a crucial role in thyroid cancer. In particular, they showed that: in PTCs, microRNAs -221 and -222 are up-regulated and play a key role into neoplastic transformation by targeting p27 (Kip1) protein, a key regulator of cell cycle (Visone et al. 2007a); in the ATCs there is a significant decrease in miR-30d, miR-125b miR-26a and miR-30a-5p, in comparison to normal thyroid tissue (Visone et al. 2007b); in FTCs, miR-191, miR-142-3p and Let-7a are downregulated, playing a role in thyroid neoplasias of the follicular histotype, by targeting proteins involved in cell cycle, Hox gene expression and adhesion, such as CDK6, ASH1L, MLL1 and FXYD5 (Colamaio et al. 2011; 2012; 2015). Moreover, the down-regulation of miR-25 and miR-30d could contribute to the process of thyroid cancer progression, leading to development of anaplastic carcinomas, targeting the polycomb protein Enhancer of Zeste Homolog 2 (EZH2) (Esposito et al. 2012b); in thyroid adenomas, goiters and

carcinomas, miR-1 expression is drastically down-regulated, in comparison with normal thyroid tissues, resulting in enhancement of proliferation and cell migration, due to the miR-1 capacity to target cyclin D2, the receptor for the stromal cell derived factor-1 (SDF-1)/CXCL12 chemokine and its ligand SDF-1/CXCL12 (Leone et al. 2011); up-regulation of miR-146b and down-regulation of miR-200b contribute to the cytotoxic effect of HDAC inhibitors on Ras-transformed thyroid cells (Borbone et al. 2013).

Recent studies have demonstrated that in FRTL5, well characterized normal rat thyroid epithelial cells, extensively used to study the molecular mechanisms of neoplastic transformation *in vitro*, the oncogene *Ras* is able to drive cell transformation toward an undifferentiated phenotype, resembling that of ATC and characterized by a high migratory and invasive aptitude (De Vita et al. 2005; Frezzetti et al. 2011; De Menna et al. 2013). Using a tamoxifen-inducible construct in these cells, De Vita and co-workers demonstrated that activation of oncogenic Ras is able to induce aberrant expression of miRNAs (Landgraf et al. 2007). Among the top scored up-regulated miRNAs, there was miR-21, which they showed to play an important role in oncogenic Ras-induced cell proliferation (Frezzetti et al. 2011), but other miRNAs, including miR-29b, appears significantly up-regulated downstream of oncogenic Ras (Landgraf et al. 2007).

At the moment, the exact biological roles of miRNAs in thyroid carcinogenesis remain to be fully elucidated but it seems reasonable that the distinctive pattern of miRNA expression in thyroid tumors compared to normal thyroid tissue may be useful in diagnosis and/or therapy of thyroid neoplasia and that different miRNA expression patterns in different types of thyroid tumors could be useful tools for their classification (Table 1).

Table1. MiRNAs deregulated in thyroid cancer (Pallante et al. 2014)

Upregulated	Downregulated
Papillary thyroid carcinoma	
miR-181a, miR-221, miR-222, miR-146, miR-155, miR-220, miR-21	miR-26a-1, miR-345, miR-138, miR-219
miR-221, miR-222, miR-181b, miR-213, miR-20	Let7f, miR-142, miR-140, miR-199, miR-151
miR-221, miR-222, miR-21, miR-31, miR-172, miR-34a, miR-213, miR-181b, miR-223, miR-224	miR-218, miR-300, miR-292, miR-345, miR-30c
	miR-30, miR-26, Let7
miR-187, miR-221, miR-222, miR-146b, miR-155, miR-122a, miR-31, miR-205, miR-224	miR-1
miR-221, miR-222, miR-200a, miR-200b, miR-200c, miR-141	miR-191
miR-146b, miR-146-3p, miR-146-5p, miR-221, miR-222, miR-222-5p, miR-375, miR-551b, miR-181-2-3p, miR-99b-3p	
miR-146a, miR-146b, miR-221, miR-222	
Follicular thyroid carcinoma	
miR-197, miR-346	
miR-96, miR-146b, miR-155, miR-187, miR-181b, miR-182, miR-200a, miR-221, miR-222, miR-224	miR-191, Let7a
miR-221, miR-222, miR-96, miR-182, miR-597	miR-199b-5p, miR-144, miR-199b-3p, miR-199a-5p, miR-144
miR-182, miR-183, miR-221, miR-222, miR-125a-3p	miR-542-5p, miR-574-3p, miR-455, miR-199a
miR-21	
Anaplastic thyroid carcinoma	
miR-21	miR-25, miR-30d, miR-125b, miR-26a, miR-30a-5p
miR-17-5p, miR-17-3p, miR-18a, miR-20a, miR-92-1	miR-200, miR-30
miR-146a	miR-1, miR-138

1.10 miR-23b and miR29b in cancer

Structure, function, and regulation of miR-29b are highly conserved in human, mouse and rat and contains miR-29b-1 and miR-29b-2 (Liu et al. 2014). MiR-29b-1 is transcribed into the same primary transcript from a locus at chromosome 7q32 and separated by 652 bases, which coincides with a common fragile site (FRA7H), while miR-29b-2 is from the same transcript, located on 1q32, separated by 507 bases; since the mature miR-29 family members share the same seed sequence, which determines the target sequences, the genes that miR-29s regulate are nearly the same (Wang et al. 2013). In the last years, several studies reported that miR-29b was highly expressed in normal tissues and down-regulated in different types of cancer, including gastric cancer, prostate cancer, breast cancer, lung cancer and glioblastomas, affecting several biological processes, such as proliferation, apoptosis, invasion and metastasis, therefore supporting, a tumor suppressor role (Wang et al. 2013). Gene expression analysis of miR-29b-overexpressing acute myeloid leukemia (AML) cells showed the suppressive effect on cell cycle regulatory factor CDK6 (Liu et al. 2014; Garzon et al., 2009). Down-regulation of miR-29b targets CDK6 directly and leads to up-regulation of CDK6 in mantle cell lymphoma (MCL). Overexpression of cyclin D1 was always found in MCL, which leads to the acceleration of G1-S cell-cycle progression. MiR-29b further attenuates cell-cycle progression and suppresses tumor cell proliferation, which demonstrated the cooperation between CDK6 and cyclin D1 (Zhao et al. 2010). The miR-29b has been shown to be correlated with good prognosis in patients with AML, and functions as a tumor suppressor in leukemic blasts by targeting proliferation pathways, apoptosis and cell cycle (Garzon et al. 2008). Moreover, in cholangiocytes/cholangiocarcinoma, miR-29b targeted MCL1, a pro-survival member of the Bcl2 family protein, and sensitized tumor cells treated with tumor necrosis factor-related apoptosis-inducing ligand (TRAIL) to apoptosis (Mott et al. 2007). Very recently, it has been shown that miR-29s (including miR-29a-c) inhibit the malignant behavior of glioblastoma cells by targeting CNMT3A and 3B (Xu et al. 2015). Finally, it has been reported that miR-29b is involved in epithelial-mesenchymal transition (EMT), a process by which epithelial cells lose their cell polarity and cell-cell adhesion, and gain migratory and invasive properties to become mesenchymal stem cells. In fact, miR-29b directly targets Snail to inhibit tumor metastasis in prostate cancer cells. (Ru et al. 2012). Consistently, exogenous expression of miR-29b inhibits Mcl-1 and MMP-2 protein expression, and affects metastatic cascade including tumor invasion, motility, cellular survival, and proliferation (Ru et al. 2012).

On the other hand, a number of papers describes an oncogenic role for miR-29b. In bladder urothelial cancer cells, miR29b-1 and miR-29c levels were higher than normal urothelial cells, which growth was suppressed by Knockdown of both

miRNAs (Xu et al. 2013). Furthermore, Pekarsky and co-workers demonstrated a crucial role for miR-29b in indolent Chronic Lymphoid Leukemia (CLL), showing it was up-regulated in indolent CLL compared to normal tissues and induces indolent CLL when overexpressed in mice (Pekarsky et al. 2006; Santanam et al. 2010). Finally, in thyroid cells, miR-29b up-regulation was induced upon a stimulus to proliferate and its overexpression inhibited thyroid cell growth, as further detailed below (Leone et al. 2012).

miR-23a and miR-23b belong to the miR- 23a/24/27a cluster, which is located on chromosome 19p13.12 and the miR-23b/27b/24-1 cluster which is located on chromosome 9q22.32, respectively (Ma et al. 2014b). Several studies reported that miR-23s are involved in acute lymphoblastic leukemia (ALL), AML, glioblastoma, hepatocellular carcinoma, gastric cancer, pancreatic cancer and uterine leiomyoma (Ma et al. 2014b; Donadelli et al. 2014; Shang et al. 2014; Cao et al. 2012; Cheng et al. 2014). As for miR-29b, also miR-23b has a dual role in carcinogenesis. In fact, it has been found to be either up-regulated or down-regulated in tumors compared with normal tissues, functioning as either tumor promoter or tumor suppressor (Li et al. 2013). In a variety of human tumors, downregulation of miR-23b have been demonstrated to promote cancer progression. For example, Li and co-workers (2014) reported that decreased expression of miR-23b was significantly correlated with tumor aggressiveness and poor prognosis of patients with epithelial ovarian cancer and could suppress ovarian cancer progression by targeting runt-related transcription factor-2; another group have demonstrated that miR-23b was involved in cytoskeletal remodelling through the enhancement of cell-cell interactions, reduction of cell motility and invasion during cancer progression (Pellegrino at al. 2013); Majid et al. (2012) have revealed that miR-23b expression was dramatically reduced in bladder cancer cell lines and tumor tissues compared to the non-malignant counterparts, and conferred proliferative advantages, cell migration and invasion traits to these cells by regulating the expression of Zeb1, a direct target of this miRNA. Although the role of miR-23b as a tumor suppressor has been well established, many studies demonstrated that it can also acts as an oncomir. For example, it has been observed that the suppression of miR-23b could inhibit tumor survival, induce apoptosis and inhibit glioma invasion (Chen et al. 2012); Tian et al. (2013) showed that a combination of four miRNAs, including miR-23b, could promote prostate cancer cell proliferation by regulating PTEN and its downstream signals. In human gastric cancer, there has been only one report indicating that miR-23b was one of 16 miRNAs upregulated in gastric cancer tissues, implying that this miRNA might be an oncomir for this cancer (Li et al. 2011).

Both miR-23b and miR-29b have been recently reported as involved in thyroid cell proliferation (Leone et al. 2012). Indeed, Leone and co-workers demonstrated that treatment of rat thyroid cells (PC Cl3) with TSH, which induces entry into S

phase of the cell cycle, is associated with the up-regulation of mir-23b and miR-29b. The expression level of these miRNAs increases as early as 30 min after TSH stimulation and lasts for at least 4 h before returning to the levels observed in quiescent cells (Figure 7). The authors also showed that both these miRNAs increase the proliferation rate of thyroid cells, leading to an increased accumulation of the PC Cl 3 cells in the S phase of the cell cycle (Figure 8). Finally, they reported experiments *in vivo* confirming that the up-regulation of miR-23b and miR-29b might have a role in thyroid cell proliferation. Indeed, both these miRNAs were found overexpressed in experimental murine PTU-induced models and in human goiters (Figure 9) (Leone at al. 2012).

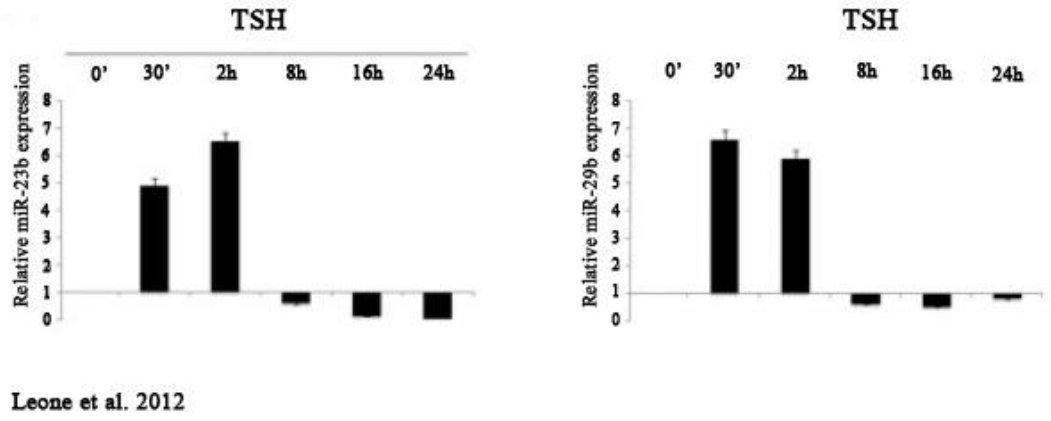

Figure 7. miR-23b, and miR-29b are up-regulated by TSH. qRT-PCR results showing expression of miR-23b (left panel) and miR-29b (right panel) in PC Cl3 rat thyroid cells at different time points of TSH treatment after starvation compared to untreated cells (Leone et al. 2012).

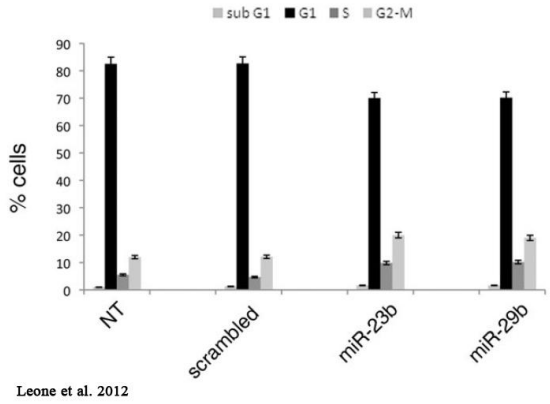

Figure 8. Flow cytometric analysis of PC Cl 3 cells untransfected (NT) or transfected with miR-23b, miR-29b, or the scrambled oligonucleotide. After transfection, the DNA of the transfected PC Cl 3 cells was analyzed 72 h later by flow cytometry after propidium iodine staining. The transfection efficiency was about 85%. Each *bar* represents the mean value _ SE from three independent experiments performed in triplicate (P _ 0.05 compared with the scrambled oligonucleotide) (Leone et al. 2012).

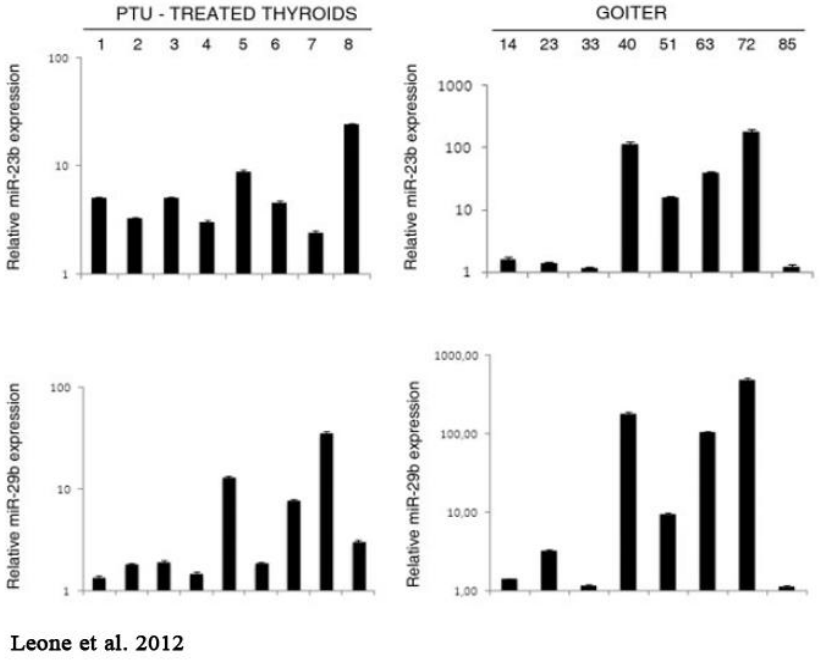

Figure 9. Up-regulation of miR-23b and miR-29b experimental and human thyroid goiters compared to normal thyroid tissues. (Left Panels) qRT-PCR showing the relative expression of miR-23b and miR-29b in goiters from a cohort of 8 mice treated with propylthyouracil, compared to thyroids from untreated mice. (Right Panels) qRT-PCR showing the relative expression of miR-23b and miR-29b in a cohort of 8 human goiters compared to normal thyroid tissue. The relative expression values indicate the relative change in the expression levels between goiters and normal thyroids, assuming that the value of normal thyroid tissue is equal to 1. The range of variability of miR-23b and miR-29b in normal thyroid tissues was less than 10% (Leone et al., 2012).

2. AIM OF THE STUDY

Carcinoma of the thyroid gland is one of the most frequent malignancies of the endocrine system and its incidence has been steadily increasing in many regions of the world. Among the most frequent genetic alterations occurring in thyroid transformation, oncogenic mutations of *Ras*-family genes (K-Ras H-Ras, and N-Ras) have been identified in all types of thyroid malignancies, leading to the suggestion that they are an early event in thyroid tumorigenesis; furthermore, mutated Ras genes are detected with higher frequency in poorly differentiated and undifferentiated thyroid cancers, suggesting that they could contribute to the partial or complete loss of differentiation, characteristic of the more aggressive thyroid cancers. Mutated Ras is also able to induce aberrant expression of miRNAs during the transformation of thyroid epithelial cells.

The POZ/BTB and AT-hook-containing zinc finger protein 1 (PATZ1) is a transcription factor whose expression is frequently de-regulated in human cancer; in particular PATZ1 results down-regulated in thyroid cancer and its restoration in human thyroid cell lines inhibits their malignant behaviors, including *in vitro* proliferation, anchorage-independent growth, migration and invasion, as well as *in vivo* tumor growth.

The first aim of my study was to understand how PATZ1 is downregulated in thyroid cancer focusing on microRNAs. Then, I intended to explore the relationship between PATZ1 and Ras-induced thyroid transformation, whether PATZ1 downregulation is a direct consequence of Ras oncogenic activation, how PATZ1 is downregulated by activated Ras and whether down-regulation of PATZ1 plays a causal role in Ras-induced thyroid transformation.

Elucidation of the molecular pathways downstream of oncogenic Ras, which are crucial for thyroid transformation, will help to find new therapeutic targets in thyroid cancer carrying Ras mutations.

3. MATERIALS AND METHODS

3.1 Bioinformatic analysis

For the identification of PATZ1 potentially targeted miRNAs it has been used on-line available tool miRanda (www.microrna.org). This tool is based on a combination of specific-base pairing rules and conservational analysis to score possible match between 3'UTR of specific genes with several miRNAs, using a dynamic programming algorithm weighted to favour 5' complementarity to enumerate initial target sites.

3.2 Cell cultures

Continues rat thyroid cell lines FRTL5 and FRTL5-Ras were cultured in Ham's F-12 medium and Coon's modification supplemented with 5% CS, 5% L-glutamine, 5% penicillin/streptomycin (GIBCO-BRL) and in the presence of a mix containing six growth factors, 6H (10 nM TSH, 10 nM hydrocortisone, 100 nM insulin, 5 mg/ml transferrin, 5 nM somatostatin, and 20 μg/ml glycyl-histidyl-lysine), in a 5% CO2 atmosphere. Human embryonic kidney HEK293 cells were cultured in DMEM supplemented with 10% FBS, 5% L-glutamine and 5% penicillin/streptomycin (GIBCO-BRL) in a 5% CO2 atmosphere. The selected cell clones of FRTL5-Ras cells and the control cells were cultured in Ham's F-12 medium and Coon's modification supplemented with 5% CS, 5% L-glutamine, 5% penicillin/streptomycin (GIBCO-BRL) and in the presence of a mix containing 6H, in a 5% CO2 atmosphere.

3.3 Transfections and plasmids

HEK293 transfections were performed by Lipofectamine 2000 (Invitrogen) according to manufacturer's instruction, with 100nM Scramble, 100nM miR-23b and 100nM miR-29b miRNA precursors (Ambion, Austin, TX) together with PGL-3-CTRL vector containing the 3'UTR of the PATZ1 variants 1/2 cloned downstream the firefly luciferase gene. For the PATZ1-3'UTR luciferase reporter construct, the 1098bp 3'-UTR region of *PATZ1* gene, variant 1/2, including binding sites for miR-32b and miR-29b was amplified from HEK293 cells DNA by using the following primers: Fw PATZ1 3'UTR V1/2: 5'-ATATGATATCGGCAGCTGCTGTGTCC-3' and Rev PATZ1 3'UTR V1/2 5'-

GCATGATATCGTACAAACATTTTTAAT-3'. The amplified fragment was cut with EcoRV and cloned into pGL3-Control firefly luciferase reporter vector (Promega, Madison, Wisconsin, USA) at the XbaI site. For stable transfection FRTL5-Ras cells were transfected by Fugene6 (Roche) according to manufacturer's instruction with HA-PATZ1 plasmid encoding for PATZ1 variant 4 or the empty vector pCEFL-HA, both expressing the gene for the resistance to neomycin. Stable transfectants were clonally selected in medium with 1μg/ml neomycin (G418) (Life Technologies) for 10 days, and cell clones were screened for PATZ1 expression by qRT-PCR and Western blot analysis.

3.4 Protein extraction, Western blotting and antibodies

Cells were lysed in buffer containing 1% Nonidet P-40, 1 mmol/liter EDTA, 50 mmol/liter Tris-HCl (pH 7.5), and 150 mmol/liter NaCl supplemented with Complete protease inhibitors (Roche Applied Science). Total proteins were resolved in a 8% polyacrylamide gel under denaturing conditions and transferred to nitrocellulose filters for Western blot analyses. Membranes were blocked with 5% BSA in TBS and incubated with the primary antibodies. Membranes were then incubated with the horseradish peroxidase–conjugated secondary antibody (1:3.000) and the reaction was detected with a Western blotting detection system (enhanced chemiluminescence; GE Healthcare). The primary antibodies used are anti-PATZ1 antibody (polyclonal antibody raised against a conserved peptide recognizing all PATZ1 isoforms of rat, mouse and human origin). To ascertain that equal amounts of protein were loaded, the membranes were incubated with antibodies against the anti-vinculin protein (sc-7649) (Santa Cruz Biotechnology, Santa Cruz, CA).

3.5 RNA extraction and qRT-PCR analysis

Total RNA was isolated using TRI-reagent solution (Sigma, St Louis, MO, USA) and treated with DNase (Invitrogen). Reverse transcription was performed according to standard procedures (Qiagen, Valencia, CA). qRT-PCR analysis was performed using the Power SYBR Green PCR Master Mix (Applied Biosystems) according to manufacters' instructions with the following primer sequences to amplify the indicated genes:

hPATZ1all-V-Fw: 5'-TACATCTGCCAGAGCTGTGG-3'
hPATZ1all-V-Rev: 5'-TGCACCTGCTTGATATGTCC-3'
hG6PD-Fw: 5'-GATCTACCGCATCGACCACT-3'
hG6PD-Rev: 5'-AGATCCTGTTGGCAAATCTCA-3'

To calculate the relative expression levels we used the 2-ΔΔCT method (Livak and Schmittgen, 2001). Primers specific for the glucose-6-phosphate dehydrogenase (G6PD) were used for normalization of qRT-PCR data.

3.6 Luciferase assay

For Luciferase assays, the pCMV-Renilla plasmid (Promega, Mannheim, Germany) was co-transfected with 3'UTR region of PATZ1 Variant 1/2. Luciferase and Renilla activities were assessed with the Dual-Light Luciferase system (Promega), according to the manufacturer's protocol, 72 h after the transfection. Luciferase activity was normalized for the Renilla activity.

3.7 Proliferation assay

For the growth curves the cells (3×10^4 cells/dish) were plated in a series of 6-cm culture dishes and counted daily for 5 consecutive days through the Bürker chamber. The count was performed in the presence of Trypan blue, a dye that penetrate in cells that have lost membrane integrity and which shows, therefore, dying cells.

3.8 Flow cytometric analysis

2 $x10^5$ cells were plated and analyzed after 24h under normal culture conditions by flow cytometry Briefly, cells were washed once with PBS, and fixed for 2 h in cold ethanol (70%). Fixed cells were washed once in PBS and treated with 40 μg/ml ribonuclease A in PBS for 30 min. They were then washed once in PBS and stained with 50 μg/ml propidium iodide (Roche, Indianapolis, IN). Stained cells were analyzed with a flow cytometer (Accuri™ C6 flow cytometer, BD Biosciences, East Rutherford, New Jersey). The data were analyzed using a BD Accuri C6 software.

3.9 Migration assays

To detect the changed capacity of tumor cell migration, we performed a wound-healing assay. Specifically, cells were digested with 0.25% trypsin and adjusted for a concentration of 5×10^5 cells/ml of cell suspension, and then inoculated into 60mm plates and cultured at 37°C overnight. In the next day, cells were cultured

in serum-free medium, reached approximately 95–100% confluence, and cell monolayer was wounded by 20 μl tips. The cells were incubated for 96 h. At 0h, 24h, 48h, 72h, and 96h, cells were photographed under an inverted microscope. The migration assay was conducted using plates Transwell cell culture chambers according to described procedures (Corning Costar Corp., Cambridge, MA). Briefly, confluent cell monolayers were harvested with trypsin/EDTA, centrifuged at 1.200 rpm for 5 min, resuspended in medium without serum and without 6H and plated (5×10^4 cells) to the upper chamber of a polycarbonate membrane filter of 8 μM pore size. The lower chamber was filled with complete medium. The cells were then incubated at 37°C in a humidified incubator in 5% CO2 for 24h. Non migrating cells on the upper side of the filter were wiped off and migrating cells on the reverse side of the filter were stained with 0.1% crystal violet in 20% methanol for 30 min, washed in PBS 7.4 (137 mM NaCl; 2.7 mM KCl, 4.3 mM NaH2PO4), photographed and counted.

3.10 Soft agar colony forming assay

For soft agar assays 7 ml of mixture of serum supplemented medium and 0.5% agar were added in a 60-mm culture dish and allowed to solidify (base agar). Next, on top of the base layer was added a mixture of serum supplemented medium and 0.35% agar (total of 2 mL) containing $2x10^5$ of FRTL5, FRTL5-Ras-ctrl and FRTL5-Ras-PATZ1 cells (obtained as described before) and allowed to solidify (top agar). Subsequently, the dishes were kept in culture incubator maintained at 37^0C and 5% CO^2 for 40 days to allow for colony growth. After 40 days the colonies were counted and photographed.

3.11 Statistical analysis.

Student's t-test was used to determine the significance for quantitative experiments. Error bars represent the standard errors (SE) of the average. Statistical significance for all the tests, assessed by calculating the p-value, was <0.05.

4. RESULTS

4.1 Identification of predicted PATZ1-targeting miRNAs

In order to identify miRNAs potentially able to down-regulate the expression of PATZ1 protein, we used the www.microRNA.org web system that is based on the miRanda application (Hohn et al. 2005) and uses the mirSVR predicted target site scoring method, giving a downregulation score and identifying a significant number of experimentally determined non-canonical and non-conserved sites (Betel et al. 2010). We searched miRNAs targeting each of the transcriptional variants of PATZ1, that share some similarities and diversity. In particular, Variant 1 and Variant 2 share a common 3'-UTR (NM_014323.2/NM_032050.1); Variant 3 includes 372 additional nucleotides (NM_032052.1) with respect to Variant 1 and 2. Conversely, PATZ1 transcript Variant 4 has a completely different 3'-UTR (NM_032051.1), both in terms of sequence and length. The analysis identified several miRNAs as potential PATZ1-targeting miRNAs (Table 2). The targeting sites of these PATZ1-targeting miRNAs on the 3'-UTR of PATZ1 are extremely conserved among different species, as resulted by the PhastCons score (Figure 10).

Table 2 PATZ1-targeting miRNAs

Variants 1/2	Variant 3	Variant 4
miR-22	miR-1271	miR-365
miR-491-5p	miR-96	miR-150
miR-216b	miR-136	miR-18a/b
miR-361-5p	miR-26a/b	miR-31
miR-544	miR-1297	miR-138
miR-339-5p	miR-185	miR-491-5p
miR-142-3p	+ all V.1-2 miRs	miR-107
miR-29a/b/c		miR-103
miR-376a/b		miR-340
miR-24		miR-590-3p
miR-421		
miR-653		
miR-134		
miR-200b/c		
miR-429		
miR-495		
miR-590-3p		
miR-448		
miR-153		
miR-490-3p		
miR-23a/b		
miR-383		
miR-543		

Due to its described up-regulation in thyroid cell proliferation and transformation (Leone et al. 2012; Landgraf et al. 2007), we focused our attention on miR-23b and miR-29b to validate their inhibitory effect on the 3'-UTR of the PATZ1 Variants 1 and 2. As shown in Figure 10, Panels A and B, in which the miR/PATZ1 alignment is shown, the mirSVR score is -0.1870 for miR-29b and -0.1391 for miR23b, predicting a significant down-regulation of PATZ1 protein and/or mRNA.

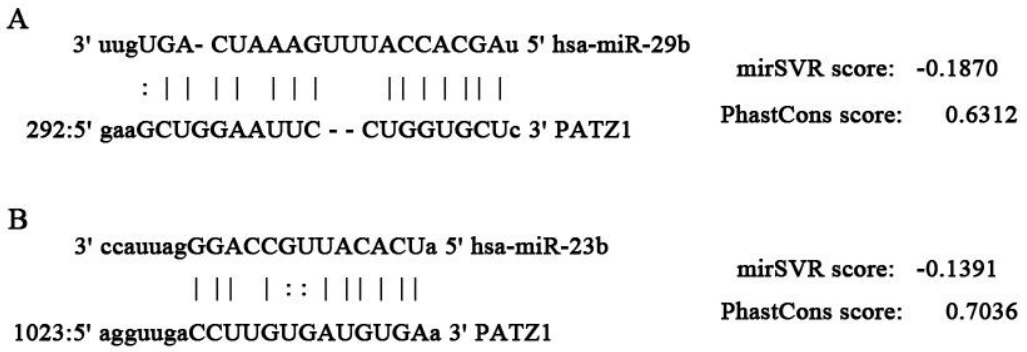

Figure 10. Representation of alignment between miR-23b/miR-29b and *PATZ1*. Schematic representation of alignment between miR-29b (A) and miR-23b (B) and 3'UTR of *PATZ1* variant 1/2. For each alignment is reported the mirSVR and Phast Conserved scores, predicting down-regulation and conservation, respectively.

4.2 PATZ1 is a direct target of miR-23b and miR-29b

In order to validate the prediction derived by the bioinformatic research, we transfected HEK293 cells, a human cell system which expresses significant levels of all Variants of PATZ1, with 100nM of either miR-23b or miR-29b synthetic miRNA precursor and evaluated PATZ1 protein levels by western blotting after 72 hours, comparing the results with those obtained in cells transfected with the same amount of a scramble synthetic miRNA precursor. As shown in Figure 11, Panel A, PATZ1 protein levels were significantly reduced in cells transfected with either miR-23b or miR-29b in comparison with the cells transfected with the scramble oligonucleotide. Moreover, to study if these two miRNAs also affected the expression of PATZ1 mRNA, quantitative real-time PCR (qRT-PCR) experiments was performed. The results indicate that miR-23b and miR-29b did not affect the expression of PATZ1 mRNA (Figure 11, Panel B). Finally, in order to

demonstrate that miR-23b and miR-29b target directly and, consequently, inhibit PATZ1 protein, we performed luciferase assays. In particular, we used a PGL-3-CTRL vector containing the 3'-UTR of the PATZ1 Variants 1-2 cloned downstream the firefly luciferase gene. This reporter vector was transfected in HEK293 cells along with 100nM of synthetic miRNA precursors or the scramble control, and luciferase activity was assessed 72h after the transfection. As shown in Figure 11, Panel C, overexpression of either miR-23b or miR-29b significantly reduced luciferase activity in comparison with the same amount of scramble control. All together these results validate both miR-23b and miR-29b as direct down-regulators of PATZ1 expression.

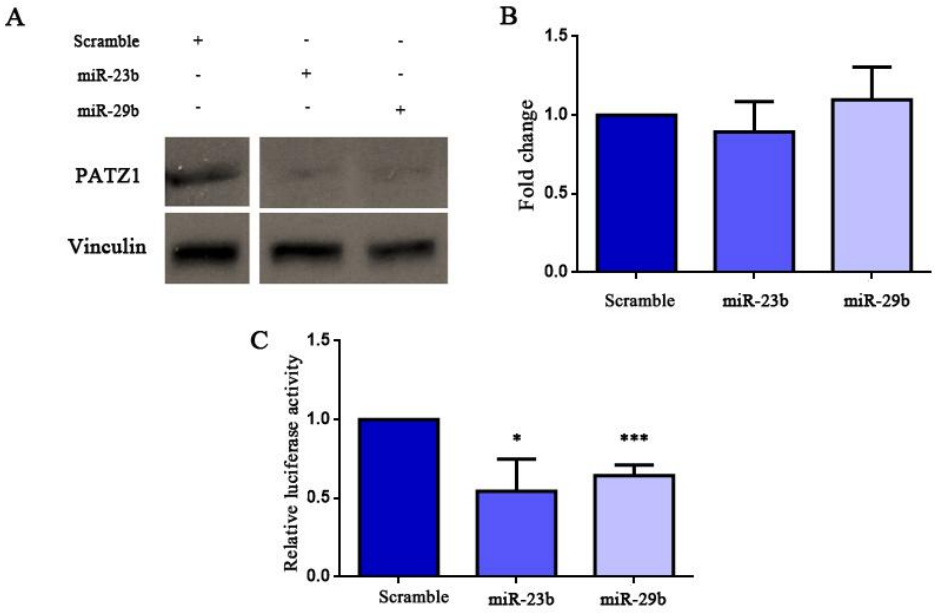

Figure 11. Effects of miR-23b and miR-29b on PATZ1. (A) 72h after transfection with miR-23b or miR-29b, PATZ1 protein expression significantly decreases, compared with the scramble control, as assessed by western blot. (B) qRT-PCR of RNA samples derived from the same experiment as in B, showing that the expression of PATZ1 mRNA does not change following transfection of either miR-23b or miR-29b. (C) In presence of either miR-23b or miR-29b the luciferase activity of a construct carrying the 3'UTR of PATZ1 Variant 1/2 significantly decreases in comparison with that of cells transfected with the scramble control. Data in B and C show mean values $\pm$ SE of three independent experiments performed in duplicate or triplicate, respectively. *, $P < 0.05$; *** $P < 0.001$, as assessed by Unpaired T test. Vinculin was used for Western Blot control; G6pd was analyzed for qRT-PCR loading control and luciferase activity was normalized for the Renilla activity.

4.3 miR-23b and miR-29b target PATZ1 in thyroid cells

To verify the effect of miR-23b and miR-29b on PATZ1 expression in a thyroid cell system, we used PC Cl3 rat thyroid cell line that keeps *in vitro* all the markers of thyroid cell differentiation, and represents an excellent system to study the mechanism regulating thyroid cell proliferation, which requires TSH for their growth (Fusco et al. 1987). Since it was previously reported that in PC CL3 cells miR-23b and miR-29b are up-regulated following stimulation with TSH (Leone et al. 2012), we analyzed the expression of *PATZ1* mRNA after TSH stimulation and correlated it to the expression of the two miRNAs. As shown in Figure 12, we found an inverse correlation between PATZ1 and miRNAs expression at 30' and 2h following treatment with TSH. Then, miR-23b and miR-29b turned back to unchanged levels at 8h, 12h and 24h of TSH stimulation, whereas PATZ1 expression was kept lowered at 8h and 12h, and even further down-regulated at 24h.

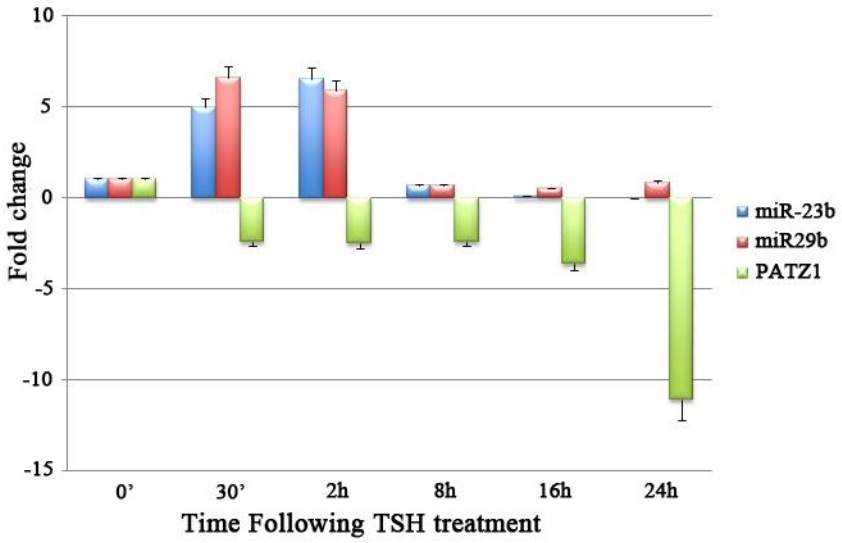

Figure 12. inverse correlation between PATZ1 and miR23b/miR29b expression following TSH treatment. miR-23b and miR29b result upregulated starting from 30' up to 2h following treatment with TSH. Conversely, the expression of PATZ1 mRNA is downregulated, starting at 30', and remains low and further downregulated at 24h. U6 and G6pd were used as loading controls. Data shown represent mean values ± SE of one experiment performed in duplicate.

Encouraged by these results, we studied the effects of both miRNAs on PATZ1 protein and mRNA expression in thyroid cells. To this aim, we transfected PC Cl3 cells with 100nM scramble control, miR-23b and miR-29b synthetic precursor and evaluated PATZ1 protein levels after 72h by western blotting. As shown in Figure 13, Panel A, PATZ1 protein levels were reduced when PC Cl3 cells were transfected with miR-29b, but not with a scramble miRNA or miR-23b precursor, indicating that in thyroid cells miR-29b is confirmed to target PATZ1, while miR-23b does not. At the same time, we analyzed the effect of both miRs on *PATZ1* mRNA, performing qRT-PCR; as reported in Figure 13, Panel B**,** we did not observe any change in the expression of *PATZ1* mRNA, confirming that miR-23b does not target PATZ1 in these cells and suggesting that targeting of PATZ1 expression by miR-29b in this cell system acts only at post-transcriptional level. This also imply that the observed inverse correlation between PATZ1 and miR-23b/miR-29b mRNA levels following TSH induction in PC Cl3 cells (Figure 12) is not a direct consequence of miRs up-regulation.

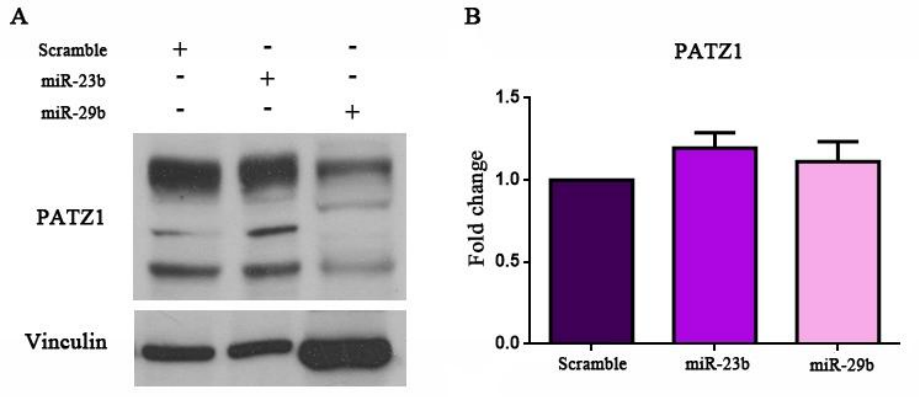

Figure 13. miR-23b and miR-29b on PATZ1 protein and mRNA. (A) Western blot analysis showing downregulation of PATZ1 protein levels in presence of 100 nM of miR-29b, but not in presence of Scramble control or miR-23b. (B) qRT-PCR analysis showing that in presence of both niR-23b and miR-29b the expression of PATZ1 mRNA does not change significantly, as assessed by Unpaired T-test. Vinculin for Western blot and G6PD for qRT-PCR were also analyzed as loading controls. Data in B show mean values ± SE of three independent experiments performed in duplicate.

4.4 Inverse correlation between PATZ1 and miR-29b in thyroid cells expressing oncogenic Ras

By screening the www.microRNA.org web system for miRNA expression in thyroid cells, we found that miR-29b was one of the most up-regulated miRNAs in FRTL-5 rat thyroid cells following expression of an oncogenic Ras gene (Figure 14, Panel A). In order to validate these findings, we used a similar cell system, in which the expression of an oncogenic Ras was induced at different time points by a tamoxifen-inducible construct (De Vita et al. 2005), and analyzed the expression of PATZ1 and miR-29b. As shown in Figure 14, Panel B, consistent with the data extracted from the web, miR-29b was up-regulated following induction of Ras as early as after 24h of treatment with tamoxifen. Opposed to miR-29b, PATZ1 was down-regulated at both mRNA and protein levels, confirming the functional miR-29b/PATZ1 interaction in thyroid cells (Figure 14, Panels B and C). The expression of miR-29b and PATZ1 was also analyzed in the two previously established V27 and V29 FRTL-5 cell clones stably expressing an oncogenic Ras (De Vita et al. 2005). As shown in Figure 14, Panels B and C, the inverse correlation between miR-29b and PATZ1 was confirmed and even emphasized in these cells. qRT-PCR analysis of FRTL-5 cells transfected with miR-29b precursor confirmed the targeting of PATZ1 in these cells at the mRNA level (Figure 14, Panel D), indicating that, differently from PC Cl3, the targeting of PATZ1 by miR-29b in FRTL-5 cells acts also at mRNA level. All together these results confirm that miR-29b targets PATZ1 in thyroid cells and suggest that PATZ1 is a downstream effector of the oncogenic Ras signaling.

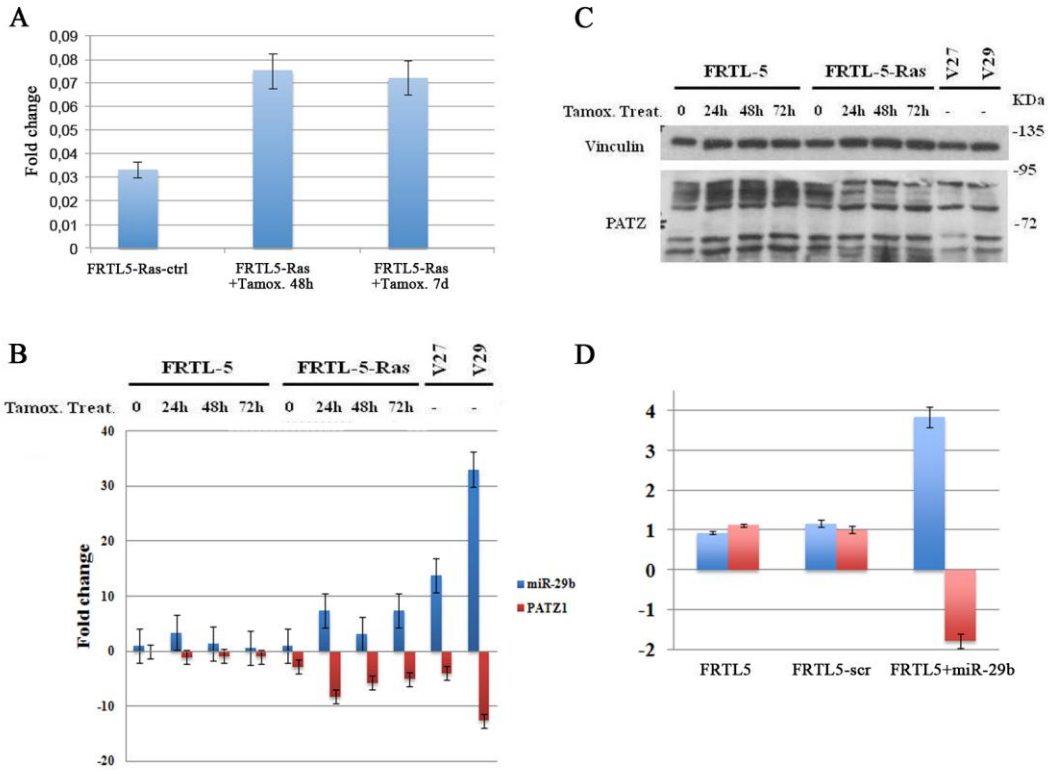

Figure 14. Inverse correlation between miR-29b and PATZ1 in Ras-induced FRTL5. (A) Results obtained by screening of www.microRNA.org, showing upregulation of miR-29b in FRTL-5 rat thyroid cells following expression of an oncogenic Ras gene. (B) qRT-PCR analysis showing miR-29b up-regulation following induction of Ras as early as after 24h of treatment with tamoxifen and in two FRTL-5 cell clones stably expressing an oncogenic Ras (V27 and V29). Opposed to miR-29b, PATZ1 resulted strongly downregulated. (C) Western blot analysis of the same samples as in B, showing downregulation of PATZ1 also at protein level. (D) 72h after transfection with miR-29b, PATZ1 mRNA decreases, compared with the scramble control, as assessed by qRT-PCR. Vinculin for Western blot; U6 and G6PD for qRT-PCR were analyzed as loading controls. Data in B and D represent mean values ± SE of three and two independent experiments performed in triplicate, respectively.

4.5 Restoration of PATZ1 expression in FRTL5-Ras cells

In order to investigate a causal role of PATZ1 in thyroid carcinogenesis induced by oncogenic Ras, we used the stable clone FRTL5 V29, in which a high overexpression of miR-29b and a strong downregulation of PATZ1 was observed (Figure 14), to restore PATZ1 expression. Following the transfection of a PATZ1-expression plasmid, and positive selection with the appropriate antibiotic, 15 PATZ1-transfected and 5 empty vector-transfected clones, plus the remaining mass populations of both transfections, were analyzed for PATZ1 expression. As shown in Figure 15, restoration of PATZ1 expression was confirmed by qRT-PCR and Western-Blot analysis in most of PATZ1-transfected clones and the mass population compared to clones and mass population transfected with the empty vector. Then, we selected 3 FRTL5-Ras-PATZ1 clones and 4 negative controls for functional studies aimed to characterize growth and malignant properties of these cells.

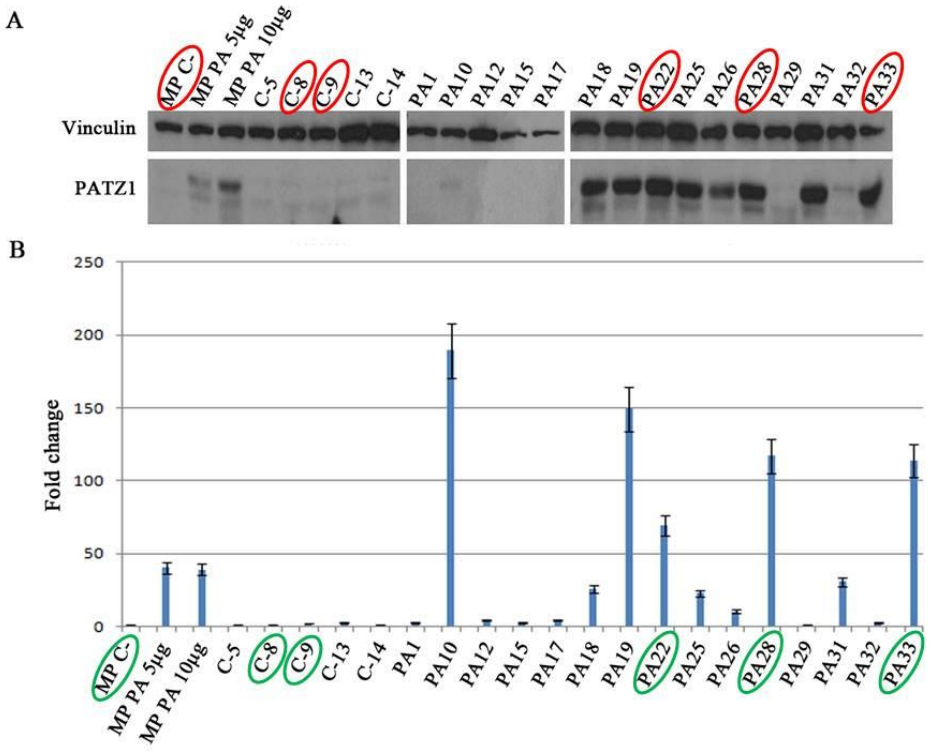

Figure 15. Restoration of PATZ1 expression in FRTL5-Ras cells. Western Blot (A) and qRT-PCR (B) analysis of PATZ1 in cell clones and mass populations (MP) obtained by transfection of either a PATZ1-expressing plasmid (PA) or the empty vector (C-). Clones and MP circled in red (Panel A) and green (Panel B) were selected for further experiments. Vinculin for Western blot and G6PD for qRT-PCR were also analyzed as loading controls. Data in B represent mean values ± SE of one experiment performed in duplicate.

4.6 PATZ1 expression in Ras-transformed thyroid cells inhibits proliferation

In order to investigate whether re-expression of PATZ1 could affect proliferation of Ras-transformed thyroid cells, we performed growth curves on the selected clones. As reported in Figure 16, FRTL5-Ras-PATZ1 cells showed a significant decrease in the proliferation rate compared to control (FRTL-Ras-ctrl). Interestingly, the growth rate of FRTL5-Ras-PATZ1 was not significantly different from that of untransformed FRTL5 cells. On the other side, as expected, FRTL5-Ras-ctrl growth curves were undistinguishable from those of parental FRTL5 V29 cells (FRTL5-Ras).

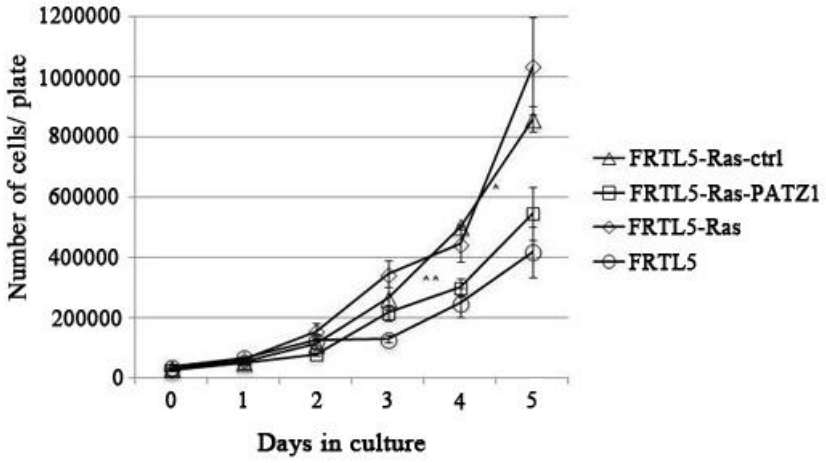

Figure 16. PATZ1 effects on the growth rate and apoptosis. Growth curves performed on different stably expressing PATZ1 cell clones of FRTL5-Ras compared to control cells expressing the empty vector (FRTL5-Ras-ctrl), parental cells (FRTL-Ras) and normal control cells (FRTL5). The curves show mean values ± SE of 3 independent cell lines for both FRTL5-Ras-ctrl and FRTL5-Ras-PATZ1. Mean values ± SE of one cell line counted in triplicate for each time point are shown for both FRTL5 and FRTL5-Ras.

Tripan Blue exclusion test, which was applied during cell counting, did not reveal any significant rate of cell death that could account for the observed differences on the growth rate (data not shown). In order to better investigate cell proliferation, we decided to analyze cell cycle by FACS. Preliminary results obtained in proliferating cells showed a decreased S and an enhanced G2/M phase in PATZ1-expressing cells compared to controls, suggesting a specific role for PATZ1 in the G2/M checkpoint (Figure 17). Further experiments, also using BrDU coupled to FACS analysis, which allows to better synchronize cells in the different phases of cell cycle, are still in progress to confirm these suggestions.

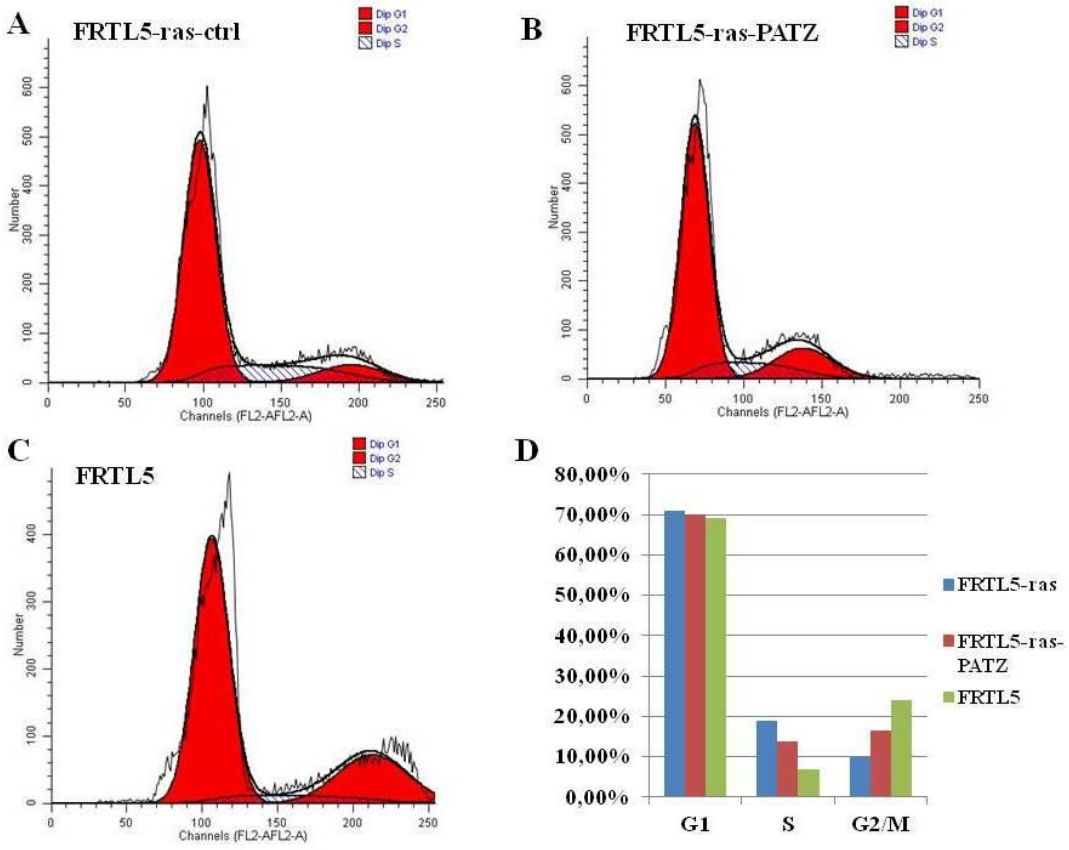

Figure 17. Propidium iodide flow cytometry (A, B, C) Representative FACS Plots of FRTL5-Ras-ctrl, FRTL5-Ras-PATZ1 and FRTL5 cells. (D) The percentage of cells in each phase, as assessed by BD Accury C6 software, of the cell cycle is represented.

4.7 PATZ1 expression in Ras-transformed thyroid cells inhibits migration

Cell migration is a key feature of cancer cells responsible for tumor progression and metastasis (Bravo-Cordero et al. 2012). To analyze whether PATZ1 re-expression affects the migratory capability in FRTL5-Ras cells, wound healing and Transwell migration assays were performed. Specifically, a wound with a 20µl tip was performed in plates in which cells were at 95% confluence. The same field was photographed at 0h, 24h, 48h, 72h and 96h (Figure18). For all time cells were starved, thus avoiding the possibility that the effect on cell proliferation could interfere with the read out of the assay. As shown in Figure 18, the migration capacity of PATZ1-transfectants was significantly reduced compared with that of control cells, suggesting that PATZ1 expression can inhibit migration of Ras-

transformed thyroid cells. However, the wound-healing assay is particularly suitable for studying the effects of cell-matrix and cell-cell interactions on cell migration, but does not give insights on migration in response to a particular chemical signal, which is usually referred to as chemotaxis. To better investigate this issue we performed a Transwell assay, analyzing cell migration across 8-μm membrane pores (Boyden chambers) in response to Calf Serum (CS) and 6H. The results of this migration assay were concordant with those of the wound healing assay, showing for all the three PATZ1-expressing clones a drastic reduction in their migration capability compared to controls (Figure19).

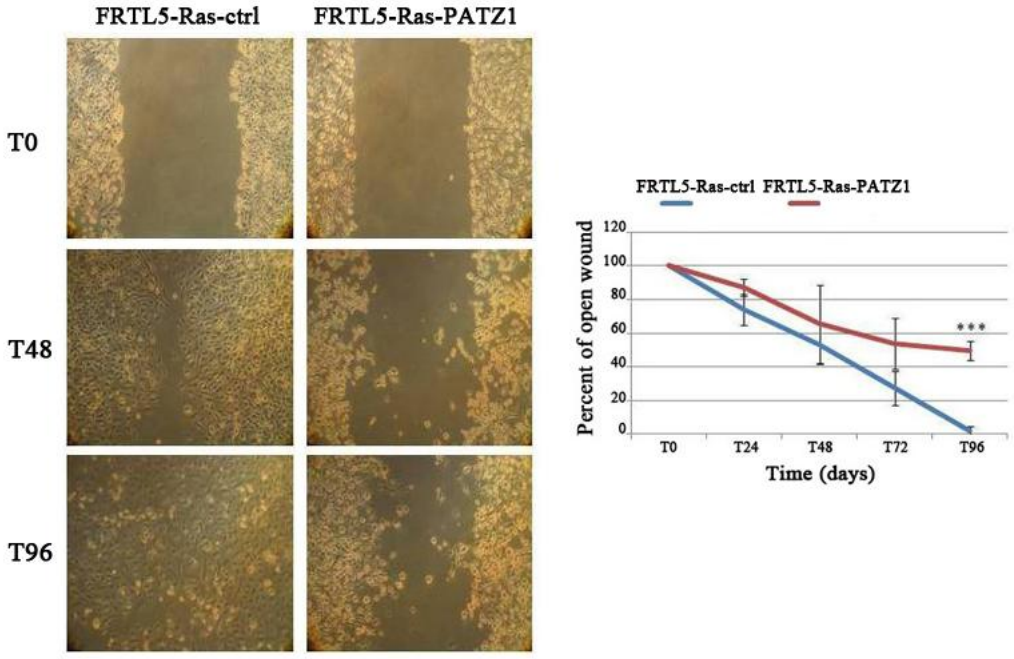

Figure 18. PATZ1 overexpression in FRTL5-Ras cells delayed wound closure. Representative images of one control clone expressing the empty vector and one clone overexpressing PATZ1. After 96h the wound was completely closed in control cells, whereas it was still unclosed in cells transfected with PATZ1. The graph shows the percent of open wound at different time points expressed as mean values ± SE of three control clones and three clones overexpressing PATZ1.

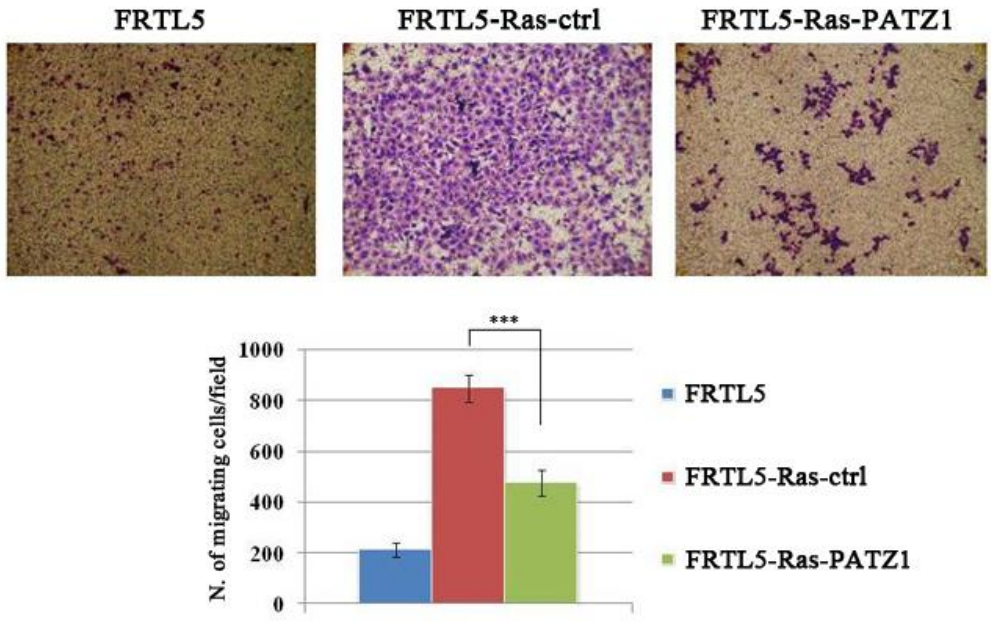

Figure 19. PATZ1 overexpression inhibits transwell migration. Representative images of a Transwell assay performed on FRTL5, FRTL5-Ras-ctrl and FRTL5-Ras-PATZ1 cells. The graph shows the mean values $\pm$ SE of three clones for each transfected construct, obtained by counting the number of cells that have migrated underneath the Boyden chamber. ***, $P < 0.001$ as assessed by Unpaired T test.

4.8 PATZ1 expression in Ras-transformed thyroid cells inhibits anchorage-independent growth

In order to confirm the hypothesis that PATZ1 may have a tumor-suppressor function in Ras-transformed thyroid cells, the malignant phenotype of the tumorigenic FRTL5-Ras cells was analyzed *in vitro* by a soft agar assay, a common method to monitor anchorage-independent growth by measuring colony formation in a semisolid culture medium. As shown in Figure 20, differently from FRTL5-Ras-ctrl cells, FRTL5-Ras-PATZ1 cells showed a drastic reduction of growth in soft agar. These results suggest that PATZ1 expression inhibits tumorigenic potential of Ras-transformed thyroid cells. However, further *in vivo* experiments, by generating xenografts in nude mice, are needed to better elucidate this issue.

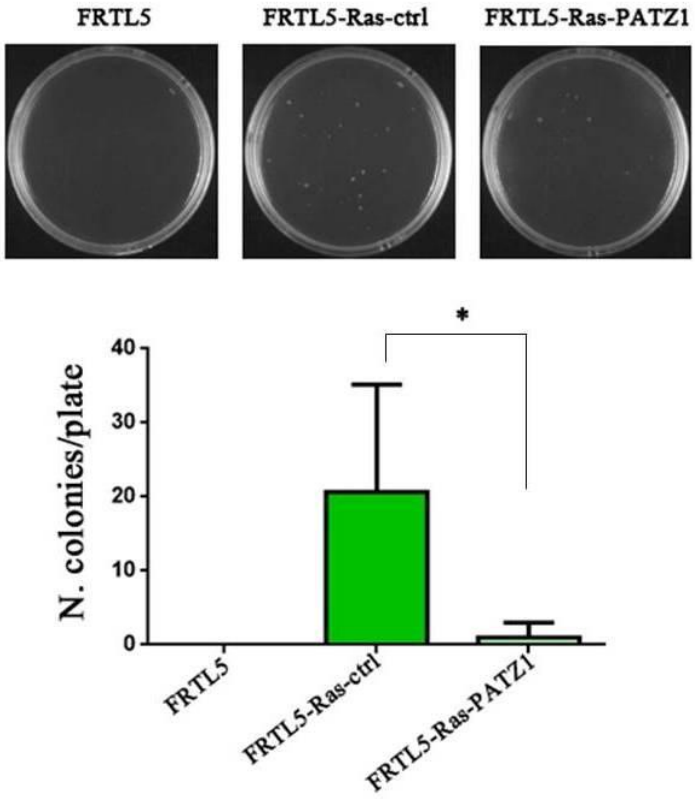

Figure 20. PATZ1 expression inhibits FRTL5-Ras capacity to grow in soft agar. Representative images of growth in soft agar of normal rat FRTL5, FRTL5-Ras-ctrl and FRTL5-Ras-PATZ1 cells. Colonies with a diameter greater than 20 μm were counted after 40 days. The experiment was performed in quadrupled. *, $P < 0.05$, as assessed by Unpaired T test.

5. DISCUSSION

Projections of cancer incidence revealed that by 2030 thyroid cancer, together with melanoma and uterine cancer, is going to surpass colorectal cancer and become the second highest diagnosis of cancer in women, and fourth in absolute cases (Rahib et al. 2014). Anyway, the average annual increase in thyroid cancer incidence is the highest among all cancers (Xing et al. 2013). Many studies have provided evidence for this increase; however, why thyroid cancer incidence keeps rising is still debated and there are conflicting reports of factors involved (Ito et al. 2013). The thyroid carcinogenesis represents a good multi-step model of cancer disease because initiation and progression occurs through gradual accumulation of various genetic and epigenetic alterations, including somatic mutations, alterations in gene expression patterns, miRNA dysregulation and aberrant gene methylation (Nikiforov and Nikiforova 2011). Based on these alterations, there are different lesions, including benign, such as goiters or adenomas, and malignant neoplasms, including carcinomas of different degree of differentiation. Indeed, among carcinomas, we can make a further classification according not only to the degree of differentiation, but also to the prognosis. At the first stage we meet well differentiated thyroid carcinoma (WDTC), associated with a favorable prognosis, which includes papillary and follicular tumors; an intermediate stage is represented by poor differentiated thyroid carcinoma (PDTC), while the last stage, combined with a poorer prognosis, is represented by undifferentiated thyroid carcinoma, also known as anaplastic thyroid cancer (ATC). PDTCs and ATCs can develop *de novo*, although many of them arise through the process of stepwise dedifferentiation of PTCs and FTCs (Nikiforov and Nikiforova 2011). The theory of sequential progression is supported by the presence of pre- or co- existing WDTC with less differentiated types and the common core of genetic loci with identical allelic imbalances in co-existing well-differentiated components (van der Laan et al. 1993). The different thyroid cancer hystotypes are characterized by distinct arrays of genetic alterations that mainly activate the Ras signaling cascade. However, in PTC, where PATZ1 is less downregulated, Ras mutations are hardly detected, while in FTC, PDTC and ATC, where PATZ1 is more strongly downregulated, mutations of Ras are more frequently found (Kondo et al. 2006; Chiappetta et al. 2014). *Ras* mutations occur as an early event in FTA and may increase the potential for malignant transformation. There are in fact recent data suggesting that *Ras* may predispose WDTC to subsequent de-differentiation into PDTC and ATC (Howell et al. 2013). Evidences that support this theory, derived in part from *in vitro* findings using normal rat thyroid cells, showed that oncogenic *Ras* can promote chromosomal instability (Saavedra et al. 2000; Abulaiti et al. 2006; Knauf et al. 2006).

However, even though critical molecular mechanisms of thyroid transformation have been clarified, other molecular steps of neoplastic progression still need to be investigated.

Recently, our research group has shown that PATZ1 exerts an onco-suppressor role in thyroid cancer through the regulation, at least in part, of p53-target genes *EpCam*, *RhoE* and *Caldesmon*, thus resulting in reduced migration and invasion *in vitro*, as well as Mesenchimal-Epithelial transition (MET) and reduced tumor growth *in vivo*. Through functional studies in undifferentiated human cancer cell lines, in which PATZ1 was strongly downregulated, we have shown that the re-expression of PATZ1 is able to revert, at least in part, the neoplastic phenotype in terms of proliferation, migration, invasiveness, soft-agar growth and *in vivo* tumorigenicity (Chiappetta et al. 2014). Starting from this study, we questioned what could be the molecular mechanism underlying the down-modulation of PATZ1 in thyroid carcinogenesis. Among possible mechanisms, we decided to focus on miRNAs, which are the actual challenge in both diagnostic and therapy for biomedical purposes. Indeed, the miRNAs signature may be an additional diagnostic tool in the management of human tumors, especially when combined with the analysis for specific genetic lesions. Moreover, innovative therapy based on restoration of downregulated miRNAs or inhibition of upregulated miRNAs by antagomirs, could improve the response to treatment of patients affected by tumors refractory to conventional radiotherapy and chemotherapy, as could be the case of ATC.

MiRNAs can act either as oncogenes or tumor suppressors, depending on the cellular context and specific diseases. This is the case of miR-23b and miR-29b, the two miRNAs that here I found to target PATZ1 in different cellular systems including thyroid cells. Several evidences suggest that miR-23b and miR-29b act as crucial regulators in a variety of cancers, influencing cell proliferation, apoptosis, differentiation, migration and/or invasivity, metastasis and chemosensitivity (Pellegrino et al. 2013; Majid et al. 2013; Liu et al. 2014; Yan et al. 2015). In thyroid cancer, a study conducted by Leone and co-workers demonstrates that up-regulation of miR-23b and miR-29b is a critical event for thyroid cell proliferation; indeed these two miRNAs promote thyroid cell growth synergizing with the traditional proliferation; moreover an increased expression of both these miRNAs were found in experimental murine PTU-induced models and in human goiters (Leone et al. 2012).

To verify the effect of miR-23b and miR-29b on PATZ1 expression in thyroid cells, I used the same cell system of Leone and co-workers (2012), showing an inverse correlation between PATZ1 and both these miRNAs at 30’ and 2h following treatment with TSH. Then, miR-23b and miR-29b turned back to unchanged levels at 8h, 12h and 24h of TSH stimulation, whereas PATZ1 expression was kept lowered at 8h and 12h, and even further down-regulated at

24h, suggesting that further events other than miR-23b and miR29b overexpression may contribute to the maintenance of PATZ1 silencing in thyroid cells induced to proliferate. These results sustain a role for PATZ1 in negative regulation of normal thyroid cell proliferation.

Interestingly, analyzing high throughput data from a study conducted by Landgraf at al. (2007), I found that miR-29b was one of the most up-regulated miRNAs in FRTL-5 rat thyroid cells following expression of an oncogenic Ras gene. Using their same cell system, in which the expression of the oncogenic Ras V12 was induced at different time points by a tamoxifen-inducible construct, as well as FRTL-5 cells in which RasV12 was stably expressed (De Vita et al. 2005), I found that the expression of PATZ1 and miR-29b were inversely correlated at both mRNA and protein level. These results support a functional miR-29b/PATZ1 interaction downstream of oncogenic Ras in thyroid cells and suggest that PATZ1 may be a negative effector of the oncogenic Ras signaling.

In order to deepen a causal role of PATZ1 downregulation in thyroid carcinogenesis induced by oncogenic Ras, I overexpressed PATZ1 in Ras transformed FRTL-5 cells, finding a significant impairment of different cellular functions related to the transformed phenotype, including proliferation, migration and capacity to grow in soft agar. This was particularly evident at the proliferation level, where growth curves obtained from PATZ1-expressing FRTL-Ras cells were undistinguishable from those of untransformed FRTL-5 cells, suggesting that re-expression of PATZ1 is potentially able to bring the proliferation rate to the normal status. Therefore, it appears that PATZ1 downregulation is indeed a crucial step in Ras oncogenic signaling, acting in different processes of cellular transformation induced by activated Ras. These data are also consistent with the role of PATZ1 that our group has demonstrated in human cancer cell lines, in which the same cellular processes have been found to be regulated by PATZ1 (Chiappetta et al. 2014).

From my data it appears that downregulation of PATZ1 is achieved by up-regulation of miR-29b in FRTL5 cells and possibly by both miR-23b and miR-29b in PC Cl3 cells. If we will be able to demonstrate by further experiments that, using antagomirs directed against one or both these miRNAs, the expression of PATZ1 in Ras transformed cells is upregulated, we can envisage a future therapy useful in thyroid cancer carrying Ras mutations.

MicroRNAs are promising candidates for drug targeting, especially when combined with the analysis for specific genetic lesions. Indeed, innovative therapies, based on modulation of miRNAs and their relative targets, are believed to improve the response to treatment of patients affected by tumors refractory to conventional radiotherapy and chemotherapy, as in the case of ATC (Pallante et al. 2014).

For these reasons, it is our intention to continue this work studying, both *in vitro* and *in vivo*, a possible effect of miR-29b antagomir on PATZ1. Our goal would be the inhibition of PATZ1-targeting miR-29b in cancer cells as a way to up-regulate PATZ1 expression and hopefully revert the transformed phenotype. It would be particularly interesting to analyze *in vivo*, by xenografts in nude mice, a possible suppressive action against tumor proliferation, following delivery of PATZ-targeting miR-29b antagomir.

6. CONCLUSION

In order to understand the mechanisms by which PATZ1 is downregulated in thyroid cancer I focused on miRNAs and found that two miRNAs, miR-23b and miR-29b, specifically target PATZ1 in thyroid cells.
Both these miRNAs are involved as both oncogenes or tumor-suppressors in different types of malignancies, depending on the cellular context, exactly as PATZ1 does. In thyroid cells both miR-23b and miR-29b are up-regulated, while PATZ1 is downregulated, following a proliferation stimulus, and miR-29b is up-regulated, while PATZ1 is downregulated, following expression of oncogenic Ras.
Focusing on the latter observation, I demonstrated that PATZ1 overexpression in Ras^{V12}-expressing thyroid cells is able to revert, at in least in part, their transformed phenotype.
All in all these results suggest that PATZ1 is a pivotal regulator acting downstream of miR29b to suppress thyroid cell transformation driven by oncogenic Ras, highlighting a new potential therapeutic target to fight highly malignant thyroid cancer.

7. ACKNOWLEDGEMENTS

I acknowledge with gratitude Prof. Lucio Nitsch, coordinator of the Genetics and Molecular Medicine Doctorate Program, for the beautiful opportunity that gave me to work at the Dipartimento di Medicina Molecolare e Biotecnologie Mediche of the Università degli Studi di Napoli Federico II.

A special thank goes to my mentor Dr. Monica Fedele for having encouraged my interest in research, for the trust shown and for all experience and knowledge made available to me.

I wish to present my sincere thank to Prof. Alfredo Fusco and Dr. Gabriella de Vita for their great collaboration.

A special thank goes to my colleague and friend Teresa, my guide! thanks for teaching me everything I know, and for having been close with a lot of patience and skill.

I thank all my colleagues for their support, the scientific and moral help, but especially for the kind moments together.

I would especially thank my family and Claudio for their unconditional support and for their infinite patience.

7. REFERENCES

Abulaiti A, Fikaris AJ, Tsygankova OM, Meinkoth JL. Ras induces chromosome instability and abrogation of the DNA damage response. Cancer Res. 2006 Nov 1;66(21):10505-12.

Apostolou, E. and Hochedlinger, K. Chromatin dynamics during cellular reprogramming. Nature. 2013. 502, 462-471.

Betel D, Koppal A, Agius P, Sander C**,** Leslie C. Comprehensive modeling of microRNA targets predicts functional non-conserved and non-canonical sites. Genome Biol. 2010;11(8):R90.

Bilic I, Koesters C, Unger B, Sekimata M, Hertweck A, Maschek R, Wilson CB, Ellmeier W. Negative regulation of CD8 expression via Cd8 enhancer-mediated recruitment of the zinc finger protein MAZR. Nat Immunol 2006; 7:392-400.

Borbone E, De Rosa M, Siciliano D, Altucci L, Croce CM, Fusco A. Up-regulation of miR-146b and down-regulation of miR-200b contribute to the cytotoxic effect of histone deacetylase inhibitors on ras-transformed thyroid cells. J Clin Endocrinol Metab. 2013 Jun;98(6):E1031-40.

Bravo-Cordero JJ, Hodgson L, Condeelis J. Directed cell invasion and migration during metastasis. Curr Opin Cell Biol. 2012 Apr; 24(2):277-83.

Burrow AA, Williams LE, Pierce LC, Wang YH. Over half of breakpoints in gene pairs involved in cancer-specific recurrent translocations are mapped to human chromosomal fragile sites. BMC Genomics 2009;10:59.

Cao M, Seike M, Soeno C, Mizutani H, Kitamura K, Minegishi Y, Noro R, Yoshimura A, Cai L, Gemma A. MiR-23a regulates TGF-β-induced epithelial-mesenchymal transition by targeting E-cadherin in lung cancer cells. Int J Oncol 2012; 41: 869-875.

Chen L, Han L, Zhang K, Shi Z, Zhang J, Zhang A, Wang Y, Song Y, Li Y, Jiang T, Pu P, Jiang C, Kang C. VHL regulates the effects of miR-23b on glioma survival and invasion via suppression of HIF-1α/VEGF and β-catenin/Tcf-4 signaling. Neuro Oncol 2012; 14: 1026-1036.

Cheng L, Yang T, Kuang Y, Kong B, Yu S, Shu H, Zhou H, Gu J. MicroRNA-23a promotes neuroblastoma cell metastasis by targeting CDH1. Oncol Lett 2014; 7: 839-845.

Chiappetta G, Valentino T, Vitiello M**,** Pasquinelli R**,** Monaco M**,** Palma G**,** Sepe R**,** Luciano A, Pallante P, Palmieri D, Aiello C, Rea D, Losito SN, Arra C, Fusco A, Fedele M. PATZ1 acts as a tumor suppressor in thyroid cancer via targeting p53-dependent genes involved in EMT and cell migration. Oncotarget. 2014 Dec 16.

Cho JH, Kim MJ, Kim KJ, Kim JR. POZ/BTB and AT-hook-containing zinc finger protein 1 (PATZ1) inhibits endothelial cell senescence through a p53 dependent pathway. Cell Death Differ. 2012 Apr; 19(4):703-12.

Colamaio M, Borbone E**,** Russo L**,** Bianco M**,** Federico A**,** Califano D, Chiappetta G, Pallante P, Troncone G, Battista S, Fusco A. miR-191 down-regulation plays a role in thyroid follicular tumors through CDK6 targeting. J Clin Endocrinol Metab**.** 2011 Dec;96(12):E1915-24.

Colamaio M, Calì G, Sarnataro D, Borbone E, Pallante P, Decaussin-Petrucci M, Nitsch L, Croce CM, Battista S, Fusco A. Let-7a down-regulation plays a role in thyroid neoplasias of follicular histotype affecting cell adhesion and migration through its ability to target the FXYD5 (Dysadherin) gene. J Clin Endocrinol Metab. 2012 Nov; 97(11):E2168-78

Colamaio M, Puca F, Ragozzino E, Gemei M, Decaussin-Petrucci M, Aiello C, Bastos AU, Federico A, Chiappetta G, Del Vecchio L**,** Torregrossa L**,** Battista S,Fusco A. miR-142-3p down-regulation contributes to thyroid follicular tumorigenesis by targeting ASH1L and MLL1. J Clin Endocrinol Metab. 2015 Jan; 100(1):E59-69.

Costoya JA. Functional analysis of the role of POK transcriptional repressors. Brief Funct Genomic Proteomic. 2007; 6(1):8-18.

Croce CM. Causes and consequences of miroRNA dysregulation in cancer. Nat Rev Genet. 2009 Oct;10(10):704-14.

DeLellis RA, Lloyd RV, Heitz PU, Eng C. Thyroid and parathyroid tumours. In World Health Organization. Classification of Tumours. Pathology and Genetics of Tumours of Endocrine Organs. 2004. pp 51-56. Lyon, France: IARC Press.

De Menna M, D'Amato V, Ferraro A, Fusco A, Di Lauro R, Garbi C, De Vita G. Wnt4 inhibits cell motility induced by oncogenic Ras. Oncogene. 2013 Aug 29;32(35):4110-9.

De Vita G, Bauer L, da Costa VM, De Felice M, Baratta MG, De Menna M, Di Lauro R**.** Dose-dependent inhibition of thyroid differentiation by RAS oncogenes. Mol Endocrinol. 2005 Jan; 19(1): 76-89.

Donadelli M, Dando I, Fiorini C, Palmieri M. Regulation of miR-23b expression and its dual role on ROS production and tumour development. Cancer Lett 2014; 349: 107-113.

Donghi R, Longoni A, Pilotti S, Michieli P, Della Porta G, Pierotti MA . Gene p53 mutations are restricted to poorly differentiated and undifferentiated carcinomas of the thyroid gland Journal of Clinical Investigation 1993; 91: 1753-1760.

Esposito F, Boscia F, Gigantino V, Tornincasa M, Fusco A, Franco R, Chieffi P.The high-mobility group A1-estrogen receptor β nuclear interaction is impaired in human testicular seminomas. J Cell Physiol**.** 2012 a Dec; 227(12):3749-55.

Esposito F, Tornincasa M, Pallante P, Federico A, Borbone E, Pierantoni GM, Fusco A. Down-regulation of the miR-25 and miR-30d contributes to the development of anaplastic thyroid carcinoma targeting the polycomb protein EZH2. J Clin Endocrinol Metab. 2012 b May; 97(5):E710-8.

Esquela-Kerscher A and Slack FJ. Oncomirs - microRNAs with a role in cancer. Nat Rev Cancer. 2006 Apr;6(4):259-69.

Fagin JA, Matsuo K, Karmakar A, Chen DL, Tang SH & Koeffler HP. High prevalence of mutations of the p53 gene in poorly differentiated human thyroid carcinomas. Journal of Clinical Investigation 1993; 91:179–184.

Faquin WC**.** The thyroid gland: recurring problems in histologic and cytologic evaluation. Arch Pathol Lab Med. 2008 Apr;132(4):622-32.

Fedele M, Berlingieri MT, Scala S, Chiariotti L, Viglietto G, Rippel V, Bullerdiek J, Santoro M, Fusco A. Truncated and chimeric HMGI-C genes induce neoplastic transformation of NIH3T3 murine fibroblasts. Oncogene**.** 1998 Jul 30;17(4):413-8.

Fedele M, Benvenuto G, Pero R, Majello B, Battista S, Lembo F, Vollono E, Day PM, Santoro M, Lania L, Bruni CB, Fusco A and Chiariotti L. A novel member of

the BTB/POZ family, PATZ, associates with the RNF4 RING finger protein and acts as a transcriptional repressor. J Biol Chem 2000; 275:7894-7901.

Fedele M, Franco R, Salvatore G, Paronetto MP, Barbagallo F, Pero R, Chiariotti L, Sette C, Tramontano D, Chieffi G, Fusco A, Chieffi P.PATZ1 gene has a critical role in the spermatogenesis and testicular tumours. J. Pathol. 2008; 215:39-47.

Fedele M and Fusco A. HMGA and cancer. Biochim Biophys Acta**.** 2010 Jan-Feb; 799(1-2):48-54.

Frattini M, Ferrario C, Bressan P, Balestra D, De Cecco L, Mondellini P, Bongarzone I, Collini P, Gariboldi M, Pilotti S, Pierotti MA, Greco A. Alternative mutations of BRAF, RET and NTRK1 are associated with similar but distinct gene expression patterns in papillary thyroid cancer. Oncogene**.** 2004 Sep 23;23(44):7436-40.

Frezzetti D, De Menna M, Zoppoli P, Guerra C, Ferraro A, Bello AM, De Luca P, Calabrese C, Fusco A, Ceccarelli M, Zollo M, Barbacid M, Di Lauro R, De Vita G. Upregulation of miR-21 by Ras in vivo and its role in tumor growth. Oncogene. 2011 Jan 20;30(3):275-86.

Fusco A, Berlingieri MT, Di Fiore PP, Portella G, Grieco M, Vecchio G. One- and two-step transformations of rat thyroid epithelial cells by retroviral oncogenes. Mol Cell Biol. 1987 Sep;7(9):3365-70.

Garzon R, Garofalo M, Martelli MP Briesewitz R**,** Wang L**,** Fernandez-Cymering C**,** Volinia S**,** Liu CG**,** Schnittger S, Haferlach T, Liso A, Diverio D, Mancini M, Meloni G**,** Foa R**,** Martelli MF, Mecucci C, Croce CM**,** Falini B. Distinctive microRNA signature of acute myeloid leukemia bearing cytoplasmic mutated nucleophosmin. Proc Natl Acad Sci U S A. 2008; 105, 3945-50.

Garzon R, Calin GA, Croce CM. MicroRNAs in Cancer. Annu Rev Med. 2009;60:167-79.

Grieco M, Santoro M, Berlingieri MT, Melillo RM, Donghi R, Bongarzone I, Pierotti MA, Della Porta G, Fusco A & Vecchio G. PTC is a novel rearranged form of the ret proto-oncogene and is frequently detected in vivo in human thyroid papillary carcinomas. Cell 1990;60 557-563.

Guan H, Ji M**,** Bao R, Yu H, Wang Y, Hou P**,** Zhang Y**,** Shan Z**,** Teng W**,** Xing M. Association of high iodine intake with the T1799A BRAF mutation in papillary thyroid cancer. J Clin Endocrinol Metab. 2009 May;94(5):1612-7.

He L, Thomson JM, Hemann MT, Hernando-Monge E, Mu D, Goodson S, Powers S, Cordon-Cardo C, Lowe SW, Hannon GJ, Hammond SM. A microRNA polycistron as a potential human oncogene. Nature. 2005 Jun 9;435(7043):828-33.

Howell GM, Hodak SP, Yip L. RAS mutations in thyroid cancer. Oncologist. 2013;18(8):926-32.

Huynh KD and Bardwell VJ. The BCL-6 POZ domain and other POZ domains interact with the co-repressors N-CoR and SMRT. Oncogene 1998; 17:2473-2484.

Iorio MV and Croce CM. MicroRNA involvement in human cancer. Carcinogenesis. 2012 Jun;33(6):1126-33.

Ito T, Seyama T, Mizuno T, Tsuyama N,Hayashi T, Hayashi Y, Dohi K, Nakamura N and Akiyama M. Unique association of p53 mutations with undifferentiated but not with differentiated carcinomas of the thyroid gland. Cancer Research 1992; 52:1369-1371.

Ito Y, Nikiforov YE, Schlumberger M, Vigneri R. Increasing incidence of thyroid cancer: controversies explored. Nat Rev Endocrinol. 2013 Mar; 9(3):178-84.

Jung CK, Little MP, Lubin JH, Brenner AV, Wells SA Jr, Sigurdson AJ, Nikiforov YE. The increase in thyroid cancer incidence during the last four decades is accompanied by a high frequency of BRAF mutations and a sharp increase in RAS mutations. J Clin Endocrinol Metab 2014; 99:E276-85.

Kebebew E, Greenspan FS, Clark OH, Woeber KA, McMillan A. Anaplastic thyroid carcinoma. Treatment outcome and prognostic factors. Cancer. 2005 Apr 1;103(7):1330-5.

Kelly KF and Daniel JM. POZ for effect--POZ-ZF transcription factors in cancer and development. Trends Cell Biol 2006;16:578-87.

Keskin N, Deniz E, Eryilmaz J, Un M, Batur T, Ersahin T, Cetin Atalay R, Sakaguchi S, Ellmeier W, Erman B. PATZ1 is a DNA damage responsive transcription factor that inhibits p53 function. Mol Cell Biol. 2015 Mar 9. pii: MCB.01475-14.

Kim TY, Kim WG, Kim WB, Shong YK. Current status and future perspective in differentiated thyroid cancer. Endocrinol Metab. 2014 Sep;29(3):217-25.

Kimura ET, Nikiforova MN, Zhu Z, Knauf JA, Nikiforov YE & Fagin JA. High prevalence of BRAF mutations in thyroid cancer: genetic evidence for constitutive activation of the RET/PTC-RAS-BRAF signaling pathway in papillary thyroid carcinoma. 2003. Cancer Research 63:1454-1457.

Knauf JA, Ouyang B, Knudsen ES, Fukasawa K, Babcock G, Fagin JA. Oncogenic RAS induces accelerated transition through G2/M and promotes defect s in the G2 DNA damage and mitotic spindle checkpoints. J Biol Chem. 2006 Feb 17;281(7):3800-9.

Kobayashi A, Yamagiwa H, Hoshino H, Muto A, Sato K, Morita M, Hayashi N, Yamamoto M, Igarashi K. A combinatorial code for gene expression generated by transcription factor Bach2 and MAZR (MAZ-related factor) through the BTB/POZ domain. Mol Cell Biol 2000; 20:1733-1746.

Kondo T, Ezzat S, Asa SL. Pathogenetic mechanisms in thyroid follicular-cell neoplasia. Nature Reviews Cancer 2006; 6: 292-306.

Kroll TG, Sarraf P, Pecciarini L**,** Chen CJ, Mueller E, Spiegelman BM, Fletcher JA. PAX8-PPARgamma1 fusion oncogene in human thyroid carcinoma. Science. 2000 Aug 25;289(5483):1357-60.

Landgraf P, Rusu M, Sheridan R, Sewer A, Iovino N, Aravin A, Pfeffer S, Rice A, Kamphorst AO, Landthaler M, Lin C**,** Socci ND, Hermida L, Fulci V, Chiaretti S,Foà R, Schliwka J, Fuchs U, Novosel A, Müller RU, Schermer B, Bissels U, Inman J, Phan Q, Chien M, Weir DB, Choksi R, De Vita G, Frezzetti D, Trompeter HI, Hornung V, Teng G, Hartmann G, Palkovits M, Di Lauro R, Wernet P, Macino G, Rogler CE, Nagle JW, Ju J, Papavasiliou FN, Benzing T, Lichter P, Tam W,Brownstein MJ, Bosio A, Borkhardt A, Russo JJ, Sander C, Zavolan M, Tuschl T. A mammalian microRNA expression atlas based on small RNA library sequencing. Cell. 2007 Jun 29;129(7):1401-14.

Lee RC, Feinbaum RL, Ambros V. The C. elegans heterochronic gene lin-4 encodes small RNAs with antisense complementarity to lin-14. Cell. 1993 Dec 3;75(5):843-54.

Lee S and Takahiro Maeda. POK/ZBTB proteins: an emerging family of proteins that regulate lymphoid development and function. Immunological Reviews. 2012 May; 247(1): 107-119.

Leone V, D'Angelo D, Pallante P, Croce CM, Fusco A.Thyrotropin regulates thyroid cell proliferation by up-regulating miR-23b and miR-29b that target SMAD3. J Clin Endocrinol Metab. 2012 Sep;97(9):3292-301.

Leone V, D'Angelo D, Pallante P, Croce CM, Fusco A. Thyrotropin regulates thyroid cell proliferation by up-regulating miR-23b and miR-29b that target SMAD3. J Clin Endocrinol Metab. 2012 Sep; 97(9):3292-301.

Li X, Luo F, Li Q, Xu M, Feng D, Zhang G, Wu W. Identification of new aberrantly expressed miRNAs in intestinal-type gastric cancer and its clinical significance. Oncol rep. 2011 Dec; 26(6): 1431-9.

Li X, Abdel-Mageed AB, Mondal D, Kandil E. MicroRNA expression profiles in differentiated thyroid cancer. A review. Int J Clin Exp Med. 2013; 6(1): 74-80.

Li W, Liu Z, Zhou L, Yao Y. MicroRNA-23b is an independent prognostic marker and suppressess ovarian cancer progression by targeting-related transcription factor-2. FEBS lett 2014 May2; 588(9): 1608-15.

Liu H, Wang B, Lin J, Zhao L. MicroRNA-29b: an emerging player in human cancer. Asian Pac J Cancer Prev. 2014;15(21):9059-64.

Livak KJ and Schmittgen TD. Analysis of relative gene expression data using real-time quantitative PCR and the 2(-Delta Delta C(T)) Method. Methods. 2001; 25(4):402-408.

Lopes JP and Fonseca E. BRAF gene mutation in the natural history of papillary thyroid carcinoma: diagnostic and prognostic implications. Acta Med Port. 2011 Dec; 24 Suppl 4:855-68.

Ma H, Ow JR, Tan BC, Goh Z, Feng B, Loh YH, Fedele M, Li H, Wu Q. The dosage of Patz1 modulates reprogramming process. Sci Rep. 2014 a Dec 17;4:7519.

Ma G, Dai W, SangA, Yang X, Gao C. Upregulation of microRNA-23a/b promotes tumor progression and confers poor prognosis in patients with gastric cancer. Int J Clin Exp Pathol. 2014 b ;7(12):8833-8840.

Majid S, Dar AA, Saini S, Deng G, Chang I, Greene K, Tanaka Y, Dahiya R, Yamamura S. MicroRNA-23b functions as a tumor suppressor by regulating Zeb1 in bladder cancer. PLoS One. 2013 Jul 2;8(7):e67686.

Mastrangelo T, Modena P, Tornielli S, Bullrich F, Testi, MA, Mezzelani A, Radice P, Azzarelli A, Pilotti S, Croce CM, Pierotti MA, Sozzi G. A novel zinc finger gene is fused to EWS in small round cell tumor. Oncogene 2000; 19:3799-37804.

Masui S, Nakatake Y, Toyooka Y, Shimosato D, Yagi R, Takahashi K, Okochi H, Okuda A, Matoba R, Sharov AA, Ko MS, Niwa H. Pluripotency governed by Sox2 via regulation of Oct3/4 expression in mouse embryonic stem cells. Nat Cell Biol. 2007 Jun;9(6):625-35.

Morii E, Oboki K, Kataoka TR, Igarashi K, Kitamura Y. Interaction and cooperation of mi transcription factor (MITF) and myc-associated zinc-finger protein-related factor (MAZR) for trascription of mouse mast cell protease 6 gene. J Biol Chem 2002; 277:8566-8571.

Mott JL, Kobayashi S, Bronk SF, Gores GJ. mir-29 regulates Mcl-1 protein expression and apoptosis. Oncogene. 2007;26, 6133-40.

Namba H, Rubin SA & Fagin JA. Point mutations of ras oncogenes are an early event in thyroid tumorigenesis. Molecular Endocrinology 1990;4:1474–1479.

Nikiforov YE. RET/PTC rearrangement in thyroid tumors. Endocrine Pathology. 2002;13 3-16.

Nikiforov YE and Nikiforova MN. Molecular genetics and diagnosis of thyroid cancer. Nat Rev Endocrinol. 2011;7(10):569-80.

Nikiforova MN, Tseng GC, Steward D, Diorio D & Nikiforov YE MicroRNA expression profiling of thyroid tumors: biological significance and diagnostic utility. Journal of Clinical Endocrinology and Metabolism. 2008; 93 1600-1608.

Nikiforova M. N, Chiosea S. I., and Y. E. Nikiforov. “MicroRNA expression profiles in thyroid tumors,” Endocrine Pathology. 2009. vol. 20, no. 2, pp. 85-91.

Nishiyama A, Xin L, Sharov AA, Thomas M, Mowrer G, Meyers E, Piao Y, Mehta S, Yee S, Nakatake Y, Stagg C, Sharova L, Correa-Cerro LS, Bassey U, Hoang, Kim HE, Tapnio R, Qian Y, Dudekula D, Zalzman M, Li M, Falco G, Yang HT, SL Lee, M Monti, I Stanghellini, MN Islam, R Nagaraja, I Goldberg, W Wang, Longo DL, Schlessinger D, Ko MS. Uncovering early response of gene regulatory networks in ESCs by systematic induction of transcription factors. Cell Stem Cell. 2009; 5:420-433.

Ow JR, Ma H, Jean A, Goh Z, Lee YH, Chong YM, Soong R, Fu XY, Yang H, Wu Q. Patz1 regulates embryonic stem cell identity. Stem Cells Dev. 2014 May 15;23(10):1062-73.

Paes JE, Ringel MD. Dysregulation of the phosphatidylinositol 3-kinase pathway in thyroid neoplasia. Endocrinol Metab Clin North Am 2008 Jun;37(2):375-87.

Pallante P, Visone R, Ferracin M, Ferraro A, Berlingieri MT, Troncone G, Chiappetta G, Liu CG, Santoro M, Negrini M, Croce CM, Fusco A MicroRNA deregulation in human thyroid papillary carcinomas. Endocr Relat Cancer. 2006 Jun;13(2):497-508.

Pallante P, Visone R, Croce CM & Fusco A. Deregulation of microRNA expression in follicular cell-derived human thyroid carcinomas. Endocrine Releated Cancer 2010; 17: F91- F104.

Pallante P, Battista S, Pierantoni GM, Fusco A. Deregulation of MicroRNA expression in thyroid neoplasias. Nat Rev Endocrinol. 2014 Feb;10(2):88-101.

Pellegrino L, Stebbing J, Braga VM, Frampton AE, Jacob J, Buluwela L, Jiao LR, Periyasamy M, Madsen CD, Caley MP, Ottaviani S, Roca-Alonso L, El-Bahrawy M, Coombes RC, Krell J, Castellano L. miR-23b regulates cytoskeletal remodeling, motility and metastasis by directly targeting multiple transcripts. Nucleic Acids Res 2013; 41: 5400-5412.

Pekarsky Y, Santanam U, Cimmino A, Palamarchuk A, Efanov A, Maximov V, Volinia S, Alder H, Liu CG, Rassenti L, Calin GA, Hagan JP, Kipps T, Croce CM. Tcl1 expression in chronic lymphocytic leukemia is regulated by miR-29 and miR-181. Cancer Res. 2006 Dec 15;66(24):11590-3.

Pero R, Lembo F, Palmieri EA, Vitiello C, Fedele M, Fusco A, Bruni CB, Chiariotti L. PATZ attenuates the RNF4-mediated enhancement of androgen receptor-dependent transcription. J Biol Chem 2002; 277:3280-3285.

Pero R, Palmieri D, Angrisano T, Valentino T, Federico A, Franco R, Lembo F, Klein-Szanto AJ, Del Vecchio L, Montanaro D, Keller S, Arra C, Papadopoulou V, Wagner SD, Croce CM, Fusco A, Chiaretti L, Fedele M. POZ-, AT-HOOK-, and zinc fingercontaining protein(PATZ) interacts with human oncogene B cell lymphoma 6 (BCL6) and is required for its negative autoregulation. J Biol Chem 2012; 287(22):18308-17.

Rahib L, Smith BD, Aizenberg R, Rosenzweig AB, Fleshman JM, Matrisian LM. Projecting cancer incidence and deaths to 2030: the unexpected burden of thyroid, liver, and pancreas cancers in the United States. Cancer Res. 2014 Jun; 74(11):2913-21.

Rossing M. Classification of follicular cell-derived thyroid cancer by global RNA profiling. J Mol Endocrinol. 2013 Mar; 18;50(2):R39-51.

Ru P, Steele R, Newhall P, Phillips NJ, Toth K, Ray RB. miRNA-29b suppresses prostate cancer metastasis by regulating epithelialmesenchymal transition signaling. Mol Cancer Ther. 2012; 11, 1166-73.

Saavedra HI, Knauf JA, Shirokawa JM, Wang J, Ouyang B, Elisei R, Stambrook PJ, Fagin JA.
The RAS oncogene induces genomic instability in thyroid PCCL3 cells via the M
APK pathway. Oncogene. 2000 Aug 10;19(34):3948-54.

Sahin M, Allard BL, Yates M, Powell JG, Wang XL, Hay ID, Zhao Y, Goellner JR, Sebo TJ, Grebe SK, Eberhardt NL, McIver B. PPARgamma staining as a surrogate for PAX8/PPARgamma fusion oncogene expression in follicular neoplasms: clinicopathological correlation and histopathological diagnostic value. J Clin Endocrinol Metab. 2005 Jan;90(1):463-8.

Sakaguchi S, Hombauer M, Bilic I, Naoe Y, Schebesta A, Taniuchi I, Ellmeier W. The zinc-finger protein MAZR is part of the transcription factor network that controls the CD4 versus CD8 lineage fate of double-positive thymocytes. Nat Immunol 2010; 11:442-448.

Santanam U, Zanesi N, Efanov A, Costinean S, Palamarchuk A, Hagan JP, Volinia S, Alder H, Rassenti L, Kipps T, Croce CM, Pekarsky Y. Chronic lymphocytic leukemia modeled in mouse by targeted miR-29 expression. Proc Natl Acad Sci U S A. 2010 Jul 6;107(27):12210-5.

Santoro M, Carlomagno F, Melillo RM, Fusco A. Dysfunction of the RET receptor in human cancer. Cell Mol Life Sci. 2004 Dec;61(23):2954-64.

Shang J, Yang F, Wang Y, Wang Y, Xue G, Mei Q, Wang F, Sun S. MicroRNA-23a antisense enhances 5-fluorouracil chemosensitivity through APAF-1/caspase-9 apoptotic pathway in colorectal cancer cells. J Cell Biochem 2014; 115: 772-784.

Soares P, Trovisco V, Rocha AS, Lima J, Castro P, Preto A, Ma´ximo V, Botelho T, Seruca R & Sobrinho-Simo˜es M. BRAF rearrangements are alternative events in the etiopathogenesis of PTC. Oncogene 2003; 22:4578-4580.

Takahashi K and Yamanaka S. Induction of pluripotent stem cells from mouse embryonic and adult fibroblast cultures by defined factors. Cell. 2006 Aug 25;126(4):663-76.

Takakura S, Mitsutake N, Nakashima M, Namba H, Saenko VA, Rogounovitch TI, Nakazawa Y, Hayashi T, Ohtsuru A, Yamashita S. Oncogenic role of miR-17-92 cluster in anaplastic thyroid cancer cells. Cancer Sci. 2008 Jun;99(6):1147-54.

Tang F, Barbacioru C, Bao S, Lee C, Nordman E, Wang X, Lao K and Surani MA. Tracing the derivation of embryonic stem cells from the inner cell mass by single-cell RNA-Seq analysis. Cell Stem Cell. 2010; 6:468-478.

Tian X, Sun D, Zhang Y, Zhao S, Xiong H, Fang J. Zinc finger protein 278, a potential oncogene in human colorectal cancer. Acta Biochim Biophys Sin (Shanghai) 2008; 40:289- 296.

Tian L, Fang YX, Xue JL, Chen JZ. Four microRNAs promote prostate cell proliferation with regulation of PTEN and its downstream signals in vitro. PLoS One. 2013 Sep 30;8(9):e75885.

Tritz R, Mueller BM, Hickey MJ, Lin AH, Gomez GG, Hadwiger P, Sah DW, Muldoon L, Neuwelt EA, Kruse CA. siRNA Down-regulation of the PATZ1 Gene in Human Glioma Cells Increases Their Sensitivity to Apoptotic Stimuli. Cancer Ther. 2008; 6:865-876.

Valentino T, Palmieri D, Vitiello M, Pierantoni GM, Fusco A, Fedele M PATZ1 interacts with p53 and regulates expression of p53-target genes enhancing apoptosis or cell survival based on the cellular context. Cell Death Dis. 2013(a) Dec 12; 4:e963.

Valentino T, Palmieri D, Vitiello M, Simeone A, Palma G, Arra C, Chieffi P, Chiariotti L, Fusco A, Fedele M. Embryonic defects and growth alteration in mice with homozygous disruption of the Patz1 gene. J Cell Physiol 2013(b);228(3):646-53.

van der Laan BF, Freeman JL, Tsang RW and Asa SL. The association of welldifferentiated thyroid carcinoma with insular or anaplastic thyroid carcinoma: evidence for dedifferentiation in tumor progression. Endocr. Pathol. 1993; 4, 215-221.

Vasko VV, Gaudart J, Allasia C, Savchenko V, Di Cristofaro J, Saji M, Ringel MD & De Micco C. Thyroid follicular adenomas may display features of follicular carcinoma and follicular variant of papillary carcinoma. European Journal of Endocrinology 2004; 151: 779-786.

Venter JC, Adams MD, Myers EW, et al. The sequence of the human genome. Science 2001; 291:1304-51.

Visone R, Russo L, Pallante P, De Martino I, Ferraro A, Leone V, Borbone E, Petrocca F, Alder H, Croce CM, Fusco A. MicroRNAs (miR)-221 and miR-222, both overexpressed in human thyroid papillary carcinomas, regulate p27Kip1 protein levels and cell cycle. Endocr Relat Cancer. 2007 (a) Sep;14(3):791-8.

Visone R, Pallante P, Vecchione A, Cirombella R, Ferracin M, Ferraro A, Volinia S, Coluzzi S, Leone V, Borbone E, Liu CG, Petrocca F, Troncone G, Calin GA,Scarpa A, Colato C, Tallini G, Santoro M, Croce CM, Fusco A. Specific microRNAs are downregulated in human thyroid anaplastic carcinomas. Oncogene. 2007 Nov (b) 29;26(54):7590-5.

Wang Y, Zhang X, Li H, Yu J, Ren X. The role of miRNA-29 family in cancer. Eur J Cell Biol. 2013 Mar;92(3):123-8.

Xing M, Haugen BR, Schlumberger M. Progress in molecular-based management of differentiated thyroid cancer. Lancet. 2013 Mar 23;381(9871):1058-69.

Xu F, Zhang Q, Cheng W, Zhang Z, Wang J, Ge J. Effect of miR-29b-1* and miR-29c knockdown on cell growth of the bladder cancer cell line T24. J Int Med Res. 2013b; 41, 1803-10.

Xu H, Sun J, Shi C, Sun C, Yu L, Wen Y, Zhao S, Liu J, Xu J, Li H, An T, Zhou X, Ren L, Wang Q, Yu S. miR-29s inhibit the malignant behavior of U87MG glioblastoma cell line by targeting DNMT3A and 3B. Neurosci Lett. 2015 Mar 17;590:40-6.

Yan B, Guo Q, Fu FJ, Wang Z, Yin Z, Wei YB, Yang JR. The role of miR-29b in cancer: regulation, function, and signaling. Onco Targets Ther. 2015 Mar 3;8:539-48.

Yang WL, Ravatn R, Kudoh K, Alabanza L, Chin KV. Interaction of the regulatory subunit of the cAMP-dependent protein kinase with PATZ1 (ZNF278). Biochem Biophys Res Commun 2010; 391:1318-1323.

Yoshikawa T, Piao Y, Zhong J, Matoba R, Carter MG, Wang Y, Goldberg I and Ko MS. High-throughput screen for genes predominantly expressed in the ICM of mouse blastocysts by whole mount in situ hybridization. Gene Expr Patterns. 2006; 6:213-224.

Zhao JJ, Lin J, Lwin T, Yang H, Guo J, Kong W, Dessureault S, Moscinski LC, Rezania D, Dalton WS, Sotomayor E, Tao J, Cheng JQ. microRNA expression profile and identification of miR-29 as a prognostic marker and pathogenetic factor by targeting CDK6 in mantle cell lymphoma. Blood. 2010; 115, 2630-9.

PATZ1 acts as a tumor suppressor in thyroid cancer via targeting p53-dependent genes involved in EMT and cell migration

Gennaro Chiappetta[1,*], Teresa Valentino[2,*], Michela Vitiello[2], Rosa Pasquinelli[1], Mario Monaco[1], Giuseppe Palma[3], Romina Sepe[2,4], Antonio Luciano[3], Pierlorenzo Pallante[2], Dario Palmieri[5], Concetta Aiello[1], Domenica Rea[3], Simona Nunzia Losito[1], Claudio Arra[3], Alfredo Fusco[2,4], Monica Fedele[2]

[1]Department of Experimental Oncology, Functional Genomic Unit, National Cancer Institute "Fondazione Giovanni Pascale", IRCCS, 80131 Naples, Italy

[2]Institute of Experimental Endocrinology and Oncology (IEOS), National Research Counsil (CNR), 80131 Naples, Italy

[3]Animal Facility, National Cancer Institute "Fondazione Giovanni Pascale", IRCCS, 80131 Naples, Italy

[4]Department of Molecular Medicine and Medical Biotechnologies, University of Naples "Federico II", 80131 Naples, Italy

[5]Departments of Molecular Virology, Immunology and Human Genetics, Comprehensive Cancer Center, Ohio State University, Columbus, OH 43210, USA

[*]These authors have contributed equally to this work

Correspondence to:
Monica Fedele, **e-mail:** mfedele@unina.it
Gennaro Chiappetta, **e-mail:** g.chiappetta@istitutotumori.na.it

Keywords: thyroid cancer, PATZ1, Epithelial-Mesenchymal Transition, cell migration

Received: July 22, 2014 ***Accepted:*** November 18, 2014 ***Published:*** January 20, 2015

ABSTRACT

PATZ1, a POZ-Zinc finger protein, is emerging as an important regulator of development and cancer, but its cancer-related function as oncogene or tumor-suppressor is still debated. Here, we investigated its possible role in thyroid carcinogenesis. We demonstrated PATZ1 is down-regulated in thyroid carcinomas compared to normal thyroid tissues, with an inverse correlation to the degree of cell differentiation. In fact, PATZ1 expression was significantly further down-regulated in poorly differentiated and anaplastic thyroid cancers compared to the papillary histotype, and it resulted increasingly delocalized from the nucleus to the cytoplasm proceeding from differentiated to undifferentiated thyroid carcinomas. Restoration of PATZ1 expression in three thyroid cancer-derived cell lines, all characterized by fully dedifferentiated cells, significantly inhibited their malignant behaviors, including *in vitro* proliferation, anchorage-independent growth, migration and invasion, as well as *in vivo* tumor growth. Consistent with recent studies showing a role for PATZ1 in the p53 pathway, we showed that ectopic expression of PATZ1 in thyroid cancer cells activates p53-dependent pathways opposing epithelial-mesenchymal transition and cell migration to prevent invasiveness. These results provide insights into a potential tumor-suppressor role of PATZ1 in thyroid cancer progression, and thus may have potential clinical relevance for the prognosis and therapy of thyroid cancer.

INTRODUCTION

Carcinoma of the thyroid gland is one of the most frequent malignancies of the endocrine system, and its incidence is predicted to become the fourth leading cancer diagnosis by 2030 [1, 2]. Thyroid carcinomas are divided into well-differentiated (WDTCs), poorly differentiated (PDTCs) and anaplastic thyroid carcinomas (ATC) [3, 4]. WDTCs encompass papillary (PTCs) and follicular carcinomas (FTCs). The PTC is the most common thyroid carcinoma (80% of cases). It is often multifocal and tends to metastasize to regional lymph nodes [3]. The FTC is a

relatively rare cancer (10% of thyroid cancers) that may develop from a pre-existing benign adenoma (FTA) or directly from the normal tissue. PDTCs and ATCs, can develop *de novo* although many of them arise through the process of stepwise dedifferentiation of PTCs and FTCs [1]. In particular, ATC is a very rare (2–5% of thyroid cancers), highly aggressive and lethal tumor characterized by very undifferentiated cells, mostly insensitive to radiotherapy and conventional chemotherapy [5, 6]. PDTC has an intermediate behavior between WDTC and ATC. Similar to other cancer types, thyroid cancer initiation and progression occurs through gradual accumulation of various genetic and epigenetic alterations. Therefore, according to the theory of sequential progression from WDTC to ATC through PDTC [7], mutations occurring in the early stages of WDTCs are also reported in PDTCs and ATCs [8]. The molecular alteration discriminating ATCs from WDTCs is the inactivation of the p53 tumor suppressor gene. P53 inactivation is observed in almost all ATCs suggesting that p53 deficiency, in association with activating mutations of oncogenes such as RAS and BRAF, drive the high proliferative index and high aggressiveness of these tumors. However, inactivating mutations of p53 observed in several types of human tumors are not frequent in thyroid cancer, but studies on p53 protein expression in a large series of thyroid tumor specimens suggest that, although not mutated, p53 activity may be inhibited in thyroid cancer by other mechanisms [9].

In spite of the progressive knowledge of the molecular mechanisms involved in thyroid transformation, the prognosis of thyroid cancer remains unpredictable and the identification of new biological markers are needed in addition to already known molecules, to correctly stratify patients at risk of recurrence and progression [10].

The POZ/BTB and AT-hook-containing zinc finger protein 1 (PATZ1) is a transcriptional regulatory factor also known as Zinc finger Sarcoma Gene (ZSG), MAZ-Related factor (MAZR) or Zinc Finger Protein 278 (ZNF278/Zfp278). PATZ1 has been demonstrated to regulate, either positively or negatively, the expression of different genes depending on the cellular context [11–17].

Several studies suggest a role for PATZ1 in cancer but its cancer-related function as oncogene or tumor suppressor is still debated. PATZ1 oncogenic role is supported by its overexpression in human malignant neoplasias, including colon and breast tumors [18, 19] and its down-regulation by siRNAs either blocks the growth or induces apoptosis of cell lines derived from colorectal cancer or gliomas, respectively [18, 20]. Similarly, we previously demonstrated that PATZ1 is overexpressed in testicular tumors, but protein localized into the cytoplasm rather than into the nucleus, suggesting a reduction of its transcriptional function [21]. Recently, we showed that PATZ1-knockout mice develop lymphomas and other neoplasias, indicating PATZ1 as a potential tumor-suppressor in lymphomagenesis and likely other tumors [17].

In this study we have analyzed PATZ1 expression and function in human thyroid cancer, identifying a potential tumor suppressor role in this type of cancer, mainly involved in inhibition of epithelial-mesenchymal transition (EMT) and cell migration.

RESULTS

PATZ1 is down-regulated and delocalized in thyroid cancer

The expression of *PATZ1* gene was analyzed, by quantitative RT-PCR (qRT-PCR), in human thyroid cancer cell lines and tissues compared to normal thyroids (NT).

The thyroid cancer cell lines used were derived from papillary (TPC1, BC-PAP), follicular (WRO) and anaplastic (FRO, FB1, ACT1, 850-5c) thyroid carcinomas. As shown in Figure 1A, in all the analyzed cell lines, *PATZ1* expression was significantly reduced compared to normal control, represented by mean value of three normal thyroid tissues.

The analysis of PATZ1 expression on tissue samples, carried out on 5 NTs, 28 PTCs, 4 FTCs, 2 PDTCs and 11 ATCs, showed a significant down-regulation of *PATZ1* in 64% of PTCs, 91% of ATCs and 100% of FTCs and PDTCs (Figure 1B). Indeed, as shown in Figure 1C, the multiple comparison analysis of the results demonstrated that PATZ1 was not only significantly downregulated in PTC ($P < 0.05$), FTC ($P < 0.01$) and PDTC/ATC ($P < 0.0001$) *versus* NT, but also it was significantly further down-regulated in PDTC/ATC *versus* PTC ($P < 0.001$).

These results indicate that PATZ1 expression is negatively associated with thyroid cancer progression, suggesting it could play a tumor suppressor role in thyroid cancer, mainly involved in the late stages of carcinogenesis.

Subsequently, we analyzed PATZ1 protein expression and localization by immunohistochemistry (IHC). The analysis was performed on paraffin embedded normal and neoplastic thyroid samples, including 27 NTs, 2 goiters, 11 FTAs, 33 PTCs, 12 FTCs, 5 PDTCs and 18 ATCs. All samples of normal thyroid parenchyma and goiters expressed PATZ1 at a high level in the nucleus, which coincides with the strong PATZ1 staining in all follicles. Conversely, compared to normal samples, PATZ1 expression in the nucleus was found to be weaker in a high percentage of FTAs (73%), PTCs (36%) and FTCs (50%), and weak or completely negative in most PDTCs (100%) and ATCs (83%) (Figure 2 and Table 1). Interestingly, PATZ1 protein showed a progressive displacement from the nucleus to the cytoplasm with a direct correlation with the undifferentiated and malignant phenotype. Indeed, in all NTs (100%, 27/27) and goiters (100%, 2/2) analyzed, PATZ1 was expressed and present only in the nucleus, while in most FTAs (64%), PTCs (82%) and FTCs (100%), PATZ1 protein was partially or completely

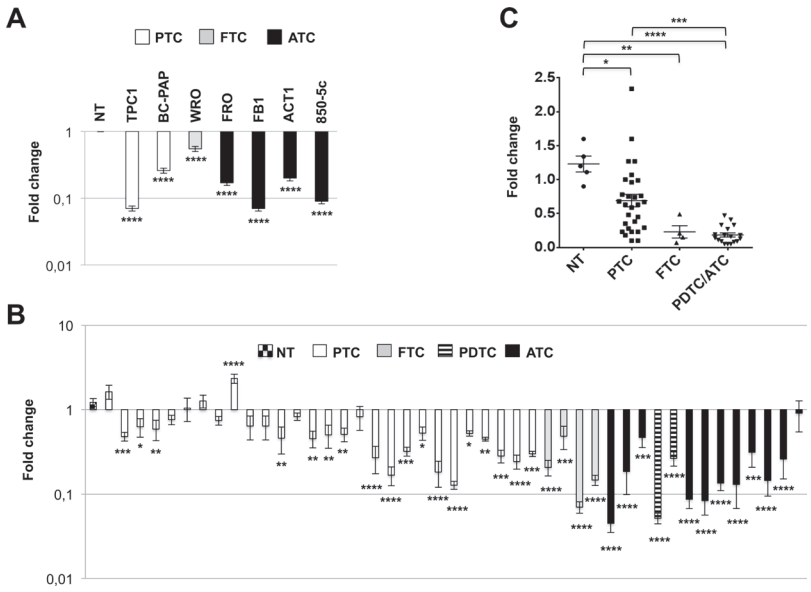

Figure 1: PATZ1 expression in human thyroid cancer cell lines and tissues. (A) qRT-PCR analysis of *PATZ1* in 2 PTC-derived cell lines (TPC1 and BC-PAP), 1 FTC-derived cell line (WRO) and 4 ATC-derived cell lines (FRO, FB1, ACT1, 850-5c) in comparison with 3 normal thyroid gland tissues, whose mean value of expression was set to 1. Mean values ± SE of triplicate samples compared to each normal control are shown. NT = mean value ± SE of the three normal thyroid tissues used as control. **(B)** qRT-PCR analysis of *PATZ1* in 28 PTCs, 4 FTCs, 2 PDTC and 11 ATCs in comparison with mean value of 5 normal thyroid samples (first lane). Mean values ± SE of two independent experiments for each sample, performed in duplicate, compared to each normal control, which has been set to 1, are shown. All values in A and B are shown in a logarithmic scale and were analyzed by one-way ANOVA followed by Dunnett's multiple comparison test. **(C)** All samples shown in B were grouped for histotype and analyzed by one-way ANOVA followed by Tukey's multiple comparison test. Mean values ± SE are shown. *, $P < 0.05$; **, $P < 0.01$; ***, $P < 0.001$; ****, $P < 0.0001$.

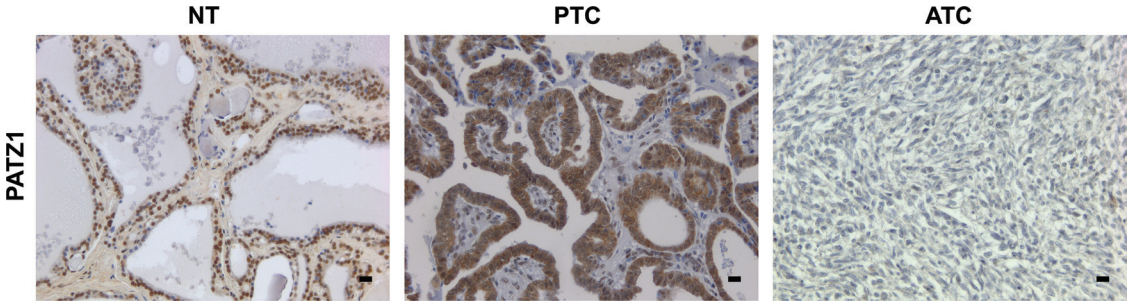

Figure 2: Representative images of PATZ1 staining in normal thyroid (NT), papillary thyroid carcinoma (PTC) and anaplastic thyroid carcinoma (ATC). PATZ1 staining was intense in the nucleus of normal thyroid tissue; it is present also in the cytoplasm of PTC; it was absent in ATC. Scale bars = 100 nm.

localized into the cytoplasm. In 60% (3/5) of PDTCs PATZ1 protein was localized only in the cytoplasm as in 11% of ATCs. Moreover, in 20% of PDTCs and in 22% of ATCs, PATZ1 expression was completely absent (Table 1). These results confirmed an inverse correlation between PATZ1 expression and the thyroid malignant phenotype.

PATZ1 expression inhibits growth of BC-PAP and FRO cells

To determine whether the expression of PATZ1 plays a role in thyroid cancer cell growth, we carried out colony-forming assays in three thyroid cancer cell lines (TPC1, BC-PAP and FRO), transfected with a vector coding for the human PATZ1 variant 4 (HA-PATZ) or the empty vector (pCEFL-HA). As shown in Figure 3A, in both BC-PAP and FRO cells an evident decrease of the colony number was detected in PATZ1 transfected cells compared to controls. Conversely, no appreciable differences were found in TPC1 cells transfected with PATZ1 or the empty vector.

Next, in order to deeply investigate a possible causal role of PATZ1 in thyroid cancer cell proliferation and other thyroid cancer cell functions, we transfected a PATZ1-EGFP-C2 plasmid carrying human PATZ1 variant 4 cDNA, or the empty vector pEGFP-C2 into the three

Table 1: PATZ1 nuclear expression and sub-cellular localization

		Nuclear anti-PATZ1 reactivity			PATZ1 sub-cellular localization			
Hystotype	**N.**	**Negative**	**Weak**	**Strong**	**Nuclear**	**Nucl/cyt**	**Cytosol**	**Negative**
NT	27	0	6 (22%)	21 (78%)	27 (100%)	0	0	0
Goiter	2	0	0	2 (100%)	2 (100%)	0	0	0
FTA	11	2 (18%)	8 (73%)	1 (9%)	4 (36%)	6 (54%)	1 (9%)	1 (9%)
PTC	33	0	12 (36%)	21 (64%)	6 (18%)	27 (82%)	0	0
FTC	12	0	6 (50%)	6 (50%)	0	12 (100%)	0	0
PDTC	5	4 (80%)	1 (20%)	0	0	1 (20%)	3 (60%)	1 (20%)
ATC	18	6 (33%)	9 (50%)	3 (17%)	7 (39%)	5 (28%)	2 (11%)	4 (22%)

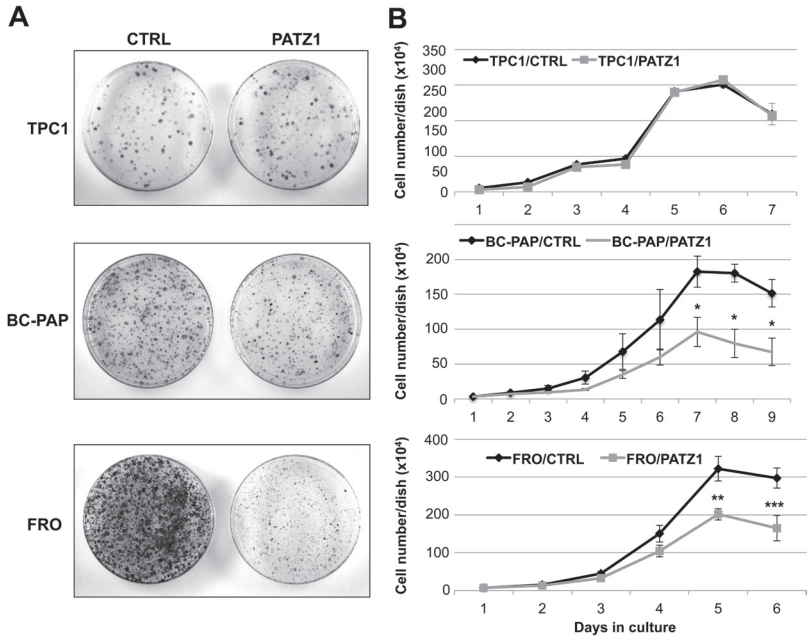

Figure 3: Analysis of cell growth in PATZ1-transfected thyroid cancer cells. (A) Colony-forming assays in human thyroid cancer cell lines transfected with PATZ1. TPC-1, BC-PAP and FRO cells were transfected with a vector expressing PATZ1 cDNA or its corresponding empty vector. Cells were cultured for 10 days, selected for resistance to G418, and stained with crystal violet. **(B)** Growth curves on different stably expressing PATZ1 cell clones and/or mass populations of TPC1, BC-PAP and FRO cells compared to controls expressing the empty vector. Mean values ± SE of at least three clones for each cell line are reported: For TPC1, clone C-1, parental TPC1 and mock-transfected mass population were used as control, whereas clones PA1, PA5 and PA6 were used as PATZ1-transfected cells; for FRO, clones C-4, C-7 and parental FRO were used as control, whereas clones PA11, PA13 and PA17 were used as PATZ1-transfected cells; for BC-PAP, clone C-1, parental BC-PAP and mock-transfected mass population (mp C-) were used as control, whereas PA2, PA3, PA7, PA10 and PATZ1-transfected mass population (mp PA) were used as PATZ1-transfected cells. PATZ1 expression in each clone or mass population is shown in supplementary Figure S1. *, $P < 0.05$; **, $P < 0.01$; ***, $P < 0.001$.

thyroid cancer cell lines already used for the colony assays and selected mass populations and/or cell clones in which PATZ1 expression was stably up-regulated compared to parental cells transfected with the empty vector (supplementary Figure S1).

To confirm the results of the colony assays and deeper investigate the cause of growth inhibition, we performed growth curves and cell viability assays on selected clones of TPC1/PATZ1, BC-PAP/PATZ1 and FRO/PATZ1 compared to their respective controls (Figure 3B). In agreement with the results from the colony assays, the growth rate of TPC-1/PATZ1 clones did not show any difference compared to control. Conversely, BC-PAP/PATZ1 clones, and FRO/PATZ1 clones, showed decreased proliferation capacity, starting to be significant at 7 or 5 days of cell culture, respectively, without differences in trypan blue incorporation (data not shown), compared to control cells.

PATZ1 expression inhibits cell migration and invasion of TPC-1, BC-PAP and FRO cells

Next, using a wound-healing assay, we tested the migration capacity of PATZ1-transfectants, showing that it was significantly reduced in FRO/PATZ1 compared with the control cells (Figure 4A–4B). Conversely, no significant differences were observed in BC-PAP and TPC1 cells (data not shown). These data indicate that PATZ1 can inhibit migration of thyroid cancer cells, but also suggest that this role is cell context-dependent. However, the wound-healing assay is particularly suitable for studying the effects of cell-matrix and cell-cell interactions on cell migration, but does not give insights on migration in response to a particular chemical signal, which is usually referred to as chemotaxis. To better investigate this issue we analyzed cell migration across 8-μm membrane pores in response to FBS. At 24 h after seeding, all PATZ1-transfected clones, including TPC1, BC-PAP and FRO cells, migrated less than empty vector control cells (Figure 4C–4D). At this experimental time, influence of PATZ1 in cell proliferation was absent (supplementary Figure S2). Next, we also directly examined the *in vitro* capacity of these cells to invade through a Matrigel-coated membrane, which has been reported to mimic the whole process of invasion, including adhesion to a substrate, dissolution of the extracellular matrix and migration [25]. Using this assay, we observed a decrease in invading capacity of PATZ1-transfected cells compared to empty vector controls, that reached significant levels in FRO and BC-PAP and was close to be significant in TPC1 cells (supplementary Figure S3). All together these results indicate that PATZ1 has a key role in suppressing migration and invasiveness of thyroid cancer cells, but also suggest that this role could involve different aspects of cell migration in different cellular contexts.

PATZ1 expression inhibits tumorigenicity of FRO cells and induces a mesenchymal-epithelial-like transition

To characterize the malignant phenotype of the stable transfectants, we analyzed their ability to grow in soft agar. Only parental and backbone vector-transfected FRO cells were able to form large, progressively growing colonies. In contrast, FRO/PATZ1 transfectants showed a drastic

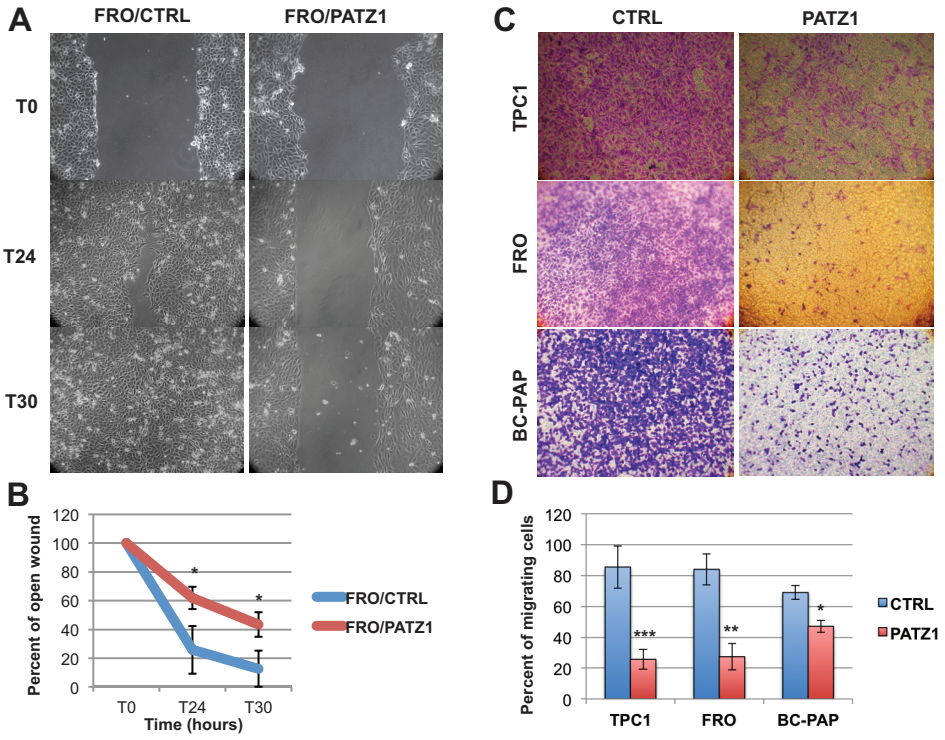

Figure 4: PATZ1 inhibits cellular migration in TPC1, FRO and BC-PAP cells. (A) Representative images of a wound healing assay in control (CTRL) and PATZ1-expressing FRO cells at 0, 24 h and 30 h after a confluent cell monolayer was wounded. **(B)** Percent of open wound calculated as mean values ± SE of two FRO/CTRL (C-4 and C-7) and four FRO/PATZ1 cell clones (PA2, PA10, PA11 and PA13). **(C)** Representative images of a transwell assay in CTRL and PATZ1-expressing TPC1, FRO and BC-PAP cells. Migrating cells were stained with crystal violet. **(D)** The number of migrating cells was calculated by measuring the percentage of stained cells. Mean values ± SE of at least 3 different clones (C-1, parental TPC1, PA1, PA5 and PA6 for TPC1; C-4, C-7, parental FRO, PA2, PA13, PA16 and PA17, for FRO; mp C-, mp PA, PA2, PA3, PA7 and PA10 for BC-PAP) in 3 independent experiments are reported. PATZ1 expression in each clone or mass population is shown in supplementary Figure S1. *, $P < 0.05$; **, $P < 0.01$; ***, $P < 0.001$.

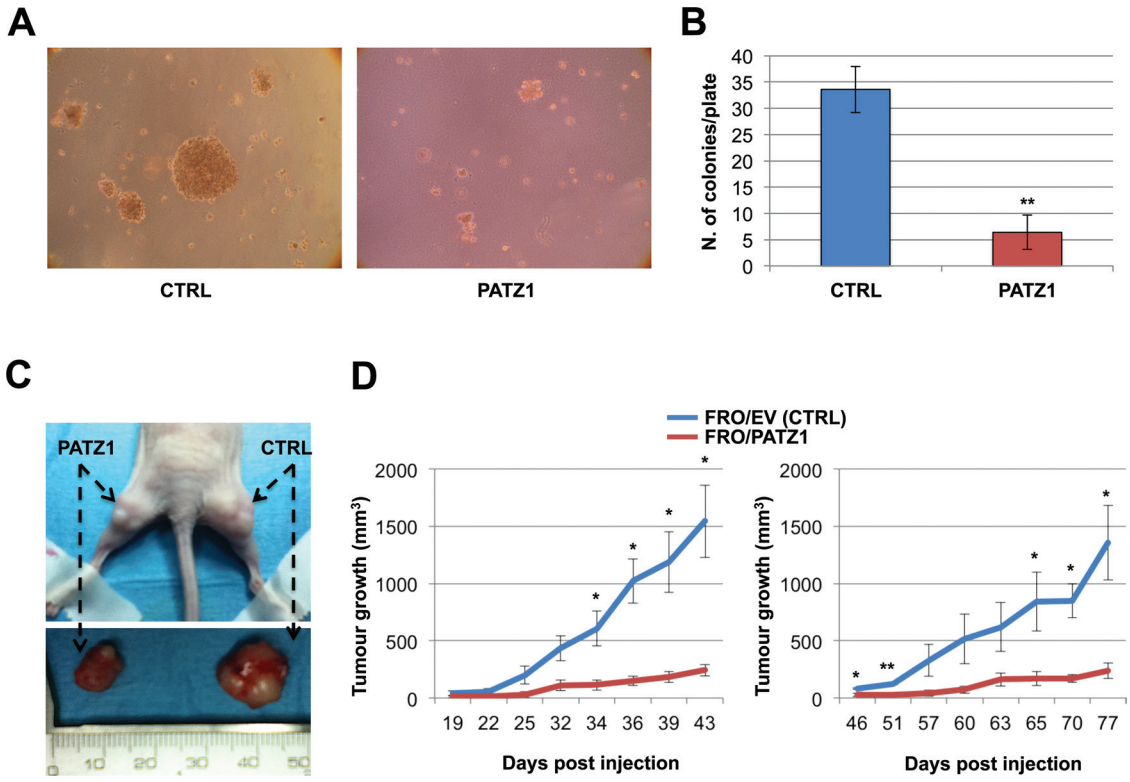

Figure 5: PATZ1 inhibits *in vitro* and *in vivo* tumorigenicity in FRO cells. (A) Representative images of growth in soft agar of control (CTRL) and PATZ1-expressing FRO cells. **(B)** Colonies larger than background (as observed in normal control cells) were counted after 2 weeks. Mean values ± SE of two controls (C-4 and parental FRO) and three PATZ1-expressing clones (PA13, PA16, PA17) are reported. PATZ1 expression in each clone is shown in supplementary Figure S1. **, $P < 0.01$. **(C)** Representative nude mouse (upper panel) injected with FRO/PATZ1 cells (clone PA13) at the left side and FRO/EV (CTRL) cells (clone C-4) at the right side. Tumors (lower panel) were excised when one of the two contralateral tumors reached the cut-off of 1500 mm^3. **(D)** Tumor growth curves in cohorts of 3 mice (left panel) and 4 mice (right panel). Mean values ± SE are reported. *, $P < 0.05$; ** $P < 0.01$. FRO/EV = empty vector-transfected FRO cells.

reduction in colony-forming efficiency (Figure 5A–5B). Both TPC1 and BC-PAP cell lines, with or without transfected PATZ1, did not form any colony in soft agar (data not shown). We next investigated the capacity of FRO/PATZ1 and their controls to generate tumor xenografts in nude mice. Tumor growth was observed in 7 out of 7 mice injected with empty vector-transfected FRO (FRO/EV) and 7 out of 7 mice xenografted with FRO/PATZ1 cells. However, size and growth rate of tumors derived from FRO/PATZ1 cells were drastically reduced compared to those of tumors generated by control cells injected into the contralateral leg (Figure 5C–5D). The histopathological analysis of the tumors, excised at the end of their growth observation, revealed that, unlike all FRO/EV-induced tumors, in which tumor tissue was composed of anaplastic cells irregularly arranged in a mass with solid aspects, 4/7 FRO/PATZ1-derived xenografts appeared heterogeneous with some areas displaying a phenotypic switch towards a better organized structure with epithelial-like features, sometimes resembling follicular structures (Figure 6). Interestingly, only in FRO/PATZ1 tumors showing follicular-like structures we observed overexpression of PATZ1, due to residual areas of cells expressing PATZ1, whereas in all the others PATZ1 expression was completely lost, as in tumors originated from control-transfected cells (supplementary Table S1 and Figure S4). It is likely that cells in which PATZ1 expression is lost are able to grow faster *in vivo*, giving rise to tumors that phenocopy the anaplastic tumor from which FRO cells originated. Conversely, PATZ1-expressing cells grow slower and the general tumor growth is likely due to those cells in which expression of PATZ1 was lost, which tend to prevail over those expressing PATZ1. Moreover, consistent with a possible association between PATZ1 expression and mesenchymal-epithelial transition, in tumor areas showing expression of PATZ1 and follicular-like structures we observed positive staining for E-cadherin (Figure 6).

PATZ1 expression activates the p53 pathway involved in the block of EMT, migration and invasiveness

To gain insight into the molecular mechanisms involved in PATZ1-mediated inhibition of cell migration, we analyzed expression of a panel of genes playing

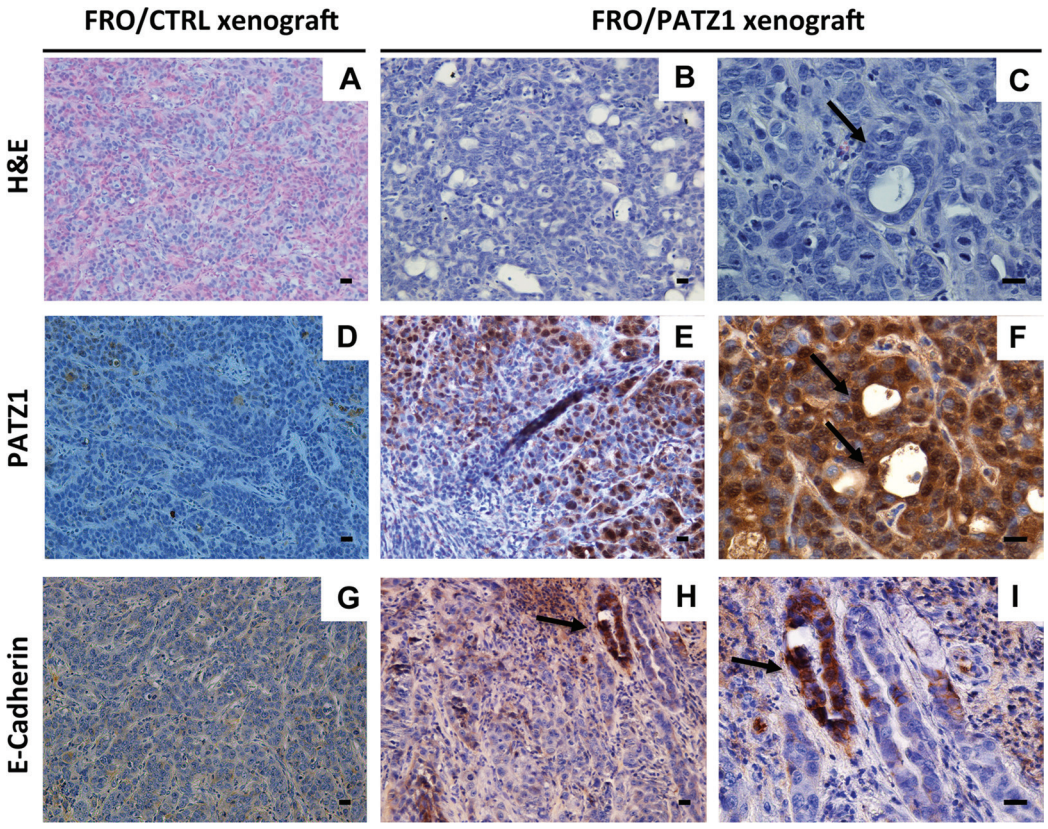

Figure 6: FRO/PATZ1 xenografts showed an epithelial-like phenotype. Representative images of tumor tissues derived from nude mice injected with FRO/PATZ1 **(B, C, E, F, H, I)** or control (CTRL) cells **(A, D, G)** from the experiments shown in Figure 5C. Tumors developed from PATZ1-expressing cells showed features of epithelial-like differentiation represented by follicular-like structures (arrows). Consistently, E-cadherin immunostaining revealed a strong positive reaction in such follicular-like structures (H, I). Immunostaining for PATZ1 showed strong expression of PATZ protein in delimited areas including cells with an epithelial-like phenotype (E, F), whereas it was negative in all the other areas of PATZ1 xenografts (E) and in CTRL counterparts (D) Scale bars = 100 nm. H&E = hematoxilin and eosin staining.

crucial roles in this key stage of metastatic progression. In particular, we focused on genes downstream of p53, because of recent data showing a functional interaction between PATZ1 and p53 [11, 26], analyzing their expression before and after a stimulus to migrate. To this aim, TPC1/PATZ1, FRO/PATZ1, BC-PAP/PATZ1 transfectants and their respective controls were starved for 48 h and then stimulated with epidermal growth factor (EGF) for 24 h. It is known that p53 maintains a transcriptional program to prevent EMT by downregulating genes, such as EpCAM, that inhibit molecules involved in stabilizing cell-cell junctions (such as E-cadherin), or by directly inhibiting components of the adhesive machinery, such as Fibronectin, that are known to contribute to cell motility through the stroma [27]. p53-regulated genes also include molecules involved in inhibition of podosome formation, such as the actin-binding protein Caldesmon, which is up-regulated by p53 [28]. Finally, p53 can also up-regulate molecules that control actin dynamics, such as RhoE and NOTCH, which both converge in the inhibition of cytoskeletal changes accompanying tumor cell migration and invasion [27]. It is noteworthy that *TP53* gene is hypo-fuctioning, but wt in FRO and TPC1 cells [29, 30], whereas it is mutated in BC-PAP cells [30]. As shown in Figure 7A, by (q)RT-PCR, expression of *EpCam* and *Caldesmon* in all three cell lines, and *RhoE* in TPC1 and BC-PAP cells, were significantly changed in PATZ1 expressing clones compared to control cells. Conversely, no changes were observed in *RhoE* and *Fibronectin* gene expression, in FRO and all three cell lines, respectively, between PATZ1-expressing clones and controls. In particular, *EpCam* expression was downregulated about 3-fold in FRO control cells following treatment with EGF, and significantly further downregulated, up to about 5-fold, in FRO clones expressing PATZ1 (Figure 7A); *Caldesmon* and RhoE were up-regulated about 2-fold and 1.5-fold, respectively, in TPC1 control cells following treatment with EGF, and further up-regulated, up to about 3- and 7-fold, respectively, in TPC1 clones expressing PATZ1 (Figure 7A). All together these results suggest that in both FRO and TPC1 cells a partial functional p53 protein, at least on the *EpCam* promoter in FRO cells and on the Caldesmon and RhoE promoters in TPC1 cells, is present

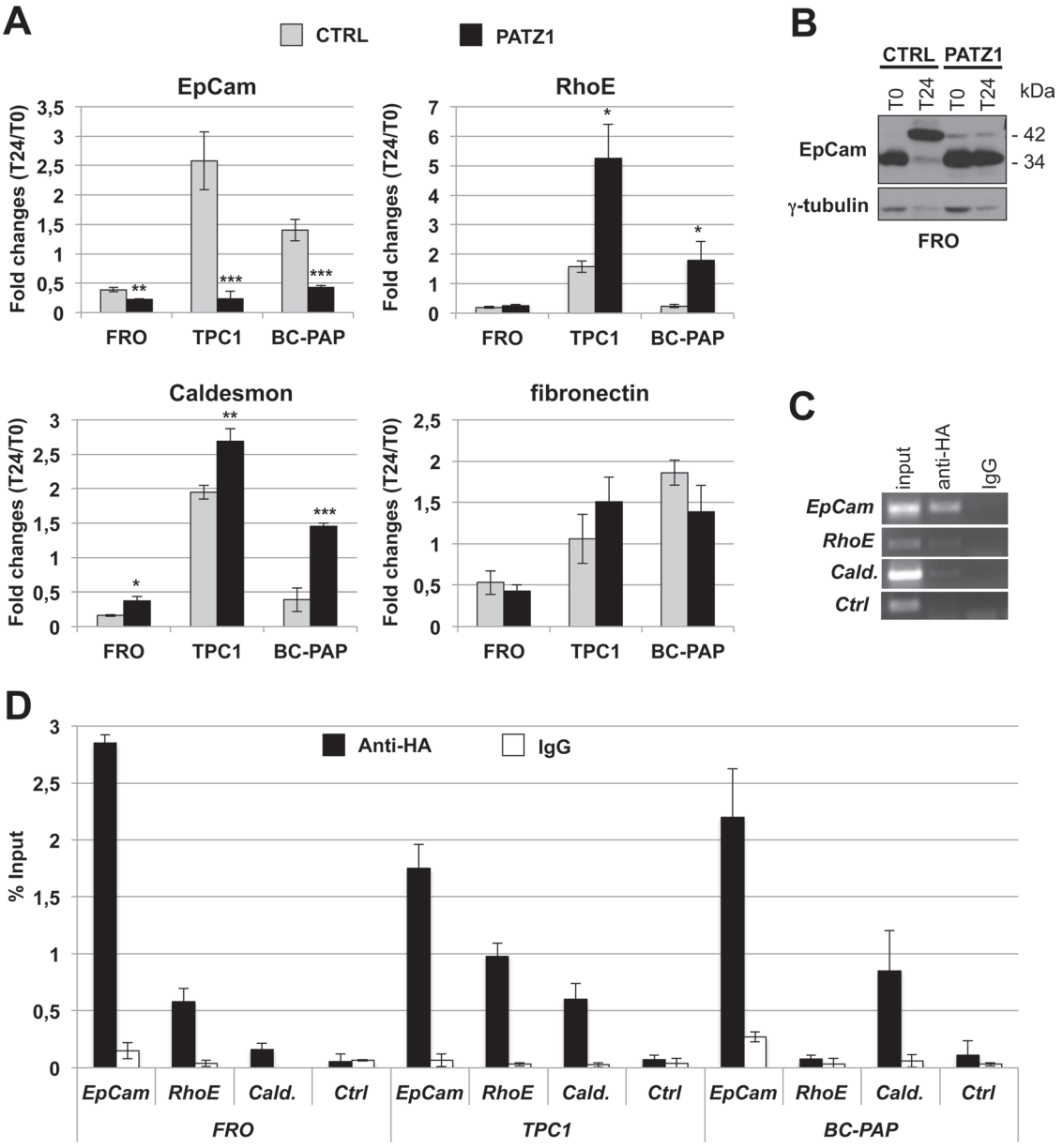

Figure 7: PATZ1 re-introduction affects expression of p53 target genes involved in EMT, migration and invasion. (A) FRO/PATZ1, TPC1/PATZ1, BC-PAP/PATZ1 transfectants and their respective controls were starved for 48 h (T0) and then stimulated with epidermal growth factor (EGF) for 24 h (T24). qRT-PCR showing expression, measured as fold changes at T24 with respect to T0, of *EpCAM*, *Caldesmon*, *RhoE* and *Fibronectin* genes. Mean values ± SE of two or three independent clones are reported. For TPC1, parental TPC1 and clone C-1 were used as control, whereas clones PA1, PA5 and PA6 were used as PATZ1-transfected cells; for FRO, clones C-4 and parental FRO were used as control, whereas clones PA11 and PA17 were used as PATZ1-transfected cells; for BC-PAP, parental BC-PAP, clone C-1 and mock-transfected mass population (mp C-) were used as control, whereas PA7, PA10 and PATZ1-transfected mass population (mp PA) were used as PATZ1-transfected cells. PATZ1 expression in each clone or mass population is shown in supplementary Figure S1. *, $P < 0.05$; ** $P < 0.01$. **(B)** Western blot analysis of EpCam expression in FRO cells at 0 h (T0) and 24 h (T24) from EGF treatment. Where indicated, CTRL = control; PATZ1 = PATZ1-expressing cells. **(C)** representative ChIP experiments in FRO cells, transiently transfected with HA-PATZ1 and immunoprecipitated with anti-HA Ab, to detect *in vivo* binding of PATZ1 to *EpCam (-218/-65)*, *RhoE (-2239/-2183)* and *Caldesmon (-106/-2)* promoter regions. IgG = not-specific Ab, *Cald*. = Caldesmon, *Ctrl = Caldesmon* region *-951/-841*, Input = PCR products with genomic DNA without immunoprecipitation. **(D)** Semi-quantitative analysis of ChIP assays on FRO, TPC1 and BC-PAP cells performed by densitometric evaluation of the gels (ImageJ64 software). Results shown are the mean values ± SD of two independent experiments for each gene and cell line, expressed as percentage of PATZ1 immunoprecipitated DNA relative to the Input. IgG and *Ctrl* abbreviations are as in (C).

but its activity can be enhanced by PATZ1, which appears to cooperate with p53 in opposing to EMT in FRO cells and to cell motility and invasiveness in TPC1 cells.

Conversely, as expected by the presence of a mutant p53 in BC-PAP cells [30], treatment with EGF in these cells resulted in an opposite regulation of the above mentioned genes, including upregulation of *EpCam* and *Fibronectin*, and down-regulation of *Caldesmon* and *RhoE*, with the consequent activation of the EMT and cell migration programs (which are not opposed by a functional p53). Importantly, in BC-PAP/PATZ1 transfectants these functions are partially or totally rescued. In fact, as shown in Figure 7, following EGF treatment, *EpCam* was up-regulated in BC-PAP control cells, whereas it was downregulated in 2 out of 3 PATZ-expressing BC-PAP clones. Similarly, *Caldesmon* and *RhoE* were downregulated in BC-PAP control cells, whereas they were upregulated in PATZ1 transfectants. Notably, *EpCam* resulted up-regulated also in TPC1 control cells following EGF treatment, but this behaviour was completely reverted in TPC1/PATZ1 clones. These results suggest that PATZ1 can activate the p53 pathway opposing EMT, migration and invasiveness also in presence of a mutant p53.

Subsequently, to assess a direct action of PATZ1 on transcription of these genes, we performed ChIP assays to avaluate PATZ1 protein binding to their promoters. Therefore, TPC1, FRO and BC-PAP cells, transiently transfected with a HA-tagged PATZ1 expression vector, were cross-linked and immunoprecipitated with anti-HA or isotype-matched preimmune IgG. Immunoprecipitation of chromatin was then analyzed by qualitative PCR, using primers spanning regions including the binding site for p53 or potential consensus elements for PATZ1. As shown in Figure 7C–7D, PATZ1 binding to *EpCam* and *Caldesmon* genes was detected in all three cell lines, binding to *RhoE* was detected in TPC1 and FRO cells, whereas a distal region on the *Caldesmon* promoter (*Ctrl*) was not amplified in any cell line, strenghtening the specificity of the binding of PATZ1 detected in the ChIP assays.

Only for EpCam, which has been recently suggested to be involved in the development of the aggressive phenotype of ATC [31] and has evoked significant interest as a target in cancer therapy [32] we analyzed protein expression changes in proliferating, starved (T0) and EGF-induced (T24) FRO, TPC1 and BC-PAP cells. Consistent with the work of Okada et al [31], reporting that EpCam protein was expressed only in anaplastic–derived thyroid cancer cell lines, we detected EpCam expression by Western blot only in FRO cells (Figure 7B and data not shown). Interestingly, EpCAM appeared to undergo a post-translational modification following treatment with EGF, as suggested by the uppershift of the protein size. This change appears to be inhibited by the presence of PATZ1 (Figure 7B).

DISCUSSION

Despite an increasing body of evidences is highlighting PATZ1 as a cancer-related gene [15–21], little is known about its function. A dual role favoring transformation or protecting from it, depending on the cellular context, seems to apply for the PATZ1 protein [11]. However, still few tumors have been analyzed for PATZ1 expression and function. Here we focus on thyroid cancer, one of the most frequent malignancies of the endocrine system, whose mechanisms of transformation are still far from being completely elucidated [1]. We first analyzed a wide panel of thyroid cancer cell lines and tissues, observing that PATZ1 is expressed at significantly lower levels compared to normal thyroid tissues. Moreover, PATZ1 protein is partially or completely delocalized from nucleus to cytoplasm in most of carcinoma samples. Interestingly, PATZ1 downregulation, as well as its cytoplasmic localization, correlates with the acquisition of a less differentiated phenotype, suggesting that PATZ1 loss and cytoplasmic localization could be considered as a valid marker of an undifferentiated, mesenchymal and aggressive phenotype. Notably, we showed that PATZ1 is strongly downregulated in all the thyroid cancer cell lines analyzed. However, despite their different origin, these cell lines have gene expression profiles more closely related to each other than to the *in vivo* differentiated tumors they were derived and have characteristics of fully dedifferentiated cells, close to undifferentiated carcinomas [33].

Therefore, choosing the thyroid cancer cell lines TPC1, BC-PAP and FRO, as cellular models for undifferentiated tumors, we showed that in all of them reintroduction of PATZ1 leads to inhibition of cellular capacity to migrate and invade, supporting a role for PATZ1 in opposing the late steps of thyroid transformation, consisting in the acquisition of a mesenchymal phenotype (EMT), capable to migrate and invade surrounding tissues, thus giving rise to local and distal metastases. Consistent with the involvement of PATZ1 in EMT, it has been recently shown that PATZ1 is part of a group of transcription factors, including proteins already linked to EMT, such as EGR-1, Sp1, Sp2, NME1, CTCF, PLAG1 and WT1, potential regulators of TGF-β1 [34]. PATZ1 reintroduction in BC-PAP and FRO cells also affected cell proliferation, suggesting a possible role for PATZ1 in this cellular function depending on the cellular context. We finally showed that PATZ1 significantly inhibits FRO tumorigenic potential both *in vitro* and *in vivo*. Interestingly, tumors grafted from PATZ1-expressing cells showed some epithelial-like features, including follicular-like structures and E-cadherin expression. Notably, the tumor areas displaying such features were also enriched in PATZ1 expression, supporting the idea that PATZ1 could have a direct role in a mesenchymal to epithelial transition (MET)-like state. Consistently, the majority

of the tumors derived from the injection of PATZ1-cells resulted mostly negative for PATZ1 expression and displayed a mesenchymal phenotype similar to those arisen from control cells. Therefore, it is likely that PATZ1 has been negatively selected *in vivo* as a way to allow an EMT phenotype.

EMT is involved in many biological processes including embryonic development, wound-healing and cancer progression [35]. In thyroid cancer it seems to be specifically involved in the development of ATCs [36], but there are evidences of its involvement also in local invasion of PTCs [37]. It is increasingly acknowledged that EMT plays an important role in the metastasis of many types of carcinomas [38, 39] and has been implicated in therapeutic resistance and tumor recurrence [40, 41]. Therefore, the identification of genes able to modulate these cellular processes has a great potential for a targeted cancer therapy. One of the major players opposing to EMT is the tumor suppressor p53 protein, whose loss has been shown to influence motility contributing to the invasive and metastatic potential of cancer cells [27]. In particular, it has been shown that p53 maintains a transcriptional program to prevent EMT and that loss of this suppression may contribute to the induction of an EMT-like phenotype [42, 43].

Recent data, showing that PATZ1 is able to interact with p53 and to directly regulate transcription of p53-regulated genes [11], suggested a possible mechanism by which PATZ1 may be involved in EMT. Consistently, we observed that PATZ1 binds *in vivo* some of the p53-regulated genes involved in preventing EMT, and its overexpression causes changes in their expression changes associated to the stimulation of cell migration by EGF. Importantly, in cells carrying a wild-type *TP53* gene, such as TPC1 and FRO, the resulting effect is a potentiation of the transcriptional program opposing EMT, migration and invasiveness. Conversely, in cells carrying a mutant *TP53* gene, such as BC-PAP, the presence of PATZ is only partially able to activate such program, indicating that PATZ1 is not sufficient to regulate these p53-dependent genes in presence of a mutant p53. Interestingly, PATZ1 expression seems to affect expression of different genes depending on the cellular context: in FRO cells it downregulates *EpCAM*, involved in the inhibition of E-cadherin [27], and upregulates *Caldesmon*, implicated in the inhibition of invadopodia [27]; in TPC1 cells it upregulates *RhoE*, implicated in the inhibition of cytoskeletal changes accompanying tumor cell migration [27], and *Caldesmon*, whereas downregulates *EpCam*; in BC-PAP cells it modulates all three of these genes. The absence of PATZ1 binding to the *RhoE* promoter in BC-PAP cells suggests that a functional p53 gene is required for this binding. However, we cannot exclude that in this cell line, EGF treatment is necessary to induce binding of PATZ1 to this gene. Further experiments are needed to better elucidate the dynamic of PATZ1 binding to these genes in the different cell lines and in relation to the presence/absence of a functional p53 protein.

Notably, when we looked at protein expression levels of EpCam, a protein that recently acquired increased interest for its multiple roles in enhancing tumorigenesis [32], and has been reported to be involved in the aggressive phenotype of ATCs [31], we found that PATZ1 expression affects hyper-glycosylation of the protein associated with the EGF treatment of the cells. According to a previous report [44], this could have effects on EpCam stability, with likely consequences on its pro-tumorigenic functionality. Therefore, PATZ1 overexpression in FRO cells affects EpCam expression at both RNA and protein levels, and this may account for the suppressor role of PATZ1 on EMT.

In conclusion, we demonstrated that PATZ1 exerts an oncosuppressor role in thyroid cancer, particularly in the progression to an anaplastic phenotype, through the regulation, at least in part, of p53-target genes *EpCam*, *RhoE* and *Caldesmon*, thus resulting in reduced migration and invasion *in vitro*, as well as MET and reduced tumor growth *in vivo*.

METHODS

Tissue collection

Thyroid tissues were collected at the Istituto dei Tumori di Napoli, Italy and the Service d'Anatamo-Pathologie, Centre Hospitalier Lyon Sud, Pierre Benite, France. For each tumor, some fragments were frozen and stored in liquid nitrogen, others were fixed in 4% paraformaldehyde and embedded in paraffin. Informed consent for the scientific use of biological material was obtained from all patients and the work has been approved by the local Ethical Committee.

RNA extraction and quantitative real time (qRT)-PCR

Total RNA extraction was performed with TRIzol reagent (Invitrogen, Carlsbad, CA), according to the manufacturer's instructions. Reverse transcription was performed according to standard procedures. qRT-PCR analysis was carried out using the Power SYBR Green PCR Master Mix (Applied Biosystems), according to manufacturer's instructions. Primer sequences were as follows: human *PATZ1* (5′-TACATCTGCCAGAGCTGTGG-3′/5′-TGCACCTGC TTGATATGTCC-3′); human *G6PD* (5′-GATCTACC GCATCGACCACT-3′/5′-AGATCCTGTTGGCAAATCT CA-3′); murine *PATZ1* (5′-GAGCTTCCCCGAGCTCAT-3′/5′-CAGATCTCGATGACCGACCT-3′); murine *G6PD*

(5′-GAAAGCAGAGTGAGCCCTTC-3′/5′-CATAGGAAT TACGGGCAAAGA-3′); *EpCam* (5′-CCATGTGCTG GTGTGTGAA-3′/5′-TGTGTTTTAGTTCAATGATGATC CA-3′); *fibronectin* (5′-CTGGCCGAAAATACATTGT AAA-3′/5′-CCACAGTCGGGTCAGGAG-3′); *Caldesmon* (5′-GAGCGTCGCAGAGAACTTAGA-3′/5′-TCCTCTG GTAGGCGATTCTTT-3′); *RhoE* (5′-AAAAACTGCGC TGCTCCAT-3′/5′-TCAAAACTGGCCGTGTAATTC-3′).

Chromatin immunoprecipitation

Chromatin immunoprecipitation (ChIP) was carried out with an acetyl-histone H3 immune precipitation assay kit (Upstate Biotechnology, Lake Placid, NY, USA) according to the manufacturer's instruction, as previously described [45]. Input and immunoprecipitated chromatin were analyzed by PCR for the presence of *EpCam, RhoE and Caldesmon* promoter, choosing regions also including p53 consensus site or putative PATZ1 consensus elements. Antibodies used to immunoprecipitate chromatin were: anti-HA (sc-805; Santa Cruz), control IgG (sc- 2027; Santa Cruz). PCR reactions were performed withAmpliTaq gold DNA polymerase (Perkin-Elmer, Monza, Italy). Primers used were: *EpCam (-218/-65)*: (5′ – ATGGAGACGAAGCACCTGG - 3′ / 5′ - GGGACTGCTCACCTCTGG-3′); *RhoE (-2239/-2183)*: (5′ - TGAGTCCACCAATGAAGCCA - 3′ / 5′ - TATGAGGAAATGCAAGTGACGT - 3′); *Caldesmon (-106/-2): (5′* - CAGGACAATGCATACCACCG - 3′ / 5′ - TAAAACTCCAGACCGCCCTT - 3′); *Caldesmon (-951/-841): (5′* - ATGAAGAGTTGGTCGGAGCA - 3′ / 5′ – ATGAAGAGACCCACCACCTG - 3′). PCR products were resolved on a 2% agarose gel and stained with ethidium bromide. Semi-quantitative analysis of the gel bands was performed by ImageJ64 software.

Histological analysis and immunohistochemistry

Mounted sections (6 μm) were stained with H&E using routine procedures. For immunohistochemistry, sections were deparaffinized, placed in a solution of absolute methanol and 0.3% hydrogen peroxide for 30 min, washed in PBS and incubated overnight at 4°C in a humidified chamber with diluted antibodies. The slides were subsequently incubated with biotinylated goat anti-rabbit IgG for 20 min (Vector Laboratories, Burlingame, CA, USA) and then with premixed reagent ABC (Vector) for 20 min. The immunostaining was performed by incubating the slides in diaminobenzidine solution (DAB-DAKO) for 5 min. After chromogen development, the slides were washed, dehydrated with alcohol and xylene and mounted with cover slips using a permanent mounting medium (Permount). The antibodies used were: anti-PATZ1 [11]; anti-E-cadherin (610181, BD Transduction laboratories). Negative controls were performed by omitting the first antibody. The proportion of cells that were positively stained with the anti-PATZ1 antibody was scored as: – (negative), no positive cells; + (low), < 10% of nuclear positive cells; ++ (moderate), 11–50% of nuclear positive cells; +++ (high), > 50% of nuclear positive cells [22]. At least 20 high-power fields were chosen randomly, and 2,000 cells were counted.

Protein extraction and western blot analysis

For protein extraction, cells were lysed in lysis buffer containing 1% NP40, 1 mM EDTA, 50 mM Tris-HCl (pH 7.5) and 150 mM NaCl, supplemented with complete protease inhibitors mixture (Roche, Monza, Italy). Total proteins were separated on a 8–10% polyacrylamide-SDS gel electrophoresis and transferred to nitrocellulose membranes (GE Healthcare, Milano, Italy) by electroblotting. Membranes were blocked with 1X TBS, 0.1% Tween-20 with 5% BSA and incubated with antibodies. The antibodies used were as follows: anti-PATZ1 (polyclonal antibody raised against a conserved peptide recognizing all PATZ isoforms of mouse and human origin), anti-EpCam (sc-25308; Santa Cruz), anti-γ-tubulin (sc-17787; Santa Cruz), anti-vinculin (sc-7649; Santa Cruz).

Cell lines, transfections and plasmids

All human thyroid carcinoma cell lines were cultured in DMEM supplemented with 10% FBS, L-glutamine, and penicillin/streptomycin (GIBCO-BRL) in a 5% CO2 atmosphere. TPC1 and FRO cells were transfected using Neon Transfection System (Invitrogen), whereas BC-PAP cells were transfected using Lipo2000 (Invitrogen), according to manufacturers' instructions. For stable transfections all the cell lines were transfected with PATZ1-EGFP-C2 plasmid carrying human PATZ1 variant 4 cDNA, or with the empty vector pEGFP-C2 (Clontech). Stable transfectants were clonally selected in complete medium containing 1 μg/ml G418 (Life Technologies). pCEFL-HA [23], and HA-PATZ1 plasmids, carrying the human PATZ1 variant 4 cDNA fused to the HA tag, were used in the colony assay.

Colony assay and growth curves

For colony assay the cells were plated at a density of 90% in 100-mm dishes, transfected with 5 μg of empty vector pCEFL-HA, or HA-PATZ1 plasmid, and supplemented with G418 (Life Technologies) 24 h later. Two weeks after the onset of drug selection, cells were fixed and stained with 0.1% crystal violet in 20% methanol for 30 min, washed with PBS and photographed.

For the growth curves the cells (4×10^4 cells/dish) were plated in a series of 6-cm culture dishes and counted

daily for 10 consecutive days through the Bürker chamber. The count was performed in the presence of trypan blue, to assess cell viability.

Migration and invasion assays

To detect the changed capacity of tumor cell migration, we performed a wound-healing assay. Specifically, cells were digested with 0.25% trypsin and adjusted for a concentration of 5×10^5 cells/ml of cell suspension, and then inoculated into 6-well plates and cultured at 37°C overnight. In the next day, cells were cultured in serum-free medium for 6 h, reached approximately 95–100% confluence, and cell monolayer was wounded by 20 μl tips. The cells were then rinsed twice with culture medium and incubated for 48 h. At 0, 6, 24 and 30 h, cells were photographed under an inverted microscope.

To evaluate tumor cell migration trans-well cell culture chambers were used, according to described procedures (Corning Costar Corp., Cambridge, MA). Briefly, confluent cell monolayers were harvested with trypsin/EDTA, centrifuged at 1.200 rpm for 5 min, re-suspended in medium without serum and plated ($3–5 \times 10^4$ cells) to the upper chamber of a polycarbonate membrane filter of 8 μm pore size. The lower chamber was filled with complete medium. The cells were then incubated at 37°C in a humidified incubator in 5% CO2 for 24 h and 48 h. Not migrating cells on the upper side of the filter were wiped off and migrating cells on the reverse side of the filter were stained with 0.1% crystal violet in 20% methanol for 30 min, washed with PBS and photographed under light microscope.

The rate of invasion was carried out by using transwell cell culture chambers in the presence of Matrigel (BD Biosciences). The chambers were pretreated with a cold solution containing serum-free medium and Matrigel (diluted 1:4) and left 45 min in incubator at a temperature of 37°C, at which Matrigel polymerizes to produce a biologically active matrix that resembles the basement membrane of mammalian cells. Then the assay was performed as the migratory assay. Stained cells were lysed in SDS and then counted by measuring their absorbance at 595 nm in three independent experiments.

In vitro and *in vivo* tumorigenic assays

Soft agar assays were performed according to the technique described [24]. Colonies larger than background colony size, set with untransformed rat thyroid cells (PC Cl 3), were counted and the results were expressed as number of colonies/plate. *In vivo* tumorigenicity was evaluated by inoculating control- and PATZ1-transfected cells (2×10^6 cells) subcutaneously into the left and right flank, respectively, of seven immunodeficient nude (7 weeks old) Foxn1 nu/nu female mice (Harlan Laboratories). Tumor occurrence was monitored by measuring with calipers at least once every three days. Tumor volume was determined as (length × width)/2. Care and use of the mice were in accordance with institutional guidelines and were approved by the local ethical committee.

Statistics

Differences among multiple groups of data were analyzed by one-way ANOVA followed by Dunnett's or Tukey's multiple comparisons test. Differences between two groups of data were analyzed by two tailed unpaired *t*-test.

ACKNOWLEDGEMENTS

This work was partially supported by Programmi di Ricerca di Interesse Nazionale (PRIN 2009) to Dr. M Fedele and AIRC (Associazione Italiana Ricerca sul Cancro) fellowship to Dr. T Valentino. The Functional Genomic Unit of the National Cancer Institute in Naples was supported by an AIRC Investigator Grant (IG-12962) to Dr. G Chiappetta. We are grateful to Lorenzo Chiariotti and his team for their support, to Laura Cerchia for critically reviewing the manuscript and to Ida Pellegrino for critical assistance in experimental procedures.

Conflict of interest

The authors declare no conflict of interest.

REFERENCES

1. Nikiforov YE, Nikiforova MN. Molecular genetics and diagnosis of thyroid cancer. Nat Rev Endocrinol. 2011; 7:569–580.
2. Rahib R, Smith BD, Aizenberg R, Rosenzweig AB, Fleshman JM, Matrisian LM. Projecting Cancer Incidence and Deaths to 2030: The Unexpected Burden of Thyroid, Liver, and Pancreas Cancers in the United States. Cancer Res. 2014; 74:2913–2921.
3. DeLellis RA, Williams ED. Thyroid and parathyroid tumours, in: DeLellis RA, Lloyd RV, Heitz PU, Eng C (Eds.), World Health Organization Classification of Tumours. Pathology and Genetics of Tumours of Endocrine Organs. IARC Press, Lyon, France 2004; pp. 51–56.
4. Nikiforov YE, Steward DL, Robinson-Smith TM, Haugen BR, Klopper JP, Zhu Z, Fagin JA, Falciglia M, Weber K, Nikiforova MN. Molecular testing for mutations in improving the fine-needle aspiration diagnosis of thyroid nodules. J Clin Endocrinol Metab. 2009; 94:2092–2098.
5. Ain KB. Anaplastic thyroid carcinoma: a therapeutic challenge. Semin Surg Oncol. 1999; 16:64–69.
6. Yau T, Lo CY, Epstein RJ, Lam AK, Wan KY, Lang BH. Treatment outcomes in anaplastic thyroid carcinoma:

survival improvement in young patients with localized disease treated by combination of surgery and radiotherapy. Ann Surgic Onc. 2008; 15:2500–2505.

7. Van der Laan BF, Freeman JL, Tsang RW, Asa SL. The association of welldifferentiated thyroid carcinoma with insular or anaplastic thyroid carcinoma: evidence for dedifferentiation in tumor progression. Endocr Pathol. 1993; 4:215–221.
8. Paes JE, Ringel MD. Dysregulation of the phosphatidylinositol 3-kinase pathway in thyroid neoplasia. Endocrinol Metab Clin North Am. 2008; 37:375–387.
9. Malaguarnera R, Vella V, Vinieri R, Frasca F. P53 family proteins in thyroid cancer. Endoc Relat Cancer. 2007; 14:43–60.
10. Cantile M, Scognamiglio G, La Sala L, La Mantia E, Scaramuzza V, Valentino E, Tatangelo F, Losito S, Pezzullo L, Chiofalo MG, Fulciniti F, Franco R, Botti G. Aberrant expression of posterior HOX genes in well differentiated histotypes of thyroid cancers. Int J Mol Sci. 2013; 14:21727–21740.
11. Valentino T, Palmieri D, Vitiello M, Pierantoni GM, Fusco A, Fedele M. PATZ1 interacts with p53 and regulates expression of p53-target genes enhancing apoptosis or cell survival based on the cellular context. Cell Death Dis. 2013; 4:e963.
12. Fedele M, Benvenuto G, Pero R, Majello B, Battista S, Lembo F, Vollono E, Day PM, Santoro M, Lania L, Bruni CB, Fusco A, Chiariotti L. A novel member of the BTB/POZ family, PATZ, associates with the RNF4 RING finger protein and acts as a transcriptional repressor. J Biol Chem. 2000; 275:7894–7901.
13. Morii E, Oboki K, Kataoka TR, Igarashi K, Kitamura Y. Interaction and cooperation of mi transcription factor (MITF) and myc-associated zinc-finger protein-related factor (MAZR) for transcription of mouse mast cell protease 6 gene. J Biol Chem. 2002; 277:8566–8571.
14. Kobayashi A, Yamagiwa H, Hoshino H, Muto A, Sato K, Morita M, Hayashi N, Yamamoto M, Igarashi K. A combinatorial code for gene expression generated by transcription factor Bach2 and MAZR (MAZ-related factor) through the BTB/POZ domain. Mol Cell Biol. 2000; 20:1733–1746.
15. Pero R, Lembo F, Palmieri EA, Vitiello C, Fedele M, Fusco A, Bruni CB, Chiariotti L. PATZ attenuates the RNF4-mediated enhancement of androgen receptor-dependent transcription. J Biol Chem. 2002; 277:3280–3285.
16. Bilic I, Koesters C, Unger B, Sekimata M, Hertweck A, Maschek R, Wilson CB, Ellmeier W. Negative regulation of CD8 expression via Cd8 enhancer-mediated recruitment of the zinc finger protein MAZR. Nat Immunol. 2006; 7:392–400.
17. Pero R, Palmieri D, Angrisano T. POZ-, AT-hook-, and zinc finger-containing protein (PATZ) interacts with human oncogene B cell lymphoma 6 (BCL6) and is required for its negative autoregulation. J Biol Chem. 2012; 287:18308–18317.
18. Tian X, Sun D, Zhang Y, Zhao S, Xiong H, Fang J. Zinc finger protein 278, a potential oncogene in human colorectal cancer. Acta Biochim Biophys Sin. 2008; 40:289–296.
19. Yang WL, Ravatn R, Kudoh K, Alabanza L, Chin KV. Interaction of the regulatory subunit of the cAMP-dependent protein kinase with PATZ1 (ZNF278). Biochem Biophys Res Commun. 2010; 391:1318–1323.
20. Tritz R, Mueller BM, Hickey MJ, Lin AH, Gomez GG, Hadwiger P, Sah DW, Muldoon L, Neuwelt EA, Kruse CA. siRNA Down-regulation of the PATZ1 Gene in Human Glioma Cells Increases Their Sensitivity to Apoptotic Stimuli. Cancer Ther. 2008; 6:865–876.
21. Fedele M, Franco R, Salvatore G, Paronetto MP, Barbagallo F, Pero R, Chiariotti L, Sette C, Tramontano D, Chieffi G, Fusco A, Chieffi P. PATZ1 gene has a critical role in the spermatogenesis and testicular tumours. J Pathol. 2008; 215:39–47.
22. Chiappetta G, Ferraro A, Vuttariello E, Monaco M, Galdiero F, De Simone V, Califano D, Pallante P, Botti G, Pezzullo L, Pierantoni GM, Santoro M, Fusco A. HMGA2 mRNA expression correlates with the malignant phenotype in human thyroid neoplasias. Eur J Cancer. 2008; 44:1015–1021.
23. Marinissen MJ, Chiariello M, Pallante M, Gutkind JS. A network of mitogen-activated protein kinases links G protein-coupled receptors to the c-jun promoter: a role for c-Jun NH2-terminal kinase, p38s, and extracellular signal-regulated kinase 5. Mol Cell Biol. 1999; 19:4289–4301.
24. Macpherson I, Montagnier L. Agar suspension culture for the selective assay of cells transformed by polyoma virus. Virology. 1964; 23:291–294.
25. Albini A. Tumor and endothelial cell invasion of basement membranes. The matrigel chemoinvasion assay as a tool for dissecting molecular mechanisms. Pathol Oncol Res. 1998; 4:230–241.
26. Cho JH, Kim MJ, Kim KJ, Kim JR. POZ/BTB and AT-hook-containing zinc finger protein 1 (PATZ1) inhibits endothelial cell senescence through a p53 dependent pathway. Cell Death Differ. 2012; 19:703–712.
27. Muller PA, Vousden KH, Norman JC. p53 and its mutants in tumor cell migration and invasion. J Cell Biol. 2011; 192:209–218.
28. Mukhopadhyay UK, Eves R, Jia L, Mooney P, Mak AS. p53 suppresses Src-induced podosome and rosette formation and cellular invasiveness through the upregulation of caldesmon. Mol Cell Biol. 2009; 29:3088–3098.
29. Fagin JA, Matsuo K, Karmakar A, Chen DL, Tang SH, Koeffler HP. High prevalence of mutations of the p53 gene in poorly differentiated human thyroid carcinomas. J Clin Invest. 1993; 91:179–184.

30. Meireles AM, Preto A, Rocha AS, Rebocho AP, Máximo V, Pereira-Castro I, Moreira S, Feijão T, Botelho T, Marques R, Trovisco V, Cirnes L, Alves C, Velho S, Soares P, Sobrinho-Simões M. Molecular and genotypic characterization of human thyroid follicular cell carcinoma-derived cell lines. Thyroid. 2007; 17:707–715.

31. Okada T, Nakamura T, Watanabe T, Onoda N, Ashida A, Okuyama R, Ito K. Coexpression of EpCAM, CD44 variant isoforms and claudin-7 in anaplastic thyroid carcinoma. PLoS One. 2014; 9:e94487.

32. Schnell U, Cirulli V, Giepmans BN. EpCAM: structure and function in health and disease. Biochim Biophys Acta. 2013; 1828:1989–2001.

33. Van Staveren WC, Solís DW, Delys L, Duprez L, Andry G, Franc B, Thomas G, Libert F, Dumont JE, Detours V, Maenhaut C. Human thyroid tumor cell lines derived from different tumor types present a common dedifferentiated phenotype. Cancer Res. 2007; 67:8113–8120.

34. Dhaouadi N, Li JY, Feugier P, Gustin MP, Dab H, Kacem K, Bricca G, Cerutti C. Computational identification of potential transcriptional regulators of TGF-β in human atherosclerotic arteries. Genomics. 2014; 103:357–370.

35. Thiery JP, Acloque H, Huang RY, Nieto MA. Epithelial-mesenchymal transitions in development and disease. Cell. 2009; 139:871–890.

36. Buehler D, Hardin H, Shan W, Montemayor-Garcia C, Rush PS, Asioli S, Chen H, Lloyd RV. Expression of epithelial-mesenchymal transition regulators SNAI2 and TWIST1 in thyroid carcinomas. Mod Pathol. 2013; 26:54–61.

37. Vasko V, Espinosa AV, Scouten W, He H, Auer H, Liyanarachchi S, Larin A, Savchenko V, Francis GL, de la Chapelle A, Saji M, Ringel MD. Gene expression and functional evidence of epithelial-to-mesenchymal transition in papillary thyroid carcinoma invasion. Proc Natl Acad Sci U S A. 2007; 104:2803–2808.

38. Kudo-Saito C, Shirako H, Takeuchi T, Kawakami Y. Cancer metastasis is accelerated through immunosuppression during Snail-induced EMT of cancer cells. Cancer Cell. 2009; 15:195–206.

39. Gjerdrum C, Tiron C, Høiby T, Stefansson I, Haugen H, Sandal T, Collett K, Li S, McCormack E, Gjertsen BT, Micklem DR, Akslen LA, Glackin C, Lorens JB. Axl is an essential epithelial-to-mesenchymal transition-induced regulator of breast cancer metastasis and patient survival. Proc Natl Acad Sci U S A. 2009; 107:1124–1129.

40. Skvortsova I, Skvortsov S, Raju U, Stasyk T, Riesterer O, Schottdorf EM, Popper BA, Schiestl B, Eichberger P, Debbage P, Neher A, Bonn GK, Huber LA, Milas L, Lukas P. Epithelial-to-mesenchymal transition and c-myc expression are the determinants of cetuximab-induced enhancement of squamous cell carcinoma radioresponse. Radiother Oncol. 2010; 96:108–115.

41. Bandyopadhyay A, Wang L, Agyin J, Tang Y, Lin S, Yeh IT, De K, Sun LZ. Doxorubicin in combination with a small TGFbeta inhibitor: a potential novel therapy for metastatic breast cancer in mouse models. PLoS One. 2010; 5:e10365.

42. Shiota M, Izumi H, Onitsuka T, Miyamoto N, Kashiwagi E, Kidani A, Hirano G, Takahashi M, Naito S, Kohno K. Twist and p53 reciprocally regulate target genes via direct interaction. Oncogene. 2008; 27:5543–5553.

43. Smit MA, Peeper DS. Deregulating EMT and senescence: double impact by a single twist. Cancer Cell. 2008; 14:5–7.

44. Munz M, Fellinger K, Hofmann T, Schmitt B, Gires O. Glycosylation is crucial for stability of tumour and cancer stem cell antigen EpCAM. Front Biosci. 2008; 13:5195–5201.

45. De Martino I, Visone R, Wierinckx A, Palmieri D, Ferraro A, Cappabianca P, Chiappetta G, Forzati F, Lombardi G, Colao A, Trouillas J, Fedele M, Fusco A. HMGA proteins up-regulate CCNB2 gene in mouse and human pituitary adenomas. Cancer Res. 2009; 69:1844–50.

OPEN

Citation: Cell Death and Disease (2013) 4, e963; doi:10.1038/cddis.2013.500

www.nature.com/cddis

PATZ1 interacts with p53 and regulates expression of p53-target genes enhancing apoptosis or cell survival based on the cellular context

T Valentino[1,2,4], D Palmieri[3,4], M Vitiello[1,2], GM Pierantoni[1,2], A Fusco[1,2] and M Fedele*[,1,2]

PATZ1 is a transcriptional factor functioning either as an activator or a repressor of gene transcription depending upon the cellular context. It appears to have a dual oncogenic/anti-oncogenic activity. Indeed, it is overexpressed in colon carcinomas, and its silencing inhibits colon cancer cell proliferation or increases sensitivity to apoptotic stimuli of glioma cells, suggesting an oncogenic role. Conversely, the development of B-cell lymphomas, sarcomas, hepatocellular carcinomas and lung adenomas in Patz1-knockout (ko) mice supports its tumour suppressor function. PATZ1 role in mouse lymphomagenesis is mainly because of the involvement of PATZ1 in BCL6-negative autoregulation. However, this does not exclude that PATZ1 may be involved in tumorigenesis by other mechanisms. Here, we report that PATZ1 interacts with the tumour suppressor p53 and binds p53-dependent gene promoters, including those of *BAX*, *CDKN1A* and *MDM2*. Knockdown of PATZ1 in HEK293 cells reduces promoter activity of these genes and inhibits their expression, suggesting a role of PATZ in enhancing p53 transcriptional activity. Consistently, Patz1-ko mouse embryonic fibroblasts (MEFs) show decreased expression of *Bax*, *Cdkn1a* and *Mdm2* compared with wild-type (wt) MEFs. Moreover, Patz1-ko MEFs show a decreased percentage of apoptotic cells, either spontaneous or induced by treatment with 5-fluorouracil (5FU), compared with wt controls, suggesting a pro-apoptotic role for PATZ1 in these cells. However, PATZ1 binds p53-target genes also independently from p53, exerting, in the absence of p53, an opposite function on their expression. Indeed, knockdown of PATZ1 in p53-null osteosarcoma cells upregulates *BAX* expression and decreases survival of 5FU-treated cells, then suggesting an anti-apoptotic role of PATZ1 in p53-null cancer cells. Therefore, these data support a PATZ1 tumour-suppressive function based on its ability to enhance p53-dependent transcription and apoptosis. Conversely, its opposite and anti-apoptotic role in p53-null cancer cells provides the perspective of PATZ1 silencing as a possible adjuvant in the treatment of p53-null cancer.

Cell Death and Disease (2013) **4,** e963; doi:10.1038/cddis.2013.500; published online 12 December 2013
Subject Category: Cancer

The human *PATZ1* gene, also known as MAZR, ZSG or ZNF278, encodes four alternatively expressed proteins, ranging from 537 to 687 amino acids, that share a common modular structure consisting of a POZ domain, an AT hook and four to seven C2H2 zinc fingers.[1–3] According to these domains, PATZ1 is a member of the POK (POZ and kruppel-like zinc finger) family, an unique group of transcription factors having key roles in development and cancer through their involvement in a variety of cellular processes, including cell proliferation, senescence and apoptosis.[4,5] Many POK proteins, such as HIC-1, Bcl6, PLZF, Nac-1 and others, have been linked directly or indirectly to p53 regulation,[5–7] and PATZ1 itself has been recently shown to inhibit endothelial cell senescence through a p53-dependent pathway.[8] However, the mechanism of action of these proteins is largely unknown.

As for other POK family members, the transcriptional activity of PATZ is dependent on the POZ-mediated oligomer formation, suggesting PATZ1 as an architectural transcription factor rather than a typical transactivator, thus working either as activator or repressor depending on the presence of the interacting proteins in the cellular context. Consistently, PATZ1 has been reported to either activate or repress *c-myc*,[1,2] to activate mast cell protease 6 and *FGF4*,[2,9] and to repress androgen receptor, *CD8* and *BCL6* genes.[10–13]

Several studies indicate a role of PATZ1 in carcinogenesis; however, it has not defined yet whether it behaves as a tumour suppressor or an oncogene. In fact, the *PATZ1* gene has been

[1]Istituto di Endocrinologia e Oncologia Sperimentale (IEOS), CNR, Naples, Italy; [2]Dipartimento di Medicina Molecolare e Biotecnologie Mediche, Università di Napoli "Federico II", Naples, Italy and [3]Department of Molecular Virology, Immunology and Medical Genetics, Comprehensive Cancer Center, The Ohio State University, Columbus, OH, USA
*Corresponding author: M Fedele, Istituto di Endocrinologia e Oncologia Sperimentale (IEOS), National Research Council, Via S. Pansini, 5-80127 Napoli, Italy. Tel: +39 81 7463054; Fax: +39 81 7463749. E-mail: mfedele@unina.it
[4]These authors contributed equally to this work.
Keywords: apoptosis; cell survival; tumour suppressor; oncogene; gene regulation
Abbreviations: Ko, knockout; MEFs, mouse embryonic fibroblasts; 5FU, 5-fluorouracil; POK, POZ and kruppel-like zinc finger; HA, hemagglutinin; Ab, antibody; GST, glutathione S-transferase; SDS, sodium dodecyl sulphate; SDS-PAGE, polyacrylamide-SDS gel electrophoresis; IP, immunoprecipitation; ChIP, chromatin immunoprecipitation; sh, short hairpins; CTRL, control; wt, wild-type; DLBCLs, diffuse large B-cell lymphomas; S.E., standard error; S.D., standard deviation; PCR, polymerase chain reaction; RT-PCR, reverse transcription PCR; qPCR or qRT-PCR, quantitative PCR or RT-PCR
Received 16.7.13; revised 06.11.13; accepted 13.11.13; Edited by G Melino

found to be rearranged with the *EWS* gene in a small round cell sarcoma where the other *PATZ1* allele is lost.[3] Moreover, loss of heterozygosity has been found at the FRA22B fragile site, where the *PATZ1* gene is located, in several solid tumours,[14] then supporting a potential tumour suppressor role for PATZ1. Furthermore, both heterozygous and homozygous Patz1-knockout (ko) mice spontaneously develop several tumours, including BCL6-expressing Non-Hodgkin lymphomas, sarcomas and hepatocellular carcinomas,[13] and *Patz1*-null mouse embryonic fibroblasts (MEFs) showed increased expression of various proteins involved in cell cycle activation, including cyclin D2, CDK4, Cyclin E, HMGA1 and HMGA2, even though they also express abundant levels of cell cycle inhibitors, arrest in both G0/G1 and G2/M phases of the cell cycle and undergo premature senescence.[15]

On the other hand, *PATZ1* overexpression has been described in various human malignant neoplasias, including colon, testicular and breast tumours,[16–18] and PATZ1 down-regulation by siRNA either blocks the growth of colorectal carcinoma cells[16] or increases sensitivity of glioma cell lines to apoptotic stimuli.[19]

We have previously demonstrated that a critical mechanism for the development of B-cell lymphoma in *Patz1*-ko mice relies on the increased Bcl6 expression levels consequent to the lack of negative regulation by PATZ1.[13] However, other mechanisms may be envisaged, especially those involved in the development of solid tumours, such as hepatocarcinomas and lung adenomas in *Patz1-ko* mice.

In order to elucidate other possible mechanisms by which PATZ1 may be involved in carcinogenesis, we decided to search for PATZ1-interacting proteins. To this aim, we screened an antibody (Ab) array that allowed us to identify several potential PATZ1 interactors. Then, we focused on the p53 tumour suppressor because of its widely demonstrated role in cancer.[20]

We first validated the PATZ1/p53 interaction by co-immunoprecipitating the endogenous proteins in mammalian cells, and then we demonstrated that the PATZ1/p53 complex is present on p53-targeted genes, where PATZ1 enhances p53 transcriptional activity. Next, we showed that PATZ binds p53-targeted genes in p53-null Saos-2 cells, where it regulates transcription in an opposite manner compared with p53. Finally, we showed that PATZ1 is endowed of both pro-apoptotic and anti-apoptotic activities, depending on the cellular context.

Results

PATZ is in the same complex with p53. In order to identify new PATZ1-interacting proteins, we employed an Ab array containing hundreds of high-quality antibodies against well-studied proteins, involved in cell cycle regulation, apoptosis and signal transduction. The array was incubated with total cell extracts from HEK293 cells transfected with the human full-length *PATZ1* cDNA, tagged with the HA-epitope and immunoblotted with anti-HA Ab. The results indicated an interaction between PATZ1 and several proteins (Supplementary Figure S1a); among these, we focused our attention on the oncosuppressor p53 because of its relevance in cancer pathogenesis.

To confirm the interaction between PATZ1 and p53, endogenous PATZ1 and p53 were co-immunoprecipitated in total cell extracts from HEK293 with anti-p53 Ab and analysed by western blotting with anti-PATZ1 Ab (Figure 1a, upper panel). Western blot with monoclonal p53 Ab confirmed the correct immunoprecipitation (IP) of the p53 protein (Figure 1a, lower panel). The reciprocal experiment performed immunoprecipitating with anti-PATZ1 Ab and revealing with anti-p53 Ab confirmed the interaction (Supplementary Figure S1b). Consistent with the specificity of this interaction, no co-IP was observed when nonspecific IgG was used to immunoprecipitate. These results demonstrate that PATZ1 and p53 are found in the same complexes in mammalian cells.

To identify the p53 domain involved in the interaction with PATZ1, pull-down assays were performed using HEK293 total cell extracts and two bacterially expressed p53 deletion mutants fused to GST (Figure 1b).[21] HA-PATZ1 was transiently transfected into HEK293 cells that were harvested 48 h later. Protein extracts were tested for their interaction with the GST-p53 deletion mutants. The complexes were immobilized on a glutathione-Sepharose matrix, separated by polyacrylamide-SDS gel electrophoresis (SDS-PAGE) and

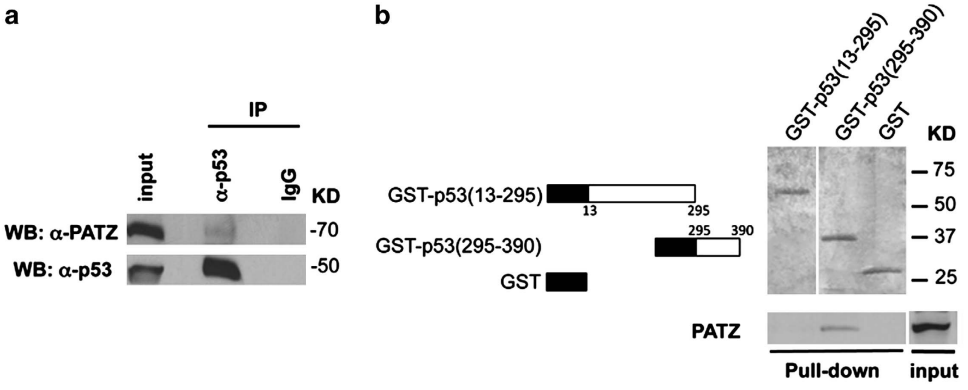

Figure 1 PATZ and p53 are in the same complex. (**a**) Co-immunoprecipitation of endogenous PATZ and p53 in HEK293 cells. (**b**) GST pull-down assay of the GST-p53 fusion proteins represented on the left with cell lysates of HEK293 cells. The bound complexes were separated by SDS-PAGE and the filter was incubated with anti-PATZ Ab (lower panel). A parallel twin gel was stained with coomassie-blue to show equal amount of the GST-fusion proteins used in the assay (upper panel). IgG = nonspecific antibody; input = total cell lysates

blotted, and the filters were hybridized with an anti-HA Ab. The GST-p53(295–390) mutant keeps the ability to bind PATZ1, whereas no binding was observed with the GST-p53(13–295) (Figure 1b, lower panel). No PATZ1 was detectable in the complexes obtained with the GST protein alone (Figure 1b, lower panel). Equal amounts of GST-fusion proteins were loaded in the pull-down assay, as shown by the blue-Coomassie staining of a parallel twin gel (Figure 1b, upper panel). These results suggest that the C-terminal domain of p53, which comprises the tetramerization (aa 323–356) and the regulatory (363–393) domains, is responsible for the interaction with PATZ1.

PATZ1 binds *BAX*, *CDKN1A* and *MDM2* promoters together or not with p53. p53 is a sequence-specific transcription factor whose DNA-binding consensus is present in a large number of promoters.[22] Similarly, PATZ1 is a transcription factor that binds DNA to specific consensus sequences in promoter regions of several genes.[23] Thus, we asked whether the physical interaction between PATZ1 and p53 takes place on promoter regions of known p53 targets. Therefore, we evaluated whether PATZ1 protein binds the promoters of p53-target genes, such as *BAX*, *MDM2* and *CDKN1A*, by performing chromatin IP (ChIP) assays. Chromatin from Raji cells was crosslinked and immunoprecipitated with anti-PATZ1 or nonspecific IgG. Immunoprecipitated chromatin was then analysed by PCR, using primers spanning the $-250/-530$ region of *BAX*, the $-400/-100$ region of *MDM2* and the $-1550/-1200$ region of *CDKN1A*, previously shown to co-immunoprecipitate with p53.[21] Occupancy by PATZ1 of the above indicated promoter regions was detectable in anti-PATZ1-precipitated chromatin. Conversely, no precipitation was observed with IgG precipitates, and when primers for the control promoter *LPL* were used, indicating that the binding of PATZ1 is specific for the selected promoters (Figure 2a). To determine whether PATZ1 occupies these promoter regions along with p53, we performed ChIP and Re-ChIP analysis on HEK293 cells transiently transfected with HA-tagged-*PATZ1*, *p53* or both expression vectors. Cells were crosslinked and immunoprecipitated (ChIP) with anti-HA Ab, and then re-immunoprecipitated (Re-ChIP) with anti-p53 Ab. In particular, a part of the anti-HA-immunoprecipitated chromatin was analysed using quantitative PCR for *BAX*, *MDM2* and *CDKN1A* promoter amplification, confirming the binding of PATZ to these promoters (Figure 2b). Another part of the PATZ1 complexes was subjected to Re-ChIP with anti-p53 Ab, and then analysed using real-time PCR for *BAX*, *MDM2* and *CDKN1A* promoters. The results shown in Figure 2c demonstrate that PATZ1 and p53 take part to the same complex on *BAX* and *CDKN1A* but not on *MDM2* promoters. The reciprocal experiments, using anti-p53 Ab for the first ChIP and anti-HA antibodies for the Re-ChIP, confirmed the results (Supplementary Figure S2). It is worth noting that ChIP and Re-ChIP experiments have been performed on exogenously expressed proteins because of the difficulty to obtain good results when endogenous proteins are not abundantly expressed.

Taken together, these results indicate that PATZ1 binds the human *BAX*, *MDM2* and *CDKN1A* promoters *in vivo*, and participate to the same DNA-bound complexes that contain p53 on the *BAX* and *CDKN1A* genes.

Interestingly, the PATZ1 protein was also capable of binding *BAX*, *MDM2* and *CDKN1A* promoters in the osteosarcoma-derived p53-null Saos-2 cells (Figure 2d), suggesting that p53 is not required for the binding of PATZ1 to these

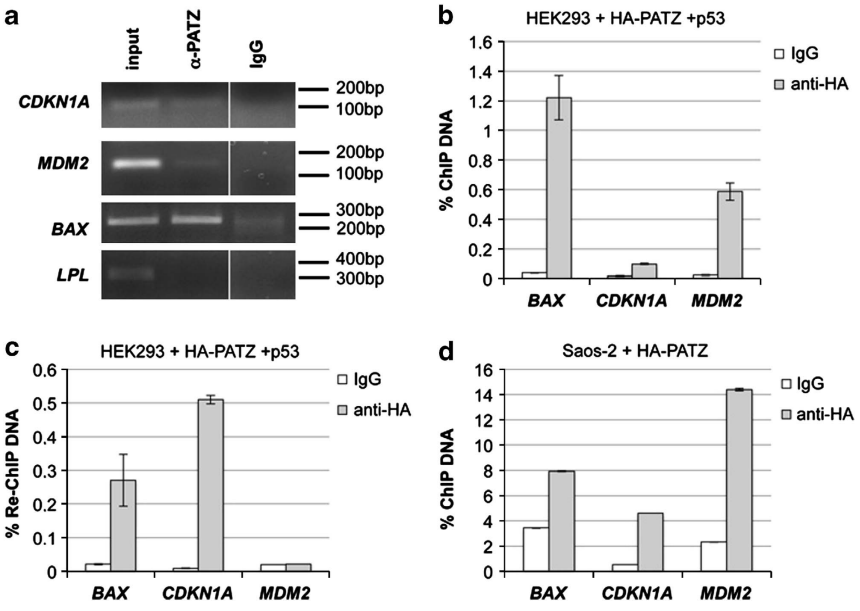

Figure 2 Binding of PATZ to p53-target genes. (**a**) ChIP assay in Raji cells to detect the endogenous *in vivo* binding of PATZ to *CDKN1A*, *MDM2* and *BAX* gene promoters, as indicated. *LPL* gene promoter was also analysed as a negative control. (**b**) ChIP assay, revealed by real-time PCR, in HEK293 cells, transiently transfected with HA-PATZ and p53, to detect the binding of PATZ to the indicated gene promoters. (**c**) Re-ChIP assay of the samples shown in **b** to detect the binding of p53 to PATZ/DNA complexes on the indicated gene promoters. (**d**) ChIP assay in Saos-2 cells, transiently transfected with HA-PATZ, to detect the binding of PATZ to the indicated gene promoters. Mean values ± S.D. of triplicates are shown in **b–d)**. IgG = nonspecific Ab

promoters. Moreover, by *in silico* analysis, using the TraFac Homology Server,[24] we found the specific responsive elements of *PATZ1* (here indicated as MAZR) in the promoter regions of *MDM2* and *CDKN1A*, suggesting that the binding of PATZ1 to these genes may be direct (Supplementary Table S1).

PATZ1 regulates transcription of p53-target genes. To study the functional consequences of the complex including PATZ1 and p53 on p53-target genes, we used reporter constructs driving luciferase gene expression under control of the BAX (BAX-luc), MDM2 (MDM2-luc) and CDKN1A (p21-luc) promoters. HEK293 cells were co-transfected with each of these reporter constructs together with plasmids expressing PATZ1, p53 or both proteins. As expected, p53 expression resulted in the upregulation of these promoters. No significant differences were observed when PATZ1 was transfected alone, whereas co-transfection of PATZ1 and p53 significantly enhances BAX promoter activity compared with that obtained by p53 alone, but had no significant effect on the other two promoters (Supplementary Figure S3). As HEK293 cells express abundant endogenous levels of PATZ1 (Figure 3a), we decided to analyse the p53-responsive promoter activities in HEK293 cells interfered for PATZ1. The knockdown of PATZ1 in these cells, by stable transfection of specific short hairpin (sh)-RNA (ShPATZ1) (Figure 3b), resulted in the reduction of *BAX*, *MDM2* and *CDKN1A* promoter activities and/or gene expression with respect to the control cells (ShCTRL) (Figures 3c and d). Furthermore, differently from ShCTRL + p53-transfected cells, in which activities of all the promoters analysed were significantly upregulated compared with ShCTRL controls, in ShPATZ1 + p53-transfected cells CDKN1A and MDM2 promoter activities were not significantly upregulated compared with ShPATZ1 controls, suggesting that p53 is not able to transactivate CDKN1A and MDM2 promoters in ShPATZ1 HEK293 cells (Figure 3c). Consistently, Patz1$^{+/-}$ MEFs showed decreased levels of endogenous *Bax*, *Mdm2* and *Cdkn1a* mRNA, compared with control wild-type (wt) cells (Figure 3e). These results suggest that PATZ1 activate expression of the *MDM2*, *CDKN1A* and *BAX* genes in both HEK293 cells and MEFs, and that it is required for proper p53 activity on MDM2 and CDKN1A promoters.

As we showed that PATZ1 is able to bind p53-dependent gene promoters also in the absence of p53, we also analysed the affects of PATZ1 knockdown on their transcriptional

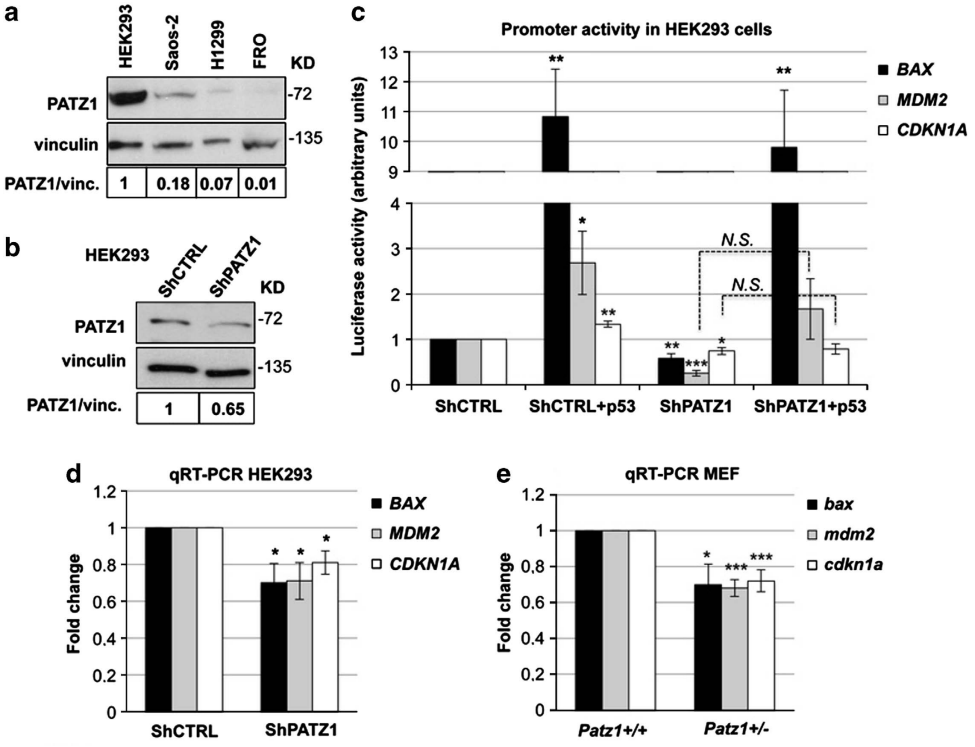

Figure 3 PATZ1 knockdown and knockout downregulates p53 activity and p53-target genes in HEK293 cells and MEFs. (**a**) Western blot analysis of PATZ expression in different cell lines, as indicated above the panels. Vinculin expression was evaluated as a loading control. Relative expression levels, compared with HEK293 cells and normalized with respect to vinculin, are indicated on the bottom. (**b**) Western blot analysis of PATZ expression in Short hairpin (Sh)PATZ1 (ShPATZ1) and backbone vector (ShCTRL)-expressing HEK293 cells. Vinculin expression was evaluated as a loading control. Relative expression levels, compared with ShCTRL cells and normalized with respect to vinculin, are indicated on the bottom. (**c**) Promoter activity of the *BAX*, *CDKN1A* and *MDM2* genes as assessed by luciferase assay in cells shown in **b**. Where indicated, p53 was co-transfected with the reporter plasmids. The data shown express the relative mean values ± S.E., compared with ShCTRL, of three or four independent experiments, each one performed in duplicate. Asterisks indicate the statistical significance compared with ShCTRL. *N.S.* = not significant. (**d**) qRT-PCR analysis of *BAX*, *MDM2* and *CDKN1A* gene expression in ShCTRL and ShPATZ1 cells. Expression levels are normalized to *GAPDH*, and the levels in ShCTRL cells were set as 1. Mean values ± S.E. of at least four independent experiments are shown. Asterisks indicate the statistical significance *versus* control cells. (**e**) qRT-PCR analysis of *bax*, *mdm2* and *cdkn1a* gene expression (normalized to *Gapdh*) in MEFs from *Patz1*$^{+/+}$ and *Patz1*$^{+/-}$ mice. Expression levels in Patz1$^{+/+}$ samples were set to 1. The data shown express the mean values ± S.E. of at least four experiments. Asterisks indicate the statistical significance compared with Patz1$^{+/+}$ MEFs

regulation in p53-null cells. To this aim, Saos-2 cells, interfered for the *PATZ1* gene, were transfected with the reporter vectors above indicated, with or without a plasmid expressing p53, and luciferase activity was analysed (Figures 4a and b). As shown in Figure 4a, the activities of *BAX*, *MDM2* and *CDKN1A* promoters were increased in cells interfered for PATZ1 (ShPATZ1) compared with control cells (ShCTRL). Moreover, the activity of a co-transfected p53 had a trend to be enhanced in ShPATZ1 cells compared with their control. Consistently, the endogenous levels of *BAX*, *MDM2* and *CDKN1A* mRNA in Saos-2 cells interfered for PATZ1 were upregulated compared with control cells (Figure 4c). To verify whether the different behaviour of PATZ in Saos-2 cells compared with HEK293 cells depends on the absence of p53, H1299 cells – another p53-null cancer cell line – were used to analyse the effect of the expression of PATZ on the BAX promoter, representing one of the above reported promoters. The results shown in Supplementary Figure S4 confirm also in this cell line an inhibitory effect of PATZ1 expression on *BAX* activity.

Therefore, at odds with the data obtained in HEK293 cells and MEFs, which endogenously express p53, these results indicate that PATZ1 downregulates the expression of the *BAX*, *MDM2* and *CDKN1A* genes in p53-null cells and suggest an oncogenic role for PATZ1 in p53-null cells.

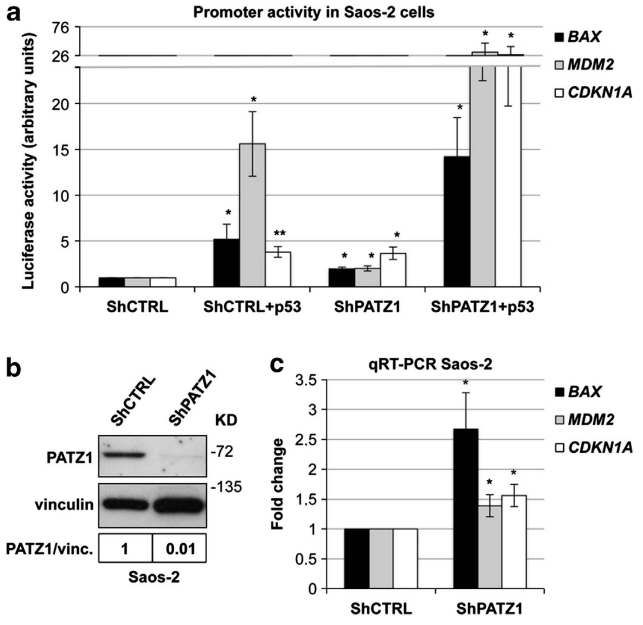

Figure 4 PATZ1 knockdown upregulates p53 activity and p53-target genes in Saos-2 cells. (**a**) Promoter activity of the *BAX*, *CDKN1A* and *MDM2* genes as assessed by luciferase assay in Saos-2 cells interfered for PATZ1 (ShPATZ1) and their backbone vector expressing control (ShCTRL). Where indicated, p53 was co-transfected with the reporter plasmids. The data shown express the mean values ± S.E. of three independent experiments. Asterisks indicate the statistical significance *versus* promoter basic activity. (**b**) Western blot analysis of PATZ expression in cells shown in **a**. Vinculin expression was evaluated as a loading control. Relative expression levels, compared with ShCTRL cells and normalized with respect to vinculin, are indicated on the bottom. (**c**) qRT-PCR analysis of *BAX*, *MDM2* and *CDKN1A* gene expression in cells shown in **a** and **b**. The data shown express the mean values ± S.E. of three independent experiments

PATZ1 can act either as a pro-apoptotic or anti-apoptotic factor depending on the cellular context. One of the main functions of p53 is the positive modulation of apoptosis in response to genotoxic conditions.[20] Therefore, to investigate the biological consequences of the functional interaction between PATZ1 and p53, we analysed the potential role of PATZ1 in apoptosis. To this aim, we analysed PARP and Caspase-3 cleavage in wt and Patz1-ko MEFs using western blot. As shown in Figure 5a, the expression of the cleaved Caspase-3, representing cells that undergo apoptosis, is lower in Patz1$^{-/-}$ MEFs compared with wt controls. Similarly, Patz1$^{-/-}$ cells also showed reduced levels of the cleaved PARP protein, another hallmark of apoptosis. Conversely, no significant differences were observed for heterozygous cells compared with wt controls. These results are consistent with reduced spontaneous apoptosis in Patz1-null MEFs compared with wt controls. Moreover, the percentage of mortality evaluated by counting viable cells after exposure to 5-fluorouracil (5FU), a known pro-apoptotic chemotherapeutic agent acting in both a p53-dependent and a p53-independent manner,[25] was significantly reduced, or tended to be reduced, in Patz1$^{-/-}$ and Patz1$^{+/-}$ MEFs, respectively, compared with wt controls (Figure 5d). These results suggest a pro-apoptotic role for PATZ1 in these cells.

Next, we analysed 5FU-induced apoptosis in HEK293 and Saos-2 cells interfered or not for PATZ1. As shown in Figure 5e, *PATZ1* silencing enhanced sensitivity of Saos-2 cells to the pro-apoptotic treatment. This was consistent with the increased levels of the *Bax* gene in Saos-2 cells interfered for PATZ1. Conversely, no significant differences were observed in HEK293 cells likely because of the high data variability among independent experiments. However, in each experiment we observed a high tendency of HEK293-interfered cells to be more sensitive to the chemotherapeutic treatment compared with control cells (Supplementary Figure S5). All together, these results suggest a dual pro-apoptotic/anti-apoptotic role for PATZ1, which depends on the cellular context, and open new interesting therapeutic possibilities in osteosarcomas.

Discussion

The development of several malignancies in Patz1-ko mice suggests a key role for the *PATZ1* gene in tumorigenesis,[13] which appears to be confirmed by its frequent misexpression in human cancer.[3,16–18] We employed an Ab array screening to identify the proteins interacting with PATZ1 in order to unveil the mechanisms by which PATZ1 is involved in tumourigenesis. From this screening we identified the tumour suppressor p53 in the same complex with PATZ1. Subsequently, we have studied the functional consequences of this interaction demonstrating that *PATZ1* interference (in HEK293 cells carrying a wt p53) results in the inhibition of the p53 activity on the transcriptional regulation of p53-target genes, including *BAX*, *MDM2* and *CDKN1A*, thus suggesting a positive role for PATZ1 on p53 transcriptional activity. Moreover, *Patz1*-null MEFs show a decreased number of apoptotic cells, either spontaneous or induced by treatment with the 5FU pro-apoptotic drug, compared with wt controls.

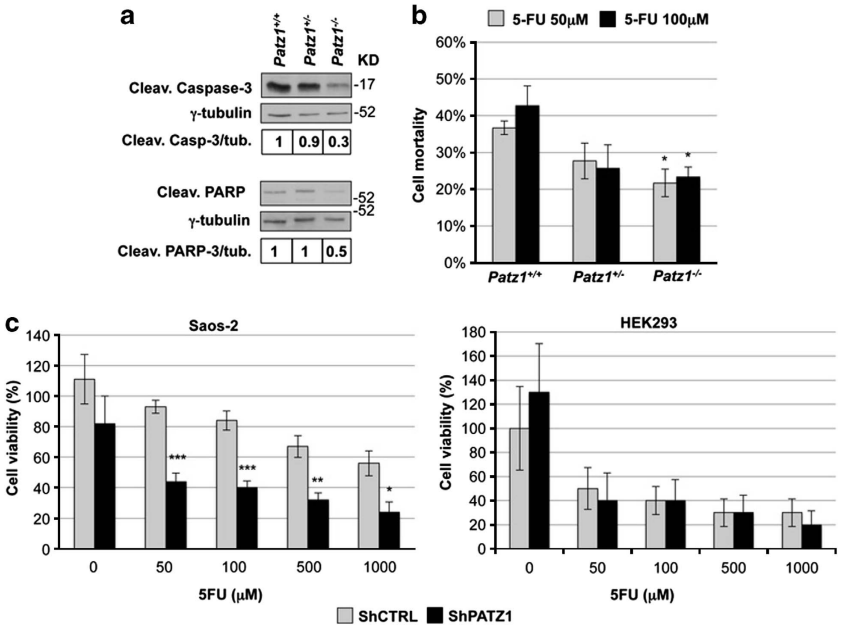

Figure 5 PATZ1 deficiency has a dual anti-apoptotic/pro-apoptotic role depending on the cellular context. (**a**) Western blot analysis of cleaved caspase-3 and PARP protein expression in Patz1$^{+/+}$, Patz1$^{+/-}$ and Patz1$^{-/-}$ MEFs. Relative expression levels, compared with Patz1$^{+/+}$ cells and normalized with respect to tubulin, are indicated on the bottom. (**b**) Cell viability assay in Patz1$^{+/+}$, Patz1$^{+/-}$ and Patz1$^{-/-}$ MEFs treated with different doses of 5FU as indicated on the top. The results show the percentage of cell mortality, expressed as mean values ± S.E. of three independent experiments, compared with not treated controls. Asterisks indicate the statistical significance compared with *Patz1*$^{+/+}$ MEFs. (**c**) Saos-2 and HEK293 cells interfered (ShPATZ1) or not (ShCTRL) for PATZ1 were treated with 5FU at different doses, as indicated at the bottom. The percentage of cell viability is shown as mean ± S.E. of four independent experiments. Asterisks indicate the statistical significance compared with ShCTRL cells

These results are in agreement with the potential tumour suppressor role of PATZ1, as it enhances the activity of a tumour suppressor gene and its loss confers resistance to apoptosis.

Whereas the positive effect of PATZ1 on p53 activity evidences a clear tumour suppressor function of PATZ1, we also describe an oncogenic potential for PATZ1. Apparently, this occurs when PATZ1 works in absence of p53. Indeed, PATZ1 knockdown upregulates transcriptional activity and expression of the *BAX*, *MDM2* and *CDKN1A* genes in the p53-null Saos-2 cells, and enhances their sensitivity to 5FU pro-apoptotic treatment. Consistently, PATZ1 expression in another p53-null cancer cell line (H1299) causes downregulation of BAX promoter activity. This is in agreement with previous results showing that siRNA downregulation of PATZ1 increases sensitivity of glioma cells (mostly carrying a mutant p53 gene and resistant to conventional chemotherapy) to apoptotic stimuli.[19] Therefore, we can speculate that targeting of *PATZ1* in p53-null tumours, which are mostly resistant to conventional chemotherapic treatment, could be envisaged as an adjuvant therapy to improve the sensitivity of the cancer cells to the conventional chemotherapy. Conversely, if a tumour retains the wt *TP53* gene and *PATZ1* is underexpressed, increasing the expression of *PATZ1* could enhance p53 activity, thus improving induction of the apoptotic process.

It has been previously shown that HMGA1, a protein interacting with PATZ1, binds to p53 and inhibits its apoptotic activity.[21,23] It would be interesting to determine whether the interaction between PATZ1 and HMGA1 might interfere with the activity of p53. We can hypothesize that in tumours carrying a wt *TP53* gene, the balance between HMGA1 and PATZ1 protein levels might have opposite effects on the activity of p53 and, consequently, in tumourigenesis and in response to anticancer treatments. It is noteworthy that in differentiated thyroid cancer, which shows a very low frequency of mutations in the *TP53* gene but a reduced p53 activity,[26] HMGA1 is overexpressed[27] and *PATZ1* is downregulated compared with normal thyroid tissue (Chiappetta *et al*., manuscript in preparation).

Recent deep-sequencing analyses confirmed earlier reports of *TP53* somatic mutations in ~20% of diffuse large B-cell lymphomas (DLBCLs),[28–30] a much lower percentage than in certain non-haematologic malignancies.[31,32] Nonetheless, 66% of DLBCLs show decreased abundance of functional p53 and reduced levels of p53 targets.[33] Therefore, additional bases of p53 deregulation in DLBCLs are still to be defined. Owing to the role of PATZ1 on p53 activity, we could speculate that the downregulation of the *PATZ1* gene might be one of the upstream events in the deregulation of p53-dependent pathways in these lymphomas. Consistently, the main malignant phenotype in Patz1-ko mice is the development of DLBCLs, where BCL6, which is known to suppress p53 expression,[34] is upregulated.[13]

In conclusion, our data demonstrate that PATZ1 is able to interact with p53 and enhance the expression of the genes regulated by p53, then increasing the susceptibility to apoptosis, according to a tumour suppressor role of PATZ. However, the absence of p53 leads PATZ1 to inhibit the same genes, enhancing cell survival. Therefore, our data seem to confirm an oncogenic or anti-oncogenic role for PATZ1 in carcinogenesis depending on the cellular context.

Materials and Methods

Cell cultures. HEK293, Saos-2 and H1299 cells were grown in DMEM containing 10% fetal bovine serum (Life Technologies, Monza, Italy), 1% glutamine (Life Technologies) and 1% penicillin/streptomycin (Life Technologies). Primary MEFs obtained from 12.5-day-old embryos of timed pregnancies between Patz1$^{+/-}$ mice, previously described,[13] were grown in DMEM (Life Technologies) containing 10% fetal bovine serum (Hyclone, Erembodegem, Belgium), 1% glutamine, 1% penicillin/streptomycin and 1% gentamicin (Life Technologies).

Plasmids, transfections, gene interference and luciferase activity assays. Full-length *PATZ1* cDNA (variant 4) for the human PATZ protein was subcloned into the *Eco*RI site of the pCEFL-HA vector, in frame with the upstream HA tag (pHA-PATZ). Expression plasmid for wt p53 (pCAG-p53) has been described previously.[35] PATZ1 knockdown in HEK293 and Saos-2 cells was carried out by stable transfection of specific sh-RNA for human PATZ1 (KH08765P; Qiagen, Milano, Italy) after selection in 1 μg/μl puromycin. pBAX-luc, pMDM2-luc or p21-luc reporter vectors have been described previously.[21] All transfections were carried out by Lipofectamine 2000 (Life Technologies) according to the manufacturer's protocol. For Luciferase assays, the pCMV-Renilla plasmid (Promega, Mannheim, Germany) was co-transfected with pHA-PATZ and/or pCAG-p53. Luciferase and Renilla activities were assessed with the Dual-Light Luciferase system (Promega), according to the manufacturer's protocol, 48 h after the transfection. Luciferase activity was normalized for the Renilla activity. All the experiments were performed at least three times in duplicate or triplicate and the mean ± S.E. was reported.

Ab array. We used an Ab array filter (Hypromatrix Incorporation, Worcester, MA, USA) in which 100 antibodies, including those against proteins involved in cell cycle regulation, apoptosis and signal transduction pathways, are immobilized on a membrane, at predetermined positions, and retained their capabilities of recognizing and capturing antigens. After incubation with total cell lysates from HEK293 cells overexpressing HA-PATZ, an immunoblot assay was performed following the manufacturer's instructions using an HRP-conjugated anti-HA Ab (sc-805 HRP; Santa Cruz Biotechnology, Dallas, TX, USA).

Protein extraction, IP and western blotting. For protein extraction, cells were lysed in lysis buffer containing 1% NP-40, 1 mM EDTA, 50 mM Tris-HCl (pH 7.5) and 150 mM NaCl, supplemented with complete protease inhibitors mixture (Roche, Monza, Italy). Total proteins were separated on a 8–10% SDS-PAGE and transferred to nitrocellulose membranes (GE Healthcare, Milano, Italy) by electroblotting. Membranes were blocked with 1 × TBS, 0.1% Tween-20 with 5% BSA and incubated with antibodies. The antibodies used were as follows: anti-p53 (DO-1/sc-126 mouse monoclonal, Santa Cruz Biotechnology; and Ab7 sheep polyclonal, Calbiochem, Billerica, MA, USA), anti-PATZ (polyclonal Ab raised against a conserved peptide recognizing all PATZ isoforms of mouse and human origin), anti-HA (sc-805; Santa Cruz Biotechnology), control IgG (sc-2027; Santa Cruz Biotechnology), anti-Myc (sc-40; Santa Cruz Biotechnology), anti-PARP (sc-7150; Santa Cruz Biotechnology) and anti-cleaved Caspase-3 (9664P; Cell Signaling Technology, Danvers, MA, USA). IP and Co-IP procedures were carried out as previously described.[36]

GST pull-down assay. Bacterial expressed GST-p53 mutant GST-p53(13–295) and GST-p53(295–390) proteins were bound to glutathione agarose and used for binding assays with total extracts from HEK293 cells transfected or not with pHA-PATZ expression plasmid. Briefly, proteins in the extracts were allowed to associate with the beads carrying either GST or GST-p53 mutants for 2 h in NETN buffer (20 mM Tris pH 8.0; 100 mM NaCl; 1 mM EDTA; 0.5% NP-40) at 4 °C. The protein complexes were washed four times in the same buffer, dissociated by boiling in loading buffer, and electrophoresed on a 12% SDS gel. The proteins were transferred to nitrocellulose and visualized with Red Ponceau staining. Subsequently, they were washed and processed with western blot for PATZ detection as described above.

ChIP and re-ChIP assays. ChIP was carried out with an acetyl-histone H3 immunoprecipitation assay kit (Upstate Biotechnology, Lake Placid, NY, USA) according to the manufacturer's instruction, and subjected to Re-ChIP as previously described.[36] Chromatin samples, derived from Raji or HEK293 cells transfected or not with pHA-PATZ and pCAG-p53, were subjected to IP with the following specific antibodies: anti-PATZ, anti-HA, anti-p53 (Calbiochem). For qPCR, 3 μl of 150 μl IP DNA was used to amplify BAX, CDKN1A and MDM2 promoter regions. IgG was used as nonspecific controls, and input DNA values were used to normalize the values from quantitative ChIP samples. Percent of IP chromatin was calculated as $2^{\Delta Ct} \times 3$, where ΔC_t is the difference between C_{tinput} and C_{tcIP}.[37] Primer sequences are available on request.

RNA extraction and quantitative (q)RT-PCR. Total RNA was extracted using TRI-reagent solution (Life Technologies) according to the manufacturer's protocol. qRT-PCR was performed with the SYBR Green PCR Master Mix (Life Technologies) under the following conditions: 10 min at 95 °C, followed by 40 cycles (15 s at 95 °C and 1 min at 60 °C). Each reaction was performed in triplicate in three independent experiments. We used the $2^{-\Delta\Delta Ct}$ method to calculate the relative expression levels.[38] Primer sequences are available upon request.

Cell viability analysis. MEF wt or ko for *Patz1*, as well as HEK293 and Saos-2 cells, interfered or not for PATZ1 were treated with 5FU and cell viability was assessed using the CellTiter-Glo Luminescent Cell Viability Assay (Promega), according to the manufacturer's instructions. Percentage of cell mortality was calculated applying the formula 1 − cell survival of treated cells/cell survival of untreated cells.

Statistical analyses. The one-way ANOVA followed by Tukey's multiple comparison test was used to compare groups of experiments. Differences between two sets of data were analysed by two-tailed unpaired *t*-test, where significance levels were set as follows: $*P \leq 0.05$; $**P \leq 0.01$; $***P \leq 0.001$.

Conflict of Interest

The authors declare no conflict of interest.

Acknowledgements. This work was supported by the Associazione Italiana Ricerca sul Cancro (AIRC-IG5728) and the Ministero Italiano dell'Università e della Ricerca scientifica (MIUR-Prin 2009). TV is recipient of a fellowship from Fondazione Italiana per la Ricerca sul Cancro (FIRC).

1. Fedele M, Benvenuto G, Pero R, Majello B, Battista S, Lembo F *et al.* A novel member of the BTB/POZ family, PATZ, associates with the RNF4 RING finger protein and acts as a transcriptional repressor. *J Biol Chem* 2000; **275**: 7894–7901.
2. Kobayashi A, Yamagiwa H, Hoshino H, Muto A, Sato K, Morita M *et al.* A combinatorial code for gene expression generated by transcription factor Bach2 and MAZR (MAZ-related factor) through the BTB/POZ domain. *Mol Cell Biol* 2000; **20**: 1733–1746.
3. Mastrangelo T, Modena P, Tornielli S, Bullrich F, Testi MA, Mezzelani A *et al.* A novel zinc finger gene is fused to EWS in small round cell tumour. *Oncogene* 2000; **19**: 3799–37804.
4. Costoya JA. Functional analysis of the role of POK transcriptional repressors. *Brief Funct Genomic Proteomic* 2007; **6**: 8–18.
5. Kelly KF, Daniel JM. POZ for effect—POZ-ZF transcription factors in cancer and development. *Trends Cell Biol* 2006; **16**: 578–587.
6. Jeon BN, Choi WI, Yu MY, Yoon AR, Kim MH, Yun CO *et al.* ZBTB2, a novel master regulator of the p53 pathway. *J Biol Chem* 2009; **284**: 17935–17946.
7. Jeon BN, Kim MK, Choi WI, Koh DI, Hong SY, Kim KS *et al.* KR-POK interacts with p53 and represses its ability to activate transcription of p21WAF1/CDKN1A. *Cancer Res* 2012; **72**: 1137–1148.
8. Cho JH, Kim MJ, Kim K, Jand Kim JR. POZ/BTB and AT-hook-containing zinc finger protein 1 (PATZ1) inhibits endothelial cell senescence through a p53 dependent pathway. *Cell Death Differ* 2012; **19**: 703–712.
9. Morii E, Oboki K, Kataoka TR, Igarashi K, Kitamura Y. Interaction and cooperation of mi transcription factor (MITF) and myc-associated zinc-finger protein-related factor (MAZR) for trascription of mouse mast cell protease 6 gene. *J Biol Chem* 2002; **277**: 8566–8571.
10. Pero R, Lembo F, Palmieri EA, Vitiello C, Fedele M, Fusco A *et al.* PATZ attenuates the RNF4-mediated enhancement of androgen receptor-dependent transcription. *J Biol Chem* 2002; **277**: 3280–3285.
11. Bilic I, Koesters C, Unger B, Sekimata M, Hertweck A, Maschek R *et al.* Negative regulation of CD8 expression via Cd8 enhancer-mediated recruitment of the zinc finger protein MAZR. *Nat Immunol* 2006; **7**: 392–400.
12. Sakaguchi S, Hombauer M, Bilic I, Naoe Y, Schebesta A, Taniuchi I *et al.* The zinc-finger protein MAZR is part of the transcription factor network that controls the CD4 versus CD8 lineage fate of double-positive thymocytes. *Nat Immunol* 2010; **11**: 442–448.

13. Pero R, Palmieri D, Angrisano T, Valentino T, Federico A, Franco R *et al.* POZ-, AT-hook-, and zinc finger-containing protein (PATZ) interacts with human oncogene B cell lymphoma 6 (BCL6) and is required for its negative autoregulation. *J Biol Chem* 2012; **287**: 18308–18317.
14. Burrow AA, Williams LE, Pierce LC, Wang YH. Over half of breakpoints in gene pairs involved in cancer-specific recurrent translocations are mapped to human chromosomal fragile sites. *BMC Genomics* 2009; **10**: 59.
15. Valentino T, Palmieri D, Vitiello M, Simeone A, Palma G, Arra C *et al.* Embryonic defects and growth alteration in mice with homozygous disruption of the Patz1 gene. *J Cell Physiol* 2012; **228**: 646–653.
16. Tian X, Sun D, Zhang Y, Zhao S, Xiong H, Fang J. Zinc finger protein 278, a potential oncogene in human colorectal cancer. *Acta Biochim Biophys Sin (Shanghai)* 2008; **40**: 289–296.
17. Fedele M, Franco R, Salvatore G, Paronetto MP, Barbagallo F, Pero R *et al.* PATZ1 gene has a critical role in the spermatogenesis and testicular tumours. *J Pathol* 2008; **215**: 39–47.
18. Yang WL, Ravatn R, Kudoh K, Alabanza L, Chin KV. Interaction of the regulatory subunit of the cAMP-dependent protein kinase with PATZ1 (ZNF278). *Biochem Biophys Res Commun* 2010; **391**: 1318–1323.
19. Tritz R, Mueller BM, Hickey MJ, Lin AH, Gomez GG, Hadwiger P *et al.* siRNA down-regulation of the PATZ1 gene in human glioma cells increases their sensitivity to apoptotic stimuli. *Cancer Ther* 2008; **6**: 865–876.
20. Zilfou JT, Lowe SW. Tumour suppressive functions of p53. *Cold Spring Harb Perspect Biol* 2009; **1**: a001883.
21. Pierantoni GM, Rinaldo C, Esposito F, Mottolese M, Soddu S, Fusco A. High Mobility Group. A1 (HMGA1) proteins interact with p53 and inhibit its apoptotic activity. *Cell Death Differ* 2006; **13**: 1554–1563.
22. Menendez D, Inga A, Resnick MA. The expanding universe of p53 targets. *Nat Rev Cancer* 2009; **9**: 724–737.
23. Fedele M, Pierantoni GM, Pallante P, Fusco A. High mobility group. A-interacting proteins in cancer: focus on chromobox protein homolog 7, homeodomain interacting protein kinase 2 and PATZ. *J Nucl Acids Inv* 2012; **3**: e1.
24. Jegga AG, Sherwood SP, Carman JW, Pinski AT, Phillips JL, Pestian JP *et al.* Detection and visualization of compositionally similar cis-regulatory element clusters in orthologous and coordinately controlled genes. *Genome Res* 2002; **12**: 1408–1417.
25. Longley DB, Harkin DP, Johnston PG. 5-fluorouracil: mechanisms of action and clinical strategies. *Nat Rev Cancer* 2003; **3**: 330–338.
26. Malaguarnera R, Vella V, Vigneri R, Frasca F. p53 family proteins in thyroid cancer. *Endocr Relat Cancer* 2007; **14**: 43–60.
27. Chiappetta G, Tallini G, De Biasio MC, Manfioletti G, Martinez-Tello FJ, Pentimalli F *et al.* Detection of high mobility group. I HMGI(Y) protein in the diagnosis of thyroid tumors: HMGI(Y) expression represents a potential diagnostic indicator of carcinoma. *Cancer Res* 1998; **58**: 4193–4198.
28. Morin RD, Mendez-Lago M, Mungall AJ, Goya R, Mungall KL, Corbett RD *et al.* Frequent mutation of histone-modifying genes in non-Hodgkin lymphoma. *Nature* 2011; **476**: 298–303.
29. Pasqualucci L, Trifonov V, Fabbri G, Ma J, Rossi D, Chiarenza A *et al.* Analysis of the coding genome of diffuse large B-cell lymphoma. *Nat Genet* 2011; **43**: 830–837.
30. Lohr JG, Stojanov P, Lawrence MS, Auclair D, Chapuy B, Sougnez C *et al.* Discovery and prioritization of somatic mutations in diffuse large B-cell lymphoma (DLBCL) by whole-exome sequencing. *Proc Natl Acad Sci USA* 2012; **109**: 3879–3884.
31. Cancer Genome Atlas Research Network. Comprehensive genomic characterization defines human glioblastoma genes and core pathways. *Nature* 2008; **455**: 1061–1068.
32. Cancer Genome Atlas Research Network. Integrated genomic analyses of ovarian carcinoma. *Nature* 2011; **474**: 609–615.
33. Monti S, Chapuy B, Takeyama K, Rodig SJ, Hao Y, Yeda KT *et al.* Integrative analysis reveals an outcome-associated and targetable pattern of p53 and cell cycle deregulation in diffuse large B cell lymphoma. *Cancer Cell* 2012; **22**: 359–372.
34. Phan RT, Dalla-Favera R. The BCL6 proto-oncogene suppresses p53 expression in germinal-centre B cells. *Nature* 2004; **432**: 635–639.
35. Baker SJ, Markowitz S, Fearon ER, Willson JK, Vogelstein B. Suppression of human colorectal carcinoma cell growth by wild-type p53. *Science* 1990; **249**: 912–915.
36. Fedele M, Visone R, De Martino I, Troncone G, Palmieri D, Battista S *et al.* HMGA2 induces pituitary tumorigenesis by enhancing E2F1 activity. *Cancer Cell* 2006; **9**: 459–471.
37. Frank SR, Schroeder M, Fernandez P, Taubert S, Amati B. Binding of c-Myc to chromatin mediates mitogen-induced acetylation of histone H4 and gene activation. *Genes Dev* 2001; **15**: 2069–2082.
38. Livak KJ, Schmittgen TD. Analysis of relative gene expression data using real-time quantitative PCR and the 2(-Delta Delta C(T)) method. *Methods* 2001; **25**: 402–408.

Supplementary Information accompanies this paper on Cell Death and Disease website (http://www.nature.com/cddis)

Journal of Cellular Physiology

Embryonic Defects and Growth Alteration in Mice With Homozygous Disruption of the *Patz1* Gene

TERESA VALENTINO,[1] DARIO PALMIERI,[1] MICHELA VITIELLO,[1] ANTONIO SIMEONE,[2] GIUSEPPE PALMA,[3] CLAUDIO ARRA,[3] PAOLO CHIEFFI,[4] LORENZO CHIARIOTTI,[1,5] ALFREDO FUSCO,[1] AND MONICA FEDELE[1]*

[1]*Istituto di Endocrinologia ed Oncologia Sperimentale del CNR and Dipartimento di Biologia e Patologia Cellulare e Molecolare, Università di Napoli "Federico II", Naples, Italy*

[2]*CEINGE, Biotecnologie Avanzate, Naples, Italy*

[3]*Istituto dei Tumori di Napoli "Fondazione G. Pascale", Naples, Italy*

[4]*Dipartimento di Psicologia, II Università di Napoli, Caserta, Italy*

[5]*Dipartimento di Chimica Farmaceutica e Tossicologica, Università di Napoli "Federico II", Naples, Italy*

PATZ1 is an emerging cancer-related gene coding for a POZ/AT-hook/kruppel Zinc finger transcription factor, which is lost or misexpressed in human neoplasias. Here, we investigated its role in development exploring wild-type and Patz1-knockout mice during embryogenesis. We report that the *Patz1* gene is ubiquitously expressed at early stages of development and becomes more restricted at later stages, with high levels of expression in actively proliferating neuroblasts belonging to the ventricular zones of the central nervous system (CNS). The analysis of embryos in which *Patz1* was disrupted revealed the presence of severe defects in the CNS and in the cardiac outflow tract, which eventually lead to a pre-mature in utero death during late gestation or soon after birth. Moreover, the Patz1-null mice showed a general growth retardation, which was consistent with the slower growth rate and the increased susceptibility to senescence of Patz1$^{-/-}$ mouse embryonic fibroblasts (MEFs) compared to wild-type controls. Therefore, these results indicate a critical role of PATZ1 in the control of cell growth and embryonic development.

J. Cell. Physiol. 228: 646–653, 2013.

The *PATZ1* gene encodes four alternatively expressed proteins, ranging from 537 to 687 amino acids, that share a common modular structure consisting of a POZ domain, two AT-hooks and four to seven C2H2 Zinc fingers (Fedele et al., 2000; Kobayashi et al., 2000; Mastrangelo et al., 2000). According to these domains, PATZ is a member of the POK (POZ and Kruppel) family of transcriptional repressors (Costoya, 2007), but it may function either as activator or repressor depending upon the cellular context. Indeed, it has been reported to either activate or repress c-myc (Fedele et al., 2000; Kobayashi et al., 2000), to activate mast cell protease 6 (Morii et al., 2002) and FGF4 (Kobayashi et al., 2000), and to repress androgen receptor (Pero et al., 2002) and CD8 (Bilic et al., 2006) genes. Consistent with the CD8 regulation, it has been recently shown that PATZ is an important part of the transcription factor network that controls the CD4 versus CD8 lineage fate of double-positive thymocytes (Sakaguchi et al., 2010). Moreover, we have previously reported that PATZ has a critical role in the spermatogenesis, by regulating the apoptotic pathways in germ cells (Fedele et al., 2008).

Several studies suggest a role of PATZ in carcinogenesis. In fact, the *PATZ1* gene maps on the FRA22B fragile site, which suffers loss of heterozygosity in several solid tumors (Burrow et al., 2009), and it has been found rearranged with the *EWS* gene in a small round cell sarcoma, with the loss of heterozygosity of the wild-type *PATZ1* allele (Mastrangelo et al., 2000), suggesting a potential tumor suppressor role. However, an oncogenic role for *PATZ1* has also been suggested since it is overexpressed in some human malignant neoplasia, including colon (Tian et al., 2008), testicular (Fedele et al., 2008), and breast (Tritz et al., 2008) tumors. Consistently, PATZ down-regulation by siRNA either blocks the growth or induces apoptosis of cell lines derived from colorectal cancers or gliomas, respectively (Tian et al., 2008; Yang et al., 2010). PATZ was found mislocalized in testicular seminomas, teratomas, and embryonal carcinomas from the nucleus to the cytoplasm, suggesting that its function could be impaired in these tumors or, alternatively, that it may acquire some new cytoplasmic function that could contribute to neoplastic transformation (Fedele et al., 2008). Interestingly, it has been recently shown that such delocalization of PATZ in testicular seminomas depends on oestrogen receptor-β levels and the translocation from cytoplasm to the nucleus is mediated by cAMP (Esposito et al., 2011), as it was previously demonstrated in other cell

Conflict of interest: none to declare.

Additional supporting information may be found in the online version of this article.

Contract grant sponsor: AIRC;
Contract grant number: IG5728.

*Correspondence to: Monica Fedele, Istituto di Endocrinologia ed Oncologia Sperimentale (IEOS) del CNR, via S. Pansini, Napoli 5-80131, Italy. E-mail: mfedele@unina.it

Manuscript Received: 29 February 2012
Manuscript Accepted: 31 July 2012

Accepted manuscript online in Wiley Online Library (wileyonlinelibrary.com): 9 August 2012.
DOI: 10.1002/jcp.24174

systems, such as PC3M prostate carcinoma cells and normal fibroblasts (Tritz et al., 2008).

Since it is known that a large number of genes involved in embryonic development are either tumor suppressor or oncogenes (Dean, 1998), we focused on studying the role of PATZ during development. To this aim we first analyzed *Patz1* expression during normal mouse development. Then, we analyzed the phenotype of mouse embryos null for *Patz1* in comparison with wild-type (WT) controls. Finally, we examined the growth characteristics of Patz1$^{-/-}$ mice and their embryo-derived fibroblasts.

Materials and Methods

In situ hybridization

The probe used for this study was a 489 bp fragment carrying a portion of the mouse *Patz1* cDNA. The same fragment, cloned in the opposite orientation in pGem3Z, was used to obtain a sense probe which we used as a control of the specificity of hybridization. Probe synthesis and labeling was carried out as previously described (Chiappetta et al., 1996). Embryos of 8.5, 10.5, 12.5, 14.5, and 17.5 days post coitum (dpc), obtained from C57/Bl6 mice mated between 9 pm and 10 pm, were collected and classified according to the Theiler staging (Theiler, 1989). Three independent embryos for each stage have been analyzed. Tissue preparation, hybridization, and washes were carried out as previously described (Chiappetta et al., 1996). Ethical Committee approval was given in all instances.

Generation and genotyping of mutant mice

The *Patz1* gene targeting vector was derived from a λΦXII phage library of a 129SvJ mouse strain (Stratagene, La Jolla, CA). It was designed to delete a 2,317-bp *Pst*I–*Xho*I fragment, including the start codon, the coding regions for the POZ domain, the AT-hook and the first four zinc fingers (Supplementary Fig. 1). It was constructed by subcloning the 5′-flanking region (the *Spe*I–*Pst*I 3 kb fragment), the *neo* cassette and the 3′-flanking region (the *Xho*I–*Xba*I 3.2 kb fragment) into the Bluescript plasmid (Stratagene) that contained a *Pac*I digestion site inserted at a distance from the multi-cloning site (Pero et al., 2012). The targeting vector was linearized with *Pac*I before electroporation into embryonic stem (ES) cells (Incyte Genomics, Palo Alto, CA).

Two correctly targeted ES cell lines were injected into C57Bl/6J blastocysts. Both ES cell lines gave rise to germ line chimeras that were backcrossed to C57Bl/6J females in order to obtain *Patz1* heterozygous offspring. For Southern blot analysis, tail DNA samples were digested with *Stu*I and probed with an external 5′ genomic fragment that detects 9.3 or 8-kb fragments, corresponding to the WT and mutant alleles, respectively. All mice were maintained under standardized nonbarrier conditions in the Laboratory Animal Facility of Istituto dei Tumori di Napoli (Naples, Italy), and all studies were conducted in accordance with Italian regulations for experimentations on animals.

Histological analysis

For histological examination, the embryos were gently immersed in Bouin solution (picric acid, 37% formaldehyde, 100% acetic acid 15:5:1). Sections (6 μm thick) were stained with hematoxylin and eosin according to standard procedures.

MEF growth and BrdU-FACS analysis

Primary MEFs, obtained from 12.5-day-old embryos, were cultured at 37°C (5% CO_2) in Dulbecco's Modified Eagle's Medium (DMEM) containing 10% fetal bovine serum (Hyclone, Logan, UT) supplemented with penicillin/streptomycin. To determine the cell doubling time, each cell line (4×10^5 cells) was plated in 6-cm culture dishes and counted daily with a hemocytometer. MEFs in logarithmic growth were incubated for 2 h with 30 μM BrdU (Becton Dickinson, San Jose, CA) and then trypsinized and fixed in 70% ethanol for cell cycle analysis by FACS. After washing with PBS, cells were re-suspended in 250 μl of PBS and incubated with 250 μl of 4M HCl for 30 min at RT followed by two washes with PBS-Tween 0.1%. Subsequently, the cells were stained, first, with 20 μl anti-BrdU-FITC (Becton Dickinson) for 1h at RT in the dark, and then washed twice with PBS-Tween 0.1% and re-stained with 5 μg/ml propidium iodide containing RNase (20 μg/ml), for 20 min at RT in the dark, and analyzed with a FACScan flow cytometer (Becton Dickinson) interfaced with a Hewlett-Packard computer (Palo Alto, CA). Gating excluded cell debris and fixation artifacts, and the G1, S, and G2/M populations were quantified using CellQuest software. In each experiment, a similar number of events was analyzed.

Senescence associated-β-galactosidase assay

Cells (4×10^4), plated 24 h before the assay, were washed twice with PBS and immersed in fixation buffer [2% (w/v) formaldehyde, 0.2% (w/v) glutaraldehyde in PBS] for 7 min. After three additional PBS washes, the cells were stained overnight in staining solution (40 mM citric acid/sodium phosphate pH 6.0, 150 mM NaCl, 2.0 mM $MgCl_2$, 1 mg/ml X-gal) at 37°C without CO_2 to avoid modification of the PH. The next day, the stained solution was replaced with PBS, and all of the cells in at least 24 fields of view were counted under the light microscope.

RNA extraction and qRT-PCR

Total RNA was extracted using TRI-reagent solution (Sigma, St Louis, MO) according to the manufacturer's protocol, treated with DNAse I (Invitrogen/Life Technologies Italia, Monza, Italy), and reverse-transcribed using random hexanucleotides as primers and MuLV reverse transcriptase (Perkin-Elmer, Waltham, MA), following manufacturer's instructions. For quantitative RT-PCR each reaction was performed three times in triplicate using SYBR Green PCR Master Mix (Applied Biosystems, Foster City, CA), as previously described (Pero et al., 2012).

Protein extraction and immunoblot analysis

Protein extraction and Western blot analysis were carried out as previously described (Melillo et al., 2001). The antibodies used were as follows: anti-p27 (610241; Becton Dickinson), anti-vinculin (sc-7649; Santa Cruz Biotechnology, Santa Cruz, CA), anti-p21 (sc-397, Santa Cruz Biotechnology), anti-p16^{Ink4a} (ab-54210; Abcam, Cambridge, UK), anti-cyclin D2 (sc-754; Santa Cruz Biotechnology), anti-p19^{arf} (ab-80; Abcam), anti-cyclin E (sc-481; Santa Cruz Biotechnology), anti-p53 (sc-126; Santa Cruz Biotechnology), anti-cdk1 (Ab-1; Calbiochem, San Diego, CA), anti-cdk2 (sc-748; Santa Cruz Biotechnology), anti-cdk4 (sc-260; Santa Cruz Biotechnology), anti-cyclin A (sc-751; Santa Cruz Biotechnology), anti-HMGA1 (Melillo et al., 2001), and anti-HMGA2 (Fedele et al., 2006).

Statistics

The one-way ANOVA followed by Tukey's multiple comparison test was used to compare groups of experiments. The statistical significant difference was considered when *P*-value was <0.05.

Results

Developmental expression of *Patz1* gene

To define the temporal and spatial profile of *Patz1* expression, we performed an in situ hybridization analysis on mouse embryos between 8.5 and 17.5 days dpc, the period during which the most critical events of organogenesis take place. In general, the expression of *Patz1* gene was ubiquitous at early stages of development and became more restricted at later stages. Interestingly, *Patz1* was expressed at high levels in the central nervous system (CNS) becoming confined at later

stages to actively proliferating neuroblasts belonging to the ventricular zones (Figs. 1 and 2).

Early gestation (8.5–10.5 dpc). At 8.5 dpc *Patz1* transcripts were widely distributed in all embryonic tissues (Fig. 1, Panel A). At 9.5 dpc *Patz1* was still expressed in the majority of the embryonic tissues even though it was markedly transcribed along the CNS, throughout the branchial arches, in the otic vescicles and in stomach primordium (Fig. 1, Panels B and C). All the other tissues showed a reduced level of expression. At 10.5 dpc (Fig. 1, Panels D and E) *Patz1* mRNA was detected at high level in the differentiating spinal and cephalic ganglia. A lower expression was also detected through the limb buds, branchial arches, stomach and the epato-biliary primordium.

Midgestation (12.5–14.5 dpc) and late gestation (17.5 dpc). At 12.5 dpc *Patz1* transcripts were detected at high level in the cephalic and spinal ganglia as well as in the brain, hindbrain, and spinal cord (Fig. 2, Panels A and B). Their distribution along the CNS was not uniform and resulted more abundant in the proliferating neuroblasts belonging to the ventricular zones (Fig. 2, Panels A–D). Additional sites of strong expression were the olfactory and respiratory epithelium in the nasal pit (Fig. 2, Panels A and B), the retina (Fig. 2, Panel C), kidney (Fig. 2, Panel A), and Rathke's pouch (Fig. 2, Panel D). At 17.5 dpc *Patz1* was detected at high level along the CNS and in specific organs such as lung, liver, and kidney (Fig. 2, Panels E–G). In the CNS, its high expression appeared at this stage clearly confined to the actively proliferating neuroblasts in the periventricular neocortical neuroepithelium. Moreover, in the telencephalon it was expressed also in the cortical plate, in the hippocampus, and in the striatal neuroepithelium and subventricular zone (Fig. 2, Panels F and G). A high expression was also found in the thymus, thyroid, salivary glands (Fig. 2, Panels E and F), and in the tooth primordia (Fig. 2, Panel G).

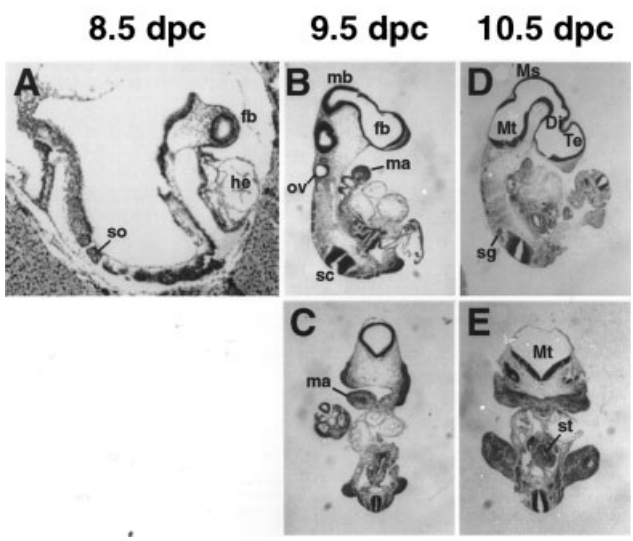

Fig. 1. Expression of the *Patz1* gene in early gestation. *Patz1* expression at 8.5 dpc (A), 9.5 dpc (B) and 10.5 dpc (D) in sagittal (A, B, D) and frontal (C, E) sections. Abbreviations stand as follows: fb and mb indicate the fore- and mid-brain, respectively; Te, Di, Ms, and Mt indicate the telencephalon, diencephalon, mesencephalon, and metencephalon, respectively; he, heart; sc, spinal cord; sg, spinal ganglia; so, somites; ov, otic vescicles; ma, mandibular arch; st, stomach.

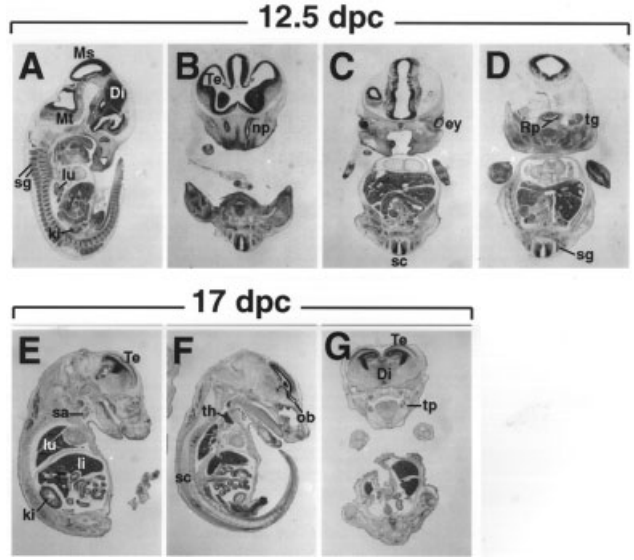

Fig. 2. Expression of the *Patz1* gene in mid- and late gestation. *Patz1* expression at 12.5 dpc (A–D) and 17 dpc (E–G) in sagittal (A, E, F) and frontal (B–D, G) sections. Abbreviations stand as in the previous figure plus: lu, lung; ki, kidney; np, nasal pit; ey, eye; Rp, rathke's pouch; tg, trigeminal ganglion; sa, salivary gland; li, liver; th, thymus; tp, tooth primordium.

Embryonic lethality and developmental defects in *Patz1*-null mice

To gain insights into the physiological role of Patz1 during development and adult life, we generated mice carrying a null mutation at the *Patz1* locus.

Mice heterozygous for the *Patz1* null allele appeared normal and were fertile. Homozygous mutant pups totaled only 4% of the newborn offspring from heterozygous intercrosses, instead of the expected 25%, indicating that most *Patz1*-null mice died during embryogenesis. Embryos from timed matings between heterozygotes were analyzed at different gestation stages (Table 1). Until 15.5 dpc all the embryos analyzed had beating hearts with no gross abnormalities except for a slight body size decrease in most of the homozygous mutant embryos (data not shown) and exencephaly in 4 out of 15 at 13.5 dpc (Fig. 3 and Supplementary Fig. 2A). Exencephaly is a cranial

TABLE 1. Embryonic lethality in Patz1$^{-/-}$ mice

	Litters	*Patz1*$^{+/+}$	*Patz1*$^{+/-}$	*Patz1*$^{-/-}$	Dead[a]	Readsorbed	Total
E8.5	2	4	11	5	0	0	20
E9.5	2	5	8	5	0	0	18
E10.5	2	2	10	3	0	0	15
E11.5	2	5	12	3	0	0	20
E12.5	5	5	10	9	0	4	24
E13.5	7	13	30	15	0	5	59
E14.5	2	4	9	3	0	2	16
E15.5	10	15	50	15	12 (80%)	10	80
E16.5	10	20	70	1	0	15	91
E18.5	10	10	40	0	—	20	50
3W[b]	24	50 (38%)	76 (58%)	5[c] (4%)	0	—	131

Embryos were isolated at the indicated time of gestation and analyzed for viability by observing heart beating. E, embryonic day; 3W, 3 weeks after birth.
[a]Percent of total *Patz1*$^{-/-}$ embryos given in parentheses.
[b]Percent of total pups given in parentheses.
[c]Growth retarded.

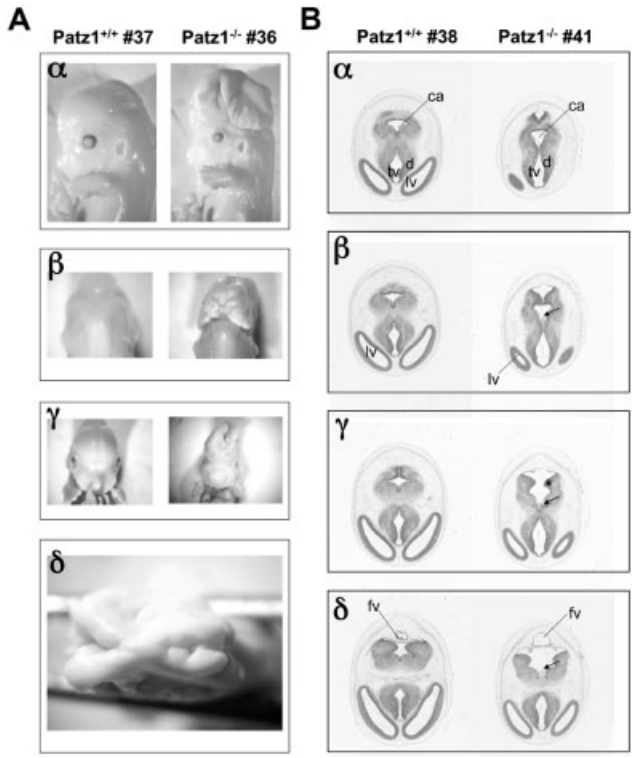

Fig. 3. CNS developmental defects in Patz1$^{-/-}$ embryos. A: Macroscopic comparison of a Patz1$^{-/-}$ embryo at 13.5 dpc with exencephaly (right side) with a normal WT embryo from the same littermate (left side). Lateral (α), dorsal (β), frontal (γ), and apical views (δ) are shown. B: Series of brain cross sections, progressively more caudal, of representative WT and Patz1$^{-/-}$ (without exencephaly) embryos at 13.5 dpc. For each panel, parallel sections are compared. Ca, cerebral aqueduct; d, diencephalon; tv, third ventricle; lv = lateral ventricle; fv, fourth ventricle; *, neuroepithelium of the isthmus; arrow indicates a tongue of cells projecting from the floor of the rhomboencephalon within the ventricular cavity.

neural tube defect, resulting from failed closure of the neural folds during neurulation. In the mouse, the neural tube initiates closure at 8.5 dpc, beginning at the cervical/hindbrain boundary. Two additional de novo closure sites occur at the caudal and rostral limits of the forebrain. Closure then spreads along the neural folds in the rostral and caudal directions. By 9.5 dpc, closure is normally complete (Juriloff et al., 1991). Differently from the WT controls, the Patz1$^{-/-}$ embryos with exencephaly (Fig. 3A and Supplementary Fig. 2A) had failure of closure of the anterior neuropore and severe malformation of the brain with the possible exception of the most caudal region of the hindbrain (caudal medulla oblongata). Histological examination of all the other 13.5 dpc homozygous mutant embryos with no exencephaly (11 out of 15) revealed some anomalies of brain development with a size and configuration roughly corresponding to 12.5–13 dpc. In particular, the brain of the mutants is smaller, the whole ventricular system is larger and, although the pattern of folding is preserved, the structures that bulge out such as the ganglionic eminence and the diencephalon are less pronounced (Fig. 3B and Supplementary Fig. 2B). Moreover, the thickness of the nervous tissue around the ventricular cavities is reduced overall, and it is particularly evident at the level of the telencephalon and diencephalon. The choroid plexus of the 4th ventricle is hypoplasic. The neuroepithelium of the isthmus and prospective cerebellum remains apart caudally (Fig. 3Bγ), although in more cranial sections the ventral part comes together (Fig. 3Bβ) and eventually fuses (Fig. 3Bα). Interestingly, in some mutant embryos (7 out of 15) a tongue of cells projects from the midline (median sulcus) of the floor of the rhomboencephalon within the ventricular cavity, extending rostrally to the region of the mesencephalon (arrows in Fig. 3B and Supplementary Fig. 2B).

Another anomaly, common to all the *Patz1*$^{-/-}$ embryos analyzed, is the origin of the aorta. In mutant embryos there is a clear malformation of the great vessels that exit the ventricular chambers of the heart. In contrast to WT embryos, where the descending aorta is located in the midline towards the left behind the esophagus (Fig. 4A, left), in 5 out of 15 mutant embryos the descending aorta is located towards the right of the midline (Fig. 4A, right). This suggests an origin from the right primitive dorsal aorta, in contrast to the normal development, in which the descending aorta originates from the left primitive dorsal aorta. From these histological sections it is not clear the real identity of the ascending aorta and pulmonary trunk. A possibility is that the identity of the two outflow trunks is the same as in the WT based on its relative position to each other. In this case, the ductus arteriosus assumes a left to right orientation, whereas the junction between the ascending aorta and the aortic arch is located on the right side. The course of the ascending aorta follows a ventral to dorsal direction with minimal displacement to the side. An alternative possibility is that the identity of the ascending aorta and pulmonary trunk is reversed in the mutant embryo, in such a way that the vessel occupying the position of the WT aorta is in reality the pulmonary trunk, and vice versa, the vessel that should be the pulmonary trunk is the ascending aorta. This malformation would be a transposition of the great vessels. In either case, the aortic arch would derive from the 4th right branchial arch artery and the ductus arteriosus from the 6th right branchial arch artery. In all the other mutants, the descending aorta is normally located in the left side of the esophagus but the aorta appears always ventral to the pulmonary trunk at its origin (Fig. 4B), suggesting outflow-tract (OFT) defects possibly including transposition or malposition of the great vessels. Consistent with these histological data, the cardiac OFT macroscopically analyzed in two agonizing newborn Patz1$^{-/-}$ pups appeared impaired by different types of vessels anomalies (Supplementary Fig. 3).

Growth retardation in *Patz1*-null mice

Almost all the *Patz1*$^{-/-}$ mice were 10–20% smaller than sex-matched littermate controls following weaning and these differences were kept almost unchanged throughout the whole of their lives (Fig. 5A,B). Similarly, their mean body weight was significantly lower than that of *Patz1*$^{+/+}$ mice in both sexes ($P < 0.01$), as depicted by the growth curves in Figure 5C. Conversely, the mean body weight of *Patz1*$^{+/-}$ mice did not differ from that of WT mice (Fig. 5C). To examine whether visceral organ size was proportional to the body weight we measured the wet weight of the heart, liver, spleen, kidney, and lung. The ratio of organ to body weight was consistently smaller in Patz1$^{-/-}$ mice as compared to WT mice (Fig. 5D).

Cell cycle profile alterations and premature senescence in *Patz1*-knockout MEFs

MEFs were prepared from *Patz1*$^{+/+}$, *Patz1*$^{+/-}$, and *Patz1*$^{-/-}$ embryos at 12.5 dpc. The growth properties of the MEFs were assessed at passage 4 by growth curves and cell-doubling time. As shown in Figure 6A–C, *Patz1*$^{-/-}$ MEFs grew significantly slower than their WT counterparts. Conversely, heterozygous *Patz1*-knockout MEFs grew significantly faster than WT MEFs.

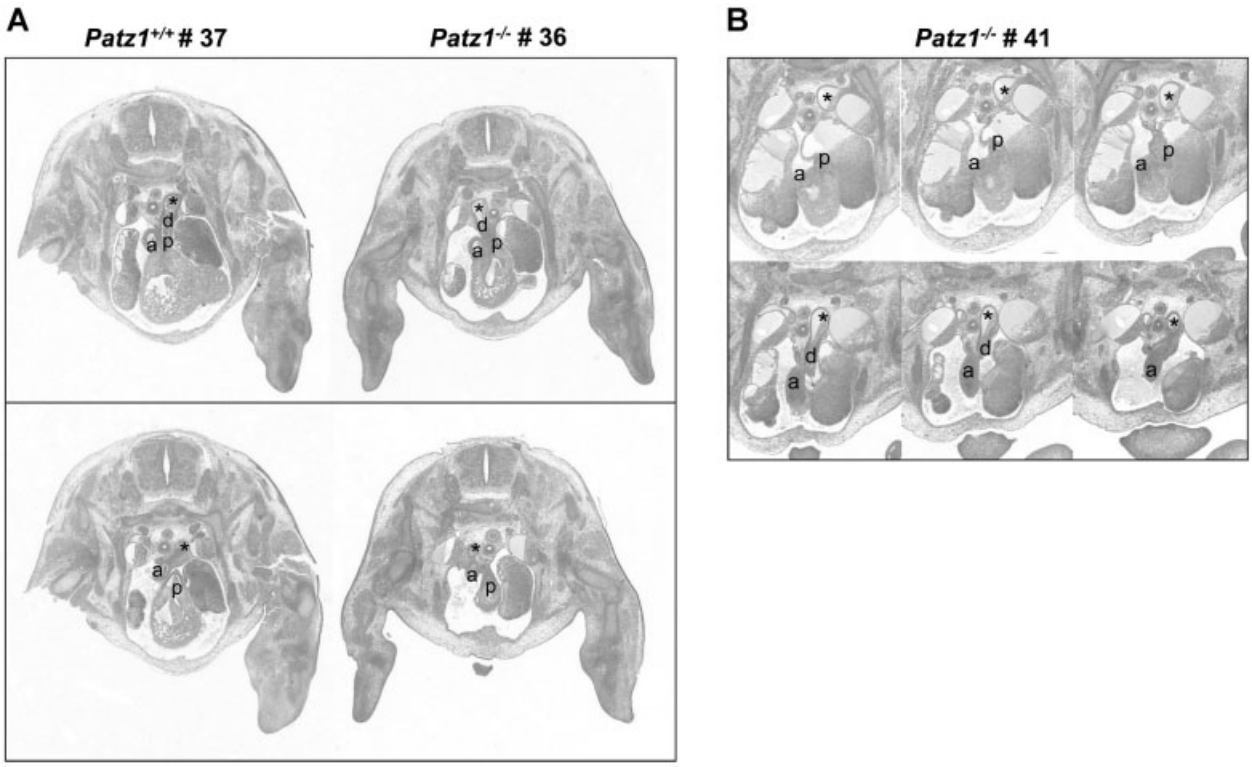

Fig. 4. Outflow-tract defects in Patz1$^{-/-}$ embryos. A: Cross sections, at the heart level, of representative WT and Patz1$^{-/-}$ embryos at 13.5 dpc. Parallel sections are aligned for comparison. B: Cross section, at the heart level, of a Patz1$^{-/-}$ embryo at 13.5 dpc different from that shown in A. All sections shown are progressively more cranial going from the top to the bottom (A) and for the left to the right (B). *, descending aorta and aortic arch; a, ascending aorta; p, pulmonary trunk; d, ductus arteriosus.

To determine whether the growth alterations observed in *Patz1*$^{-/-}$ and *Patz1*$^{+/-}$ MEFs were due to altered progression through the different phases of the cell cycle, proliferating MEFs in the logarithmic phase were analyzed by bromodeoxyuridine (BrdU) incorporation and flow cytometry. A drastic reduction in BrdU incorporation was observed in *Patz1*$^{-/-}$ compared to both WT and *Patz1*$^{+/-}$ cells, suggesting a significant decrease in S phase entrance in Patz1-null MEFs. Consistently, staining with propidium iodide for DNA content confirmed that the cell population in S phase was significantly decreased in *Patz1*$^{-/-}$ compared to both WT and heterozygous cells (Fig. 6D). Conversely, an increased number of *Patz1*$^{-/-}$ cells in both G0/G1 and G2/M has been observed compared to WT and *Patz1*$^{+/-}$ MEFs (Fig. 6D).

We next examined the susceptibility to senescence of the MEFs at different culture passages by measuring senescence-associated β-gal activity. As shown in Figure 6, Panels E and F, *Patz1*$^{-/-}$ MEFs entered into premature cellular senescence when they were cultured beyond seven passages.

To further investigate the mechanisms underlying the cell cycle profile alterations of *Patz1*-knockout MEFs, we examined the expression of cyclins, CDKs and CDK-inhibitor proteins in *Patz1*$^{+/+}$, *Patz1*$^{+/-}$, and *Patz1*$^{-/-}$ cells. Proteins involved in cell cycle activation, such as HMGA1 and HMGA2, were also examined. Consistent with the slow growth rates (Fig. 6A–C) and the increased susceptibility to senescence of *Patz1*$^{-/-}$ MEFs (Fig. 6E,F), an increased expression of cell cycle inhibitors, including p53, p21, p27, p16, and p19, was observed in *Patz1*$^{-/-}$ MEFs compared to their WT and heterozygous counterparts. Paradoxically, *Patz1*$^{-/-}$ cells also showed increased expression of various proteins involved in cell cycle activation, including cyclin D2, CDK4, Cyclin E, HMGA1, and HMGA2 (Fig. 6G). It is likely that conflicting signals could account for cell cycle arrest (hypermitogenic arrest) that might then induce premature senescence (Blagosklonny, 2003).

Collectively, these data suggest that cells devoid of two *Patz1* alleles enter the cell cycle more slowly than WT cells do, arrest in both G0/G1 and G2/M phases of the cell cycle and undergo premature cellular senescence. Conversely, heterozygous MEFs cells grow faster than WT controls but do not show significant differences in BrdU uptake and cell cycle profile, compared to WT cells.

Discussion

PATZ is an emerging cancer-related transcription factor, whose role in cancer pathogenesis is not clear, due to controversial reports supporting either a tumor suppressive or a tumor inducing activity (Mastrangelo et al., 2000; Fedele et al., 2008; Tian et al., 2008; Tritz et al., 2008; Yang et al., 2010; Pero et al., 2012). From the analysis of Patz1-null mice, we previously reported an important role for the *PATZ1* gene in testis development and spermatogenesis. Indeed, the lack of the *Patz1* gene led to increased apoptosis of the spermatocytes and total absence of spermatids and spermatozoa, with the subsequent loss of tubular structure and male infertility (Fedele et al., 2008). Consistent with these data, among the germ cells, PATZ1 is exclusively expressed in spermatogonia (Fedele et al., 2008), in which, as Plzf, another member of the POK family, it could regulate the maintaining of a stem cell pool (Buaas et al., 2004; Costoya et al., 2004). Also by generating Patz1-null mice, but focusing on T-cell development, it has been subsequently

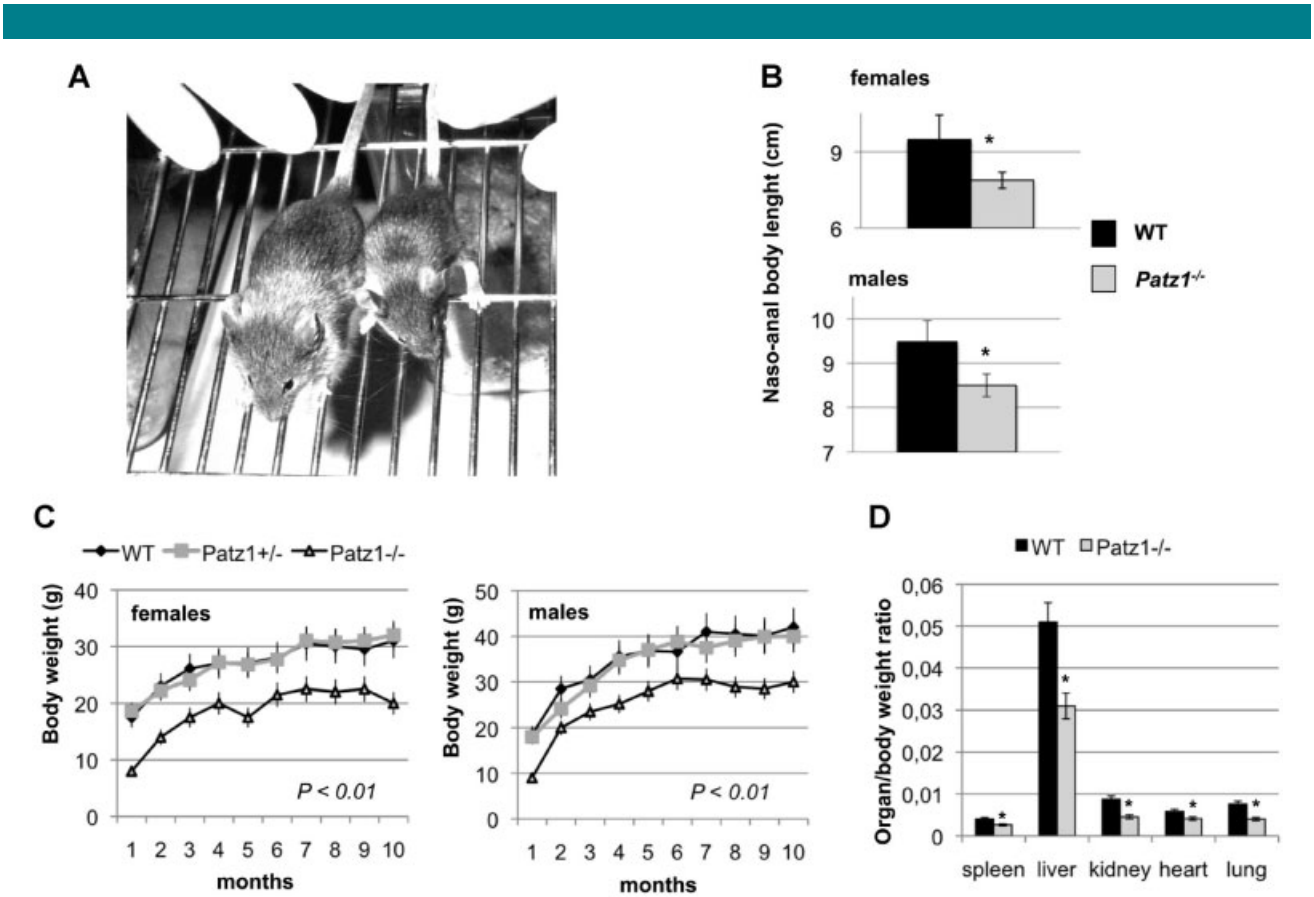

Fig. 5. Growth retardation of *Patz1*$^{-/-}$ mice. A: Gross appearance of a representative 1-year-old *Patz1*-null mouse (right) in comparison with a sex-matched wild-type sibling (left). B: Naso-anal length of cohorts of 10 mice, males or females, was measured at 12 months of age. Values are mean ± SD, **P* < 0.05. C: Body weights curves of cohorts of 10 WT, 10 *Patz1*$^{+/-}$ and 10 *Patz1*$^{-/-}$ female (left) and male (right) mice as a function of age. Value are mean ± SD. The curves of *Patz1*$^{-/-}$ mice were significantly lower than both *Patz1*$^{+/+}$ and *Patz1*$^{+/-}$ mice (*P* < 0.01), as calculated by ANOVA + Tukey test. D: Ratio of organ to body weight on mean values of four mice for each genotype above indicated. **P* < 0.05.

shown that PATZ regulates transcription of the *cd8* gene and is part of the transcription factor network that controls the fate of double positive thymocytes (Sakaguchi et al., 2010).

In the present work, we have more deeply studied the expression of PATZ during development, extending the analysis to the whole embryo. Interestingly, we found that it is widely expressed at high levels during embryogenesis, especially in the CNS, where it is clearly restricted to the actively proliferating neuroblasts in the periventricular neocortical neuroepithelium, in the telencephalic cortical plate, in the hippocampus, and in the striatal neuroepithelium and subventricular zone, suggesting the involvement of PATZ in CNS development, as then validated by the phenotype of *Patz1*$^{-/-}$ embryos. In fact, they show defects in the CNS with a clear reduction of periventricular cells. The critical role of PATZ in CNS development is consistent with previously published data reporting that PATZ is strongly expressed in the midbrain region (Kobayashi et al., 2000) and that it is one of the transcriptional factors that regulate a group of candidate genes for susceptibility to the fetal alcoholic syndrome, which is characterized by severe defects at the CNS (Lombard et al., 2007).

Interestingly, most of the CNS districts, where PATZ1 expression is confined at later stages of development, harbor embryonic neural stem cells (NSCs; Temple, 2003), once again suggesting a crucial role of PATZ1 in maintaining a stem cell pool. This is consistent with the reduction of the subventricular zone, which is one of the key neurogenic sites harboring the adult NSC niche (Doetsch, 2003), in Patz1-null embryos. It is noteworthy that in adult mammals, NSCs generate new neurons that are important for specific types of learning and memory (Yamasaki et al., 2007; Zhang et al., 2008). The control of adult NSC number and function is fundamental for preserving the stem cell pool and ensuring proper levels of neurogenesis throughout life. Indeed, decreased neurogenesis is implicated in the development of pre-mature aging and disorders in learning, memory, and cognition (Lemaire et al., 2000; Drapeau and Abrous, 2008; Kitamura et al., 2009). Therefore, the definition of the mechanisms underlying NSC maintaining may open the possibility of preventing the onset or progression of these disorders by therapeutically enhancing neurogenesis.

Another interesting phenotype, observed by the morphological analysis of *Patz1*$^{-/-}$ embryonic tissues at 12.5 dpc, and subsequently confirmed by macroscopic observations in newborn pups, was the altered positioning of the cardiac OFT. It is likely that these defects are responsible for the intrauterine or early neonatal death of most Patz1-null mice. In fact, the wrong positioning of the vessels that carry blood to and from the heart can cause birth asphyxia due to respiratory distress following the transition from placental to pulmonary-based breathing (Ranjit, 2000). Similar cardiovascular defects are reminiscent of common congenital heart defects, most of them known as DiGeorge syndrome, seen in human newborns.

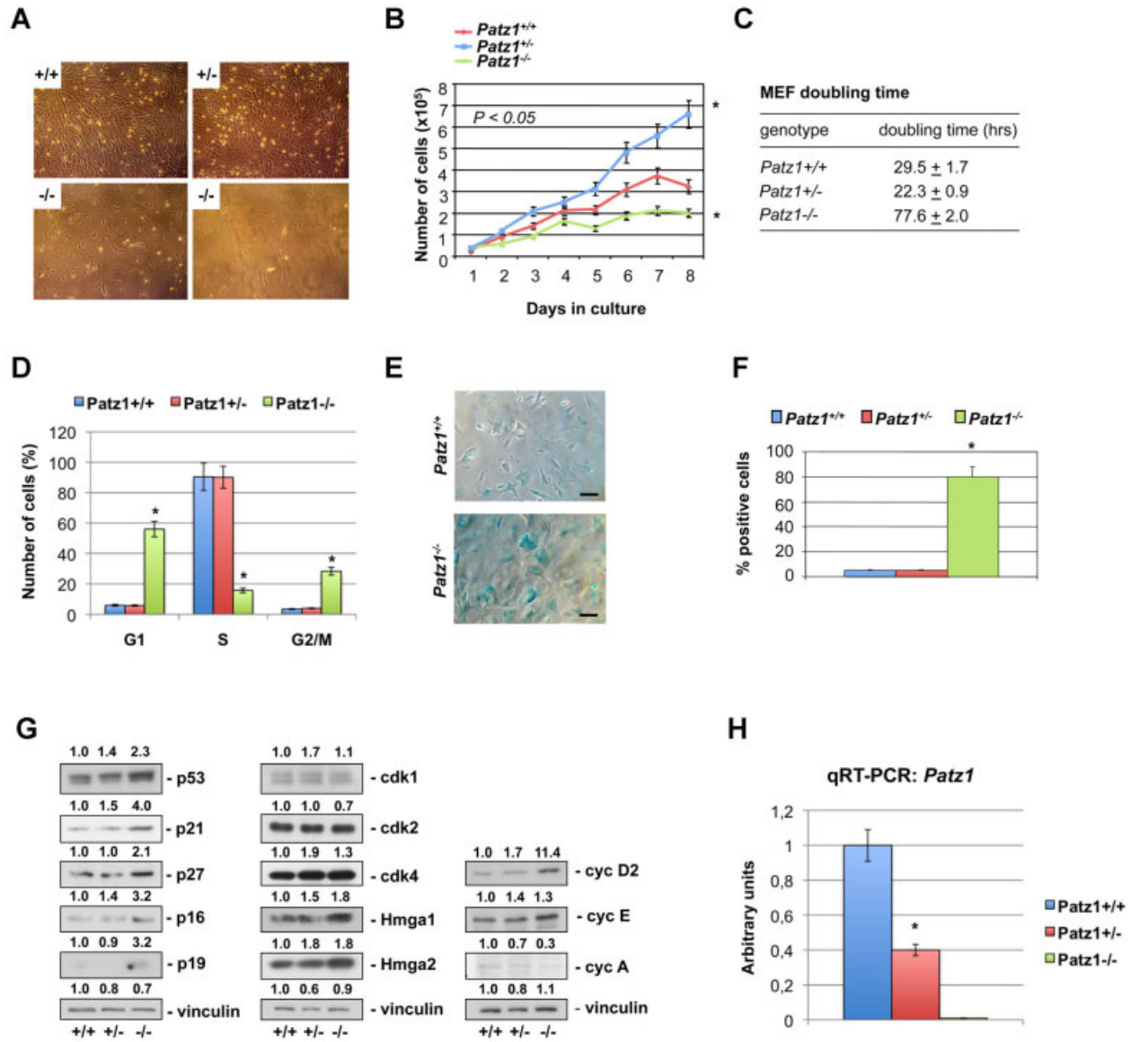

Fig. 6. Growth alterations in *Patz1*-knockout embryonic fibroblasts. A: MEFs were prepared from *Patz1*$^{+/+}$, *Patz1*$^{+/-}$, and *Patz1*$^{-/-}$ embryos at 12.5 dpc. At passage 4 their growth properties were examined in vitro. Representative clones from each genotype, as indicated in the figure, are shown 3 days after plating an equal number of cells from each. B: Growth curves of MEFs as described in (A). MEFs were plated equally and counted daily for 8 days. The values are the mean ± SE of three different cell clones (each originating from a different embryo) for each genotype. C: Cell-doubling time of MEFs as described in (A), calculated 4 days after plating. The values represent the mean ± SD of three different cell clones as described in (B). D: BrdU + Propidium iodide flow cytometry of asynchronous MEFs as described in (A). The percentage (expressed as mean ± SD) of cells in each phase of the cell cycle is indicated. E: Light microscopy of representative WT and homozygous *Patz1*-knockout MEFs stained for β-galactosidase activity at culture passage 8 (Scale bare: 10 μm). F: Quantification of the percent of cells positive for β-galactosidase activity (i.e., senescent cells) in *Patz1*$^{+/+}$, *Patz1*$^{+/-}$, and *Patz1*$^{-/-}$ MEFs is expressed as mean ± SD of three independent experiments. G: Expression of cell cycle and senescence regulators in representative MEFs from each genotype, as indicated on the bottom, was determined by Western blot. Relative expression levels, compared to WT cells and normalized with respect to vinculin, are indicated on the top of each panel. H: Relative *Patz1* expression in MEFs as in the previous panels, evaluated by qRT-PCR. Values are the mean ± SD of three independent experiments in three different clones for each genotype.

This disease has an incidence of 1 of 4,000 born and is caused by the alteration of several genes located in 22q11-22q12 (Schinke and Izumo, 2001). Since *PATZ1* is also located on chromosome 22q12, and many human newborns with aortic arch and/or OFT defects do not display characteristic mutations in well known genes associated to the DiGeorge syndrome (DGS), such as TBX1, *PATZ1* might be a good candidate among the genes responsible for some types of DGS. It is noteworthy, at this regard, that many experimental models of DSG focus on the cardiac neural crest cells, a unique subset of cells that migrate from the dorsal aspect of the neural tube to remodel the pharyngeal arch arteries and the septation of the cardiac OFT into two individual vessels: the pulmonary trunk and ascending aorta (Hutson and Kirby, 2007). Therefore, the two main pathological phenotypes observed in Patz1$^{-/-}$ embryos (neural tube and cardiac OFT defects) could be linked by a common pathological event in the neural crest cells.

The few mice Patz1$^{-/-}$ that survive to the birth harbor no or just slight cardiovascular defects (decrease in the diameter of a vessel), having a quite normal life expectancy, except for those which die prematurely for the onset of lymphomas (Pero et al., 2012). Interestingly, most of these adult mice are growth-retarded since they are 10–20% smaller and 40–50% lighter than their WT and *Patz1*$^{+/-}$ sex and age-matched controls. This phenotype is compatible with defects in the CNS development (Shanske et al., 1997). Nevertheless, the analysis of MEF growth properties suggest that this phenotype may be due, at least in part, to alterations in cell cycle progression and premature senescence. Indeed, cell cycle analysis of *Patz1*$^{-/-}$ MEFs shows arrest at or beyond the restriction point, in either G1 or G2 phase, which is compatible with a hypermitogenic arrest (Blagosklonny, 2003). Indeed, Patz1-null MEFs showed conflicting signals due to increased levels at the same time of both mitogenic cyclins and CDK inhibitors. This could conceivably create an oncogenic stress, which would be responsible for premature senescence (Serrano et al., 1997).

The results obtained on the Patz1-null MEFs are consistent with very recent data showing growth inhibition and accelerated senescence in human endothelial cells interfered for PATZ1 expression (Cho et al., 2011). Apparently, this anti-senescence function seems to conflict with the role of tumor suppressor that we envisaged for PATZ (Pero et al., 2012). However, the different cellular context may play a critical role in the effect of PATZ on cell fate. Moreover, a dual tumor suppressor/anti-senescence role has been previously reported for other genes (Pan et al., 2011). Indeed, differently from apoptosis that leads cells to death, senescence is a stable and metabolically active state, which in fibroblasts is associated with resistance to apoptosis caused by radiation (Yeo et al., 2000).

In conclusion, our findings in Patz1-knockout mice highlight the critical role that PATZ plays during neural and cardiac OFT development, deficiencies of which dramatically impact on embryonic development and postnatal growth. Moreover, they also indicate that *PATZ1* gene can affect cell-cycle decision, supporting its cancer-related function.

Acknowledgments

We thank Sara Sancho-Oliver from Frimorfo for embryos analysis, Francesco D'Agnello for technical assistance with artwork and Sabrina Battista for critically reviewing the article.

Literature Cited

Bilic I, Koesters C, Unger B, Sekimata M, Hertweck A, Maschek R, Wilson CB, Ellmeier W. 2006. Negative regulation of CD8 expression via Cd8 enhancer-mediated recruitment of the zinc finger protein MAZR. Nat Immunol 7:392–400.

Blagosklonny MV. 2003. Cell senescence and hypermitogenic arrest. EMBO Rep 4:358–362.

Buaas FW, Kirsh AL, Sharma M, McLeann DJ, Morris JL, Griswold MD, de Rooij DG, Braun RE. 2004. Plzf is required in adult male germ cells for stem cell self-renewal. Nat Genet 36:647–652.

Burrow AA, Williams LE, Pierce LC, Wang YH. 2009. Over half of breakpoints in gene pairs involved in cancer-specific recurrent translocations are mapped to human chromosomal fragile sites. BMC Genomics 10:59.

Chiappetta G, Avantaggiato V, Visconti R, Fedele M, Battista S, Trapasso F, Merciai BM, Fidanza V, Giancotti V, Santoro M, Simeone A, Fusco A. 1996. High level expression of the HMGI (Y) gene during embryonic development. Oncogene 13:2439–2446.

Cho JH, Kim MJ, Kim KJ, Kim JR. 2012. POZ/BTB and AT-hook-containing zinc finger protein 1 (PATZ1) inhibits endothelial cell senescence through a p53 dependent pathway. Cell Death Differ 19:703–712.

Costoya JA. 2007. Functional analysis of the role of POK transcriptional repressors. Brief Funct Genomic Proteomic 6:8–18.

Costoya JA, Hobbs RM, Barna M, Cattoretti G, Manova K, Sukhwani M, Orwig KE, Wolgemuth DJ, Pandolfi PP. 2004. Essential role of Plzf in maintenance of spermatogonial stem cells. Nat Genet 36:653–659.

Dean M. 1998. Cancer as a complex developmental disorder—Nineteenth Cornelius P. Rhoads Memorial Award Lecture. Cancer Res 58:5633–5636.

Doetsch F. 2003. A niche for adult neural stem cells. Curr Opin Genet Dev 13:543–550.

Drapeau E, Abrous DN. 2008. Stem cell review series: Role of neurogenesis in age-related memory disorders. Aging Cell 7:569–589.

Esposito F, Boscia F, Franco R, Tornincasa M, Fusco A, Kitazawa S, Looijenga LH, Chieffi P. 2011. Down-regulation of oestrogen receptor-β associates with transcriptional co-regulator PATZ1 delocalization in human testicular seminomas. J Pathol 224: 110–120.

Fedele M, Benvenuto G, Pero R, Majello B, Battista S, Lembo F, Vollono E, Day PM, Santoro M, Lania L, Bruni CB, Fusco A, Chiariotti L. 2000. A novel member of the BTB/POZ family, PATZ, associates with the RNF4 RING finger protein and acts as a transcriptional repressor. J Biol Chem 275:7894–7901.

Fedele M, Visone R, De Martino I, Troncone G, Palmieri D, Battista S, Ciarmiello A, Pallante P, Arra C, Melillo RM, Helin K, Croce CM, Fusco A. 2006. HMGA2 induces pituitary tumorigenesis by enhancing E2F1 activity. Cancer Cell 9:459–471.

Fedele M, Franco R, Salvatore G, Paronetto MP, Barbagallo F, Pero R, Chiariotti L, Sette C, Tramontano D, Chieffi G, Fusco A, Chieffi P. 2008. PATZ1 gene has a critical role in the spermatogenesis and testicular tumours. J Pathol 215:39–47.

Hutson MR, Kirby ML. 2007. Model systems for the study of heart development and disease. Cardiac neural crest and conotruncal malformations. Semin Cell Dev Biol 18:101–110.

Juriloff DM, Harris MJ, Tom C, MacDonald KB. 1991. Normal mouse strains differ in the site of initiation of closure of the cranial neural tube. Teratology 44:225–233.

Kitamura T, Saitoh Y, Takashima N, Murayama A, Niibori Y, Ageta H, Sekiguchi M, Sugiyama H, Inokuchi K. 2009. Adult neurogenesis modulates the hippocampus-dependent period of associative fear memory. Cell 139:814–827.

Kobayashi A, Yamagiwa H, Hoshino H, Muto A, Sato K, Morita M, Hayashi N, Yamamoto M, Igarashi K. 2000. A combinatorial code for gene expression generated by transcription factor Bach2 and MAZR (MAZ-related factor) through the BTB/POZ domain. Mol Cell Biol 20:1733–1746.

Lemaire V, Koehl M, Le Moal M, Abrous DN. 2000. Prenatal stress produces learning deficits associated with an inhibition of neurogenesis in the hippocampus. Proc Natl Acad Sci USA 97:11032–11037.

Lombard Z, Tiffin N, Hofmann O, Bajic VB, Hide W, Ramsay M. 2007. Computational selection and prioritization of candidate genes for fetal alcohol syndrome. BMC Genomics 8:389.

Mastrangelo T, Modena P, Tornielli S, Bullrich F, Testi MA, Mezzelani A, Radice P, Azzarelli A, Pilotti S, Croce CM, Pierotti MA, Sozzi G. 2000. A novel zinc finger gene is fused to EWS in small round cell tumor. Oncogene 19:3799–37804.

Melillo RM, Pierantoni GM, Scala S, Battista S, Fedele M, Stella A, De Biasio MC, Chiappetta G, Fidanza V, Condorelli G, Santoro M, Croce CM, Viglietto G, Fusco A. 2001. Critical role of the HMGI(Y) proteins in adipocytic cell growth and differentiation. Mol Cell Biol 21:2485–2495.

Morii E, Oboki K, Kataoka TR, Igarashi K, Kitamura Y. 2002. Interaction and cooperation of mi transcription factor (MITF) and myc-associated zinc-finger protein-related factor (MAZR) for trascription of mouse mast cell protease 6 gene. J Biol Chem 277:8566–8571.

Pan J, Zhong J, Gan LH, Chen SJ, Jin HC, Wang X, Wang LJ. 2011. Klotho, an anti-senescence related gene, is frequently inactivated through promoter hypermethylation in colorectal cancer. Tumour Biol 32:729–735.

Pero R, Lembo F, Palmieri EA, Vitiello C, Fedele M, Fusco A, Bruni CB, Chiariotti L. 2002. PATZ attenuates the RNF4-mediated enhancement of androgen receptor-dependent transcription. J Biol Chem 277:3280–3285.

Pero R, Palmieri D, Angrisano T, Valentino T, Federico A, Franco R, Lembo F, Klein-Szanto AJ, Del Vecchio L, Montanaro D, Keller S, Arra C, Papadopoulou V, Wagner SD, Croce CM, Fusco A, Chiariotti L, Fedele M. 2012. POZ-, AT-hook-, and zinc finger-containing protein (PATZ) interacts with human oncogene B cell lymphoma 6 (BCL6) and is required for its negative autoregulation. J Biol Chem 287:18308–18317.

Ranjit MS. 2000. Cardiac abnormalities in birth asphyxia. Indian J Pediatr 67:529–532.

Sakaguchi S, Hombauer M, Bilic I, Naoe Y, Schebesta A, Taniuchi I, Ellmeier W. 2010. The zinc-finger protein MAZR is part of the transcription factor network that controls the CD4 versus CD8 lineage fate of double-positive thymocytes. Nat Immunol 11:442–448.

Schinke M, Izumo S. 2001. Deconstructing DiGeorge syndrome. Nat Genet 27:238–240.

Serrano M, Lin AW, McCurrach ME, Beach D, Lowe SW. 1997. Oncogenic ras provokes premature cell senescence associated with accumulation of p53 and p16INK4a. Cell 88:593–602.

Shanske A, Caride DG, Menasse-Palmer L, Bogdanow A, Marion RW. 1997. Central nervous system anomalies in Seckel syndrome: Report of a new family and review of the literature. Am J Med Genet 70:155–158.

Temple S. 2003. The development of neural stem cells. Nature 414:112–117.

Theiler K. 1989. The house mouse (atlas of embryonic development), ed. New York: Springer-Verlab.

Tian X, Sun D, Zhang Y, Zhao S, Xiong H, Fang J. 2008. Zinc finger protein 278, a potential oncogene in human colorectal cancer. Acta Biochim Biophys Sin (Shanghai) 40:289–296.

Tritz R, Mueller BM, Hickey MJ, Lin AH, Gomez GG, Hadwiger P, Sah DW, Muldoon L, Neuwelt EA, Kruse CA. 2008. siRNA down-regulation of the PATZ1 gene in human glioma cells increases their sensitivity to apoptotic stimuli. Cancer Ther 6:865–876.

Yamasaki TR, Blurton-Jones M, Morrissette DA, Kitazawa M, Oddo S, LaFerla FM. 2007. Neural stem cells improve memory in an inducible mouse model of neuronal loss. J Neurosci 27:11925–11933.

Yang WL, Ravatn R, Kudoh K, Alabanza L, Chin KV. 2010. Interaction of the regulatory subunit of the cAMP-dependent protein kinase with PATZ1 (ZNF278). Biochem Biophys Res Commun 391:1318–1323.

Yeo EJ, Hwang YC, Kang CM, Choy HE, Park SC. 2000. Reduction of UV-induced cell death in the human senescent fibroblasts. Mol Cell 10:415–422.

Zhang CL, Zou Y, He W, Gage FH, Evans RM. 2008. A role for adult TLX-positive neural stem cells in learning and behaviour. Nature 451:1004–1007.

PIT1 upregulation by HMGA proteins has a role in pituitary tumorigenesis

Dario Palmieri[1,2], Teresa Valentino[1,2], Ivana De Martino[1], Francesco Esposito[1,2], Paolo Cappabianca[3], Anne Wierinckx[4,5], Michela Vitiello[1,2], Gaetano Lombardi[6], Annamaria Colao[6], Jacqueline Trouillas[4,5], Giovanna Maria Pierantoni[1], Alfredo Fusco[1,2] and Monica Fedele[1,2]

[1]Dipartimento di Biologia e Patologia Cellulare e Molecolare, [2]Istituto di Endocrinologia ed Oncologia Sperimentale (IEOS) del Consiglio Nazionale delle Ricerche and [3]Dipartimento di Scienze Neurologiche, Divisione di Neurochirurgia, Università degli Studi di Napoli 'Federico II', via Pansini 5, 80131 Naples, Italy
[4]INSERM U1028; CNRS UMR5292; Lyon Neuroscience Research Center, Neuro-oncology and Neuro-inflammation Team, Lyon F-69372, France
[5]University Lyon1, F-69000 Lyon, France
[6]Dipartimento di Endocrinologia, Università degli Studi di Napoli 'Federico II', 80131 Naples, Italy

(Correspondence should be addressed to A Fusco; Email: alfusco@unina.it)

Abstract

We have previously demonstrated that HMGA1B and HMGA2 overexpression in mice induces the development of GH and prolactin (PRL) pituitary adenomas mainly by increasing E2F1 transcriptional activity. Interestingly, these adenomas showed very high expression levels of PIT1, a transcriptional factor that regulates the gene expression of *Gh*, *Prl*, *Ghrhr* and *Pit1* itself, playing a key role in pituitary gland development and physiology. Therefore, the aim of our study was to identify the role of *Pit1* overexpression in pituitary tumour development induced by HMGA1B and HMGA2. First, we demonstrated that HMGA1B and HMGA2 directly interact with both PIT1 and its gene promoter *in vivo*, and that these proteins positively regulate *Pit1* promoter activity, also co-operating with PIT1 itself. Subsequently, we showed, by colony-forming assays on two different pituitary adenoma cell lines, GH3 and αT3, that *Pit1* overexpression increases pituitary cell proliferation. Finally, the expression analysis of *HMGA1*, *HMGA2* and *PIT1* in human pituitary adenomas of different histological types revealed a direct correlation between *PIT1* and HMGA expression levels. Taken together, our data indicate a role of *Pit1* upregulation by HMGA proteins in pituitary tumours.

Endocrine-Related Cancer (2012) **19** 123–135

Introduction

Pituitary adenomas are one of the most frequent intracranial tumours with a prevalence of clinically apparent tumours close to one in 1000 of the general population and are the third most common intracranial tumour type after meningiomas and gliomas (Scheithauer *et al*. 2006). They are mostly non-metastatising monoclonal neoplasms arising from adenohypophyseal cells in the anterior pituitary, and exhibit a wide range of hormonal and proliferative activity. The most common types (about 50%) of pituitary adenomas are prolactinomas, while GH- or ACTH-secreting adenomas account for 20 and 10% of pituitary tumours respectively, and TSH-secreting adenomas are rare (1%) (Llyod *et al*. 2004). About one-third of pituitary adenomas are named non-functioning adenomas because they do not exhibit signs of hypersecretion or gonadotrophin adenomas related to FSH–LH immunoreactivity (Trouillas *et al*. 1986). They are usually large tumours diagnosed following local compressive effects on brain structures and cranial nerves.

Pituitary tumorigenesis is generally considered a model of the multi-step process of carcinogenesis, in which molecular genetic alterations represent the initialising event that transforms cells, and hormones and/or growth factors promote cell proliferation (Asa & Ezzat 2002). However, the molecular events leading

DOI: 10.1530/ERC-11-0135
1351–0088/12/019–123
Online version via http://www.endocrinology-journals.org

to pituitary tumour development are still unclear, since somatic mutations identified in other neoplasias, such as the *BRAF* and *RAS* genes, are rare events in pituitary adenomas (Lania *et al*. 2003, De Martino *et al*. 2007*a*). Activating mutations of *Gsα* (the so-called *gsp* mutations) are the most important somatic mutation in pituitary adenomas, being present in up to 40% of GH-secreting adenomas (Lyons *et al*. 1990). Mutations of *MEN1A*, the gene mutated in the MEN-1 syndrome, which includes pituitary adenomas, are uncommon in sporadic tumours (Zhuang *et al*. 1997, Schmidt *et al*. 1999). Similarly, other genes involved in familial pituitary adenomas, such the *AIP* gene, responsible for familial isolated pituitary adenomas, or the *CDKN1B* gene, mutated in the MEN-1-like syndrome MEN-4, have been found to be mutated in about 3% of sporadic GH-secreting adenoma or never in sporadic pituitary adenomas respectively (Occhi *et al*. 2010). However, epigenetic events, such as hypermethylation and/or microRNA-dependent impairment of protein translation, are likely to be responsible for the down-regulation of gene and/or protein expression associated with pituitary tumorigenesis (Amaral *et al*. 2009, Dudley *et al*. 2009, Tateno *et al*. 2010). Moreover, a parental-specific methylation pattern of the *Gsα* gene, responsible for a tissue-specific near-exclusive expression of Gsα from the maternal allele, is relaxed in the majority of GH-secreting pituitary adenomas negative for *gsp* (Hayward *et al*. 2001). Therefore, both genetic and epigenetic alterations appear to be involved in pituitary tumorigenesis. Our recent studies have identified a crucial role for the high-mobility group A (HMGA) proteins in pituitary tumour development (Fedele *et al*. 2002, 2005).

HMGA protein family includes four members, HMGA1A, HMGA1B and HMGA1C, splicing isoforms of the *HMGA1* gene, and HMGA2, encoded by the *HMGA2* gene (Fusco & Fedele 2007). They are small acidic non-histone nuclear factors that bind the minor groove of AT-rich DNA sequences through their amino-terminal region containing three short basic repeats, the so-called AT-hooks (Fusco & Fedele 2007). HMGA proteins do not have transcriptional activity *per se*, but regulate gene expression interacting with other transcription factors and modifying the structure of DNA, in order to modulate the formation of stereo-specific complexes on the promoter/enhancer regions of target genes (Thanos & Maniatis 1992, Falvo *et al*. 1995).

Both *HMGA* genes have a critical role during embryogenesis, when they are widely expressed, whereas their expression is absent or low in normal adult tissues (Zhou *et al*. 1995, Chiappetta *et al*. 1996). Conversely, they are frequently overexpressed in several human cancers including thyroid (Chiappetta *et al*. 1998, 2008), prostate (Tamimi *et al*. 1993, Winkler *et al*. 2007), cervix (Bandiera *et al*. 1998), colorectum (Fedele *et al*. 1996) and pancreas carcinoma (Abe *et al*. 2000, 2003), and several studies indicate that HMGA proteins are causally involved in tumour development (Fusco & Fedele 2007). In fact, overexpression of both *HMGA1* and *HMGA2* results in the transformation of rat1a fibroblast and human lymphoblastoid cells (Wood *et al*. 2000) while inhibition of their expression prevents thyroid transformation induced by mouse transforming retroviruses (Vallone *et al*. 1997) or induces apoptosis in two different thyroid anaplastic carcinoma cell lines (Scala *et al*. 2000).

Several data support a critical role for *HMGA2* (and probably for *HMGA1*) in the generation of human pituitary adenomas (Fedele *et al*. 2010). Indeed, *HMGA2* was found amplified and overexpressed in a large set of human prolactinomas (Finelli *et al*. 2002), and pituitary adenomas secreting prolactin (PRL) and GH developed in transgenic mice overexpressing HMGA1B or HMGA2 (Fedele *et al*. 2002, 2005). Our previous studies demonstrated that HMGA2 induces pituitary tumour development by enhancing E2F1 activity (Fedele *et al*. 2006). Indeed, following the interaction with the retinoblastoma protein pRB, HMGA2 displaces histone deacetylase 1 (HDAC1) from the pRB/E2F1 complex, increasing E2F1 acetylation and transcriptional activity. Consistently, functional loss of E2F1 activity (obtained by mating *Hmga2* transgenic and *E2f1* knockout mice) strongly reduced the incidence of pituitary tumours (Fedele *et al*. 2006). However, *Hmga2* mice still develop pituitary neoplasias also in an *E2f1* knockout background, although with a lower frequency and a less aggressive phenotype, suggesting that other molecular pathways may be involved in pituitary tumour development induced by HMGA overexpression. Recently, using a genechip microarray approach, we have shown that HMGA proteins can contribute to pituitary cell transformation through the transcriptional modulation of target genes, such as *Mia* (*Cd-rap*) (De Martino *et al*. 2007*b*) and *Ccnb2* (De Martino *et al*. 2009).

Our previous findings also showed a very abundant expression of *Pit1* (whose expression was not detectable in adult mouse pituitary) in pituitary adenomas from *Hmga1b* and *Hmga2* transgenic mice (Fedele *et al*. 2002, 2005). PIT1, also named GHF1, is a member of the POU transcription factor family (Delhase *et al*. 1996), and plays a key role in the specification, expansion and survival of three specific pituitary cell types (somatotropes, lactotropes and a subset of thyrotropes) during the development of the

anterior pituitary (Lefevre *et al*. 1987, Nelson *et al*. 1988, Li *et al*. 1990), and its transcriptional activity on many genes, such as *GH*, *PRL*, *TSHB*, *GHRHR* and *PIT1* itself, is crucial for pituitary gland physiology (Lefevre *et al*. 1987, Nelson *et al*. 1988, Chen *et al*. 1990, Li *et al*. 1990, McCormick *et al*. 1990). Moreover, *PIT1* is overexpressed in GH, PRL and TSH pituitary adenomas (Asa *et al*. 1993, Delhase *et al*. 1993, Friend *et al*. 1993, Pellegrini *et al*. 1994, Pellegrini-Bouiller *et al*. 1997).

The aim of the present study was to investigate the role of *Pit1* overexpression in the generation of pituitary adenomas in *Hmga1b* and *Hmga2* transgenic mice.

Here, we demonstrate that both HMGA1B and HMGA2 bind both PIT1 and PIT1-responsive DNA elements, thus positively modulating *Pit1* promoter activity. Functional studies show that *Pit1* overexpression enhances pituitary adenoma cell proliferation. Finally, a correlation was found between *PIT1* and *HMGA* overexpression in human pituitary adenomas, further supporting a role of HMGA-mediated *PIT1* overexpression in pituitary tumours.

Materials and methods

Plasmids, siRNAs, recombinant proteins and antibodies

Expression vector containing the V5-tagged full-length cDNA for *Pit1* sub-cloned in the pcDNA3.1/GS vector was purchased from Invitrogen. HA-tagged HMGA1B and HMGA2 expression plasmids were previously described (Fedele *et al*. 2001, 2006). The *PIT1* promoter construct, carrying the region −1321 to +15, related to the transcriptional start site, of the human *PIT1* gene fused to the luciferase cDNA (PIT-1-Luc), was a generous gift of Dr M Delhase (Brussels, Belgium). The pBABE-puro vector was previously described (Monaco *et al*. 2001). The siRNA anti-HMGA1 was purchased from Santa Cruz Biotechnology (Santa Cruz, CA, USA). GST- and His-HMGA1B and HMGA2 fusion proteins were expressed in *Escherichia coli* strain BL21 (DE3) and purified using glutathione sepharose or nickel beads as described previously (Baldassarre *et al*. 2001, Pierantoni *et al*. 2001). Full-length PIT1 protein, anti-HA (sc-805) and anti-PIT1 supershift antibodies (sc-442X) were purchased from Santa Cruz Biotechnology, whereas anti-V5 (R960-25) antibody was purchased from Invitrogen. Anti-HMGA1 and anti-HMGA2 antibodies were previously described (Fedele *et al*. 2006, Pierantoni *et al*. 2007).

Cell cultures and transfections

Human embryonic kidney (HEK) 293T, rat pituitary adenoma GH3 and mouse pituitary adenoma αT3 cells were cultured in DMEM supplemented with 10% FCS (GIBCO-BRL, Life Technologies). DNA was transfected by the calcium phosphate procedure, as described previously (Graham & Van der Eb 1973), in HEK293T, and by Lipofectamine 2000 (Invitrogen), according to the manufacturer's instructions, in GH3 and αT3 cells.

GST pull-down assay, protein extraction and co-immunoprecipitation

For *in vitro* protein–protein binding, 5 μg PIT1 recombinant protein were incubated with 5 μg resin conjugated to GST, GST-HMGA1B or GST-HMGA2 recombinant proteins. Reactions and analysis of the protein–protein interactions were performed as described previously (Pierantoni *et al*. 2001). A similar procedure was also applied to HEK293T cells transiently transfected with the Pit1-V5 expression vector. Briefly, 500 μg total protein extracts were incubated with 5 μg resin conjugated to GST, GST-HMGA1B or GST-HMGA2 recombinant proteins. The protein–protein complexes formed on the resin were pulled down by centrifugation. The resin was washed five times at 4 °C with 1 ml cold NETN buffer containing 0.1% NP-40, 1 mM EDTA, 50 mM Tris–HCl (pH 7.5), 150 mM NaCl, 20 mM pirophosphate, 0.2 μg aprotinin, 4 mM PMSF, 25 mM sodium fluoride, 10 mM activated sodium orthovanadate (Sigma) and a cocktail of protease inhibitors (Roche Applied Science).

Protein extracts were obtained by lysing cells and tissues in NETN buffer and then processed for co-immunoprecipitation as described previously (Pierantoni *et al*. 2001).

Electrophoretic mobility shift assay

Recombinant proteins (5 ng) were incubated for 15 min at RT in binding buffer (10 mM Tris–HCl, pH 7.5, 50 mM NaCl, 1 mM DTT, 2 μg BSA, 1 μg poly-dCdG) with a ^{32}P-end-labelled double-strand (DS) oligonucleotides (specific activity, 8000–20 000 c.p.m./fmol), corresponding to the PIT1 consensus (sc-2541; Santa Cruz Biotechnology) or to the same element mutated in the PIT1 binding site (sc-2542). Up to 400-fold excess of specific unlabelled competitor oligonucleotide was added as the control. Supershift analysis was carried out by incubating the reaction mix with 1 μg antibody for 30 min in ice. The DNA–protein complexes were resolved on 6%

non-denaturing acrylamide gels and visualised by exposure to autoradiographic films.

Chromatin immunoprecipitation

Chromatin immunoprecipitation (ChIP) was carried out with an acetyl-histone H3 immune precipitation assay kit (Upstate Biotechnology, Lake Placid, NY, USA) according to the manufacturer's instruction, as described previously (De Martino *et al*. 2009). Input and immunoprecipitated chromatin were analysed by PCR for the presence of the *Pit1* promoter sequence. PCR were performed with AmpliTaq gold DNA polymerase (Perkin–Elmer, Monza, Italy). Primers used to amplify the sequence of the *Pit1* promoter were 5′-GCACCAACCTATCATTAC-3′ (forward) and 5′-TGCTACTAACACAATTGC-3′ (reverse). PCR products were resolved on a 2% agarose gel, stained with ethidium bromide, and scanned using a Typhoon 9200 scanner. The intensity of the bands was quantified by densitometric analysis using ImageQuant software (GE Healthcare, Milan, Italy).

Luciferase and colony assays

For the luciferase assay, a total of 2×10^5 cells were seeded into each well of a six-well plate and transiently transfected with 1 μg PIT-1-Luc and with the indicated amounts of HA-HMGA1B and HA-HMGA2, together with 0.5 μg Renilla and various amounts of the backbone vector to keep the total DNA concentration constant. Transfection efficiency, normalised for the Renilla expression, was assayed with the dual luciferase system (Promega Corporation). All transfection experiments were repeated at least three times.

For the colony assay, GH3 and αT3 cells were seeded at a density of 2.5×10^6 per 10 mm dish. Two days after, the cells were transfected with 10 μg pcDNA3.1 or 10 μg pcDNA3.1/Pit1-V5 or 5 μg *Pit1* shRNA (Santa Cruz Biotechnology) or 5 μg scrambled shRNA (Santa Cruz Biotechnology) plus 2 μg pBABE-puro. After about 15 days of positive selection in puromycin, the cells were stained with 500 mg/ml crystal violet in 20% methanol, and the resulting colonies were counted.

Tissue samples

The human pituitary adenoma samples were obtained from 46 surgical excision biopsies, including 13 GH and 33 PRL adenomas) from patients of 'Federico II' University (Naples) and Neurosurgical Department (Pr Jouanneau E) of Hospices Civils de Lyon (France). One part of each pituitary adenoma was saved for routine histopathology evaluation, including immunohistochemistry with the systematic detection of GH, PRL, ACTH, TSH, FSH and LH, and the other one immediately frozen at −80 °C until the extraction of nucleic acids. Informed consent for the scientific use of biological material was obtained from all patients.

RNA extraction and real-time RT-PCR

Total RNA was extracted from tissues using TRI REAGENT (Molecular Research Center, Inc., Cincinnati, OH, USA) solution, according to the manufacturer's instructions. The RNA integrity was verified by denaturing agarose gel electrophoresis (virtual presence of sharp 28S and 18S bands) and spectrophotometry. One microgram of total RNA of each sample was reverse-transcribed with the QuantiTect Reverse Transcription (Qiagen) using an optimised blend of oligo-dT and random primers according to the manufacturer's instructions. To ensure that RNA samples were not contaminated with DNA, negative controls were obtained by performing the PCR on samples that were not reversed-transcribed but identically processed. Quantitative PCR was performed with the SYBR Green PCR Master Mix (Applied Biosystems, Foster City, CA, USA) as follows: 95 °C for 10 min and 40 cycles (95 °C for 15 s and 60 °C for 1 min). A dissociation curve was run after each PCR in order to verify amplification specificity. Each reaction was performed in duplicate. To calculate the relative expression levels, we used the $2^{-\Delta\Delta C_t}$ method (Livak & Schmittgen 2001).

Primer sequences are available upon request.

Statistical analyses

For the comparison between two groups of experiments, Student's *t*-test was used. Three or more groups of experiments were compared using the one-way ANOVA followed by Tukey's multiple comparison test. All results are expressed as mean ± S.D. The statistical significant difference was considered when P value was <0.05. Linear regression analysis was performed to determine the association of *PIT1* with *HMGA1* or *HMGA2* expression levels in human pituitary adenomas. The square of correlation coefficient (R^2) close to 1 was considered to be indicative of a significant direct correlation.

Results

HMGA proteins interact with PIT1

To investigate the role of HMGA proteins in the modulation of PIT1 function, we first hypothesised that HMGA proteins directly bind PIT1 protein. The finding

that other members of the POU transcription factor family, such as Oct-6 and Oct-2A, interact with HMGA proteins through their POU domain supports this hypothesis (Abdulkadir *et al*. 1995, Leger *et al*. 1995, Zwilling *et al*. 1995). Therefore, we performed a GST pull-down assay incubating the PIT1 recombinant protein with GST-HMGA1B or GST-HMGA2 fusion proteins. As shown in Fig. 1A, PIT1 was able to directly interact with both GST-HMGA1b and GST-HMGA2, but not with GST alone. To confirm this interaction in a cellular context, we transfected HEK293T cells with expression vectors containing the full-length cDNAs for PIT1, HMGA1b or HMGA2, fused to the V5 (Pit-1-V5) and HA (HA-HMGA1b and HA-HMGA2) tags respectively. Total cell extracts were immunoprecipitated with anti-V5 antibody and analysed by immunoblot with anti-HA antibody. As shown in Fig. 1B (left panels), HA-HMGA1b and HA-HMGA2 were immunoprecipitated by the anti-V5 antibody only when transfected along with Pit-1-V5. This result was confirmed by reverse co-immunoprecipitation carried out by immunoprecipitating with anti-HA antibody and analysing with anti-V5 antibody (Fig. 1B, right panels). The negative result obtained by blotting for the unrelated and endogenous E2F1 protein confirmed the specificity of the PIT1/HMGA interactions. Ethidium bromide was added to the immunoprecipitation reaction to prevent DNA-mediated interaction between proteins. Interestingly, cells co-transfected with PIT1 and each of the HMGA proteins show more abundant levels of HMGA proteins than those transfected with HMGA1b or HMGA2 alone (input in Fig. 1B, middle panels), suggesting that PIT1 can positively influence their expression. Western blot anti-V5 or anti-HA antibody, for samples immunoprecipitated with anti-V5 or anti-HA antibody respectively was performed to control the successful immunoprecipitation reactions (Fig. 1B).

Finally, to validate the HMGA/PIT1 interaction in the context of the pituitary tumours, we pulled down pituitary adenoma extracts from *Hmga1b* or *Hmga2* transgenic mice, where PIT1 is abundantly expressed (Fedele *et al*. 2002, 2005), from GST-HMGA1B or GST-HMGA2 beads. Figure 1C shows that both GST-HMGA1B and GST-HMGA2, but not GST, interacted with endogenous PIT1 protein in transgenic mouse tumours. These data demonstrate that HMGA proteins are direct molecular partners of PIT1 both *in vitro* and *in vivo*.

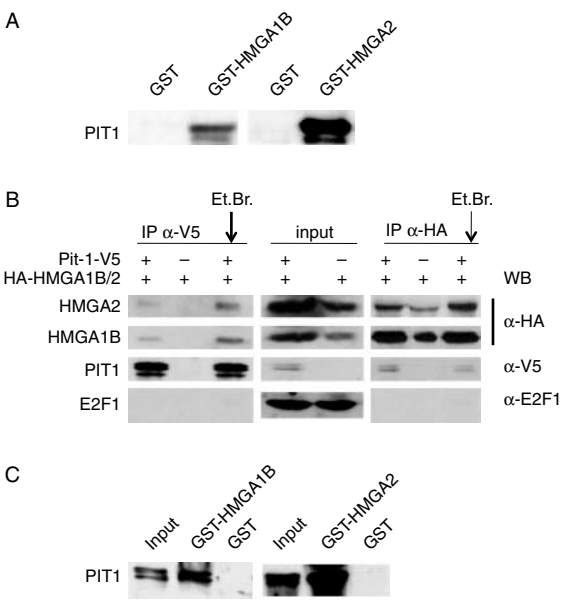

Figure 1 *In vitro* and *in vivo* interaction between PIT1 and HMGA proteins. (A) Recombinant PIT1 protein was incubated with immobilised GST-HMGA1B, GST-HMGA2 or GST alone in a GST pull-down assay. (B) HEK293T cells were transiently transfected with the Pit-1-V5, HA-HMGA1B and HA-HMGA2 expression plasmids where indicated. Protein extracts were immunoprecipitated (IP) with the anti-V5 or anti-HA, and probed with either anti-HA, anti-V5 or anti-E2F1 antibodies, as indicated on the right. Proteins detected are indicated on the left. Ethidium bromide was added to the IP reaction to make sure that the interaction was not mediated by any contaminating DNA. Western blot anti-V5 (lower panel) was done as a positive control of the IP reaction. Fifty micrograms of total cell extracts before IP were loaded as the control (input). (C) Protein extracts from pituitary adenoma tissues developed by *Hmga1b* (blot on the left) and *Hmga2* transgenic mice (blot on the right) were incubated with immobilised GST-HMGA1B, GST-HMGA2 or GST alone in a GST pull-down assay, and then probed with anti-PIT1 antibody.

HMGA proteins bind to and activate the *Pit1* promoter

PIT1 is able to directly regulate the expression of several genes with a key role in pituitary gland physiology such as *PRL*, *GH*, *GHRHR* and *PIT1* itself (Lefevre *et al*. 1987, Nelson *et al*. 1988, Chen *et al*. 1990, Li *et al*. 1990, McCormick *et al*. 1990). Since HMGA proteins physically interact with PIT1, we investigated whether this interaction may affect PIT1 activity. HMGA1B or HMGA2 recombinant proteins were incubated with a ^{32}P-end-labelled DS oligonucleotide corresponding to the consensus site recognised by PIT1 in an electrophoretic mobility shift assay (EMSA). As shown in Fig. 2A, both HMGA1B and HMGA2 were able to bind the PIT1 responsive element (Pit-1-RE) *in vitro*. The specificity of the binding was assessed using a 100- and 400-fold molar excess of the specific unlabelled DS oligonucleotide or a 100-fold molar excess of the same unlabelled, but single-strand (SS) oligonucleotide as specific and non-specific competitors respectively. Moreover, the

binding was also abolished pre-incubating the reaction mix with anti-HMGA1 and anti-HMGA2 antibodies, which, as reported previously (Martinez Hoyos *et al.* 2009), specifically displace HMGA proteins from their target DNA (data not shown). As shown in Fig. 2B, the binding of HMGA proteins to the Pit-1-RE does not interfere with the binding of PIT1 to the same oligonucleotide. Moreover, as shown by the absence of a slower migrating spot when both HMGA and PIT1 proteins are incubated with the probe, it appears that they do not form a unique complex, but independently bind the same DNA response element. We also used, as a control of specificity of the PIT1 binding, an oligonucleotide mutated in a key residue within the PIT1 consensus site, which was incapable of binding PIT1 (Fig. 2C, lane 1). Interestingly, this mutant oligonucleotide still binds HMGA1B with the same efficiency of the wild-type Pit-1-RE, whereas the binding to HMGA2 was highly compromised (Fig. 2C, lanes 2 and 3). Therefore, it is likely that HMGA1B and HMGA2 do not bind exactly to the same residues nearby the PIT1 consensus site.

Next, since one of the PIT1 targets is *Pit1* gene itself, we focused on the potential role of HMGA in PIT1-dependent *Pit1* gene regulation in pituitary adenomas. For this purpose, we first performed a ChIP assay in pituitary adenomas from *Hmga1b* or *Hmga2* transgenic mice. Chromatin was immunoprecipitated using specific anti-HMGA1 or anti-HMGA2 antibody, or IgG as the negative control, and analysed by PCR using primers specific for the mouse *Pit1* promoter. Figure 3A shows the *in vivo* binding of both *Hmga1* and *Hmga2* to the *Pit1* promoter, while no amplification was obtained in the negative control. Then, we investigated the functional effect of the physical interaction between HMGA proteins and PIT1 on the *PIT1* promoter activity by luciferase assays. HEK293T cells were transiently transfected with a reporter vector (PIT1-1-Luc), containing the luciferase gene under the control of the *PIT1* promoter, along with vectors coding for HA-HMGA1B, HA-HMGA2 or Pit-1-V5 proteins. As shown in Fig. 3B, only HA-HMGA2, but not HA-HMGA1B, was able to positively regulate the activity of the *PIT1* promoter. Moreover, a strong and significant cooperation between HMGA2 and PIT1 was observed ($P<0.001$), while HMGA1 only slightly but significantly increased the positive transcriptional effect of PIT1 on its promoter ($P<0.05$). To confirm these data in a pituitary context, we transiently transfected GH3 cells, derived from a rat pituitary PRL- and GH-secreting adenoma expressing high levels of endogenous PIT1 (Fig. 3D), with HMGA1B or HMGA2 expression vectors, along with the Pit-1-Luc

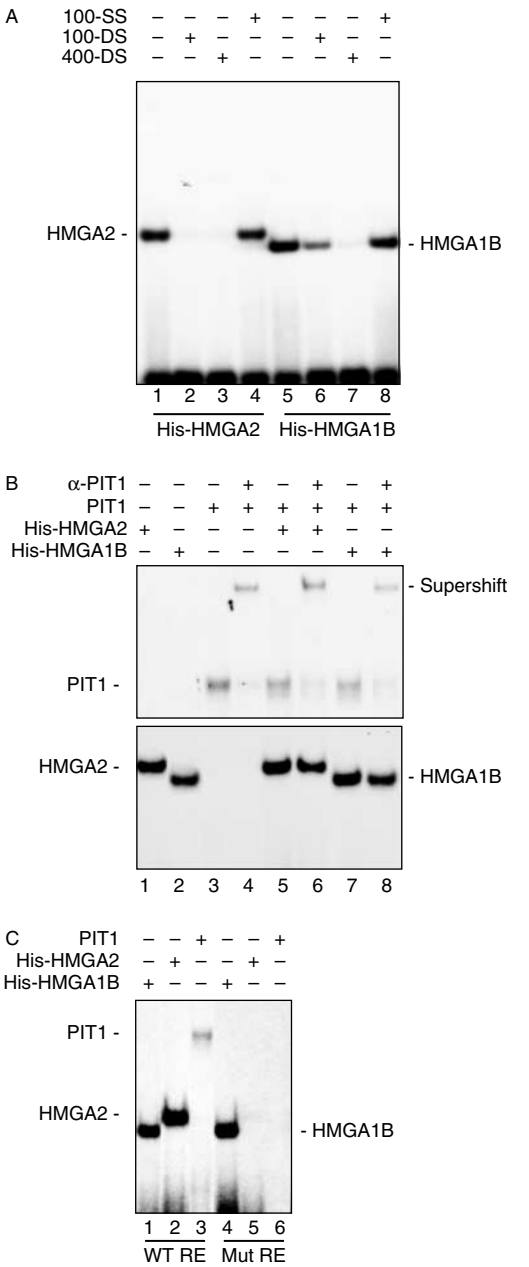

Figure 2 *In vitro* binding of HMGA proteins to the PIT1 consensus site. (A) Electrophoretic mobility shift assay (EMSA) performed with the radiolabelled PIT1 consensus site incubated with recombinant His-HMGA1B and His-HMGA2 as indicated. To assess the specificity of the binding, a 100- and 400-fold excess of unlabelled double-strand (DS) oligonucleotide was added as a specific competitor, and a 100-fold excess of unlabelled single-strand (SS) oligonucleotide was added as a non-specific competitor. (B) EMSA performed with the same oligonucleotide as in (A), incubated with recombinant PIT1, His-HMGA1B and His-HMGA2 as indicated. Supershift assay was performed with anti-PIT1 antibody where indicated. Two different autoradiographic exposure times were needed to allow a good view of both the binding of HMGA proteins and that of PIT1: upper panel, 18 h; lower panel, 1 h. (C) The same EMSA as in (B), but with an oligonucleotide mutated in the PIT1 consensus site.

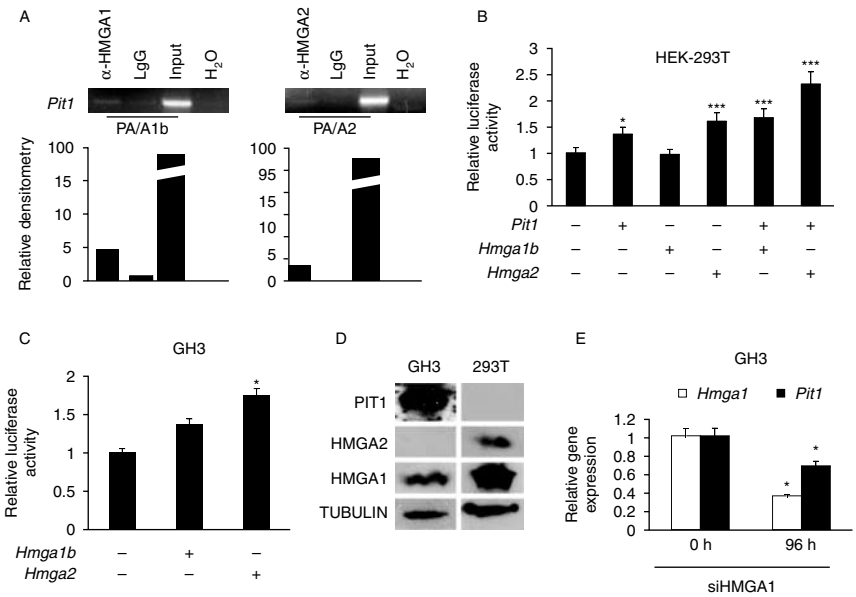

Figure 3 *In vivo* binding and activation by HMGA of the *PIT1* promoter. (A) Chromatin immunoprecipitation (ChIP) assay performed on pituitary adenomas from *Hmga1b* and *Hmga2* transgenic mice to detect the endogenous *in vivo* binding of HMGA proteins to the *Pit1* promoter gene, as indicated. As an immunoprecipitation control, IgG was used. *Input*, PCR products with genomic DNA without immunoprecipitation. All the PCR products were quantified with ImageQuant software and reported in the histograms below each band. (B and C) Luciferase activity (fold of activation vs promoter basic activity) of the *PIT1* promoter in HEK293T (B) and GH3 (C) cells. Where indicated, *PIT1* and/or either *Hmga1b* or *Hmga2*, or both, expression vectors were co-transfected with the PIT1-1-Luc plasmid. Data express mean ± S.D. of three independent experiments. Asterisks indicate the statistical results of a multiple comparison test vs promoter basic activity. $*P<0.05$; $***P<0.001$. (D) Western blot analysis to detect HMGA1, HMGA2 and PIT1 expression in GH3 and HEK293T cells. (E) qRT-PCR analysis of *Pit1* and *Hmga1* expression in GH3 cells interfered for HMGA1 with 100 nM of siHMGA1 for 96 h. The reported data (mean ± S.D. of three independent experiments) are normalised with respect to scrambled siRNA-treated cells. $*P<0.05$.

vector. As shown in Fig. 3C, HA-HMGA2 expression led to a significant increase in *Pit1* promoter activity, while only a slight but not significant increase was observed after the transfection of the HA-HMGA1B construct. These data clearly demonstrate that HMGA2 is able to positively regulate *PIT1* promoter activity in co-operation with PIT1, whereas they suggest that HMGA1 shows only a very weak effect on the regulation of *PIT1* gene expression. The abundant expression of HMGA1 in GH3 cells, in contrast to the total absence of HMGA2 expression (Fig. 3D), could probably account for the lack of a significant effect of HMGA1 transfection on *PIT1* promoter activity. To further evaluate the role of endogenous HMGA1 on *Pit1* expression in pituitary cells, *Pit1* expression was analysed in GH3 cells interfered for HMGA1, through an anti-HMGA1 siRNA, in comparison with GH3 cells treated with a scrambled siRNA. As shown in Fig. 3E, *Pit1* mRNA levels were significantly decreased in cells knocked down for HMGA1 compared with their scrambled-treated controls. Therefore, both HMGA1 and HMGA2 play a crucial role in the regulation of *Pit1* expression in GH3 cells.

Overexpression of *Pit1* increases the proliferation rate of pituitary adenoma cells

To evaluate the role of *Pit1* overexpression in cell proliferation in a pituitary context, we performed a colony-forming assay in GH3 cells. As shown in Fig. 4A, the number of colonies obtained, after puromycin selection, by transfection of a Pit1 expression vector, was significantly higher (a fourfold increase) compared with that obtained by transfecting the empty vector. Consistently, the knock-down of the endogenous PIT1 in GH3 cells caused a significant decrease in their growth in a colony-forming assay (data not shown). Similar results were obtained using a different pituitary cell type, such as the mouse gonadotroph cell line αT3. Indeed, as shown in Fig. 4B, *Pit1* overexpression caused a twofold increase in the number of colonies with respect to the backbone vector. Since αT3 cells do not express *Pit1* normally, we asked whether the exogenous expression of *Pit1* upregulates the classical PIT1 targets, such as *Gh* and *Ghrhr*. To answer this question, we performed RT-PCR analysis in αT3 cell clones stably expressing *Pit1*, with the result that *Gh* was not expressed in these

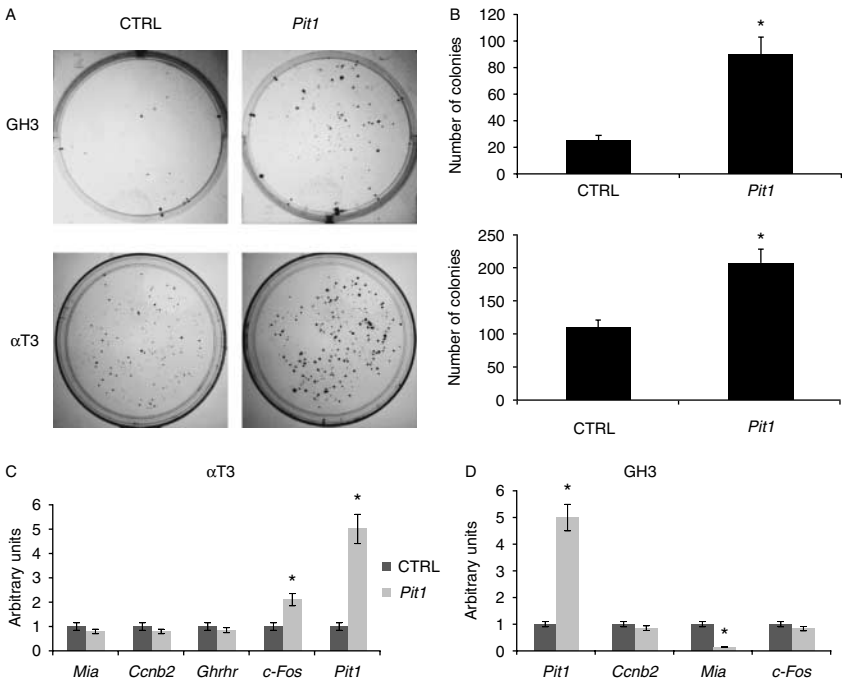

Figure 4 Effect of *Pit1* expression on pituitary adenoma cell proliferation. (A) Representative colony-forming assay performed on GH3 and αT3 cells transfected with a vector expressing *PIT1*. As a negative control, the empty vector (CTRL) was used. (B) The results of three colony-forming assays performed as in (A) were expressed as mean±S.D. (C and D) qRT-PCR analysis of gene expression changes upon transfection of *Pit1* in αT3 (C) and GH3 (D) cells. The resulting mean±S.D. of three independent experiments are reported. The genes analysed are indicated below the *x*-axis. *$P<0.05$.

cells (data not shown), and *Ghrhr* expression did not change significantly between parental and *Pit1*-transfected cells (Fig. 4C). Similarly, the expression of *Pit1* in these cell clones does not lead to a different expression, compared with the parental cells, of genes, such as *Ccnb2* and *Mia* (*Cd-rap*) (Fig. 4C), that are directly regulated by HMGA proteins in pituitary adenomas (De Martino *et al*. 2007*a*,*b*, 2009). Conversely, as reported for other cell systems (Gaiddon *et al*. 1999), the expression of *Pit1* in αT3 cells, but not in GH3 cells, leads to the upregulation of *c-Fos* (Fig. 4C and D). Surprisingly, overexpression of *Pit1* in GH3 cells inhibits the expression of *Mia* (*Cd-rap*) (Fig. 4D). These findings indicate that *Pit1* overexpression positively regulates pituitary cell proliferation through different mechanisms depending on the specific pituitary cellular context.

Positive correlation between *HMGA* and *PIT1* expression in human pituitary adenomas

Overexpression of *PIT1* is a common feature of GH-, PRL- and TSH-, but not of ACTH-, FSH-, LH- or non-functioning human pituitary adenomas (Pellegrini-Bouiller *et al*. 1997). Moreover, we have previously demonstrated that *HMGA1* and *HMGA2* expression levels are significantly increased in human pituitary adenomas compared with normal gland (De Martino *et al*. 2009). To evaluate whether there is a direct correlation between *HMGA1/2* and *PIT1* mRNA levels, we analysed a panel of 46 human pituitary adenomas (including 13 GH and 33 PRL adenomas) for the expression of *PIT1*, *HMGA1* and *HMGA2* mRNAs by quantitative RT-PCR. As shown in Fig. 5, a direct correlation between *PIT1* and *HMGA1* or *HMGA2* mRNA levels was observed. In fact, the correlation coefficients for the fold changes between adenomas and normal gland, calculated in both *PIT1* and *HMGA1*, as well as *PIT1* and *HMGA2* expression levels, were $R^2=0.82$ ($P<0.001$) and $R^2=0.61$ ($P<0.001$) respectively.

Discussion

Various studies support a critical role of HMGA proteins in the development of human pituitary adenomas (Finelli *et al*. 2002, De Martino *et al*. 2009, Qian *et al*. 2009, Wang *et al*. 2010). However, the mechanism by which they act in pituitary tumour development is still not completely known. We have previously demonstrated, using mouse models over-expressing HMGA2 and knockout for E2F1, that

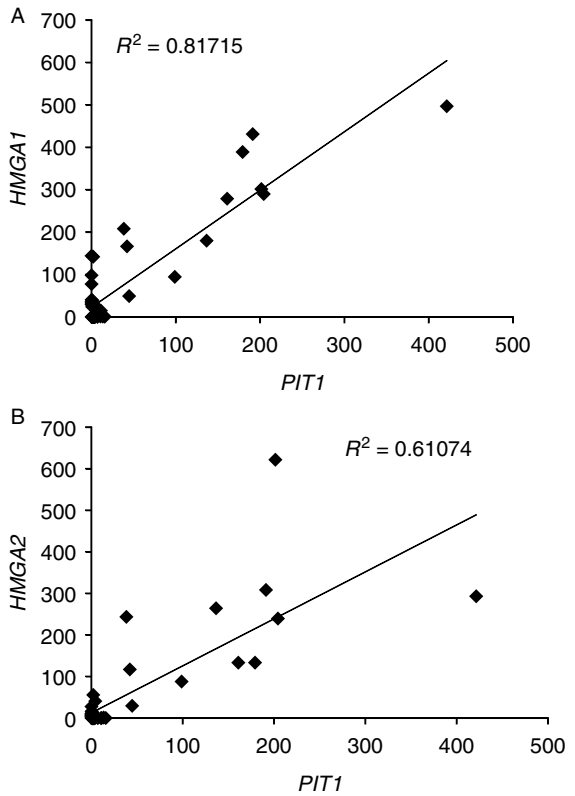

Figure 5 qRT-PCR analysis of *PIT1* mRNA in correlation with *HMGA1* and *HMGA2* expression in human pituitary adenomas. (A and B) Statistical analysis of the correlation between *PIT1* and *HMGA1* (A) or *HMGA2* (B) relative expression, as analysed by qRT-PCR, in pituitary adenomas vs normal gland. R^2, correlation coefficient.

induction of pituitary adenomas in *Hmga2* transgenic mice is mainly due to E2F1 activation (Fedele *et al*. 2006). Nevertheless, alternative pathways that may co-operate in the achievement of the full pituitary phenotype have been envisaged because of the incomplete rescue of the pituitary tumour phenotype in double *HMGA2/E2F1* mutants (Fedele *et al*. 2006). Analysing the gene expression profile of pituitary adenomas from *Hmga2* transgenic mice in comparison with normal pituitary glands from control mice (De Martino *et al*. 2007*b*), we identified *Mia* (*Cd-rap*) and *Ccnb2* genes as directly downregulated or upregulated respectively by both HMGA1 and HMGA2 proteins, and able to affect pituitary cell proliferation (De Martino *et al*. 2007*b*, 2009).

Here we report another mechanism, based on *Pit1* induction, by which HMGA overexpression may induce the development of pituitary adenomas. Indeed, we previously demonstrated that *Pit1* is expressed at high levels in pituitary adenomas developed by *Hmga* transgenic mice (Fedele *et al*. 2002, 2005), and here we show that HMGA proteins bind both PIT1 and PIT1-responsive DNA elements, thus positively modulating the PIT1 promoter activity, also synergistically co-operating with *Pit1*. Moreover, we demonstrated that *Pit1* overexpression drastically enhances (up to fourfold) pituitary cell proliferation by inducing the expression of *c-Fos* in gonadotroph cells or by inhibiting the expression of *Mia* (*Cd-rap*) in GH/PRL-secreting cells. Therefore, these results indicate a potential causal role of the aberrant *Pit1* expression in the cell biology of pituitary tumour.

We can envisage two different, but not mutually excluding, mechanisms by which HMGA-mediated *Pit1* upregulation may contribute to pituitary cell transformation:

a) HMGA overexpression may upregulate *Pit1* levels in pituitary adenoma cells of the *Pit1* lineage, enhancing their proliferation.
b) The enhancement of *Pit1* expression by HMGA during development might lead to abnormal growth of the embryonic cells secreting GH and PRL, which results in pituitary adenoma during adult life.

Interestingly, high expression levels of *PIT1* represent a constant feature of human pituitary GH, PRL and TSH adenomas (Asa *et al*. 1993, Delhase *et al*. 1993, Friend *et al*. 1993, Pellegrini *et al*. 1994, Pellegrini-Bouiller *et al*. 1997), and several previous studies suggested a potential role for *PIT1* in cell proliferation, the prevention of apoptotic death and the pathogenesis of pituitary tumours (Castrillo *et al*. 1991, Gaiddon *et al*. 1999, Salvatori *et al*. 2002, Pellegrini *et al*. 2006). In fact, microinjection of *Pit1* antisense sequences blocks cell growth in the GC somatotroph cell line (Castrillo *et al*. 1991) and dominant-negative mutants of *Pit1* reduce cell viability by decreasing the growth rate and inducing apoptosis via a caspase-independent pathway (Pellegrini *et al*. 2006). Moreover, PIT1 can also upregulate the expression of genes, such as *c-Fos* (Gaiddon *et al*. 1999) and *Ghrhr* (Salvatori *et al*. 2002), involved in cell proliferation. Interestingly, recent studies have identified an increased expression of PIT1 also in breast tumours (Ben-Batalla *et al*. 2010), suggesting a potential role of PIT1 in the proliferation of different cell types.

In conclusion, our data demonstrate that the high expression of *Pit1* in the pituitary adenomas of *Hmga* transgenic mice is induced by a positive regulation by HMGA proteins of *Pit1* transcription and support a role for *Pit1* overexpression in pituitary tumour.

Declaration of interest

The authors declare that there is no conflict of interest that could be perceived as prejudicing the impartiality of the research reported.

Funding

This work was supported by grants from Associazione Italiana Ricerca sul Cancro (AIRC), CNR (DG.RSTL. 030.001) and MIUR (PRIN 2008). D Palmieri and F Esposito are recipients of fellowships from Fondazione Italiana Ricerca sul Cancro (FIRC).

Acknowledgements

We thank Mireille Delhase for providing us the Pit-1 promoter plasmids, Angelo Ferraro for performing real-time PCR on human tissues and Luigi Di Guida for animal care.

References

Abdulkadir SA, Krishna S, Thanos D, Maniatis T, Strominger JL & Ono SJ 1995 Functional roles of the transcription factor Oct-2A and the high mobility group protein I/Y in HLA-DRA gene expression. *Journal of Experimental Medicine* **182** 487–500. (doi:10.1084/jem.182.2.487)

Abe N, Watanabe T, Masaki T, Mori T, Sugiyama M, Uchimura H, Fujioka Y, Chiappetta G, Fusco A & Atomi Y 2000 Pancreatic duct cell carcinomas express high levels of high mobility group I(Y) proteins. *Cancer Research* **60** 3117–3122.

Abe N, Watanabe T, Suzuki Y, Matsumoto N, Masaki T, Mori T, Sugiyama M, Chiappetta G, Fusco A & Atomi Y 2003 An increased high-mobility group A2 expression level is associated with malignant phenotype in pancreatic exocrine tissue. *British Journal of Cancer* **89** 2104–2109. (doi:10.1038/sj.bjc.6601391)

Amaral FC, Torres N, Saggioro F, Neder L, Machado HR, Silva WA Jr, Moreira AC & Castro M 2009 MicroRNAs differentially expressed in ACTH-secreting pituitary tumors. *Journal of Clinical Endocrinology and Metabolism* **94** 320–323. (doi:10.1210/jc.2008-1451)

Asa SL & Ezzat S 2002 The pathogenesis of pituitary tumours. *Nature Reviews. Cancer* **2** 836–849. (doi:10.1038/nrc926)

Asa SL, Puy LA, Lew AM, Sundmark VC & Elsholtz HP 1993 Cell type-specific expression of the pituitary transcription activator pit-1 in the human pituitary and pituitary adenomas. *Journal of Clinical Endocrinology and Metabolism* **77** 1275–1280. (doi:10.1210/jc.77.5.1275)

Baldassarre G, Fedele M, Battista S, Vecchione A, Klein-Szanto AJ, Santoro M, Waldmann TA, Azimi N, Croce CM & Fusco A 2001 Onset of natural killer cell lymphomas in transgenic mice carrying a truncated HMGI-C gene by the chronic stimulation of the IL-2 and IL-15 pathway. *PNAS* **98** 7970–7975. (doi:10.1073/pnas.141224998)

Bandiera A, Bonifacio D, Manfioletti G, Mantovani F, Rustighi A, Zanconati F, Fusco A, Di Bonito L & Giancotti V 1998 Expression of HMGI(Y) proteins in squamous intraepithelial and invasive lesions of the uterine cervix. *Cancer Research* **58** 426–431.

Ben-Batalla I, Seoane S, Garcia-Caballero T, Gallego R, Macia M, Gonzalez LO, Vizoso F & Perez-Fernandez R 2010 Deregulation of the Pit-1 transcription factor in human breast cancer cells promotes tumor growth and metastasis. *Journal of Clinical Investigation* **120** 4289–4302. (doi:10.1172/JCI42015)

Castrillo JL, Theill LE & Karin M 1991 Function of the homeodomain protein GHF1 in pituitary cell proliferation. *Science* **253** 197–199. (doi:10.1126/science.1677216)

Chen RP, Ingraham HA, Treacy MN, Albert VR, Wilson L & Rosenfeld MG 1990 Autoregulation of pit-1 gene expression mediated by two cis-active promoter elements. *Nature* **346** 583–586. (doi:10.1038/346583a0)

Chiappetta G, Avantaggiato V, Visconti R, Fedele M, Battista S, Trapasso F, Merciai BM, Fidanza V, Giancotti V, Santoro M *et al.* 1996 High level expression of the HMGI (Y) gene during embryonic development. *Oncogene* **13** 2439–2446.

Chiappetta G, Tallini G, De Biasio MC, Manfioletti G, Martinez-Tello FJ, Pentimalli F, de Nigris F, Mastro A, Botti G, Fedele M *et al.* 1998 Detection of high mobility group I HMGI(Y) protein in the diagnosis of thyroid tumors: HMGI(Y) expression represents a potential diagnostic indicator of carcinoma. *Cancer Research* **58** 4193–4198.

Chiappetta G, Ferraro A, Vuttariello E, Monaco M, Galdiero F, De Simone V, Califano D, Pallante P, Botti G, Pezzullo L *et al.* 2008 HMGA2 mRNA expression correlates with the malignant phenotype in human thyroid neoplasias. *European Journal of Cancer* **44** 1015–1021. (doi:10.1016/j.ejca.2008.02.039)

Delhase M, Vergagni P, Malur A, Trouillas J & Hooghe-Peters EL 1993 Pit-1/GHF-1 expression in pituitary adenomas: further analogy between human and rat SMtTW tumors. *Journal of Molecular Endocrinology* **11** 129–139. (doi:10.1677/jme.0.0110129)

Delhase M, Castrillo JL, de la Hoya M, Rajas F & Hooghe-Peters EL 1996 AP-1 and Oct-1 transcription factors down-regulate the expression of the human PIT1/GHF1 gene. *Journal of Biological Chemistry* **271** 32349–32358. (doi:10.1074/jbc.271.50.32349)

De Martino I, Fedele M, Palmieri D, Visone R, Cappabianca P, Wierinckx A, Trouillas J & Fusco A 2007*a* B-RAF mutations are a rare event in pituitary adenomas. *Journal of Endocrinological Investigation* **30** RC1–RC3.

De Martino I, Visone R, Palmieri D, Cappabianca P, Chieffi P, Forzati F, Barbieri A, Kruhoffer M, Lombardi G, Fusco A *et al.* 2007*b* The Mia/Cd-rap gene expression is down-regulated by the HMGA proteins in mouse pituitary adenomas. *Endocrine-Related Cancer* **14** 875–886. (doi:10.1677/ERC-07-0036)

De Martino I, Visone R, Wierinckx A, Palmieri D, Ferraro A, Cappabianca P, Chiappetta G, Forzati F, Lombardi G, Colao A *et al.* 2009 HMGA proteins up-regulate *CCNB2* gene in mouse and human pituitary adenomas. *Cancer Research* **69** 1844–1850. (doi:10.1158/0008-5472.CAN-08-4133)

Dudley KJ, Revill K, Clayton RN & Farrell WE 2009 Pituitary tumours: all silent on the epigenetics front. *Journal of Molecular Endocrinology* **42** 461–468. (doi:10.1677/JME-09-0009)

Falvo JV, Thanos D & Maniatis T 1995 Reversal of intrinsic DNA bends in the IFN beta gene enhancer by transcription factors and the architectural protein HMG I(Y). *Cell* **83** 1101–1111. (doi:10.1016/0092-8674(95)90137-X)

Fedele M, Bandiera A, Chiappetta G, Battista S, Viglietto G, Manfioletti G, Casamassimi A, Santoro M, Giancotti V & Fusco A 1996 Human colorectal carcinomas express high levels of high mobility group HMGI(Y) proteins. *Cancer Research* **56** 1896–1901.

Fedele M, Pierantoni GM, Berlingieri MT, Battista S, Baldassarre G, Munshi N, Dentice M, Thanos D, Santoro M, Viglietto G *et al.* 2001 Overexpression of proteins HMGA1 induces cell cycle deregulation and apoptosis in normal rat thyroid cells. *Cancer Research* **61** 4583–4590.

Fedele M, Battista S, Kenyon L, Baldassarre G, Fidanza V, Klein-Szanto AJ, Parlow AF, Visone R, Pierantoni GM, Outwater E *et al.* 2002 Overexpression of the *HMGA2* gene in transgenic mice leads to the onset of pituitary adenomas. *Oncogene* **21** 3190–3198. (doi:10.1038/sj.onc.1205428)

Fedele M, Pentimalli F, Baldassarre G, Battista S, Klein-Szanto AJ, Kenyon L, Visone R, De Martino I, Ciarmiello A, Arra C *et al.* 2005 Transgenic mice overexpressing the wild-type form of the HMGA1 gene develop mixed growth hormone/prolactin cell pituitary adenomas and natural killer cell lymphomas. *Oncogene* **24** 3427–3435. (doi:10.1038/sj.onc.1208501)

Fedele M, Visone R, De Martino I, Troncone G, Palmieri D, Battista S, Ciarmiello A, Pallante P, Arra C, Melillo RM *et al.* 2006 HMGA2 induces pituitary tumorigenesis by enhancing E2F1 activity. *Cancer Cell* **6** 459–471. (doi:10.1016/j.ccr.2006.04.024)

Fedele M, Palmieri D & Fusco A 2010 HMGA2: a pituitary tumour subtype-specific oncogene? *Molecular and Cellular Endocrinology* **326** 19–24. (doi:10.1016/j.mce.2010.03.019)

Finelli P, Pierantoni GM, Giardino D, Losa M, Rodeschini O, Fedele M, Valtorta E, Mortini P, Croce CM, Larizza L *et al.* 2002 The high mobility group A2 gene is amplified and overexpressed in human prolactinomas. *Cancer Research* **62** 2398–2405.

Friend KE, Chiou YK, Laws ER Jr, Lopes MB & Shupnik MA 1993 Pit-1 messenger ribonucleic acid is differentially expressed in human pituitary adenomas. *Journal of Clinical Endocrinology and Metabolism* **77** 1281–1286. (doi:10.1210/jc.77.5.1281)

Fusco A & Fedele M 2007 Roles of HMGA proteins in cancer. *Nature Reviews. Cancer* **7** 899–910. (doi:10.1038/nrc2271)

Gaiddon C, de Tapia M & Loeffler JP 1999 The tissue-specific transcription factor Pit-1/GHF-1 binds to the c-fos serum response element and activates c-fos transcription. *Molecular Endocrinology* **13** 742–751. (doi:10.1210/me.13.5.742)

Graham FL & van der Eb AJ 1973 Transformation of rat cells by DNA of human adenovirus 5. *Virology* **54** 536–539. (doi:10.1016/0042-6822(73)90163-3)

Hayward BE, Barlier A, Korbonits M, Grossman AB, Jacquet P, Enjalbert A & Bonthron DT 2001 Imprinting of the G(s)alpha gene GNAS1 in the pathogenesis of acromegaly. *Journal of Clinical Investigation* **107** R31–R36. (doi:10.1172/JCI11887)

Lania A, Mantovani G & Spada A 2003 Genetics of pituitary tumors: focus on G-protein mutations. *Experimental Biology and Medicine* **228** 1004–1017.

Lefevre C, Imagawa M, Dana S, Grindlay J, Bodner M & Karin M 1987 Tissue-specific expression of the human growth hormone gene is conferred in part by the binding of a specific trans-acting factor. *EMBO Journal* **6** 971–981.

Leger H, Sock E, Renner K, Grummt F & Wegner M 1995 Functional interaction between the POU domain protein Tst-1/Oct-6 and the high-mobility-group protein HMG-I/Y. *Molecular and Cellular Biology* **15** 3738–3747.

Li S, Crenshaw EB III, Rawson EJ, Simmons DM, Swanson LW & Rosenfeld MG 1990 Dwarf locus mutants lacking three pituitary cell types result from mutations in the POU-domain gene pit-1. *Nature* **347** 528–533. (doi:10.1038/347528a0)

Livak KJ & Schmittgen TD 2001 Analysis of relative gene expression data using real-time quantitative PCR and the 2(−Delta Delta *C*(T)). *Methods* **25** 402–408. (doi:10.1006/meth.2001.1262)

Llyod RV, Kovacs K, Young WF Jr, Farrell WE, Asa SL, Trouillas J, Kontogeorgos G, Sano T, Scheithauer BW & Horvath E 2004 Pituitary tumours: introduction. In chapter 1: tumours of the pituitary. In *World Health Organization Classification of Tumours-Pathology and Genetics of Tumours of Endocrine Organs*, pp 10–13. Eds RA DeLellis, RV Lloyd, PU Heitz & C Eng. Lyon: IARC Press.

Lyons J, Landis CA, Harsh G, Vallar L, Grünewald K, Feichtinger H, Duh QY, Clark OH, Kawasaki E, Bourne HR

et al. 1990 Two G protein oncogenes in human endocrine tumors. *Science* **249** 655–659. (doi:10.1126/science.2116665)

Martinez Hoyos J, Ferraro A, Sacchetti S, Keller S, De Martino I, Borbone E, Pallante P, Fedele M, Montanaro D, Esposito F *et al.* 2009 HAND1 gene expression is negatively regulated by the High Mobility Group A1 proteins and is drastically reduced in human thyroid carcinomas. *Oncogene* **28** 876–885. (doi:10.1038/onc.2008.438)

McCormick A, Brady H, Theill LE & Karin M 1990 Regulation of the pituitary-specific homeobox gene GHF1 by cell-autonomous and environmental cues. *Nature* **345** 829–832. (doi:10.1038/345829a0)

Monaco C, Visconti R, Barone MV, Pierantoni GM, Berlingieri MT, De Lorenzo C, Mineo A, Vecchio G, Fusco A & Santoro M 2001 The RFG oligomerization domain mediates kinase activation and re-localization of the RET/PTC3 oncoprotein to the plasma membrane. *Oncogene* **20** 599–608. (doi:10.1038/sj.onc.1204127)

Nelson C, Albert VR, Elsholtz HP, Lu LI & Rosenfeld MG 1988 Activation of cell-specific expression of rat growth hormone and prolactin genes by a common transcription factor. *Science* **239** 1400–1405. (doi:10.1126/science.2831625)

Occhi G, Trivellin G, Ceccato F, De Lazzari P, Giorgi G, Dematté S, Grimaldi F, Castello R, Davì MV, Arnaldi G *et al.* 2010 Prevalence of AIP mutations in a large series of sporadic Italian acromegalic patients and evaluation of CDKN1B status in acromegalic patients with multiple endocrine neoplasia. *European Journal of Endocrinology* **163** 369–376.

Pellegrini I, Barlier A, Gunz G, Figarella-Branger D, Enjalbert A, Grisoli F & Jaquet P 1994 Pit-1 gene expression in the human pituitary and pituitary adenomas. *Journal of Clinical Endocrinology and Metabolism* **79** 89–96. (doi:10.1210/jc.79.1.189)

Pellegrini I, Roche C, Quentien MH, Ferrand M, Gunz G, Thirion S, Bagnis C, Enjalbert A & Franc JL 2006 Involvement of the pituitary-specific transcription factor pit-1 in somatolactotrope cell growth and death: an approach using dominant-negative pit-1 mutants. *Molecular Endocrinology* **20** 3212–3227. (doi:10.1210/me.2006-0122)

Pellegrini-Bouiller I, Morange-Ramos I, Barlier A, Gunz G, Enjalbert A & Jaquet P 1997 Pit-1 gene expression in human pituitary adenomas. *Hormone Research* **47** 251–258. (doi:10.1159/000185472)

Pierantoni GM, Fedele M, Pentimalli F, Benvenuto G, Pero R, Viglietto G, Santoro M, Chiariotti L & Fusco A 2001 High mobility group I (Y) proteins bind HIPK2, a serine–threonine kinase protein which inhibits cell growth. *Oncogene* **20** 6132–6141. (doi:10.1038/sj.onc.1204635)

Pierantoni GM, Rinaldo C, Esposito F, Mottolese M, Soddu S & Fusco A 2007 High mobility group A1 (HMGA1) proteins interact with p53 and inhibit its apoptotic activity. *Cell Death & Differentiation* **13** 1554–1563. (doi:10.1038/sj.cdd.4401839)

Qian ZR, Asa SL, Siomi H, Siomi MC, Yoshimoto K, Yamada S, Wang EL, Rahman MM, Inoue H, Itakura M *et al.* 2009 Overexpression of HMGA2 relates to reduction of the let-7 and its relationship to clinicopathological features in pituitary adenomas. *Modern Pathology* **22** 431–441. (doi:10.1038/modpathol.2008.202)

Salvatori R, Fan X, Mullis PE, Haile A & Levine MA 2002 Decreased expression of the GHRH receptor gene due to a mutation in a Pit-1 binding site. *Molecular Endocrinology* **16** 450–458. (doi:10.1210/me.16.3.450)

Scala S, Portella G, Fedele M, Chiappetta G & Fusco A 2000 Adenovirus-mediated suppression of HMGI(Y) protein synthesis as potential therapy of human malignant neoplasias. *PNAS* **97** 4256–4261. (doi:10.1073/pnas.070029997)

Scheithauer BW, Gaffey TA, Lloyd RV, Sebo TJ, Kovacs KT, Horvath E, Yapicier O, Young WF Jr, Meyer FB, Kuroki T *et al.* 2006 Pathobiology of pituitary adenomas and carcinomas. *Neurosurgery* **59** 341–353. (doi:10.1227/01.NEU.0000223437.51435.6E)

Schmidt MC, Henke RT, Stangl AP, Meyer-Puttlitz B, Stoffel-Wagner B, Schramm J & von Deimling A 1999 Analysis of the MEN1 gene in sporadic pituitary adenomas. *Journal of Pathology* **188** 168–173.

Tamimi Y, van der Poel HG, Denyn MM, Umbas R, Karthaus HF, Debruyne FM & Schalken JA 1993 Increased expression of high mobility group protein I(Y) in high grade prostatic cancer determined by *in situ* hybridization. *Cancer Research* **53** 5512–5516.

Tateno T, Zhu X, Asa SL & Ezzat S 2010 Chromatin remodeling and histone modifications in pituitary tumors. *Molecular and Cellular Endocrinology* **326** 6670. (doi:10.1016/j.mce.2009.12.028)

Thanos D & Maniatis T 1992 The high mobility group protein HMG I(Y) is required for NF-kappa B-dependent virus induction of the human IFN-beta gene. *Cell* **71** 777–789. (doi:10.1016/0092-8674(92)90554-P)

Trouillas J, Girod C, Sassolas G & Claustrat B 1986 The human gonadotropic adenoma: pathological diagnosis and hormonal correlations in 26 tumors. *Seminars in Diagnostic Pathology* **3** 42–57.

Vallone D, Battista S, Pierantoni GM, Fedele M, Casalino L, Santoro M, Viglietto G, Fusco A & Verde P 1997 Neoplastic transformation of rat thyroid cells requires the junB and fra-1 gene induction which is dependent on the HMGI-C gene product. *EMBO Journal* **16** 5310–5321. (doi:10.1093/emboj/16.17.5310)

Wang EL, Qian ZR, Rahman MM, Yoshimoto K, Yamada S, Kudo E & Sano T 2010 Increased expression of HMGA1

correlates with tumour invasiveness and proliferation in human pituitary adenomas. *Histopathology* **56** 501–509. (doi:10.1111/j.1365-2559.2010.03495.x)

Winkler S, Murua Escobar H, Meyer B, Simon D, Eberle N, Baumgartner W, Loeschke S, Nolte I & Bullerdiek J 2007 HMGA2 expression in a canine model of prostate cancer. *Cancer Genetics and Cytogenetics* **177** 98–102. (doi:10.1016/j.cancergencyto.2007.06.008)

Wood LJ, Maher JF, Bunton TE & Resar LM 2000 The oncogenic properties of the HMG-I gene family. *Cancer Research* **60** 4256–4261.

Zhou X, Benson KF, Ashar HR & Chada K 1995 Mutation responsible for the mouse pygmy phenotype in the developmentally regulated factor HMGI-C. *Nature* **376** 771–774. (doi:10.1038/376771a0)

Zhuang Z, Ezzat SZ, Vortmeyer AO, Weil R, Oldfield EH, Park WS, Pack S, Huang S, Agarwal SK, Guru SC *et al.* 1997 Mutations of the MEN1 tumor suppressor gene in pituitary tumors. *Cancer Research* **57** 5446–5451.

Zwilling S, König H & Wirth T 1995 High mobility group protein 2 functionally interacts with the POU domains of octamer transcription factors. *EMBO Journal* **14** 1198–1208.

Received in final form 9 December 2011
Accepted 23 December 2011
Made available online as an Accepted Preprint
23 December 2011

factors responsible for bone loss before and after OLT and to examine the predictive value of changes in BMD for risk of fracture in these patients.

DOI: 10.1530/endoabs.32.OC2.4

OC2.5

Genetic analysis of *CDKN1B* gene in familial primary hyperparathyroidism

Elena Pardi[1], Simona Borsari[1], Federica Saponaro[1], Chiara Banti[1], Natalia Pellegata[3], Misu Lee[3], Edda Vignali[1], Antonella Meola[1], Marco Mastinu[2], Stefano Mariotti[2], Claudio Marcocci[1] & Filomena Cetani[1]
[1]Department of Clinical and Experimental Medicine, University of Pisa, Pisa, Italy; [2]Endocrinology Unit, Department of Medical Sciences, Policlinico di Monserrato, University of Cagliari, Cagliari, Italy; [3]Institute of Pathology, Helmholtz Zentrum München-German Research Center for Environmental Health, Neuherberg, Germany.

Primary hyperparathyroidism (PHPT) is usually a sporadic disorder, but in $<10\%$ of cases occurs as part of hereditary syndromes, including multiple endocrine neoplasia types 1 and 2A (MEN1 and MEN2A), hyperparathyroidism-jaw tumor syndrome (HPT-JT) and familial isolated hyperparathyroidism (FIHP).
MEN 1 is an autosomal dominant disorder characterized by tumours in multiple endocrine glands, most commonly parathyroid, enteropancreatic and anterior pituitary glands. To date, germline mutations in the *MEN1* gene have been identified in 70–80% of *MEN1* kindreds. FIHP has a heterogeneous molecular ethiology, since germline mutations in *MEN1*, *HRPT2* and *CASR* genes have been reported. Recently, germline mutations of cyclin dependent kinase inhibitor 1B (*CDKN1B*) gene, encoding the p27 protein, have been identified in 8 kindreds with MEN1 syndrome which were negative to the MEN1 genetic screening.
The aim of this study was to perform a genetic screening of *CDKN1B* gene in patients with MEN1 syndrome and FIHP (33 and 17, respectively). All MEN1 and FIHP probands were negative for MEN1 gene mutations at genetic testing.
Genomic DNA from index cases was analyzed by PCR amplification of the entire coding region and splice sites, and direct sequencing was performed by a 16-capillaries automatic sequencer.
A novel frameshift germline mutation in *CDKN1B* gene, c.372_373delCT/p.Asn124AsnfsX2, was identified in a MEN1 proband. A construct expressing p27_c.372_373delCT was generated to assess the functional properties of the mutant protein *in vitro*. Indirect immunofluorescence demonstrated that the mutant protein is mainly retained in the cytoplasm, affecting the cell cycle inhibitory function of p27 in the nucleus. Our results confirm that germline CDKN1B mutations are involved, althought rarely, in parathyroid tumorigenesis.

DOI: 10.1530/endoabs.32.OC2.5

OC2.6

Hypomineralized teeth as biomarkers of exposure to endocrine disruptors

Katia Jedeon[1,2], Muriel Molla De La Dure[2,3], Steven Brookes[4], Clemence Marciano[1], Marie-Chantal Canivenc-Lavier[5], Ariane Berdal[1,3] & Sylvie Babajko[1]
[1]INSERM UMRS 872, Laboratory of Molecular Oral Pathophysiology, Paris, France; [2]Université Paris-Diderot, UFR d'Odontologie, Paris, France; [3]Reference Centre for Rare Malformations of the Face and Oral Cavity, Hospital Rothschild, Paris, France; [4]Department of Oral Biology, Leeds Dental Institute, Leeds, UK; [5]INRA UMR 1324, Université de Bourgogne, Dijon, France.

MIH for Molar Incisor Hypomineralization is a recently described pathology affecting around 18% of six year old children. Although a number of putative factors have been hypothesized, etiology of MIH remains unknown. The parallel increase of exposure to endocrine disruptors (EDs) and the prevalence of MIH led us to investigate a possible relationship between both events.
Rats were orally exposed daily to low dose of bisphenol A (BPA), genistein, vinclozolin, alone (for BPA) or in combination, from the conception to the sacrifice, mimicking human environmental exposure. Macroscopic observation of male rat incisors showed that the phenotype induced by BPA was the most evident with 75% of rats presenting random opaque white spots comparable to those observed in human MIH, whereas only 50% of GEN and VINCLO treated rats shared similar phenotype. Human MIH and BPA treated rat teeth were analyzed in parallel by scanning electron microscopy (SEM) - Energy dispersive X-ray (EDX) and histology. Both of them exhibited the same hypomineralization phenotype. BPA targeted specifically the expression of two major enamel genes, enamelin and kallikrein 4 (Klk4) at the transcriptional level. Rat ameloblastic HAT-7 cells were stably transfected with plasmids containing KLK4 promoter, and treated with 1 nM BPA, 1 nM GEN, 1 nM VINCLO. BPA decreased both KLK4 mRNA level and KLK4 promoter activity. Conversely, GEN increased KLK4 expression whereas VINCLO had no effect on this gene, a possible reason for the lesser effect on enamel hypomineralization.
Our data strongly support a role for EDs acting as BPA in MIH pathology. In conclusion, MIH teeth may represent a much needed early biomarker, easily accessible, for ED exposure in humans.

DOI: 10.1530/endoabs.32.OC2.6

Thyroid

OC3.1

Targeting of *PATZ1* by miR-29b is a downstream effect of oncogenic Ras signalling in thyroid cells

Michela Vitiello[1,2], Teresa Valentino[1,2], Marta De Menna[2], Luigia Serpico[1], Sonia Mansueto[1], Gabriella De Vita[2], Alfredo Fusco[1,2] & Monica Fedele[1]
[1]Istituto di Endocrinologia ed Oncologia Sperimentale del CNR, Naples, Italy; [2]Dipartimento di Biologia e Patologia Cellulare e Molecolare, Università degli Studi di Napoli "Federico II", Naples, Italy.

PATZ1, a member of the POZ-ZF protein family of transcription factors is emerging as an important cancer-associated factor that can act either as oncogene or tumour-suppressor depending on the cellular context. Consistent with a tumour-suppressor role in thyroid cells, we have shown that PATZ1 is highly downregulated in anaplastic thyroid carcinomas compared to normal thyroid tissue and is a powerful inhibitor of anaplastic thyroid cancer cell survival, migration, invasiveness and tumorigenicity.
Looking for the upstream signalling pathway regulating PATZ1 expression in thyroid cells, we searched for microRNAs targeting PATZ1. In order to identify miRNAs predicted to bind the 3′UTR of PATZ1 we used bioinformatics free tools, based on the miRanda application and the mirSVR predicted target site scoring method. Among the miRNAs identified by this analysis we validated miR-29b. Indeed, we demonstrated that it is able to target PATZ1 and cause downregulation of PATZ1 expression at both mRNA and protein level in different cell systems, including rat thyroid cells. Interestingly, miR-29b is induced by Ras during transformation of FRTL-5 rat thyroid cells toward an undifferentiated phenotype, resembling that of anaplastic carcinomas and characterized by the acquisition of a migratory and invasive behaviour. In these cells, we observed a strong down-regulation of PATZ1 expression, which starts as early as 2 h after Ras induction, and an inverse correlation between the expression of miR-29b and PATZ1 mRNA and protein levels.
These results are consistent with the suppressor role of PATZ in thyroid carcinogenesis and suggest that down-regulation of PATZ1 expression, through miR-29b, may be a downstream effect of the oncogenic Ras signalling in thyroid cell transformation.

DOI: 10.1530/endoabs.32.OC3.1

OC3.2

Mitochondrial mass and function is regulated by PI3K signaling in thyroid cancer cells

K Alexander Iwen, Erich Schröder, Julia Resch, Ulrich Lindner, Peter König, Hendrik Lehnert, Nina Perwitz, Saleh Ibrahim & Georg Brabant
Universität zu Lübeck, Lübeck, Germany.

Objective
Abnormal mitochondria are well known in oxyphilic thyroid tumors but recent data also confirm profound mitochondrial alterations in other thyroid carcinomas. These changes are linked to the aggressiveness of the tumors. Our group recently demonstrated in an *in vivo* model, that inhibition of phosphoinositide 3-kinase (PI3K) signalling suppressed the invasive and metastatic behaviour of thyroid cancer cells. Here, we evaluated whether a modulation of PI3K signalling changes mitochondrial mass and function.
Methods
We used follicular (FTC-133, WRO) and anaplastic (8505C) carcinoma cell lines to characterize mitochondrial mass and function both under baseline conditions and inhibition of PI3K signaling. Therefore, we transfected phosphatase and tensin homolog (PTEN) mutated FTC-133 cells with *wild type* PTEN or empty vector. We compared these chronic effects with an acute inhibition of PI3K signaling over 18 h using the pan-PI3K inhibitor GDC-0941 in all cell lines.

Conclusion: This study correlates the expression of UBE2C to radio and chemo resistance of breast cancer cells, providing a potential target in a subset of patients whose tumors express high levels of UBE2C in breast cancer.

168 L597VBRAF Acts as an Epistatic Modifier of G12DKRAS

L. Cheung[1], C. Andreadi[1], T. Kamata[1], S. Giblett[1], B. Patel[1], R. Marais[1], C. Pritchard[1]. [1]*University of Leicester, Biochemistry, Leicester, United Kingdom*

Introduction: The RAS/RAF/MEK/ERK signalling pathway plays a crucial role in the control of cell growth and is a mutational target in human cancer. Oncogenic *BRAF* and *RAS* mutations are detected in ~7% and 30% of samples respectively. ^{L597V}*BRAF* is the fifth most common residue in BRAF mutated in human cancers and gives rise to a mutant with moderately elevated BRAF kinase activity. Unlike the most common BRAF mutation, ^{V600E}*BRAF*, ^{L597V}*BRAF* co-exists with other oncogenic driver mutations, particularly *KRAS* mutations. *RAS* and *BRAF* mutations have also been found in a group of developmental syndromes, collectively known as RASopathies that have heart, skin and facial abnormalities with some predisposition to cancer. ^{L597V}*BRAF* is one of only seven mutations in BRAF detected in both cancer and RASopathies, and my research is aimed at addressing how this mutant can contribute to both pathologies.
Material and Method: A conditional knock-in, Cre-lox-regulated mouse model (Braf$^{+/LSL-L597V}$) was used to express the ^{L597V}Braf mutation in mouse tissues and embryonic fibroblasts (MEFs). To examine cooperation between ^{L597V}Braf and oncogenic RAS, Braf$^{+/LSL-L597V}$ mice were intercrossed with the Jacks/Tuveson Kras$^{+/LSL-G12D}$ conditional knockin mice. The effects of the mutations on cancer hallmarks and downstream signalling pathway activation were examined
Results and Discussion: Constitutive expression of endogenous ^{L597V}Braf induced Braf activity by ~2-fold and led to weak activation of the downstream Mek/Erk pathway. This was associated with induction of RASopathy hallmarks including facial dysmorphia, short stature and cardiac hypertrophy but was not sufficient to transform MEFs in vitro or induce tumours in vivo. By co-expressing ^{L597V}*Braf* with oncogenic ^{G12D}*Kras*, the two mutations synergised to induce Mek/Erk signalling to levels comparable to that induced by the high activity mutant ^{V600E}Braf. Morphological transformation of MEFs was more similar to that induced by ^{V600E}Braf than ^{G12D}Kras and microarray analysis confirmed that the double mutant cells had a gene expression signature more similar to ^{V600E}Braf than ^{G12D}Kras. In the lung, there was also a shift from predominantly adenomatous alveolar hyperplasia lesions, normally induced by ^{G12D}Kras, to predominantly adenomas, as occurs with ^{V600E}Braf. However, we show using siRNA that, unlike ^{V600E}Braf, Mek/Erk pathway activation was mediated by both Craf and Braf in the ^{L597V}Braf mutant cells and, furthermore, ATP-competitive RAF inhibitors induced paradoxical Mek/Erk pathway activation in a similar way to cells expressing ^{WT}Braf.
Conclusion: Weak activation of the Mek/Erk pathway underpins RASopathy conditions but, for cancer, ^{L597V}Braf works to epistatically modify the transforming effects of driver oncogenes by enhancing Mek/Erk signalling.

169 Oxidative Stress Regulation is Abrogated by Loss of NKX3.1 Expression in Acute and Chronic Inflammation

B. Debelec-Butuner[1], C. Alapinar[2], K.S. Korkmaz[3]. [1]*Ege University, Pharmaceutical Biotechnology, Izmir, Turkey*, [2]*Ege University, Institute of Science Dept of Biotechnology, Izmir, Turkey,* [3]*Ege University, Faculty of Engineering Dept. of Bioengineering, Izmir, Turkey*

Background: Prostatic inflammation is associated with the development of carcinoma, which was reported in previous studies. Inflammatory microenvironment leads to generation of reactive oxygen species (ROS) during inflammation and alters many cellular mechanisms, which contributes to tumorigenesis. In this study, we aimed to identify the components of oxidative stress response during acute and chronic inflammation, and the role of NKX3.1 protein loss, which was induced by pro-inflammatory cytokines in deregulated antioxidant defense.
Material and Methods: Inflammatory microenvironment was mimicked by treatment of prostate cell lines with inflammatory conditioned media. Then cellular responses were determined by immuno-blotting, RT-PCR and real-time cell proliferation system. Cellular ROS was measured with DCFH on flow-cytometer.
Results: We established an inflammation model of prostate by treating prostate cells with inflammatory conditioned media (CM) with known cytokine concentrations. For the production of CM, U937 monocytes were differentiated into macrophages and induced by lipopolysaccharide for the secretion of inflammatory cytokines into media. Following induction of acute inflammation in prostate cells, ROS generation and subsequent DNA damage increased, and these changes were suppressed by ectopic expression of NKX3.1. Further, oxidative stress genes such as ENOX2, GPX2, GPX3, PRDX6 and QSCN6 were found deregulated in the absence of NKX3.1. In addition, abnormal morphological changes and increased proliferation were also evident during inflammation, and these alterations were suppressed by NKX3.1 expression as well as antioxidant N-acetyl-L-cysteine treatment. In a conclusion, prostatic inflammation leads to sustained oxidative damage, and NKX3.1 related mechanisms influence ROS scavenging to regulate the growth of prostate cells.
Conclusion: These results suggest that antioxidant effect of NKX3.1 is considerably significant for its tumor suppressor function.

170 PATZ1 is a New Candidate Tumour-suppressor Gene in Thyroid Cancer

T. Valentino[1], M. Vitiello[1], R. Pasquinelli[2], D. Palmieri[3], M. Monaco[2], G. Palma[2], C. Arra[2], A. Fusco[1], G. Chiappetta[2], M. Fedele[1]. [1]*Università Federico 2º, Istituto di Endocrinologia ed Oncologia Sperimentale del CNR, Naples, Italy,* [2]*Istituto dei Tumori di Napoli Fondazione G. Pascale, Naples, Italy,* [3]*MVIMG The Ohio State University, Columbus. Ohio, USA*

Background: Thyroid carcinoma arising from the thyroid follicular epithelium represents the most frequent endocrine malignancy and is mainly associated with gene rearrangements, generating RET/PTC and TRK oncogenes, as well as BRAFV600E and RASV12 activating point mutations. Except for p53, which appears to be involved only in poorly differentiated and aggressive histotypes, a role of tumour-suppressor genes in the pathogenesis of thyroid cancer is still poorly known.
We found that the POZ/AT-hook/kruppel Zinc finger 1 (*PATZ1*) gene, encoding a transcription factor that has been proposed to be involved in cancer, is down-regulated, with an inverse correlation to the degree of malignancy and loss of differentiation, in a vast majority of thyroid cancer cell lines and tumours compared to normal thyroid.
Materials and Methods: Papillary thyroid cancer (PTC)-derived TPC1 and anaplastic thyroid cancer (ATC)-derived FRO cell lines stably expressing peGFP-C2 empty vector or peGFP-PATZ1 plasmid, were generated. In these cell lines we performed different functional assays (i.e. growth curves, FACS, colony forming, TUNEL, wound healing, trans-well migration, soft agar growth and xenograft in nude mice) to characterize differences in growth, death, migration, invasive capacity and malignancy, with or without PATZ1.
Results: Restoration of *PATZ1* expression had no effect on the growth of both cell lines. Conversely, it led FRO cells to apoptosis and highly reduced migratory and invasive capabilities of both TPC1 and FRO cells. Finally, differently from the FRO parental cell lines expressing the empty vector, the PATZ1 transfectants did not form colonies in soft agar and had reduced transforming ability *in vivo* compared to their controls.
Conclusions: Our data suggest that downregulation of *PATZ1* expression exerts a functional role in the pathogenesis of thyroid cancer, and are also consistent with a specific role of PATZ1 in the signaling pathways involved in cell survival and metastatic progression in both papillary and anaplastic thyroid cancer.

171 Bcl-2 Family Members and Survival Under Stress Conditions in Multidrug Resistant Leukemic Cells

D. Cerezo[1], M. Lencina[1], C. Bernal[1], M. Canovas[1], P. Garcia-Peñarrubia[1], E. Martin-Orozco[1]. [1]*University of Murcia, Biochemistry and Molecular Biology B and Immunology, Murcia, Spain*

Over-expression of several anti-apoptotic Bcl-2 family members has been reported in hematologic malignancies and has been associated with survival and/or chemotherapy resistance in various human cancers. Thus, differential expression of a single Bcl-2 family member can disturb the balance between life and death and the permutations for pro-survival signaling in the context of cancer cells. In an attempt to address this question in leukemic cells we have investigated the Bcl-2 family expression profile in MDR leukemic cells (L1210R) compared with its parental cell line, L1210 and with P-gp-transfected parental cells (CBMC-6). We have undertaken the study comparing two different kinds of stress conditions: cold temperature and daunomycin exposure. Cold temperature induces preferential cell death in leukemic MDR cells meanwhile daunomycin treatment induces cell death in parental but not in sensitive cells. We have focus here in the study of Bcl-xL and Bcl-2, as anti-apoptotic members; and Bax (belonging to the multi-domain or Bax subfamily) and Bad (belonging to the BH3-only subfamily) as pro-apoptotic members. By using western-blot techniques, we have detected expression levels of Bcl-2 family members in leukemic cells treated with daunomycin for different doses and/or time points. Furthermore, we have performed silencing experiments in order to analyze the contribution of each individual member of the Bcl-2 family to the survival of parental (L1210), resistant (L1210R) and P-gp-transfected (CBMC-6) leukemic cells in presence of the chemotherapeutic agent. We have compared these data with those obtained previously by using the model of cold stress-induced cell death. Together, these findings demonstrate that during the process of drug resistance, leukemic cells undergo alterations on Bcl-2 family members expression that could influence their response to different types of stress.

Thyroid basic

OC15.1

PATZ1 is a new candidate tumour-suppressor gene in thyroid cancer

G. Chiappetta[2], T. Valentino[1], M. Vitiello[1], R. Pasquinelli[2], M. Monaco[2], G. Palma[2], C. Arra[2], A. Fusco[1] & M. Fedele[1]
[1]Istituto di Endocrinologia e Oncologia Sperimentale del CNR, Napoli, Italy; [2]Istituto dei Tumori di Napoli Fondazione G. Pascale, Napoli, Italy.

Thyroid carcinoma arising from the thyroid follicular epithelium represents the most frequent endocrine malignancy and is mainly associated with gene rearrangements generating RET/PTC and TRK oncogenes, as well as BRAFV600E and RASV12 activating point mutations. Except for p53, which appears to be involved only in poorly differentiated and aggressive histotypes, a role of tumor-suppressor genes in the pathogenesis of thyroid cancer is still poorly known.

We found that the POZ/AT-hook/kruppel Zinc finger 1 (PATZ1) gene is down-regulated, with an inverse correlation to the degree of malignancy and differentiation, in the vast majority of thyroid tumours compared to normal thyroid, suggesting a tumour-suppressor role mainly involved in the late stages of thyroid carcinogenesis.

To explore this possibility, we performed functional studies in the papillary thyroid cancer (PTC)-derived TPC1 and the anaplastic thyroid cancer (ATC)-derived FRO cell lines, in which the expression of *PATZ1* is strongly down-regulated with respect to normal thyroid cells. Restoration of *PATZ1* expression, by stable DNA transfection, had no effect on the growth rate of both cell lines. Conversely, it led FRO cells to death and highly reduced migratory and invasive capabilities of both cell lines. Finally, we examined the transformed phenotype of the FRO cell transfectants expressing *PATZ1*, by analyzing their ability to grow in soft agar and to induce tumours in athymic mice. Differently from the parental cell line expressing the empty vector, these transfectants did not form colonies in soft agar and had reduced transforming ability *in vivo* compared to their controls. These data indicate that the loss of *PATZ1* expression exerts a functional role in the pathogenesis of thyroid cancer, and they are consistent with a specific role of PATZ1 in the signaling pathways involved in cell survival and metastatic progression.

Declaration of interest
The authors declare that there is no conflict of interest that could be perceived as prejudicing the impartiality of the research project.
Funding
This work was supported, however funding details are unavailable.

OC15.2

Ligand bound-thyroid hormone receptor contributes to reprogramming of pancreatic exocrine cells to insulin-producing cells via induction of Ngn3 and MafA

F. Furuya, H. Shimura, T. Endo & T. Kobayashi
University of Yamanashi, Chuo, Japan.

Introduction
One goal of diabetic regenerative medicine is to instructively convert mature pancreatic exocrine cells into insulin-producing cells. We recently reported that liganded thyroid hormone receptor α (TRα) plays a critical role in expansion of the β-cell mass during postnatal development.
Materials and Methods
AdTRα is a recombinant adenoviral vector that expresses human TRα1 under the control of the cytomegalovirus promoter. To analyze whether TRα gene transfer induces reprogramming of pancreatic exocrine cells to insulin-producing cells, AdTRα were injected into the pancreas of immunodeficient mice. Rat pancreatic AR42J cells that possess exocrine and neuroendocrine properties were infected with AdTRα. The expression of transcription factors that are involved in the differentiation of pancreatic endocrine cells was then analyzed by quantitative RT-PCR, western blot or immunocytochemistry. To explore whether liganded-TRα-induced reprogramming of pancreatic exocrine cells is direct or indirect effect, AdTRα-infected AR42J cells were concomitantly transfected with siRNA of Ngn3 or MafA.
Results
Small scattered clusters of insulin-producing cells, which also expressed lipase, were observed in AdTRα-infected mice. T3-treatment of AR42J cells that were infected with AdTRα and pretreated with activin A increased the mRNA and protein expression levels of Ngn3 and MafA, compared to no T3-treatment. Overexpression of TRα together with T3-treatment also induced insulin expression in activin A-treated AR42J cells. The siRNA-induced inhibition of expression of Ngn3 or MafA significantly inhibited AdTRα-induced reprogramming of AR42J cells into insulin-producing cells.
Conclusions
These results suggested that combination of liganded-TRα and activin A leads to reprogramming pancreatic exocrine cells to insulin-producing cells via induction of Ngn3 and MafA. Our findings also support the hypothesis that liganded-TRα plays a critical role in β-cell regeneration during postnatal development.

Declaration of interest
The authors declare that there is no conflict of interest that could be perceived as prejudicing the impartiality of the research project.
Funding
This research did not receive any specific grant from any funding agency in the public, commercial or not-for-profit sector.

OC15.3

Radioiodine therapy of non-thyroidal cancer following systemic sodium iodide symporter (NIS) gene transfer using Transferrin-receptor (Tfr) targeted non-viral gene delivery vectors

K. Klutz[1], G. Grünwald[1], M. Willhauck[1], N. Schwenk[1], A. Vetter[2], W. Rödl[2], M. Hacker[2], C. Zach[2], R. Senekowitsch-Schmidtke[3], E. Wagner[2], B. Göke[1], M. Ogris[2] & C. Spitzweg[1]
[1]Campus Grosshadern, University Hospital of Munich, Munich, Germany; [2]Ludwig-Maximilians-University, Munich, Germany; [3]University Hospital Klinikum rechts der Isar, Munich, Germany.

We have recently demonstrated the high potential of non-viral polyplexes for tumor-specific delivery of the sodium iodide symporter (NIS) after systemic application. In the current study we used novel polymers based on linear polyethylenimine (LPEI), shielded by polyethylene glycol (PEG), and coupled with the synthetic peptide B6 (LPEI-PEG-B6) as a transferrin (Tf)-receptor specific ligand to achieve active tumor targeting to human hepatocellular cancer (HuH7) cells after systemic delivery of NIS DNA.

We complexed LPEI-PEG-B6 with a NIS-expressing plasmid and analyzed levels of functional NIS expression after transfection of HuH7 (high Tf-receptor expression level) as compared to control cancer cells with low Tf-receptor expression level (colon cancer, RKO) *in vitro* and *in vivo*.

In vitro incubation of HuH7 cells with LPEI-PEG-B6/NIS resulted in a 9-fold increase in iodide uptake activity as compared to RKO cells. After establishment of subcutaneous HuH7 and RKO tumors in nude mice, NIS-conjugated nanoparticles or control vectors were injected i.v. followed by analysis of radioiodine biodistribution using I-123 scintigraphy. After injection of LPEI-PEG-B6/NIS, a significant perchlorate-sensitive iodide accumulation (8.5–10.9% ID/g I-123; eff. half-life of 5 h) was observed in HuH7 tumors resulting in a tumor absorbed dose of 50 mGy/MBq I-131 after systemic NIS gene transfer using LPEI-PEG-B6/NIS polyplexes. Tumoral iodide uptake activity and NIS mRNA expression were significantly lower in RKO cells confirming the specificity of Tf-receptor targeted nanoparticle vectors. After four cycles of polymer application followed by therapeutic application of I-131 (55.5 MBq), tumor growth was significantly reduced as compared to control groups.

These results clearly demonstrate that systemic *in vivo* NIS gene transfer using nanoparticle vectors coupled with a Tf-receptor targeting ligand is capable of inducing tumor-specific radioiodide uptake, which represents a promising innovative strategy for the NIS gene therapy approach in metastatic cancer.

Declaration of interest
The authors declare that there is no conflict of interest that could be perceived as prejudicing the impartiality of the research project.
Funding
This work was supported, however funding details are unavailable.

OC15.4

The DNA methylation as a predisposition factor in the pathogenesis of congenital hypothyroidism in premature infants

F. Marelli[1,4], D. Gentilini[1], G. Weber[2], M. Vigone[2], G. Radetti[3] & L. Persani[1,4]
[1]IRCCS Istituto Auxologico Italiano, Cusano Milanino, Italy; [2]HSR Istutito Salute e Vita San Raffaele, Milan, Italy; [3]Compensorio sanitario di Bolzano, Bolzan, Italy; [4]University of Milan, Milan, Italy.

Introduction
Epidemiological data indicate that children born prematurely have a risk 3–5 fold higher of congenital hypothyroidism (CH). In addition premature infants born small for gestational age (SGA) have a risk of 12% higher to develop IC compared to prematures with appropriate development (AGA). The mechanisms that justify the increased risk of IC are still unknown. Some studies report a